

# **The role of the nucleoporin Nup93 sub-complex in regulating HOXA gene expression**

A thesis  
submitted in partial fulfillment of the requirements

for the degree of  
Doctor of Philosophy

By

**Ajay S. Labade**

20112006

Under the guidance of

**Dr. Kundan Sengupta**



**INDIAN INSTITUTE OF SCIENCE EDUCATION AND RESEARCH, PUNE**

**2018**



भारतीय विज्ञान शिक्षा एवं अनुसंधान संस्थान, पुणे  
INDIAN INSTITUTE OF SCIENCE EDUCATION AND RESEARCH (IISER), PUNE  
(An Autonomous Institution, Ministry of Human Resource Development, Govt. of India)  
Dr. Homi Bhabha Road, Pashan, Pune - 411 008

DOCTORAL STUDIES OFFICE

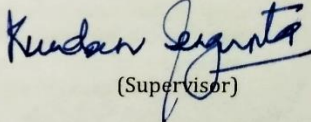
Form for submission of Ph.D. Thesis

**Certificate by Supervisor**

I certify that the thesis entitled The role of the nucleoporin-Nup93 sub-complex in regulating HoxA gene expression presented by Mr/Ms Ajay Shankar Lebade represents his/~~her~~ original work which was carried out by him/~~her~~ at IISER, Pune under my guidance and supervision during the period from 01/08/2013 to 17/08/2018.

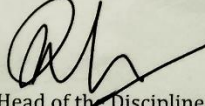
The work presented here or any part of it has not been included in any other thesis submitted previously for the award of any degree or diploma from any other University or institutions. I further certify that the above statements made by him/~~her~~ in regard to his/~~her~~ thesis are correct to the best of my knowledge.

Date: 14.08, 2018

  
(Supervisor)

**Recommended and Forwarded**

Date: 16/8/18

  
Head of the Discipline

**Received the Thesis**

Date:

Dean, Doctoral studies

**Enclosures (check list)**

1. Abstract of Thesis
2. Electronic copy of the Thesis
3. Consolidated Progress Report as per funding agencies format
4. Copy of online generate Thesis Submission payment receipt

(I/II)

Ph: +91-20-25908122 | Fax: +91-20-20251566

Email: [doctoraloffice@iiserpune.ac.in](mailto:doctoraloffice@iiserpune.ac.in)

DSO 13

DSO 13



भारतीय विज्ञान शिक्षा एवं अनुसंधान संस्थान, पुणे  
INDIAN INSTITUTE OF SCIENCE EDUCATION AND RESEARCH (IISER), PUNE  
(An Autonomous Institution, Ministry of Human Resource Development, Govt. of India)  
Dr. Homi Bhabha Road, Pashan, Pune - 411 008

DOCTORAL STUDIES OFFICE

Form for submission of Ph.D. Thesis

Declaration by student

Name of Student: Ajay Shankar Labade Reg. No.: 20112006

Thesis Supervisor(s): Dr. Kundan Sengupta Department: Biology

Date of joining: 01/08/2013 Date of Pre-Synopsis Seminar: 14/03/2018

Title of Thesis: The role of nucleoporin Nup93 sub-complex  
in regulating HOXA gene expression.

I declare that this written submission represents my idea in my own words and where others' ideas have been included; I have adequately cited and referenced the original sources. I also declare that I have adhered to all principles of academic honesty and integrity and have not misrepresented or fabricated or falsified any idea/data/fact/source in my submission. I understand that violation of the above will be cause for disciplinary action by the Institute and can also evoke penal action from the sources which have thus not been properly cited or from whom proper permission has not been taken when needed.

The work reported in this thesis is the original work done by me under the guidance of  
Dr. Kundan Sengupta

Date: 14/08/2018

Signature of the student

(I/II)

Ph: +91-20-25908122 | Fax: +91-20-20251566

Email: [doctoraloffice@iiserpune.ac.in](mailto:doctoraloffice@iiserpune.ac.in)

Dedicated to my parents and their love for science



## **Acknowledgements**

Foremost, I would like to express my sincere gratitude to my Ph.D. advisor Dr. Kundan Sengupta for his continuous support and guidance of my Ph.D. and research, for his motivation, enthusiasm, knowledge, and patience. I have had a great time working with him, giving me complete freedom to think independently and develop new techniques in the lab. Kundan is a great scientist, always willing to discuss and explore new ideas and debate on confusing results. His constant and insightful inputs helped me all the time to shape my research work. His guidance helped me a lot to improve my writing skills during manuscript and thesis writing.

I would like to thank my research advisory committee (RAC) members, Prof. M. S. Madhusudhan (IISER Pune), Dr. Jomon Joseph (NCCS), Dr. Krishanpal Karmodiya (IISER Pune) critically evaluating my work and their timely suggestions during my RAC meetings. I especially thank Dr. Krishanpal Karmodiya for help in ChIP-seq data analysis. I thank Prof. Sanjeev Galande (IISER Pune) and his laboratory members for reagents and suggestions. I thank Dr. Girish Deshpande for his critical comments on the manuscript. I thank Ralph Kehlenbach and Radha Chauhan for the GR2-GFP2-M9 and Nup93 overexpression constructs, respectively.

I have had the great fortune of being the Ph.D. student of Chromosome Biology Lab (CBL). Lab members of CBL have been friendly and supportive, always willing to help, share reagents and discuss novel ideas. I would like to thank all CBL members, past and present for their valuable inputs in my manuscript and thesis. I thank my seniors Devika and Ayantika who helped me a lot to start my Ph.D. project. I thank Maithilee, Roopali, Shalaka, and Maryuresh for their constant support. I would further like to thank Adwait Salvi, without whom I could not have been able to complete Nup93-HOXA project in NT2/D1 cells. I would like to thank all my friends in IISER Pune, especially Piyush and Kalpesh for their constant help.

I am extremely grateful to IISER, Pune for all its support in the form of equipment, infrastructure, management (Mrinalini Virkar, Kalpesh Thakare, Piyush Gadekar, Rupali Jadhav, Shabnam Patil, Mahesh Rote). I also thank the IISER Pune Microscopy facility (Vijay, Santosh, and Aditi). I thank Dinesh who provided help with lab chores. I thank IISER Pune for funding my fellowship and Wellcome-DBT India Alliance for funding the work. I would also like to thank Infosys India for the travel fellowship.

Finally, I would like to thank my family for their continuous support throughout my Ph.D. I thank my parents Shankar Labade and Manda Labade for always encouraging my love for science and being a constant source of happiness. I thank my brother Anurag and sister Komal, who have always encouraged me for completing my Ph.D.

## Table of Contents

- Abstract
- Synopsis
- List of abbreviations

	Page No.
<b>Chapter 1: Introduction and Review of Literature</b> .....	1
<b>1. Introduction</b> .....	2
1.1 Nuclear architecture and nuclear landmarks .....	2
1.2 The nuclear envelope.....	4
1.3 Functional organization of the genome at the nuclear periphery .....	7
1.4 The nuclear pore complex.....	12
1.5 Nuclear pore complex assembly.....	19
1.6 Transport independent functions of the NPC.....	21
1.7 Mechanism of chromatin contact with NPC .....	27
<b>Chapter 2: Materials and Methods</b> .....	30
<b>2.1 Commonly used methods throughout the study</b> .....	31
2.1.1 Cell culture.....	31
2.1.2 Metaphase spread preparation .....	31
2.1.3 Transient siRNA mediated knockdown .....	32
2.1.4 DNA transfections .....	33
2.1.5 Protein extraction and immunoblotting .....	34
2.1.6 Reverse transcription-PCR and real-time quantitative PCR .....	37
2.1.7 Immunoprecipitation (IP) and Co-IP .....	39
2.1.8 Chromatin Immunoprecipitation (ChIP) and ChIP-qPCR .....	39
2.1.9 Three-dimensional fluorescence in situ hybridization (3D-FISH) .....	44
2.1.10 RNA FISH.....	45
2.1.11 Microscopy and Image analysis .....	46
2.1.12 Poly(A) Fluorescence <i>In situ</i> Hybridization (FISH) .....	47

2.1.13 Nuclear import assay .....	47
<b>2.2 Materials and method specific for Chapter 4 .....</b>	<b>49</b>
2.2.1 ChIP-sequencing .....	49
2.2.2 ChIP-seq analysis .....	49
<b>2.3 Materials and method specific for Chapter 5 .....</b>	<b>54</b>
2.3.1 NT2/D1 cell culture and differentiation.....	54
2.3.2 CTCF and Nup93 ChIP in DLD-1 cells.....	55
2.3.3 CTCF and Nup93 ChIP in NT2/D1 cells .....	55
2.3.4 Nup93 and CTCF knockdown followed by RA treatment.....	55
2.3.5 3D-FISH for HOXA locus in NT2/D1 cells.....	55
<b>Chapter 3: Nup93 sub-complex mediated repression of HOXA gene cluster in differentiated cells.....</b>	<b>56</b>
<b>3.1 Introduction.....</b>	<b>57</b>
<b>3.2 Results.....</b>	<b>63</b>
3.2.1 Effect of Nup93 depletion on nuclear morphology, nuclear volume, and ploidy levels .....	63
3.2.2 Nup93 associates with the HOXA gene locus.....	67
3.2.3 Nup93 interacts with Nup188 and Nup205.....	71
3.2.4 Nup93 requires Nup188 and Nup205 to associate with the HOXA1 promoter .....	73
3.2.5 Interdependence of Nup93 sub-complex proteins .....	75
3.2.6 HOXA gene expression is upregulated in Nup93, Nup188 or Nup205 depleted cells .	77
3.2.7 Overexpression of Nup93 in the background of Nup188 and Nup205 depletion does not rescue de-repression of HOXA.....	80
3.2.8 Rescue of HOXA upregulation .....	82
3.2.9 HOXA gene locus is untethered from the nuclear periphery in Nup93, Nup188, Nup205 depleted cells.....	84
3.2.10 HOXA transcripts are enriched upon Nup93 depletion .....	86
3.2.11 Nup93 depletion alters the relative occupancy of histone marks on the HOXA1 promoter.....	88
3.2.12 Nuclear import in cells depleted of Nup93, Nup188 or Nup205.....	91
3.2.13 Nuclear export in cells depleted of Nup93, Nup188 or Nup205 .....	95
3.2.14 Nup93 does not interact with CTCF or PRC2 complex proteins .....	97
<b>3.3 Discussion .....</b>	<b>99</b>
3.3.1 Implications of the association of nucleoporins with chromatin .....	100

3.3.2 Role of nucleoporins in nuclear transport and chromatin organization .....	102
3.3.3 Potential mechanisms of nucleoporin-chromatin interactions.....	103
3.3.4 Nucleoporins as repressors of HOXA gene expression in differentiated cells.....	106
<b>Chapter 4: Genome-wide functions of Nup93 .....</b>	<b>108</b>
<b>4.1 Introduction.....</b>	<b>109</b>
<b>4.2 Results .....</b>	<b>112</b>
4.2.1 Validating the specificity of Nup93 antibody ChIP-sequencing .....	112
4.2.2 Optimizing chromatin immunoprecipitation assay to determine putative chromatin binding sites of Nup93 .....	118
4.2.3 Analysis of ChIP Seq data to investigate the genome-wide binding of Nup93.....	119
4.2.4 Mapping of Nup93 peaks to the human genome .....	124
4.2.5 Characterizing the location of Nup93 peaks .....	128
4.2.6 GO term analysis of Nup93 associated genes reflects its possible role during differentiation.....	131
4.2.7 DNA binding motifs enriched in Nup93 binding sequences.....	137
4.2.8 Transcription factors enriched within Nup93 binding regions .....	139
4.2.9 Co-occupancy of Nup93 and CTCF .....	141
4.2.10 Overlapping role of Nup93 and CTCF in gene regulation .....	144
4.2.11 Nup93 binding sites are enriched for repressive histone marks .....	147
<b>4.3 Discussion .....</b>	<b>150</b>
<b>Chapter 5: Role of Nup93 and CTCF in the regulation of HOXA gene expression during differentiation .....</b>	<b>157</b>
<b>5.1. Introduction.....</b>	<b>158</b>
<b>5.2 Results.....</b>	<b>163</b>
5.1.1 Nup93 and CTCF binding sites do not overlap with each other on HOXA locus.....	163
5.1.2 HOXA is upregulated upon Nup93 depletion independent of CTCF.....	166
5.1.3 Nup93 depletion increases occupancy of CTCF on its conserved binding sites .....	168
5.1.4 Effect of Nup93-CTCF on the dynamics of the HOXA gene cluster in RA mediated differentiation of NT2D1 cells .....	170
5.1.5 RA mediated activation of HOXA gene cluster in NT2/D1 cells.....	173
5.1.6 Expression levels of Nup93 and CTCF are unaffected upon differentiation .....	175
5.1.7 Antagonistic effect of Nup93 and CTCF depletion on HOXA gene expression.....	177

5.1.8 RA mediated induction of HOXA gene expression in Nup93 or CTCF depleted cells .....	178
5.1.9 Dynamic association of HOXA locus with the nuclear periphery during differentiation .....	181
5.1.10 Dynamic association of Nup93 and CTCF with HOXA locus during differentiation .....	185
<b>5.3 Discussion .....</b>	<b>188</b>
<b>Chapter 6: Conclusions and Potential Future Directions .....</b>	<b>195</b>
<b>6.1 Conclusions.....</b>	<b>196</b>
<b>6. 2 Potential Future Directions .....</b>	<b>208</b>
<b>References .....</b>	<b>212</b>



## **Abstract**

The nuclear pore complex (NPCs) is required for the regulated import and export of RNA and proteins. NPC is a megadalton multiprotein channel composed of ~ 30 nucleoporins (Nups). In addition to transport, nucleoporins are involved in the regulation of chromatin organization and gene expression. Here we investigated the role of nucleoporin Nup93 in the regulation of HOXA gene expression. HOXA expression is restricted to early stages of development and differentiation, while its aberrant expression in differentiated cells is associated with cancers. We showed that Nup93 is associated with HOXA1, HOXA3, and HOXA5 promoters and represses HOXA expression, in a manner assisted by its interacting partners Nup188 and Nup205. Single cell imaging by 3D-Fluorescence in situ hybridization (3D-FISH) analyses, revealed that the depletion of Nup93 untethers the HOXA gene locus from the nuclear periphery, which we also ascertained by RNA-FISH. We propose a novel role for the Nup93 sub-complex in repressing HOXA gene locus thereby preventing its untimely expression in differentiated cells. To address the genome-wide role of Nup93 in gene regulation, we performed Chromatin Immunoprecipitation (ChIP) of Nup93 followed by whole-genome sequencing. Analyses of Nup93 ChIP-seq data shows that Nup93 specifically associates with genes involved in development and differentiation. Furthermore, Nup93 associates with genomic regions similar to the repressive histone mark (H3K27me3), suggesting a repressive role of Nup93 in gene regulation. In addition, Nup93 enriched regions also overlap with CTCF - a major genome organizer, suggesting a crosstalk between Nup93 and CTCF in gene regulation.

To further understand the role of Nup93 and CTCF during differentiation, we performed Retinoic acid-mediated differentiation of NT2/D1 cells in the background of Nup93 and CTCF depletion. We found that Nup93 depletion in NT2/D1 cells upregulates HOXA gene cluster. In contrast, CTCF depletion downregulates HOXA gene cluster. Surprisingly, we found that retinoic acid treatment in Nup93 depleted cells significantly enhances HOXA gene expression. In contrast, RA treatment in CTCF depleted cells reduces HOXA gene expression. 3D-FISH analyses revealed that HOXA gene locus shows a dynamic repositioning from the nuclear periphery during differentiation to the nuclear interior upon activation and relocates to the nuclear periphery that correlates with repression. We found that the untethering of HOXA locus from the nuclear periphery correlates with the reduced occupancy of Nup93 and increased occupancy of CTCF on the HOXA1 promoter during differentiation. In summary, our results suggest that Nup93 and CTCF have an antagonistic role in the regulation of HOXA gene expression during differentiation.

# Synopsis

## *Background*

The nucleus stores genetic information in the form of DNA, which is replicated transcribed and transmitted faithfully to daughter cells upon cell division. In human cells, ~ 2 m long genomic DNA is organized in the form of chromosome territories in the nucleus of a diameter of ~10 $\mu$ m. Despite its highly compact organization, the nucleus is functionally compartmentalized. Several studies have shown that gene loci and chromosomal domains occupy cell type-specific locations inside the nucleus, consistent with their transcriptional status (Fritz et al., 2016; Gibcus and Dekker, 2013; Li et al., 2018; Stancheva and Schirmer, 2014; Talamas and Capelson, 2015). These findings have uncovered that the functional compartmentalization of the genome is essential for cell type-specific gene expression. However, how this functional compartmentalization is faithfully maintained inside the nucleus remains poorly understood.

Nuclear landmarks such as the nuclear envelope proteins, lamins, nucleolus and nuclear bodies among others, are essential for the structural and functional organization of the genome (Mekhail and Moazed, 2010). A substantial fraction of the genome is organized relative to nuclear landmarks and nuclear bodies (Quinodoz et al., 2018). The Nuclear pore complex (NPC) is one such nuclear landmark, which has been implicated in the functional organization of the genome (D'Angelo, 2018; Liang and Hetzer, 2011). Beyond their vital role in nuclear-cytoplasmic transport, how NPC components regulate the genome organization and gene expression is largely uncertain (Ibarra and Hetzer, 2015; Raices and D'Angelo, 2018).

Nuclear pore complex is a large multiprotein channel (~120 MDa) that connects nucleoplasm to the cytoplasm and assists in nuclear transport (D'Angelo and Hetzer, 2008). It is composed of multiple copies of 30 different proteins known as nucleoporins. Structurally, nucleoporins are divided into two categories - scaffold nucleoporins and peripheral nucleoporins. Scaffold nucleoporins such as Nup93-subcomplex and Nup107 subcomplex forms the core scaffold of the NPC, while peripheral nucleoporins constitutes the central channel, inner and outer ring of the NPC (D'Angelo and Hetzer, 2008). Scaffold nucleoporins are largely immobile and tethered to the nuclear periphery by transmembrane nucleoporins (Pom121, Ndc1, and Gp210) (Doucet and Hetzer, 2010; Mansfeld et al., 2006; Stavru et al., 2006a, 2006b). Peripheral nucleoporins (e.g. Nup98, Nup50) are mobile and they show dynamic movement from the nuclear pore complex (Sakiyama et al., 2017). In addition to their function in nuclear transport, nucleoporins also regulate chromatin organization and gene regulation (Ibarra and Hetzer, 2015). Nucleoporins function in both transcriptional activation and repression either at the nuclear periphery or in the nucleoplasm (D'Angelo, 2018). Mobile nucleoporins translocate into the nucleus and associates with gene regulatory elements such as promoters for the control of gene expression (Casolari et al., 2004; Sood and Brickner, 2014). Scaffold nucleoporins associate with gene loci at the nuclear periphery and regulate their expression (Ibarra et al., 2016).

Gene regulatory function of nucleoporins has been largely studied in yeast, *Drosophila*, and *C.elegans*. In yeast, NPC is involved in the silencing of telomeric chromatin at the nuclear periphery (Van deaaa 1Vosse et al., 2013). Similarly, inducible genes such as INO1, GAL1, and HXK1 move from the nuclear interior to the NPC upon

activation (Brickner and Walter, 2004; Light et al., 2010; Taddei et al., 2006; Texari et al., 2013). The recruitment of genes to the NPC is DNA sequence dependent. Additionally, mediator proteins such as SAGA complex and TREX are involved in gene recruitment at the NPC (Cabal et al., 2006; Schneider et al., 2015). In *Drosophila*, mobile nucleoporins such as Nup98 and Nup50 re-localize to the nucleoplasm, associate with chromatin and participate in gene regulation (Capelson et al., 2010a, 2010b). Nup153 and Megator, associate with ~25% of the *Drosophila* genome at nucleoporin associated regions (NARs) and coordinate the dosage compensation by binding to X chromosome (Vaquerizas et al., 2010). A mobile nucleoporin Nup98 shows preferential localization of active genes involved in development and differentiation (Kalverda et al., 2010). Although nucleoporins are shown to regulate either activation or repression of gene expression, the molecular mechanisms that allow them to differentiate between these two-different gene regulatory functions is not yet understood.

Gene regulatory functions of nucleoporins in mammals are not extensively studied as compared to yeast and *Drosophila*. Nucleoporins such as Nup98, Nup93, Nup210, Nup153, and Nup50 regulate gene expression in mammals (Brown et al., 2008; D'Angelo et al., 2012; Ibarra et al., 2016; Liang et al., 2013). Nup98 shows differential binding with developmentally regulated genes (e.g. GRIK1, NRG1, and MAP) during differentiation of neural progenitor cells (Liang et al., 2013). Interestingly, transmembrane nucleoporin Nup210 shows cell type-specific expression pattern during differentiation of C2C12 cells into myotubes (D'Angelo et al., 2012). Nup210 regulates the expression of genes (Asb2, Cand2, Clic5, GDF5) involved in the differentiation (D'Angelo et al., 2012). Similarly, a stable nucleoporin Nup93, associates with super enhancers of cell identity genes (Ibarra et

al., 2016). Both Nup93 and Nup210 are immobile nucleoporins and are located at the core of the nuclear pore complex. Nucleoporins might function as regulators of developmental gene expression by providing a stable platform for gene regulation. However, underlying mechanisms of chromatin-nucleoporin association at the nuclear periphery is unclear.

In yeast and *Drosophila*, transcription factors mediate the interaction between chromatin and NPC (Brickner et al., 2012; Pascual-Garcia et al., 2017). In mammals, Nup210 interacts with the transcription factor complex Mef2C and regulate the activation of muscle structural genes (Raices et al., 2017). Similarly, Nup155- a part of the Nup93 subcomplex, associates with HDAC4 and inhibits the expression of sarcomeric genes (*Nppb*, *Acta1*, *Cacna1*) at the nuclear periphery (Kehat et al., 2011). These studies indicate the role of transcription factors and chromatin modulator in mediating nucleoporin-chromatin interaction. However, how a stable nucleoporin directly associates with chromatin is not clear from these studies. How does nucleoporin regulate cell type-specific gene expression? Furthermore, if nucleoporins regulate the expression of developmental genes, how do they dynamically associate with these genes during differentiation? We have focused on some of these unanswered questions in our study by examining the role of a stable nucleoporin Nup93, in the regulation of the organization and function of the HOXA gene locus in differentiated colorectal cancer (DLD-1 cells) and during the differentiation of embryonal carcinoma (NT/2D1) cells.

Nup93 is one of the most stable nucleoporins in the nuclear pore complex (Rabut et al., 2004). It has a relatively low turnover rate and long life at the nuclear pore complex as revealed by postmitotic turnover analysis ((D'Angelo et al., 2009; Savas et al., 2012; Toyama et al., 2013). The nucleoporin Nup93 sub-complex is composed of Nup93,



Nup188, Nup205, Nup155 and Nup53 (Grandi et al., 1997; Kosinski et al., 2016; Miller et al., 2000; Sachdev et al., 2012; Vollmer and Antonin, 2014). Gene regulatory function of Nup93 has previously been demonstrated in *Caenorhabditis elegans* and *Drosophila* (Breuer and Ohkura, 2015; Brown et al., 2008; Ibarra et al., 2016; Rohner et al., 2013). In *Caenorhabditis elegans*, an ortholog of Nup93 tethers *hsp16.2* promoter to the nuclear periphery (Rohner et al., 2013). Additionally, NPP-13 associates with Polymerase-III transcribed genes, including snoRNA (small nucleolar RNA) and t-RNA genes (Ikegami and Lieb, 2013). Interestingly, in *Drosophila*, Nup62 and Nup93 function as negative regulators of chromatin attachment to the NPC by suppressing chromatin interaction with Nup155 (Breuer and Ohkura, 2015). Together, these studies demonstrate the chromatin binding function of a stable nucleoporin Nup93.

In humans, chromatin immunoprecipitation with a stable nucleoporin Nup93, showed that Nup93 associates with heterochromatic regions of chromosome 5, chromosome 7 and chromosome 16 in HeLa cells (Brown et al., 2008). For the first time, this study was able to demonstrate that a stable nucleoporin can contact chromatin in human cells. Interestingly, Nup93 associates with the HOXA gene cluster on chromosome 7 (Brown et al., 2008). However, the functional relevance of Nup93-HOXA cluster association remains to be understood. Furthermore, whether Nup93 associates with all human chromosomes in the interphase nucleus was not clear from this study. A more recent study showed that Nup93 associates with super-enhancers of cell identity genes in human U2OS cells (Ibarra et al., 2016). Depletion of Nup93 showed a global change in the expression of super enhancer-associated genes (Ibarra et al., 2016). Furthermore, careful analysis of RNA seq data showed that the depletion of Nup93 leads to an overexpression

of HOXA genes in U2OS cells (Ibarra et al., 2016). Altogether, both these studies with different human cell lines revealed the connection of Nup93 in the regulation of HOXA genes.

The HOXA genes encode for 11 transcription factors that are essential for development and involved in pattern formation in early development (Rousseau et al., 2014). Expression of HOXA gene is restricted to early stages of development and differentiation. HOXA expression levels are dysregulated in breast carcinoma, human cutaneous melanoma and oral cancers (Bhatlekar et al., 2014; Bitu et al., 2012; Maeda et al., 2005; Makiyama et al., 2005; Mustafa et al., 2015; Novak et al., 2006). Chromosome conformation capture studies have shown that the repressed HOXA gene cluster adopts a compact chromatin state organized as “multiple chromatin loops” for instance in undifferentiated NT2/D1 cells (Bermejo et al., 2012; Narendra et al., 2015; Xu et al., 2014). These loops of the HOXA gene loci are disrupted by the combined action of retinoic acid treatment and depletion of CTCF or PRC2 that transcriptionally activate HOXA gene expression (Xu et al., 2014). Surprisingly, ChIP with Nup93 in two different human cell lines (U2OS and HeLa) suggest a possible role of Nup93 in the regulation of the HOXA gene cluster (Ibarra et al., 2016). Interestingly, these studies were performed in differentiated cells, where HOXA genes are typically in a repressed state. The role of Nup93 in the regulation of HOXA gene cluster remains elusive from these studies.

In this thesis, we have attempted to address the following questions to understand the role of Nup93 in the regulation of the HOXA gene cluster.

1. Does Nup93 regulate the expression of the HOXA gene cluster in differentiated cells?
2. What is the role of the interactors of Nup93 i.e Nup188 and Nup205, in the regulation of Nup93 associated genes? And does the Nup93 sub-complex tether the HOXA genomic locus?
3. Does Nup93 have a genome-wide role in gene regulation?
4. Since CTCF is a well-known genome organizer, does Nup93 participate with CTCF in the organization of the HOXA?
5. Does Nup93 associate and organize the HOXA locus during of differentiation?

I have attempted to answer these questions with the following aims in my thesis

### ***Specific Aims***

**Aim 1.** To investigate the role of the Nup93-subcomplex in the repression of the HOXA gene cluster at the nuclear periphery.

We examined the occupancy of Nup93 on the HOXA gene locus by performing chromatin immunoprecipitation (ChIP) followed by qPCR analysis for HOXA1, HOXA3, and HOXA5 promoters. We found that Nup93 specifically associates with specific sub-regions of HOXA1, A3, and A5 promoters. We demonstrate that Nup93 interacts with Nup188 and Nup205. To investigate the role of Nup188 and Nup205 in mediating Nup93-HOXA interaction, we performed ChIP with Nup93 in Nup188 or Nup205 depleted cells. These

results revealed that Nup188 and Nup205 are required for Nup93-HOXA interaction. Depletion of Nup188 or Nup205 abolishes occupancy of Nup93 on HOXA1 the promoter.

The qRT-PCR analysis revealed that depletion of Nup93, Nup188 or Nup205 de-represses the entire HOXA gene cluster (HOXA1 to A13) in DLD-1 cells. The de-repression of HOXA gene locus is accompanied by an increase in active histone marks (H3K9Ac) and decrease in repressive histone mark (H3K27me3) on HOXA1 promoter with a concomitant increase in elongation mark (H3K36me3) on the HOXA1 gene body. Furthermore, 3D-FISH analyses revealed that the depletion of Nup93 or its interacting partners - Nup188 or Nup205, untethers HOXA gene locus from the nuclear periphery.

**Aim 2.** To investigate the genome-wide role of Nup93 in gene regulation

Since Nup93 is localized at the nuclear periphery in the NPC, we determined the genome-wide occupancy of Nup93 in differentiated DLD-1 cells. We performed Chromatin immunoprecipitation of Nup93 followed by whole genome sequencing (Nup93 ChIP-seq) and examined the enrichment of Nup93 across different genomic regions such as promoters, introns, exons, upstream and downstream regions of the gene. ChIP-seq analysis revealed that Nup93 is enriched around transcription start sites and exon-intron boundaries of various genes. Functional, characterization of these genes by Gene Ontology analysis revealed that Nup93 associates with genes involved in development and differentiation. Transcription factor enrichment analysis of Nup93 peaks revealed that Nup93 peaks significantly overlap with CTCF peaks suggesting its possible role in genome

organization. Furthermore, Nup93 peaks showed an enrichment of the repressive histone mark (H3K27me3) indicating its global role in transcriptional silencing.

**Aim 3.** Role of Nup93 in the regulation of HOXA gene cluster during differentiation  
HOXA gene expression is temporally regulated during differentiation. We asked if Nup93 is involved in the regulation of HOXA gene expression during the differentiation of human embryonal carcinoma cell line - NT2/D1. Since ChIP-seq analysis revealed a significant overlap between Nup93 and CTCF, we sought to determine if Nup93 exerts a co-regulatory role on HOXA expression along with CTCF. Since CTCF is a well-known genome organizer. To determine the role of Nup93 and CTCF in HOXA gene regulation, we knocked down Nup93 and CTCF in NT2/D1 cells followed by retinoic acid treatment. Surprisingly, we found that retinoic acid treatment in Nup93 depleted cells significantly enhances HOXA expression. In contrast, RA treatment in CTCF depleted cells reduces HOXA gene expression. This suggests an antagonistic role of Nup93 and CTCF in the regulation of HOXA gene expression. 3D-FISH analysis of the HOXA locus revealed that HOXA locus shows a dynamic association with respect to the nuclear periphery during different stages of differentiation. In support of this observation, preliminary results of Nup93 and CTCF ChIP-PCR on HOXA1 promoter indicates that Nup93 and CTCF show mutually exclusive association with the HOXA1 promoter at different stages of differentiation.

## ***Summary***

Taken together, our studies unravel a novel role for nucleoporins Nup93 and its interactors Nup188 and Nup205 in mediating the repression and tethering of the HOXA gene cluster to the nuclear periphery in diploid DLD1 cells. Depletion of Nup93, Nup188 or Nup205 significantly enhances HOXA gene expression. The elevated levels of HOXA gene expression upon the depletion of Nup93 or its interactors—Nup188 and Nup205, is associated with an increase in the occupancy of active histone marks and decreased levels of inactive histone marks with a concomitant increase in transcriptional elongation marks within the HOXA gene. Furthermore, we show that Nup93 peaks overlap with CTCF peaks suggesting its potential role in genome organization. In addition, we show that Nup93 associates with genes involved in development and differentiation. Nup93 associated peaks are enriched for repressive histone marks, suggesting a repressive role of Nup93 in gene regulation. We have identified a novel antagonistic role of Nup93 and CTCF in regulating HOXA gene expression during differentiation. In this thesis, we have attempted to show the functional importance of Nup93-HOXA interaction in regulating HOXA gene cluster silencing.

## **References**

- Bermejo, R., Kumar, A., and Foiani, M. (2012). Preserving the genome by regulating chromatin association with the nuclear envelope. *Trends Cell Biol.* 22, 465–473.
- Bhatlekar, S., Fields, J.Z., and Boman, B.M. (2014). HOX genes and their role in the development of human cancers. *J. Mol. Med.* 92, 811–823.
- Bitu, C.C., Destro, M.F. de S.S., Carrera, M., da Silva, S.D., Graner, E., Kowalski, L.P., Soares, F.A., and Coletta, R.D. (2012). HOXA1 is overexpressed in oral squamous cell carcinomas and its expression is correlated with poor prognosis. *BMC Cancer* 12, 146.



- Breuer, M., and Ohkura, H. (2015). A negative loop within the nuclear pore complex controls global chromatin organization. *Genes Dev.* 29, 1789–1794.
- Brickner, J.H., and Walter, P. (2004). Gene recruitment of the activated INO1 locus to the nuclear membrane. *PLoS Biol.* 2, e342.
- Brickner, D.G., Ahmed, S., Meldi, L., Thompson, A., Light, W., Young, M., Hickman, T.L., Chu, F., Fabre, E., and Brickner, J.H. (2012). Transcription factor binding to a DNA zip code controls interchromosomal clustering at the nuclear periphery. *Dev. Cell* 22, 1234–1246.
- Brown, C.R., Kennedy, C.J., Delmar, V.A., Forbes, D.J., and Silver, P.A. (2008). Global histone acetylation induces functional genomic reorganization at mammalian nuclear pore complexes. *Genes Dev.* 22, 627–639.
- Cabal, G.G., Genovesio, A., Rodriguez-Navarro, S., Zimmer, C., Gadal, O., Lesne, A., Buc, H., Feuerbach-Fournier, F., Olivo-Marin, J.-C., Hurt, E.C., et al. (2006). SAGA interacting factors confine sub-diffusion of transcribed genes to the nuclear envelope. *Nature* 441, 770–773.
- Capelson, M., Liang, Y., Schulte, R., Mair, W., Wagner, U., and Hetzer, M.W. (2010a). Chromatin-bound nuclear pore components regulate gene expression in higher eukaryotes. *Cell* 140, 372–383.
- Capelson, M., Doucet, C., and Hetzer, M.W. (2010b). Nuclear pore complexes: guardians of the nuclear genome. *Cold Spring Harb. Symp. Quant. Biol.* 75, 585–597.
- Casolari, J.M., Brown, C.R., Komili, S., West, J., Hieronymus, H., and Silver, P.A. (2004). Genome-wide localization of the nuclear transport machinery couples transcriptional status and nuclear organization. *Cell* 117, 427–439.
- D'Angelo, M.A. (2018). Nuclear pore complexes as hubs for gene regulation. *Nucleus* 9, 142–148.
- D'Angelo, M.A., and Hetzer, M.W. (2008). Structure, dynamics and function of nuclear pore complexes. *Trends Cell Biol.* 18, 456–466.
- D'Angelo, M.A., Raices, M., Panowski, S.H., and Hetzer, M.W. (2009). Age-dependent deterioration of nuclear pore complexes causes a loss of nuclear integrity in postmitotic cells. *Cell* 136, 284–295.
- D'Angelo, M.A., Gomez-Cavazos, J.S., Mei, A., Lackner, D.H., and Hetzer, M.W. (2012). A change in nuclear pore complex composition regulates cell differentiation. *Dev. Cell* 22, 446–458.
- Doucet, C.M., and Hetzer, M.W. (2010). Nuclear pore biogenesis into an intact nuclear envelope. *Chromosoma* 119, 469–477.
- Fritz, A.J., Barutcu, A.R., Martin-Buley, L., van Wijnen, A.J., Zaidi, S.K., Imbalzano, A.N., Lian, J.B., Stein, J.L., and Stein, G.S. (2016). Chromosomes at work: organization of chromosome territories in the interphase nucleus. *J. Cell Biochem.* 117, 9–19.
- Gibcus, J.H., and Dekker, J. (2013). The hierarchy of the 3D genome. *Mol. Cell* 49, 773–782.
- Grandi, P., Dang, T., Pané, N., Shevchenko, A., Mann, M., Forbes, D., and Hurt, E. (1997). Nup93, a vertebrate homologue of yeast Nic96p, forms a complex with a novel 205-kDa protein and is required for correct nuclear pore assembly. *Mol. Biol. Cell* 8, 2017–2038.
- Ibarra, A., and Hetzer, M.W. (2015). Nuclear pore proteins and the control of genome functions. *Genes Dev.* 29, 337–349.
- Ibarra, A., Benner, C., Tyagi, S., Cool, J., and Hetzer, M.W. (2016). Nucleoporin-mediated regulation of cell identity genes. *Genes Dev.* 30, 2253–2258.
- Ikegami, K., and Lieb, J.D. (2013). Integral nuclear pore proteins bind to Pol III-transcribed genes and are required for Pol III transcript processing in *C. elegans*. *Mol. Cell* 51, 840–849.

- Kalverda, B., Pickersgill, H., Shloma, V.V., and Fornerod, M. (2010). Nucleoporins directly stimulate expression of developmental and cell-cycle genes inside the nucleoplasm. *Cell* 140, 360–371.
- Kehat, I., Accornero, F., Aronow, B.J., and Molkentin, J.D. (2011). Modulation of chromatin position and gene expression by HDAC4 interaction with nucleoporins. *J. Cell Biol.* 193, 21–29.
- Kosinski, J., Mosalaganti, S., von Appen, A., Teimer, R., DiGuilio, A.L., Wan, W., Bui, K.H., Hagen, W.J.H., Briggs, J.A.G., Glavy, J.S., et al. (2016). Molecular architecture of the inner ring scaffold of the human nuclear pore complex. *Science* (80- ). 352, 363–365.
- Li, Y., Hu, M., and Shen, Y. (2018). Gene regulation in the 3D genome. *Hum. Mol. Genet.* 27, R228–R233.
- Liang, Y., and Hetzer, M.W. (2011). Functional interactions between nucleoporins and chromatin. *Curr. Opin. Cell Biol.* 23, 65–70.
- Liang, Y., Franks, T.M., Marchetto, M.C., Gage, F.H., and Hetzer, M.W. (2013). Dynamic association of NUP98 with the human genome. *PLoS Genet.* 9, e1003308.
- Light, W.H., Brickner, D.G., Brand, V.R., and Brickner, J.H. (2010). Interaction of a DNA zip code with the nuclear pore complex promotes H2A.Z incorporation and INO1 transcriptional memory. *Mol. Cell* 40, 112–125.
- Maeda, K., Hamada, J.-I., Takahashi, Y., Tada, M., Yamamoto, Y., Sugihara, T., and Moriuchi, T. (2005). Altered expressions of HOX genes in human cutaneous malignant melanoma. *Int. J. Cancer.* 114, 436–441.
- Makiyama, K., Hamada, J.-I., Takada, M., Murakawa, K., Takahashi, Y., Tada, M., Tamoto, E., Shindo, G., Matsunaga, A., Teramoto, K.-I., et al. (2005). Aberrant expression of HOX genes in human invasive breast carcinoma. *Oncol. Rep.* 13, 673–679.
- Mansfeld, J., Güttinger, S., Hawryluk-Gara, L.A., Panté, N., Mall, M., Galy, V., Haselmann, U., Mühlhäusser, P., Wozniak, R.W., Mattaj, I.W., et al. (2006). The conserved transmembrane nucleoporin NDC1 is required for nuclear pore complex assembly in vertebrate cells. *Mol. Cell* 22, 93–103.
- Mekhail, K., and Moazed, D. (2010). The nuclear envelope in genome organization, expression and stability. *Nat. Rev. Mol. Cell Biol.* 11, 317–328.
- Miller, B.R., Powers, M., Park, M., Fischer, W., and Forbes, D.J. (2000). Identification of a new vertebrate nucleoporin, Nup188, with the use of a novel organelle trap assay. *Mol. Biol. Cell* 11, 3381–3396.
- Mustafa, M., Lee, J.-Y., and Kim, M.H. (2015). CTCF negatively regulates HOXA10 expression in breast cancer cells. *Biochem. Biophys. Res. Commun.* 467, 828–834.
- Narendra, V., Rocha, P.P., An, D., Raviram, R., Skok, J.A., Mazzoni, E.O., and Reinberg, D. (2015). CTCF establishes discrete functional chromatin domains at the Hox clusters during differentiation. *Science* (80- ). 347, 1017–1021.
- Novak, P., Jensen, T., Oshiro, M.M., Wozniak, R.J., Nouzova, M., Watts, G.S., Klimecki, W.T., Kim, C., and Futscher, B.W. (2006). Epigenetic inactivation of the HOXA gene cluster in breast cancer. *Cancer Res.* 66, 10664–10670.
- Pascual-Garcia, P., Debo, B., Aleman, J.R., Talamas, J.A., Lan, Y., Nguyen, N.H., Won, K.J., and Capelson, M. (2017). Metazoan Nuclear Pores Provide a Scaffold for Poised Genes and Mediate Induced Enhancer-Promoter Contacts. *Mol. Cell* 66, 63–76.e6.
- Quinodoz, S.A., Ollikainen, N., Tabak, B., Palla, A., Schmidt, J.M., Detmar, E., Lai, M.M., Shishkin, A.A., Bhat, P., Takei, Y., et al. (2018). Higher-Order Inter-chromosomal Hubs Shape 3D Genome Organization in the Nucleus. *Cell* 174, 744–757.e24.
- Rabut, G., Doye, V., and Ellenberg, J. (2004). Mapping the dynamic organization of the nuclear pore complex inside single living cells. *Nat. Cell Biol.* 6, 1114–1121.

- Raices, M., and D'Angelo, M.A. (2018). Nuclear pore complexes in the organization and regulation of the mammalian genome. In *Nuclear Pore Complexes in Genome Organization, Function and Maintenance*, M. D'Angelo, ed. (Cham: Springer International Publishing), pp. 159–182.
- Raices, M., Bukata, L., Sakuma, S., Borlido, J., Hernandez, L.S., Hart, D.O., and D'Angelo, M.A. (2017). Nuclear pores regulate muscle development and maintenance by assembling a localized *mef2c* complex. *Dev. Cell* 41, 540–554.e7.
- Rohner, S., Kalck, V., Wang, X., Ikegami, K., Lieb, J.D., Gasser, S.M., and Meister, P. (2013). Promoter- and RNA polymerase II-dependent *hsp-16* gene association with nuclear pores in *Caenorhabditis elegans*. *J. Cell Biol.* 200, 589–604.
- Rousseau, M., Crutchley, J.L., Miura, H., Suderman, M., Blanchette, M., and Dostie, J. (2014). Hox in motion: tracking HoxA cluster conformation during differentiation. *Nucleic Acids Res.* 42, 1524–1540.
- Sachdev, R., Sieverding, C., Flötenmeyer, M., and Antonin, W. (2012). The C-terminal domain of Nup93 is essential for assembly of the structural backbone of nuclear pore complexes. *Mol. Biol. Cell* 23, 740–749.
- Sakiyama, Y., Panatala, R., and Lim, R.Y.H. (2017). Structural dynamics of the nuclear pore complex. *Semin. Cell Dev. Biol.* 68, 27–33.
- Savas, J.N., Toyama, B.H., Xu, T., Yates, J.R., and Hetzer, M.W. (2012). Extremely long-lived nuclear pore proteins in the rat brain. *Science* (80-. ). 335, 942.
- Schneider, M., Hellerschmied, D., Schubert, T., Amlacher, S., Vinayachandran, V., Reja, R., Pugh, B.F., Clausen, T., and Köhler, A. (2015). The Nuclear Pore-Associated TREX-2 Complex Employs Mediator to Regulate Gene Expression. *Cell* 162, 1016–1028.
- Sood, V., and Brickner, J.H. (2014). Nuclear pore interactions with the genome. *Curr. Opin. Genet. Dev.* 25, 43–49.
- Stancheva, I., and Schirmer, E.C. (2014). Nuclear envelope: connecting structural genome organization to regulation of gene expression. *Adv. Exp. Med. Biol.* 773, 209–244.
- Stavru, F., Hülsmann, B.B., Spang, A., Hartmann, E., Cordes, V.C., and Görlich, D. (2006a). NDC1: a crucial membrane-integral nucleoporin of metazoan nuclear pore complexes. *J. Cell Biol.* 173, 509–519.
- Stavru, F., Nautrup-Pedersen, G., Cordes, V.C., and Görlich, D. (2006b). Nuclear pore complex assembly and maintenance in POM121- and gp210-deficient cells. *J. Cell Biol.* 173, 477–483.
- Taddei, A., Van Houwe, G., Hediger, F., Kalck, V., Cubizolles, F., Schober, H., and Gasser, S.M. (2006). Nuclear pore association confers optimal expression levels for an inducible yeast gene. *Nature* 441, 774–778.
- Talamas, J.A., and Capelson, M. (2015). Nuclear envelope and genome interactions in cell fate. *Front. Genet.* 6, 95.
- Texari, L., Dieppo, G., Vinciguerra, P., Contreras, M.P., Groner, A., Letourneau, A., and Stutz, F. (2013). The nuclear pore regulates *GAL1* gene transcription by controlling the localization of the SUMO protease Ulp1. *Mol. Cell* 51, 807–818.
- Toyama, B.H., Savas, J.N., Park, S.K., Harris, M.S., Ingolia, N.T., Yates, J.R., and Hetzer, M.W. (2013). Identification of long-lived proteins reveals exceptional stability of essential cellular structures. *Cell* 154, 971–982.
- Vaquerez, J.M., Suyama, R., Kind, J., Miura, K., Luscombe, N.M., and Akhtar, A. (2010). Nuclear pore proteins nup153 and megator define transcriptionally active regions in the *Drosophila* genome. *PLoS Genet.* 6, e1000846.
- Vollmer, B., and Antonin, W. (2014). The diverse roles of the Nup93/Nic96 complex proteins - structural scaffolds of the nuclear pore complex with additional cellular functions. *Biol. Chem.* 395, 515–528.

Van de Vosse, D.W., Wan, Y., Lapetina, D.L., Chen, W.-M., Chiang, J.-H., Aitchison, J.D., and Wozniak, R.W. (2013). A role for the nucleoporin Nup170p in chromatin structure and gene silencing. *Cell* 152, 969–983.

Xu, M., Zhao, G.-N., Lv, X., Liu, G., Wang, L.Y., Hao, D.-L., Wang, J., Liu, D.-P., and Liang, C.-C. (2014). CTCF controls HOXA cluster silencing and mediates PRC2-repressive higher-order chromatin structure in NT2/D1 cells. *Mol. Cell. Biol.* 34, 3867–3879.

## List of abbreviations

ChIP	Chromatin Immunoprecipitation
Nup	Nucleoporin
NPC	Nuclear Pore Complex
CCL	Cancer Cell Line Encyclopedia
HPA	Human Protein Atlas
ENCODE	Encyclopedia Of DNA Elements
TSS	Transcription Start Site
FISH	Fluorescence in-situ hybridization
kDa	Kilo Dalton
Kd	Knockdown
UT	Untreated
3C	Chromosome Conformation Capture
4C	Circular Chromosome Conformation Capture
5C	Chromosome Conformation Capture Carbon Copy
CBS	CTCF binding site
ChIP-chip	Chromatin Immunoprecipitation-chip
ChIP-seq	Chromatin Immunoprecipitation - sequencing
CTCF	CTCCC-binding factor
HDAC	Histone deacetylase
PRC	Polycomb repressive complex
DNA	Deoxyribonucleic acid
EDTA	Ethylenediaminetetraacetic acid
HOX	Homeotic complex
IgG	Immunoglobulin G
NE	Nuclear envelope
STED	Stimulated Emission Depletion
INM	Inner nuclear membrane nuclear
ONM	Outer nuclear membrane
siRNA	small interfering RNA
GFP	Green fluorescent protein





## **Chapter 1: Introduction and Review of Literature**

# **1. Introduction**

## **1.1 Nuclear architecture and nuclear landmarks**

The cell is the structural and functional unit of all living organisms. It is an autonomous unit that multiplies by cell division. Cells have heritable genetic information in the form of DNA. Both prokaryotic and eukaryotic cells duplicate their genome before division. The prokaryotic genome is not enclosed within the membrane-bound compartment, while the eukaryotic genome is enveloped within a membrane-bound compartment - the nucleus. The genome of a cell is enclosed within the nucleus as a highly compact DNA with histones referred to as chromatin. The chromatin undergoes further compaction to form chromosomes. The nucleus is divided into sub-compartments, which further contribute to chromatin organization. Chromosomes occupy a specific sub-volume in the interphase nucleus referred to as chromosome territories (Croft et al., 1999) (Figure 1.1).

In humans there are 22 pairs of autosomes and two sex chromosomes, accommodating over 30,000 genes (Ferrai et al., 2010). Chromosomes inside the nucleus are non-randomly arranged i.e. gene-rich chromosomes are centrally located inside the nucleus and gene-poor chromosomes are peripherally located (Croft et al., 1999; Hübner and Spector, 2010) (Figure 1.1). The nuclear periphery is rich in heterochromatin - a repressive zone for gene expression (Croft et al., 1999). The nucleus also consists of nuclear bodies devoid of the membrane. The nucleus is constituted by a double bilayer membrane and a network of lamins (Figure 1.1). Lamins are intermediate filament proteins at the inner nuclear membrane that impart mechanical stability to the nucleus (Foisner, 2001) (Figure 1.1). Apart from their structural role, they maintain nuclear architecture and

regulate gene expression. Recent reports suggest that gene loci e. g. CFTR, contact nuclear lamins and are repressed, but become active upon detachment from the lamins (Ferrai et al., 2010). Lamins function as nuclear landmarks since they impart structural and functional role inside the nucleus. The nucleolus is another important nuclear landmark inside the nucleus which plays an important role in the organization of the genome (Figure 1.1). The major function of the nucleolus is rRNA synthesis and ribosome assembly (Leary and Huang, 2001). The nucleolus is also involved in tethering chromosome 13,14,15, 21 and 22 through their nucleolar organizer regions (NOR) (van Koningsbruggen et al., 2010) (Figure 1.1). Nuclear bodies like PML bodies, Cajal bodies, nuclear speckles, coiled bodies are also important in the functional organization of the genome (Mao et al., 2011) (Figure 1.1). PML bodies are shown to be involved in gene regulation (Ching et al., 2005). Nuclear speckles contain serine/arginine-rich proteins that are involved in mRNA processing (Spector and Lamond, 2011) (Figure 1.1).

Nuclear pore complex is one of the major nuclear landmark present in the nuclear envelope. The nuclear pore complex is essential for the transport of small molecules across the nuclear membrane. In addition to its role in nuclear transport, NPC is also emerging as a major hub for gene regulation and genome organization. In this study, we have mainly focused on the role of NPC in gene regulation. NPC is a part of the nuclear envelope. Therefore, before we discuss the structure and function of the NPC, it is important to understand the composition and role of the nuclear envelope in the functional organization of the genome

**Figure 1.1**

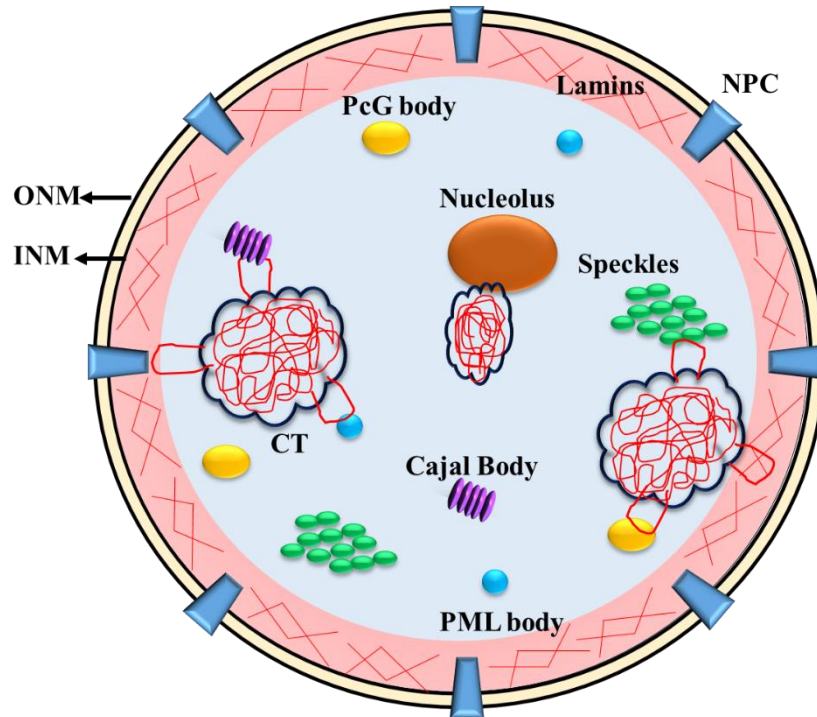


**Figure 1.1. Schematic representation of the Nuclear architecture:** Eukaryotic nucleus is bound by double bilayer membranes; Inner nuclear membrane (INM) and Outer nuclear membrane (ONM). Two nuclear membranes are fused together at the nuclear pore complex (NPC). Nucleus is surrounded by intense network of intermediate filament proteins called (Fedorova and Zink, 2008) as Lamins. Nucleus also consist of many membrane less proteinaceous entities referred as nuclear bodies (Nucleolus, PcG body, Cajal body, Speckles, PML body etc). Chromatin inside the nucleus is non-randomly organized in the form of chromosome territories. Gene rich chromosomes are positioned at the nuclear periphery while gene poor chromosomes are positioned at the center. Chromatin inside the nucleus make functional contacts with various nuclear bodies and nuclear landmarks inside the nucleus.

## 1.2 The nuclear envelope

The nuclear envelope (NE) is an important nuclear landmark which separates nucleoplasm from the cytoplasm. It is composed of a double lipid bilayer membrane which is continuous with the endoplasmic reticulum. NE is important for spatial separation of nuclear functions from the cytoplasmic in the cell. Nuclear membrane consists of two phospholipid bilayers,

outer nuclear membrane (ONM) and inner nuclear membrane (INM) (Figure 1.2). Both ONM and INM have a diverse group of integral membrane proteins which are involved in various nuclear activities such as signal transduction, nuclear transport, mechanotransduction, and chromatin organization (Figure 1.2). Proteins present in INM interact with chromatin and participate in genome organization and gene regulation (Figure 1.2). Most abundant group of proteins that are present in the nuclear envelope are Nuclear pore complex (NPC) proteins (Figure 1.2). More than 2000 NPCs perforate nuclear envelope and regulate the transport of small molecules such as mRNA and proteins in and out of the nucleus. Another group of NE proteins- the Nuclear envelope transmembrane proteins (NETs) specifically localizes to the INM (Batrakou et al., 2009) (Figure 1.2). More than eighty transmembrane proteins have been identified but very few of them have been fully characterized (Batrakou et al., 2009; Worman and Schirmer, 2015). NETs such as Lamin B Receptor (LBR), lamina-associated polypeptide (LAP)1, LAP2, emerin, and MAN1 interact with Lamins and chromatin (Figure 1.2). Improper localization and malfunction of these NETs have been linked to various diseases such as muscular dystrophy (emerin, nesprin) (Meinke et al., 2011; Zhang et al., 2007), osteopoikilosis (MAN1) (Hellemans et al., 2004) or Pelger-Huet anomaly (LBR) (Turner and Schlieker, 2016). Interestingly, INM proteins play an important role in chromatin organization and gene regulation (Andrulis et al., 1998; Reddy et al., 2008; Thanisch et al., 2017). For example, LBR interacts with chromatin-associated protein HP1 $\alpha$  and tethers heterochromatin at the nuclear periphery (Solovei et al., 2013) (Figure 1.2). In addition, the interaction of LBR with XIST is required for silencing and recruitment of X chromosome at the nuclear lamina (Chen et al., 2016). Lamins are NE proteins that

constitute the nuclear lamina, a meshwork of intermediate filament proteins presents just below the nuclear membrane and required for structural integrity of the nucleus. The nuclear lamina is composed of A-type lamins and B-type lamins. Although the lamina is required for nuclear stability, it is becoming increasingly clear that lamins also play major roles in chromatin organization and gene expression (Collas et al., 2014; Shimi et al., 2008) (Figure 1.2). Mutations in lamins have been linked with various human diseases such as Laminopathies and premature aging (Broers et al., 2006). In summary, NE plays a critical role in separating genome form cytoplasm and its highly specialized membrane provides an essential platform for chromatin tethering and gene regulation.

**Figure 1.2**

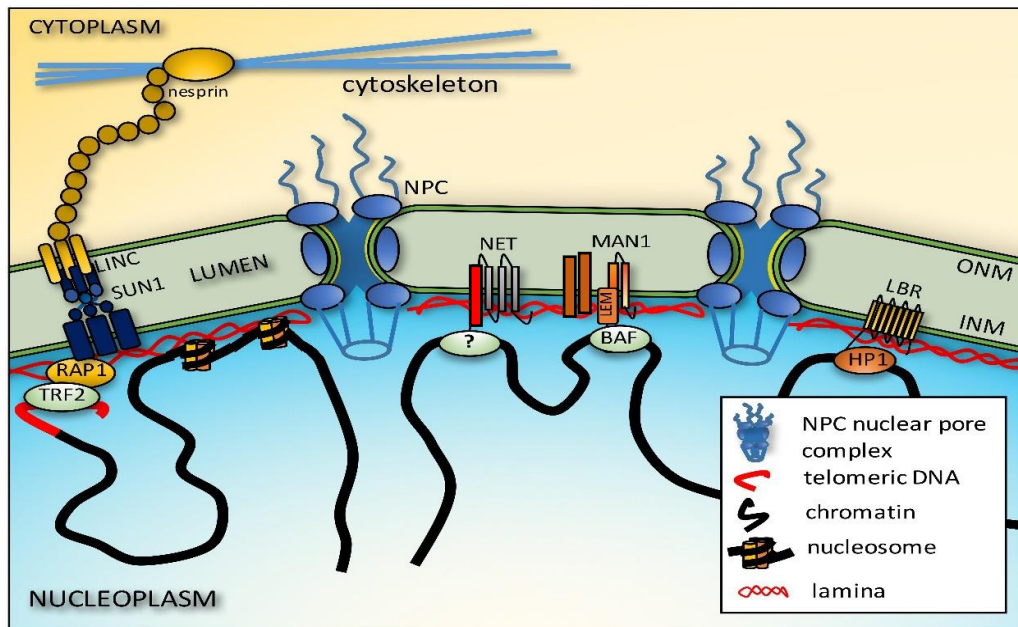


**Figure 2. Topology of the Nuclear Envelope:** Nuclear envelope consists of the inner nuclear membrane (INM) and outer nuclear membrane (ONM) separated by perinuclear space (Lumen). Various nuclear transmembrane proteins (NET) are embedded into the INM. NET interacts with nuclear lamina and chromatin. Interaction of outer nuclear membrane proteins (LINC complex) with inner nuclear membrane proteins (SUN domain proteins) connects nucleus to the cytoskeleton. LINC complex proteins interact with Nesprin in the cytoplasm. Various INM proteins (LBR, MAN1, etc.) contacts chromatin. Members of the LEM (lamina-assoMAN1) interact with chromatin through barrier-to-autointegration factor (BAF). LBR interacts with HP1 alpha to tether heterochromatin at the nuclear periphery. INM and ONM fuse with each other at the NPC. The image is adapted with permission from (Czapiewski et al., 2016)

### 1.3 Functional organization of the genome at the nuclear periphery

The genome is non-randomly organized inside the nucleus. Electron microscopy studies have shown that the electron dense heterochromatin is concentrated near the nuclear periphery and around the nucleoli, whereas euchromatin is present at the center of the nucleus (Albiez et al., 2006; Cherkezyan et al., 2014) (Figure 1.3). Nuclear envelope provides a huge surface for the organization of chromatin at the nuclear periphery. Heterochromatin present at the nuclear periphery is highly compact and is mostly gene poor. Therefore, the nuclear periphery is a repressive zone for gene expression. Lamins, NETs, and some NPC proteins such as Nup98, Nup153, and Nup50 directly associate with chromatin or transcriptional regulators and regulate gene expression. Lamins regulate heterochromatin organization at the nuclear periphery (Solovei et al., 2013). In addition, the interaction between lamins and chromatin is mediated by specific DNA sequence

**Figure 1.3**

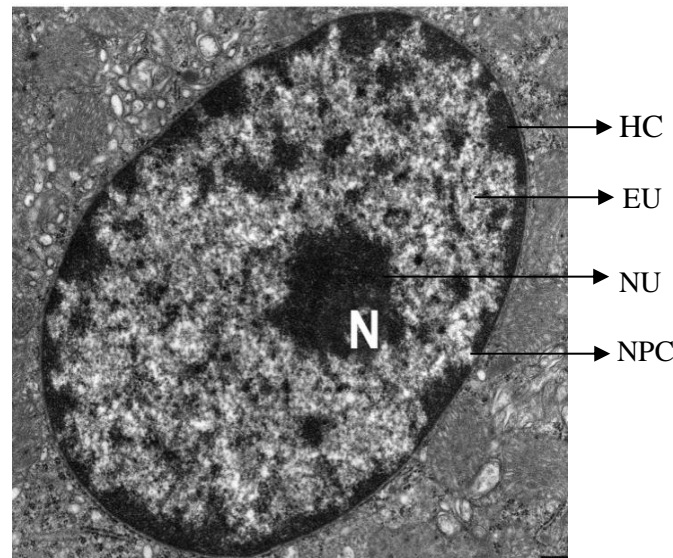


**Figure 1.3. Electron micrograph of the nucleus:** Electron dense heterochromatin (HC) is enriched at the nuclear periphery and at the nucleolus (NU). Euchromatin (EU) is more lightly stained as compared to heterochromatin. Heterochromatin at the nuclear periphery is not continuous but it is interrupted by the presence of Nuclear pore complex. Image is obtained with permission from (Fedorova and Zink, 2008).

enriched for GAGA repeats and is required for silencing of IgH and Cyp3A loci at the nuclear periphery (Zullo et al., 2012). Proteomic studies have revealed that the nuclear envelope proteome possesses a high degree of tissue specificity and this tissue-specific proteome can influence genome organization and its function (Batrakou et al., 2009; Korfali et al., 2012). Nuclear periphery is largely but not entirely heterochromatic. Cell type-specific proteomics of the nuclear periphery gives us an idea about the important role of the nuclear periphery in functional chromatin organization at the nuclear periphery. Heterochromatin is defined by the presence of inactive histone marks such as histone H3 lysine 9 dimethylation and trimethylation (H3K9me2 and H3K9me3). Immunofluorescence studies for inactive histone marks show enrichment of inactive marks at the NE (Fišerová et al., 2017). Similarly, heterochromatin protein 1 alpha (HP1 $\alpha$ ) shows a distinct subpopulation at the NE (Poleshko and Katz, 2014). However, the precise mechanism of gene repression and chromatin organization at the nuclear periphery remains unclear.

During the 18<sup>th</sup> century, Carl Rabl made the first basic description of the nonrandom organization of centromeric foci at the nuclear periphery in the nuclei of salamander larvae referred as “Rabl configuration” (Mekhail and Moazed, 2010). Along with centromeres, telomeric regions are located at the nuclear periphery, required for telomeric gene silencing (Crabbe et al., 2012). In *S. cerevisiae* telomere regions of chromosomes tend to cluster together at the nuclear periphery and becomes silent (Taddei et al., 2006) In addition to centromeres and telomeres, gene-poor chromosomes also tend to localize at the nuclear periphery (Figure 1.4). Over 100 years ago, Theodor Boveri first suggested the nonrandom organization of chromosomes inside the interphase nucleus. Later fluorescence in situ



hybridization (FISH) revealed that in human fibroblasts gene-poor chromosome 18 is positioned at the nuclear periphery while gene-rich chromosome 19 is positioned at the nuclear interior (Croft et al., 1999). Chromosome positioning is largely dependent on gene density. For example, artificially introduced human chromosome 7, 18 and 19 in DLD-1 cells maintain their conserved spatial localization in the nucleus where gene-poor Chromosome 7 and 18 positioned at the nuclear periphery and Chromosome 19 at the nuclear interior (Sengupta et al., 2007). In contrast, chromosome positioning is not entirely dependent on gene density, since chromosomes also show tissue- or cell type-specific positioning inside the nucleus. For example mouse chromosome 5 is peripherally positioned in lung cells and internally positioned in liver cells (Parada et al., 2004). Similarly, human chromosome 6 is peripheral in CD8<sup>+</sup> T-cells but internal in CD4<sup>+</sup> T-cells (Kim et al., 2004). However, the molecular mechanism that determines tissue- or cell type-specific positioning of the chromosome is not yet clear. In this regard, cell type-specific patterning of heterochromatin (as mentioned previously) at the nuclear periphery could be one determining a factor for specific chromosome positioning (Solovei et al., 2013; Zuleger et al., 2013). For example, tissue and cell type-specific expression of certain nuclear envelope proteins such as Lamin B receptor (LBR) and lamin family proteins could contribute to the tethering of specific chromosomes at the nuclear periphery (Dechat et al., 2008; Ranade et al., 2017; Solovei et al., 2013). Whether the tissue-specific expression of nuclear envelope proteins is a prominent determinant of chromosomal positioning is yet to be determined.

**Figure 1.4**

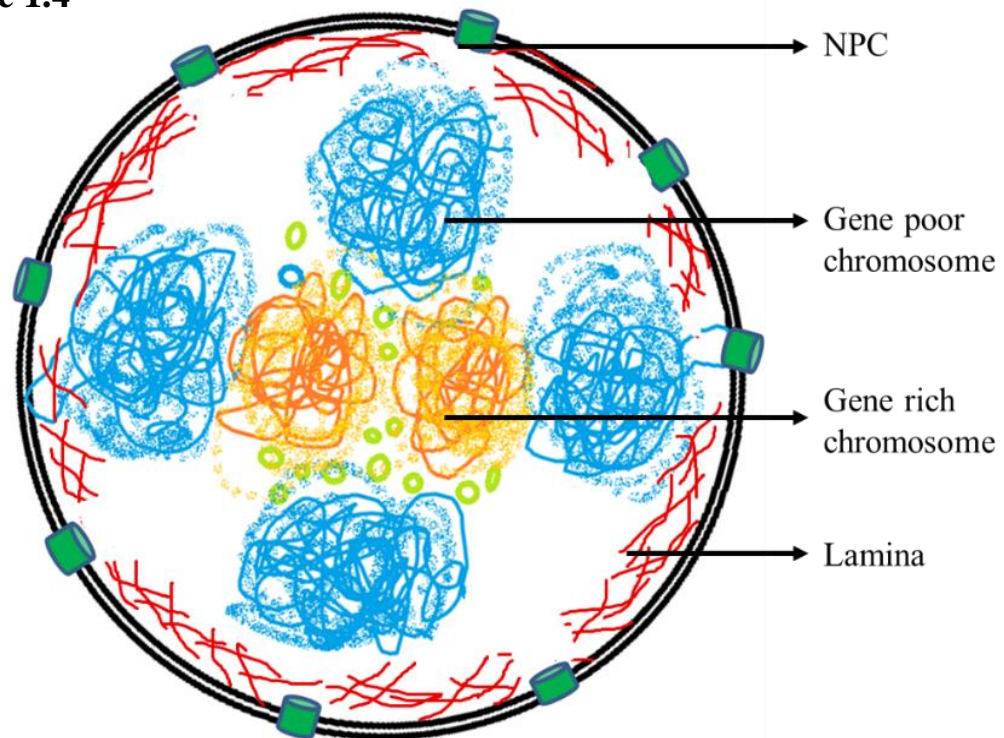


**Figure 1.4 Chromosome positioning inside the nucleus:** Nuclear periphery plays an important role in chromosome positioning inside the nucleus. Gene poor chromosomes are positioned at the nuclear periphery while gene rich chromosomes are positioned at the nuclear interior. Intense network of nuclear lamina at the nuclear periphery is important for positioning of chromosomes at the nuclear periphery.

Gene loci are typically in the range of ~1-10 kb and orders of magnitude lower in DNA content than chromosome territories (~100 Mbp) relatively smaller in size as compared to chromosomes. Gene loci also occupy specific position inside the nucleus which is correlated with its activity (activation or repression). For example, an insulator sequence *gypsy* in *Drosophila* is always positioned at the NE (Gerasimova et al., 2000). When *gypsy* sequence along with a reporter gene was incorporated in the internally located reporter gene, it moved towards the periphery and with reduced expression of a reporter gene (Gerasimova et al., 2000). Similarly, inactive X chromosome or Barr body is located

at the nuclear periphery (Walker et al., 1991). Certain gene locus like CFTR gene when present at the nuclear periphery is repressed but upon detachment from the nuclear periphery get expressed (Zink et al., 2004). Also, Mash1 (Ascl1) locus is untethered from the periphery during neurogenesis (Williams et al., 2006). Mechanism of gene repression at the nuclear periphery is not yet well understood. Genes are typically repressed when associated with nuclear envelope-associated proteins such as LBR, Sun family proteins, INM proteins, Nucleoporins and Lamins (Mattout-Drubezki and Gruenbaum, 2003; Nikolakaki et al., 1996; Reddy et al., 2008; Steglich et al., 2013). For example, *ZNF570* gene is associated with nuclear Lamins at the nuclear periphery but moves away from the nuclear periphery upon Lamin B2 depletion consistent with its overexpression (Ranade et al., 2017). Mapping of lamina-associated sequences to the mammalian genome by DamID seq technique has helped to find Lamina associated domains (LADs) in a genome-wide manner (Guelen et al., 2008). LADs are present on all chromosomes and their size varies ~0.1 to 1 Mb. LADs associate with repressive histone marks (H3K27me3 and H3K9me2), again suggesting a repressive role of the nuclear periphery in gene regulation (Guelen et al., 2008).

In summary, the nuclear periphery is a repressive compartment in the nucleus. In contrast, there are many contradictory findings in this field which showed that nuclear periphery is not always a silencing zone, but many gene loci are expressed at the nuclear periphery. In yeast, genes situated at the nuclear periphery when contacts nuclear pore complex protein like Nup2 become active and get expressed (Schmid et al., 2006). Using the LacO/GFP lacI method it is possible to visualize the relocation of certain gene loci like INO1 in heterochromatic exclusion zone upon activation (Brickner and Walter, 2004).

According to gene gating hypothesis, genes are relocated to the nuclear pore complex upon activation to facilitate the mRNA export (Blobel, 1985). For example, the GAL1 gene locus is relocated to the nuclear pore complex in a transcription-dependent manner (Cabal et al., 2006). Above examples of gene activation at nuclear periphery are contradictory to the earlier consideration that nuclear periphery is a repressive zone.

In the context of this study, I will mainly focus on NPC proteins and their additional roles in genome organization and gene regulation. Before we start discussing the additional roles of NPC, it is important to understand structural details of the nuclear pore complex.

#### **1.4 The nuclear pore complex**

The nuclear pore complex is an important landmark of the nucleus that helps in transport of macromolecules between nucleoplasm and cytoplasm. There are more than two thousand nuclear pores present on each mammalian nucleus. Each NPC is a large multiprotein channel composed of multiple copies of 30 different proteins called nucleoporins (NUPs) arranged in octagonal symmetry along the central axis (Figure 1.5). The majority of NUPs are evolutionarily conserved and have the well-characterized function of mediating macromolecular transport (Wälde and Kehlenbach, 2010). Selective transport of macromolecules across the nuclear membrane is required for the accurate progression of most major nuclear and cellular processes. However, our understanding of the nucleoporins function is rapidly evolving as accumulating evidence suggest that they can directly associate with DNA and regulate genome functions (Raices and D'Angelo, 2018). Among these, one of the most remarkable and well-supported roles of the NUPs is to regulate the transcription of their associated genes. It is still uncertain how NPC components could modulate gene expression. This study is focussed on the gene regulatory

function of the NPC, in relation to one of the subcomplexes in the pore, The Nup93 subcomplex. It is important to first understand the basic structure and composition of the NPC before discussing further details about transport independent functions of the NPC.

NPC is a large macromolecular assembly embedded into the nuclear envelope to form a hollow channel. These are one of the largest protein complexes in the eukaryotic cell, with a molecular mass of approximately ~ 60 MDa in yeast and ~ 120 MDa in humans (Alber et al., 2007). They are composed of multiple (8–64) copies of 30 different nuclear pore proteins called nucleoporins (NUPs) (Figure 1.5). Most of the nucleoporins are conserved across eukaryotes. The entire NPC structure integrates approximately 500–1000 Nups (D'Angelo and Hetzer, 2008). Early EM studies have shown that NPC has an eightfold rotational symmetry for the entire structure. Various electron microscopy techniques including cryo-electron microscopy have resolved the high-resolution structure and density map of the NPC with human cell lines (U2OS) and *Xenopus* oocyte specimen (Eibauer et al., 2015; Knockenhauer and Schwartz, 2016; von Appen et al., 2015). The principal structural components of the NPC include three-ring moieties: the cytoplasmic ring, inner pore ring, and nucleoplasmic ring. Three rings are sandwiched between the nuclear basket and cytoplasmic filaments (Figure 1.5). The inner pore ring resides at the fusion point of inner and outer nuclear membranes. The nuclear and cytoplasmic rings are anchored to the inner pore ring. The nuclear basket and the cytoplasmic filaments are peripheral parts of the NPC emerging from the nuclear and cytoplasmic sides. The external diameter of the NPC is ~100-125 nm, at the cytoplasmic. The nuclear side is ~60-65 nm and the central channel is ~25-45nm (Jamali et al., 2011) (Figure 1.5).

It is now evident that out of 30 different nucleoporins, 20 are highly conserved among all eukaryotes and remaining 10 show species-specific differences (DeGrasse et al., 2009; Neumann et al., 2010). NUPs are organized into small subcomplexes which are composed of several directly interacting NUPs and they act as building blocks of the NPC

**Figure 1.5**

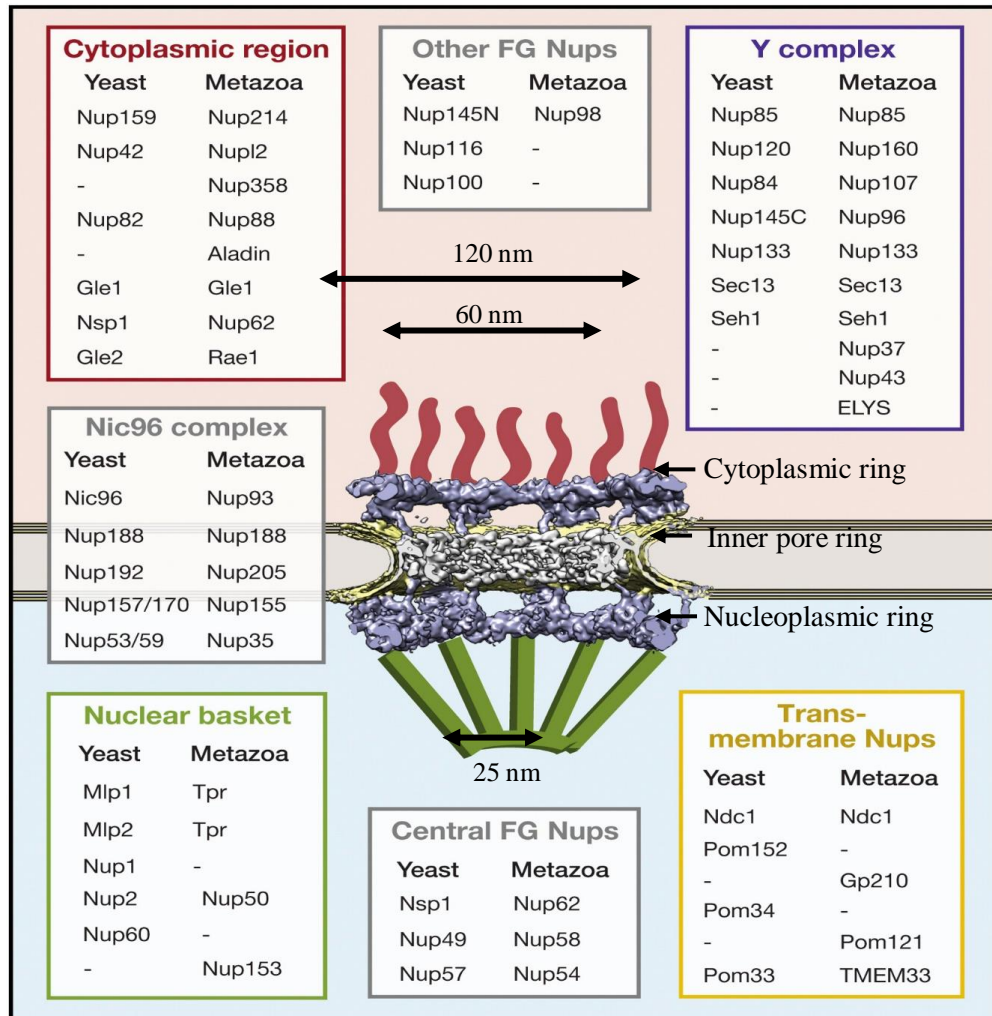


**Figure 1.5. Human nuclear pore complex:** Cryo-ET reconstruction of the human NPC from HeLa cells (EMDB code 3103. Von Appen et al, 2015). Cut view of the NPC showing cytoplasmic ring, inner pore ring and nucleoplasmic ring. Approximate positions of the different nucleoporins are mapped inside the NPC. Nucleoporins are grouped according to their position inside the NPC. Image is modified with permission from Knochenhauer and Schwartz, 2016.

(Alber et al., 2007) (Figure 6). Co-immunoprecipitation studies have shown the interaction between Nups within these smaller subcomplexes (Alber et al., 2007; Theerthagiri et al., 2010). In vertebrates, there are three major subcomplexes: The well-known highly conserved Y-complex (NUP107-Nup160 complex in humans), Nup93 complex and the NUP62 complex (Grandi et al., 1997; Siniossoglou et al., 1996; Ulrich et al., 2014; Walther et al., 2003) (Figure 1.5 and 1.6). These complexes are assembled together along with the existing pool of free nucleoporins to form NPC (Figure 1.5).

In vertebrates, Nup107-Nup160 complex is the largest sub-complex composed of six nucleoporins: Nup107, Nup85, Nup160, Nup133, Nup96 and Sec13 (Kelley et al., 2015). The yeast homolog of Nup107-160 complex is Nup84 complex. The electron microscopy structure showed the Y-shaped structure of the Nup107-160 complex (Kelley et al., 2015; Walther et al., 2003). Y sub-complex is the principal component of the nuclear and cytoplasmic rings. Nup107-160 complex is one of the early sub-complexes which binds to chromatin through interaction with Mel28-ELYS (a nucleoporin that binds to chromatin via AT hook) (Rasala et al., 2008).

The second major sub-complex within the NPC is the Nup93 sub-complex, which is the major focus of this study. Nup93 sub-complex is positioned at the center of the NPC, forming a central ring (Alber et al., 2007; Sachdev et al., 2012). In vertebrates, it is composed of five nucleoporins: Nup205, Nup188, Nup155, Nup93 and Nup35 (Figure 1.6) (Grandi et al., 1997; Sachdev et al., 2012; Theerthagiri et al., 2010; Vollmer and Antonin, 2014). Nup93 is involved in tethering NPC to the nuclear membrane via Nup53-Ndc1 (transmembrane nucleoporin) interaction (Mansfeld et al., 2006; Onischenko et al., 2009). Nup53 interacts with Nup93, Nup155, and Nup205 within the complex members

(Hawryluk-Gara, 2005). Similarly, Nup93 directly interacts with Nup188 and Nup205 but Nup188 does not interact with Nup205 (Theerthagiri et al., 2010). In vertebrates, Nup93 exists as two separate complexes, Nup93-Nup188 complex and Nup93-Nup205 complex (Miller et al., 2000; Theerthagiri et al., 2010). Immuno-depletion studies in *Xenopus* egg extracts have shown that Nup93 is required for NPC assembly (Grandi et al., 1997). In *C. elegans*, depletion of Nup93 causes embryonic lethality with a change in nuclear size and chromatin condensation at the nuclear periphery (Galy et al., 2003).

The Nup62 complex is composed of nucleoporins Nup54, as well as Nup58 and its splice variant Nup45 (Sharma et al., 2015). This sub-complex comprises FG repeat-containing nucleoporins that line the central channel of the pore and participate in nuclear transport. Certain nucleoporins are present as individual proteins, either towards the cytosolic or peripheral side of the NPC. These nucleoporins include Nup153, Nup50, TPR, Nup98, Nup88, Nup214, Nup358, Aladin and Rae1 (Sampathkumar et al., 2013; von Appen et al., 2015). Nup98 is GLFG repeat containing nucleoporin which is not a part of nucleoporin sub-complex and is present on both nucleoplasmic and cytoplasmic sides of the NPC. Nup98 is involved in nuclear export of mRNA (Wu et al., 2001). Three transmembrane nucleoporins Ndc1, Pom121, and Nup210 are involved in anchoring NPC to the nuclear envelope (Funakoshi et al., 2011; Onischenko et al., 2009; Stavru et al., 2006b). Ndc1 directly interacts with Nup53 and Pom121 interacts with Nup155 (Eisenhardt et al., 2014; Mitchell et al., 2010). This interaction is required for tethering of NPC to the nuclear membrane.

NPCs are generally static structures at the nuclear periphery, in contrast to the highly mobile importins and exportins (Nuclear transport receptors). Single NPCs do not



show any planar movement in the nuclear membrane, they move in dynamic in arrays during nuclear shape change events (Daigle et al., 2001). In contrast to the whole NPC, individual nucleoporins can be very dynamic, for example, Nup98 and Nup50 are highly dynamic nucleoporin. The residence time of different nucleoporins at the NPC have been determined by FRAP studies. The residence time of nucleoporins at NPCs range from seconds to days, both in dividing and non-dividing cells (D'Angelo et al., 2009; Rabut et al., 2004; Toyama et al., 2013). NUPs are classified into two broad categories-Scaffold NUPs, which are highly stable and provide structural integrity to the NPC. Peripheral NUPs extends into the cytoplasm or into the central channel and show high mobility rates (Sakiyama et al., 2017; Sampathkumar et al., 2013). Scaffold NUPs such as Nup107-160 complex and the Nup93 complex is stably associated with the NPC with low diffusion rates (D'Angelo and Hetzer, 2008; Kim et al., 2014; Rabut et al., 2004) . Nup93 is one the most stable components of the nuclear pore complex with a relatively high residence time of ~72h, and with a relatively low diffusion rate [ $K_{off} = 40 \pm 3.4 \times 10^{-6} (s^{-1})^a$ ] (Rabut et al., 2004). In contrast, peripheral NUPs such as Nup153, Nup50, and Nup98 are highly dynamic in nature with relatively low residence time at the NPC ranging from seconds to minutes (Rabut et al., 2004). Peripheral NUPs contains phenylalanine-glycine repeats (FG repeats) which are involved in nuclear-cytoplasmic transport (Liang and Hetzer, 2011; Liang et al., 2013). Nup50 is a dynamic nucleoporin with a residence time of 26s and diffusion rate [ $K_{off} = 5.0 \pm 1.1 \times 10^{-2}(s^{-1})^a$ ] (Rabut et al., 2004). Studies in yeast and *Drosophila* reveal that mobile NUPs leave the nuclear pore complex and contact chromatin (Schmid et al., 2006), underscoring their role in gene regulation by off-pore interactions.

**Figure 1.6**

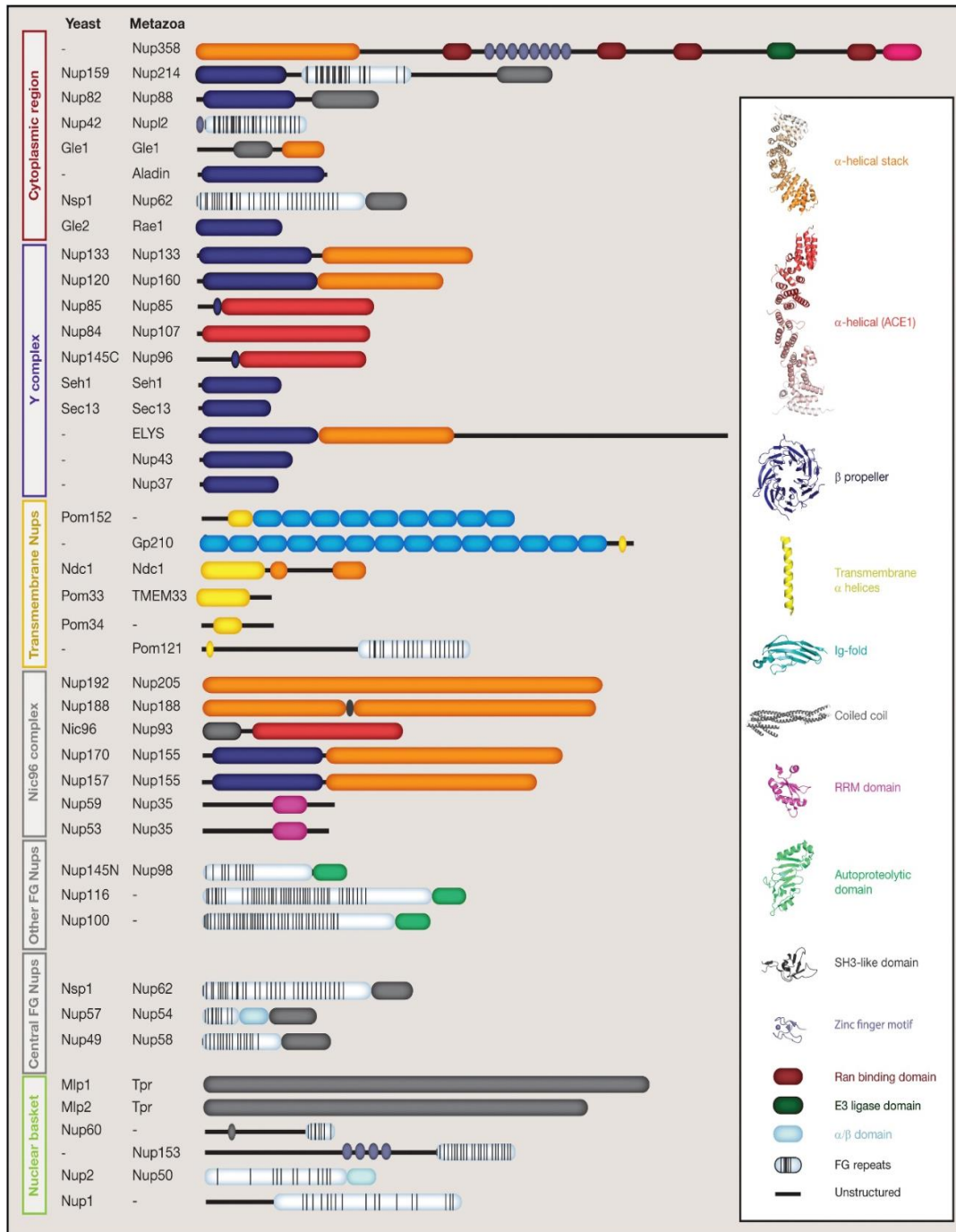


**Figure 1.6. Domain organization of different nucleoporins:** Domain organization of different nucleoporins is predicted based on X-ray crystallographic data and structure prediction software. Nucleoporins are grouped into different subcomplexes. Color code indicates different structural elements as mentioned in the right-side box. Image is adopted from Knockenhauer and Schwartz, 2016.

## 1.5 Nuclear pore complex assembly

In the context of nucleoporin-chromatin interactions, it is also important to understand the mechanism of NPC assembly during early stages of NE formation. Nucleoporins are one of the early proteins that associate with chromatin during NE reformation. In metazoan cells undergoing open mitosis, NE breaks down and NPC disassembles at the onset of mitosis. NE breakdown is essential for spindle fibers to access chromosomes. Upon exit from mitosis at the end of telophase, the entire NE reforms and NPCs reassemble around the segregated chromatin. NPC assembly after mitosis is postmitotic NPC assembly. While NPC also assembles during interphase as the number of NPC must double at the end of the G2 phase in interphase NPC assembly. There are two different mechanisms of post-mitotic and interphase NPC assembly.

At the onset of mitosis, mitotic kinases (Cyclin-Dependent Kinase1) phosphorylate different nuclear envelope proteins (Nups, Lamins and Inner nuclear membrane protein) in order to release chromatin from the nuclear envelope (Schooley et al., 2012). Regulated phosphorylation of different NUPs is required for disassembly of NPC. Nup98 is the first NUP that dissociates from NPC upon phosphorylation followed by Nup53, Nup107-160 complex, Nup62 complex, Ndc1 and Pom121 (Antonin et al., 2008; Dultz et al., 2008). However, how phosphorylation of NUPs modulates their function is not yet understood. After disassembly, nucleoporins are dispersed into the cytoplasm either as individual proteins or as sub-complexes. When NE is reformed, NPC assembly must be coordinated with NE reformation. NPC assembly has been extensively studied by cell-free nuclear reassembly assays using *Xenopus* egg extracts. There are two models for postmitotic NPC assembly. One is the pre-pore model where chromatin is first bound by nucleoporins, which

forms a seeding point for nuclear membrane formation. In another model, chromatin is first surrounded by a membrane and then NPCs are inserted into the membrane.

At the very early stage, the nucleoporin ELYS associates with chromatin via its DNA binding AT-hook and forms a seeding point for NPC assembly (Rasala et al., 2008). Then Nup107-160 complex associates with ELYS followed by Nup153 and Nup50 (Dultz et al., 2008; Walther et al., 2003). The initial stage of NPC assembly involves the inner ring components such as Ndc1, Nup155, and Nup53 that are recruited to the NE (Dultz et al., 2008; Eisenhardt et al., 2014; Otsuka et al., 2014). This initial recruitment of inner ring components is required for the formation of pre-pore complexes. ER membrane spreads laterally around pre-pore complexes. Transmembrane NUPs - Ndc1 and Pom121 then associate with pre-pores by interacting with Nup107-Nup160 complex and tethers the membrane to pre-pores (Antonin et al., 2008; Mansfeld et al., 2006). Depletion of both Pom121 and Nup107-160 complex blocks NE reformation and NPC assembly (Pascual-Garcia et al., 2017; Rasala et al., 2008). The pre-pore assembly recruits Nup93 sub-complex through the interaction between Nup155, Nup53, Pom121 and Ndc1 (Mitchell et al., 2010; Theerthagiri et al., 2010). In later stages, NPC assembly is completed by recruitment of Nup62 complex and other peripheral nucleoporins such as Nup98, Nup153, Nup50, Nup214, TPR and Gp210 (Dultz et al., 2008; Hase and Cordes, 2003)

Interphase NPC assembly is not well understood. Various studies using human cells and *Xenopus* egg extracts have identified molecular players including reticulon and DP1/Yop1p family proteins, membrane deforming and curvature sensing nucleoporins such as Nup53 and Nup133, INM protein Sun1 which recruits Pom121 to INM (Talamas and Hetzer, 2011). Interphase NPC assembly is a slow process and has a different order of

recruitment for nucleoporins than post-mitotic assembly. The interaction between Pom121 and Nup133 is essential for interphase NPC assembly (Funakoshi et al., 2011). Interestingly interaction between ELYS and Nup107-160 complex is not involved in this process (Doucet and Hetzer, 2010). Recent EM tomography studies have revealed different intermediates involved in interphase NPC assembly (Otsuka et al., 2016). This study showed the asymmetric mode of NPC assembly, starting with an asymmetric de novo fusion event between INM and ONM. During interphase assembly, INM membrane evaginate from inside to outside, until it fuses with the ONM (Otsuka et al., 2016)

### **1.6 Transport independent functions of the NPC**

Chromosome conformation capture (3C) studies have shown that transcriptional regulation of genes involves physical contact between chromatin and transcriptional regulators. However, this contact is spatially confined to a shorter distance. This spatial restriction makes it difficult for chromatin to loop out of its territory and make a long-range contact with the transcriptional regulator. Nuclear pore complex is situated at the nuclear periphery and a small fraction of chromatin is in direct contact with NPC. Electron micrographs and high-resolution imaging studies of the nucleus reveal that electron dense heterochromatin at the nuclear periphery is not continuous, but is absent just below the NPC (Fišerová et al., 2017). The zone below the NPC is referred to as the heterochromatic exclusion zone. Nevertheless, nuclear pore components contact with chromatin. NPC and chromatin contact are of two types based on their location (i) On-pore contacts (ii) Off-pore contacts.

### **1.6.1 Off pore interactions**

Nucleoporin chromatin contacts away from the NPC are Off-pore contacts. In yeast Nup98 and Nup153 are involved in Off-pore contact with chromatin inside the nucleoplasm (Griffis et al., 2004). Gene regulation by nucleoporin inside the nucleus was observed in *Drosophila*, where Nup98 was found to be associated with chromatin inside the nucleus (Capelson et al., 2010a; Kalverda et al., 2010). In *Drosophila*, nucleoporins such as Nup98, Sec13 and Nup50 re-localize to the nucleoplasm and contact chromatin (Capelson et al., 2010). In mammals, Nup98 shows transcription-dependent mobility inside the nucleus (Griffis et al., 2002). Nup98 is important for the transcriptional memory of several genes such as *HLA-DRA* (Light et al., 2013). Nup153 is another dynamic nucleoporin which shows transcription-dependent mobility (Griffis et al., 2004) (Griffis et al., 2004). Nup153 and Mtor are two nucleoporins which determine transcriptionally active domains of the *Drosophila* genome inside the nucleus by interacting with chromatin (Vaquerizas et al., 2010). In mouse ESCs, Nup153 associates with the transcription start site of developmental genes (Jacinto et al., 2015). The nup170p yeast homolog of mammalian Nup170 contacts chromatin in association with chromatin remodeling complex and Sir4p and helps in sub-telomeric gene silencing (Van de Vosse et al., 2013). Another finding that supports the intranuclear role of nucleoporins in gene regulation showed that the soluble form of Pom121 (Transmembrane nucleoporin) interacts with Nup98 at many gene promoters inside the nucleus (Franks et al., 2016)

### **1.6.2 On pore interactions**

Experimental findings have also suggested that Nup's are involved in On-Pore interactions. In budding yeast, telomeric silencing is achieved by recruitment of telomeres to the nuclear

**Table 1: Role of nucleoporins in functional genome organization**

No	Nucleoporin	Location	Chromatin associated role	Reference
1	Nup98	Nuclear basket	<ul style="list-style-type: none"> <li>• Association with Human genes GRIK1, NRG1, MAP2, GPM6B, SOX5, ERBB4, ARHGAP26, ZBTB16</li> <li>• Association with <i>Drosophila</i> developmental genes</li> </ul>	(Liang et al., 2013)
2	Nup93	Core	<ul style="list-style-type: none"> <li>• HoxA1, HoxA3, HoxA5, CFTR, PHF14, DGKB, GRM8</li> <li>• Associate with super-enhancers and developmental genes</li> </ul>	(Brown et al., 2008b)
3	Mlp1	Nuclear basket	<ul style="list-style-type: none"> <li>• No specific gene loci, Associate with peripheral heterochromatin</li> </ul>	(Tan-Wong et al., 2009)
4	Nup153	Nuclear basket	<ul style="list-style-type: none"> <li>• Double stranded break foci</li> </ul>	(Lemaître et al., 2012))
5	Nup88	Cytoplasmic filament	<ul style="list-style-type: none"> <li>• Inactive gene loci in <i>Drosophila</i></li> </ul>	(Capelson et al., 2010)
6	Sec13	Core	<ul style="list-style-type: none"> <li>• Associate with RNA Pol-II foci in <i>Drosophila</i></li> </ul>	(Capelson et al., 2010)
7	Nup210	Transmembrane Nup	<ul style="list-style-type: none"> <li>• Skeletal muscle-specific genes</li> </ul>	Gomez-Cavazos and Hetzer, 2015
8	Nup50	Nuclear basket	<ul style="list-style-type: none"> <li>• Differentiation-related genes</li> </ul>	(Buchwalter et al., 2014)
9	Nup153	Nuclear basket	<ul style="list-style-type: none"> <li>• Associates with active chromosomal domains in <i>Drosophila</i></li> <li>• Require for repression of developmental genes in Mouse</li> <li>• Regulation of cardiac gene expression</li> </ul>	(Jacinto et al., 2015) (Vaquerizas et al., 2010)
	Megator	Nuclear basket	<ul style="list-style-type: none"> <li>• Associates with active chromosomal domains in <i>Drosophila</i></li> </ul>	(Jacinto et al., 2015)
	Nup170		<ul style="list-style-type: none"> <li>• Sub-telomeric gene silencing</li> </ul>	(Van de Vosse et al., 2013)
	Pom121	Transmembrane	<ul style="list-style-type: none"> <li>• Associate with promoters along Nup98</li> </ul>	(Franks et al., 2016)

periphery by interaction with nucleoporin Mlp (Tpr) (Crabbe et al., 2012; Galy et al., 2000; Scherthan et al., 2000). Yeast genes such as *GAL1*, *HXK1*, *INO1* relocate to NPCs upon activation. It is well established that NPC-gene association is required for transcriptional memory of those genes (Schneider et al., 2015; Sood and Brickner, 2014). In mammal's association of genes with NPC for their activation or repression is an emerging field of gene regulation. Consistent with the gene regulation at the NPC, a study in 2008 in HeLa cells showed for the first time that Nup93 (Highly stable nucleoporin) associates with human chromosome 5,7 and 16. This study revealed that Nup93 largely associates with inactive chromatin (Brown et al., 2008). Another study supporting the On-pore interaction of chromatin with NPC suggests that in embryonic stem cells and Neural progenitor cells chromatin contacts nuclear pore complex by looping out from its territory (Liang et al., 2013). Similarly, *GAL1* gene loci contacts NPC bound protein Mlp1 and Mlp2 on NPC (Texari et al., 2013). During development of neurons, many gene loci show dynamic association with NPC depending upon the developmental stage of the cell (Liang et al., 2013). In embryonic stem cell stage, Nup98 binding target *GRIK1* is located away from the nuclear membrane but is re-localized to the nuclear membrane in neural progenitor cells and to the nuclear center in neurons (Liang et al., 2013). Nup98 is a phenylalanine-glycine (FG) repeat-containing mobile nucleoporin that has dual localization both at the NPC and in the nuclear interior. Mobile fraction of the Nup98 shows intranuclear accumulation in GLFG bodies (Griffis et al., 2002).

Nup98 is important for gene regulation both at the NPC and inside the nucleus (Franks and Hetzer, 2013). During different stages of neuronal differentiation Nup98 associates with repressed genes at the NPCs and with active genes inside the nucleus (Liang



et al., 2013). While in cardiomyocytes, sarcomere genes and calcium handling genes are relocated to the NPC for their activation (Kehat et al., 2011). Similarly, tissue-specific nucleoporin - Nup210, is required for regulation of skeletal muscle-specific genes at the NPC (Gomez-Cavazos and Hetzer, 2015). Nup93 associates with super-enhancers in the genome at the nuclear periphery suggesting on pore interaction of chromatin with the NPC. Although many studies suggest that On-pore interaction is for repression of genes, various contradictory reports showed that On-pore interactions are also important in the activation of gene loci (Brown et al., 2008; Liang et al., 2013; Light et al., 2013). Together these findings have created a new area of interest in the field of nuclear pore complex and gene regulation.

Gene gating hypothesis suggests that gene loci meet nuclear pore complex simply to facilitate the mRNA export out of the nucleus. But this is not the only explanation for this idea, nuclear pore complex proteins play an important role in the initiation of transcription and gene regulation. More complicated role of nuclear pore complex component was suggested in one of the early studies, which shows that Nup2 act as a boundary element separating active and inactive chromatin from each other (Schmid et al., 2006). Another study showed the active role of NPC in transcription by means of Sac3-Thp1 mRNA export complex making direct contact with Nup1 (Fischer et al., 2002). Artificial targeting of certain nucleoporins to the promoter of reporter gene activates gene expression (Taddei, 2007). Various studies have shown the profound role of nucleoporins in development and differentiation (Buchwalter et al., 2014; Gomez-Cavazos and Hetzer, 2015; Jacinto et al., 2015; Liang et al., 2013; Pascual-Garcia et al., 2014). For example, Nup93 have been shown to associate with super-enhancers of developmental genes (Ibarra

et al., 2016). Depletion of Nup50 in mouse myoblast cells C2C12 inhibits their differentiation into myotubes suggesting an important role of Nup50 in differentiation (Buchwalter et al., 2014). Overexpression of Nup98 in neural progenitor stem cell increases the expression level of Nup98 associated gene loci (Liang et al., 2013). Some nucleoporins such as Nup153 are also involved in accurate regulation of DNA damage response process (Lemaître et al., 2012; Palancade et al., 2007). In addition, Nup84 have been shown to play an important role in the DNA damage response pathway (Nagai et al., 2008). Mlp1 is implicated in maintaining the transcriptional memory (Tan-Wong et al., 2009). In mammals, Nup98 plays an important role in epigenetic memory (Light et al., 2013). GAL 1 gene expression is controlled by its association with Mlp1 and Mlp2 through Ulp1 (SUMO protease) at the Nuclear pore complex (Texari et al., 2013). Mlp1 also helps in transcriptional memory by facilitating faster association of RNA pol-II to the promoter of HXK1 gene and Mlp1 mutant loses the transcriptional memory (Tan-Wong et al., 2009). Hsp 16 gene in *C. elegans* is relocated to the NPC upon heat-shock induction, with the promoter sequence being sufficient for the peripheral localization of this gene (Rohner et al., 2013). NPP13 is a *C. elegans* ortholog of vertebrate Nup93 binds to the Pol-III transcribed genes and is required for the processing of snoRNA and tRNA transcripts (Ikegami and Lieb, 2013). In yeast, one of the core component of NPC, Nup170p is required for tethering telomere to the nuclear envelope (Van de Vosse et al., 2013). Chromatin immunoprecipitation in *Drosophila* has shown that Nup153 and Megator bind to more than 25% of the genome in continuous domains of about ~10 to 500 kb. These domains show active marks of transcription like RNA Pol –II enrichment (Vaquerizas et al., 2010b).

Stability of genome is primarily depending upon the proper functioning of DNA-damage and repair (DDR) pathway. Any change or alteration in this process leads to DNA mutation and instability. Genomic instability is one of the important hallmarks of the cancer cell. Few experimental evidence has shown the role of NPCs in DNA damage and repair pathway [Reviewed in (Bukata et al., 2013)]. Mutation in Nup84 and Nup60 complex leads to the alteration in the DDR pathway (Palancade et al., 2007). Similarly, a recent study in yeast has shown that whole replication fork containing double-stranded break is relocated to NPC during the repair via SUMO-Ulp1 pathway (Nagai et al., 2008). In conclusion, the role of NPC in the DDR pathway is SUMO-Ulp1 dependent and disturbance in any of these pathway leads to an increase in DNA damage and ultimately genome instability. However, the role of NPC in DDR in mammals remains unclear. Deletion or down-regulation of Nup153 in mammalian U2OS cells increases DNA damage and activation of DNA damage checkpoints (Lemaître et al., 2012). The mechanisms of NPCs in DDR are unclear, as it may be attributed to the direct interaction of chromatin with NPC or defects in transport of certain DNA damage repair proteins. All the above findings summarize the importance of nucleoporin-chromatin contacts in various aspects of functional genome organization.

### **1.7 Mechanism of chromatin contact with NPC**

The mechanisms by which chromatin contacts nuclear pore complex is not yet known. Chromatin looping is an emerging phenomenon potentially involved in this process. Long-range chromosomal contacts can be facilitated by the formation of chromatin loops and are important for expression of co-regulated genes. TALEN based cleavage of such intra- and

inter-chromosomal chromatin loops leads to the inactivation of co-regulated genes (Fanucchi et al., 2013). Therefore, chromatin looping could also be involved in nucleoporin mediated gene regulation.

In yeast, transcription factors (for example Put3, Ste12, Gcn4 and TREX-2) are known to regulate the association of genes with NPCs (Dieppo and Stutz, 2010; Randise-Hinchliff et al.; Schneider et al., 2015). In *Drosophila*, a nuclear hormone receptor, ecdysone is recruited to the nuclear periphery for regulation of NPC associated genes (Pascual-Garcia et al., 2017). Nup210 regulates structural genes of the muscle at the nuclear periphery by recruitment of the transcription factor Mef2C (Raices et al., 2017). Surprisingly, Nup210 is not required for gene localization to the nuclear periphery (Raices et al., 2017). In addition to transcription factors, histone deacetylase, HDAC4 interacts with Nup155 and prevents the association of sarcomeric genes at the nuclear periphery (Kehat et al., 2011).

The Nup98 fusion protein interacts with several transcriptional and chromatin modulators such as CREB binding protein (CBP) and mixed lineage leukemia (MLL) (Pascual-Garcia and Capelson, 2014; Pritchard et al., 1999). The Nup98-HoxA9 fusion protein interacts with Crm1 and regulates HOXA gene expression (Oka et al., 2016). Nup98 also interacts with DNA helicase DHX9 (Capitanio et al., 2017). The interaction between Nup98 and DHX9 is required for its recruitment to specific gene loci for its regulation (Capitanio et al., 2017). The mobile nucleoporin Nup153 interacts with polycomb repressive complex 1 (PRC1) and represses developmental genes (Jacinto et al., 2015). Yeast nucleoporin Mlp1 interacts with the chromatin-bound coactivator complex

SAGA (Spt-Ada-Gcn5-Acetyltransferase) and regulate gene activation (Schmid et al., 2006).

In summary, these findings implicate transcription factors and chromatin modulators in mediating Nucleoporin-chromatin interactions. However, the spatial restriction of chromatin movement inside the nucleus makes it difficult for chromatin to access the core component of the nuclear pore complex. Some reports suggest that mRNA export complex itself brings chromatin in the proximity of NPC (Fischer et al., 2002). The recent finding showed that chromatin is a flexible and dynamic fiber between 5- 24 nm, supporting the idea of dynamic chromatin looping in long-range chromatin-nuclear landmark interaction (Ou et al., 2017). Understanding the mechanism behind chromatin contact with NPC is important because that will help us to uncover the role of nucleoporins in gene regulation. But the mechanism behind nucleoporin-chromatin contact might not be universal, instead, it could cell type specific.

## **Chapter 2: Materials and Methods**

## **2.1 Commonly used methods throughout the study**

### **2.1.1 Cell culture**

Colorectal adenocarcinoma cell line - DLD1 was a gift from the lab of Dr. Thomas Ried, NCI/NIH, Bethesda, USA and cultured in RPMI media (Invitrogen, 11875), supplemented with 10% fetal bovine serum (FBS, Invitrogen, 6140-079, Carlsbad, USA), 100 U/ml penicillin/100 µg/ml of streptomycin (Gibco, 15070-063) at 37°C with 5% CO<sub>2</sub>. Cells were sub-cultured when ~60-70% confluent and utilized in ~10-15 passages for all experiments.

We ensured that cultures were free of Mycoplasma contamination by DAPI staining cells periodically. The authenticity of DLD1 cells was validated periodically by DAPI karyotyping.

DLD-1 cells: Modal chromosomal number = 44-46

### **2.1.2 Metaphase spread preparation**

To induce metaphase block DLD-1 cells were treated with 0.1 µg/ml Colcemid (Roche 10 295 892 001) for 90 min. Cells were then harvested by trypsinization and treated with hypotonic solution (using 0.075 M KCl) for 30 min. Hypotonic treatment was stopped by fixing the cells with 4–5 drops of fixative (Methanol: Acetic Acid, 3:1) followed by a spin at 1000 rpm for 10min at 4°C. The cell pellet was washed 3 times with a fixative solution. After 3 washes cells were suspended in fixative solution at an appropriate dilution and dropped onto clean glass slides. Metaphases were stained with DAPI (0.05µg/ml in 1X PBS, pH-7.0)

### **2.1.3 Transient siRNA mediated knockdown**

Transient knockdowns were performed using siRNA oligonucleotides from Dharmacon, USA. Briefly, DLD1 / NT2/D1 cells ( $\sim 0.2 \times 10^6$ ) were plated in individual wells of a 6-well plate, 24 hours prior to transfection for cells to attain a confluency of  $\sim 50\text{-}60\%$ . The cells were transfected with siRNA oligonucleotides (50 nM) using RNAiMax (Invitrogen, 13778) in reduced serum Opti-MEM (Gibco, 31985) for 6 h, after which cells were transferred to complete medium and incubated for 48h. After 48h of knockdown Cells were processed for Western blots or RNA extraction.

For recovery experiment, cells were allowed to recover in culture for 8 days after 48 hours of Nup93, Nup188, and Nup205 depletion. Nup93 knockdown was performed by using a combination of oligo-1 and oligo-2 at 25 nM each. Two independent siRNA oligos against Nup188, Nup205, and Nup98 were tested for their knockdown efficiency. CTCF knockdown was performed using a single oligo at a final concentration of 50 nM. On-target Plus nontargeting siRNA, respective scramble siRNAs and siLacZ siRNA, were used as negative controls. List of all siRNAs used in this study is given in Table 2.1.1.



**Table 2.1.1: List of siRNAs used in this study**

Nup93_1	5' GCGCTAATTTACTACTGCA 3'	3'dTdT	Dharmacon	100nM
Nup93_2	5' AGAGTGAAGTGGCGGACAA 3'	3'dTdT	Dharmacon	50nM
Nup93_1_Scr	5' ATATACTCGCGTACGATTC 3'	3'dTdT	Dharmacon	100nM
Nup98	5' TGTCAGACCCTAAGAAGAA 3'	3'dTdT	Dharmacon	10nM
Nup98_Scr	5' AGGTGAACGAATAGGTAGA 3'	3'dTdT	Dharmacon	100nM
Nup205_1	5' GGAAUUAUCCAGAACUAUU 3'	3'dTdT	Dharmacon	100nM
Nup205_2	5' AGAUGGUGAAGGAGGAAUAUU 3'	3'dTdT	Dharmacon	50nM
Nup205_1_Scr	5' GCAATCCGACTTATAGAATTA 3'	3'dTdT	Dharmacon	100nM
Nup205_2_Scr	5' GTGAGAGAATAGGGATGTATA 3	3'dTdT	Dharmacon	100nM
Nup188_1	5' GGUAGUAGGCAGACCAUAUU 3'	3'dTdT	Dharmacon	50nM
Nup188_2	5' GCCTTTCTGCGCTTGATCACCACCC 3'	3'dTdT	Dharmacon	50nM
Nup188_1_Scr	5' GCCGAATGTAACGGTAAAGTT 3'	3'dTdT	Dharmacon	100nM
Nup188_2_Scr	5' GCTCCTCTCGCCCACCGTTTAGCTA 3'	3'dTdT	Dharmacon	100nM
CTCF_1	5' ACAAGAATGAGAAGCGCTT 3'	3'dTdT	Dharmacon	50nM
CTCF_2	5' CAAGAAGCGGAGAGGACGA 3'	3'dTdT	Dharmacon	50nM

#### 2.1.4 DNA transfections

For plasmid maxi preps, ~250 ml bacterial cultures were grown overnight at 37°C at 180 rpm shaking. Extraction of DNA was performed using the PureLink Maxiprep DNA Extraction Kit (Invitrogen), eluted in nuclease-free water (NFW) and used for transfecting mammalian cells. All plasmids used in this study were confirmed by sequencing. Cells were transfected with plasmids using Lipofectamine LTX with Plus reagent (Invitrogen, 15338-100) in OptiMEM for 6h after which cells were transferred to complete medium or using Trans-IT 2020 (Mirus) in complete medium. Constructs used in this study are mentioned in Table.2.1.2.

**Table 2.1.2: DNA construct used in this study**

Sr. No	Construct	Use	Source
1	Nup93-GFP (pEGFP-C1)	Overexpression upon Nup188 and Nup205 depletion, High-resolution imaging using STED and SIM microscopes	From Dr. Radha Chauhan (NCCS Pune, India)
2	GR2-GF2-M9	For nuclear import assay	Prof.Ralph Kehlenbach (Uni. of Goettingen)
3	BAC clone (RP11-1132K14)	HOXA DNA FISH analysis	BACPAC Home BACPAC Resources Center (BPRC)

### 2.1.5 Protein extraction and immunoblotting

Cells were lysed in RIPA buffer (50mM Tris-Cl pH-7.4, 150mM NaCl, 0.1% SDS, 0.1% sodium azide, 0.5% Na-deoxycholate, 1mM EDTA, 1% NP40, 1X Protease inhibitor cocktail) and centrifuged at 13,000 g for 10 min at 4°C. The supernatant was separated and used for protein estimation using a BCA kit (cat no.23225). Total protein (20 µg, estimated to be within the linear range of detection) was used for each sample preparation. Samples were lysed in 1X Laemmli buffer (Tris-HCl pH 6.8, 2% SDS, 20% glycerol, 0.2% bromophenol blue, 0.025% β-mercaptoethanol) and denatured at 95°C for 5 minutes. Protein samples were resolved by SDS-PAGE and were transferred to activated polyvinylidene fluoride membrane (PVDF, Millipore, cat no. IPVH00010), followed by blocking with 5% non-fat dried skim milk/1X TBST (Tris-buffer saline, 0.1% Tween 20) for 1 hour at RT. Primary antibodies were diluted in 0.5% milk/1X TBST buffer. All antibody dilutions are within the linear range of detection. Rabbit anti-Nup93 (1:500, sc-292099, Lot-E0211, Santa Cruz Biotechnology, CA), rabbit anti-Nup188, (1:1000, Abcam, ab86601, Lot-GR43443-4), mouse anti-Nup98 (1:500, sc-74553, Lot-H0108, Santa Cruz Biotechnology, Santa Cruz, CA), rabbit anti-Nup205 antibody (1:500, HPA024574, Lot-

R11937, ATLAS antibodies), rabbit anti-EED (1:500, ab4469, Lot-GR51357-1), rabbit anti EZH2 (1:500, ab3748, Lot-GR252135-1), rabbit anti-Suz12 (1:500, ab12073, Lot-GR79631-1) and rabbit anti-CTCF antibody (1:500, 07-729, Lot-2375606, Millipore). Secondary antibodies: Donkey anti-rabbit immunoglobulin G horseradish peroxidase (1:10,000, GE NA9340V) and Sheep anti-mouse immunoglobulin G-HRP (1: 10,000, NA9310V) were diluted in 0.5% milk (1X TBST). The blots were developed using enhanced chemiluminescence detection reagents (ECL Prime, 89168-782) at incremental exposures of 10 seconds acquired under a chemiluminescence system LAS4000 (GE). Densitometry analysis of western blots was done using ImageJ software from three independent biological replicates. GAPDH was used as internal control for normalization.

**Table 2.1.3: List of antibodies used in this study**

No	Antibody	Cat. Number	Western blot	IP	ChIP	IFA
1	Rabbit anti-Nup93	sc-292099	1:500	2µg / 500 µg of protein	2µg / 100 µg of chromatin	1:300
2	Rabbit anti-Nup188	ab86601	1:1000	2µg / 500 µg of protein	— (Not used)	—
3	Rabbit anti-Nup205	HPA024574	1: 500	—	—	
4	Rouse anti-Nup98	sc-74553	1:500	2µg / 500 µg of protein	—	1:300
5	Rabbit anti-EED	ab4469	1:500	—	—	—
6	rabbit anti EZH2	ab3748	1:500	—	—	—
7	rabbit anti-Suz12	ab12073	1:500	—	—	—
8	rabbit anti-CTCF	07-729	1:500	—	2µg / 100 µg of chromatin	1:500
9	Rabbit anti-H3K9Ac	ab4441	1:5000	—	2µg / 100 µg of chromatin	—
10	Mouse anti 3K27me3	ab6002	1:1000	—	2µg / 100 µg of chromatin	—
11	Anti-pan H3	ab1791	1:5000	—	2µg / 100 µg of chromatin	—
12	Anti-H3K36me3	ab9050	1:1000	—	2µg / 100 µg of chromatin	—
13	Anti-GAPDH	G9545	1:5000	—	—	—
14	Mouse Anti-Oct4	PCRP-POU5F1-1D2	1:500	—	—	1:100
15	Anti-rabbit antibody–Alexa Fluor 488	Molecular Probes	—	—	—	1:1000
16	Anti-rabbit antibody–Alexa Fluor 568	Molecular Probes	—	—	—	1:1000
17	Anti-mouse antibody–Alexa Fluor 488	Molecular Probes	—	—	—	1:1000
18	Anti-mouse antibody–Alexa Fluor 488	Molecular Probes	—	—	—	1:1000
19	Anti-mouse antibody–Alexa Fluor 568	Molecular Probes	—	—	2µg / 100 µg of chromatin	1:1000
20	Anti-mouse antibody–Alexa Fluor 633	Molecular Probes	—	—	—	1:1000
21	Donkey anti-rabbit antibody–horseradish peroxidase	GE-NA9340V	1:10000	—	—	—
22	Sheep anti-mouse antibody–horseradish peroxidase	GE-NA9310V	1:10000	—	—	—
23	Normal rabbit IgG	—	—	2µg / 500 µg of protein	—	—
24	Phalloidin-Alexa 488	—	—	—	—	1:200

### **2.1.6 Reverse transcription-PCR and real-time quantitative PCR**

Cells were washed with 1X PBS and total RNA was extracted using the Trizol method (Rio et al., 2010), cDNA was synthesized from total RNA with the ImProm-II reverse transcription system using Oligo(dT) primers (Promega, A3800), cDNA was used as a template and RT-PCR was carried out using intron-exon junction primers (Table-1).  $\beta$ -actin and Glyceraldehyde-3-phosphate dehydrogenase (GAPDH) were used as internal controls. The template cDNA was serially diluted to optimize the extent of amplification in the linear range. Real-time quantitative PCR was performed using BioRad RT-PCR instrument (CFX96 Touch) in 10  $\mu$ l of reaction mixtures containing KAPA SYBR Green RT-PCR mix and 2  $\mu$ M each of the forward and reverse primer respectively (Table-2.1.4). Fold change was calculated by double normalization of Ct values to the internal control and untreated samples by  $2^{-\Delta\Delta C_t}$  method (Livak and Schmittgen, 2001).

**Table 2.1.4 List of qRT-PCR primers used in this study**

No	Gene name	Sequence
1	Nup93	F-AGAAGACGCCCTTGACTTTAC R-GATATAAATTTGCCGCGCATAGG
2	Nup188	F-CTGGGCAATCAGCAGGATATAA R-AATGATCCCAAGGCCAGAAG
3	Nup205	F-GACCCTAGAACTCAGTCCAGA R-CTGTGACACCAGCGTAAGAA
5	CTCF	F-CGTTACTGTGATGCTGTGTTTC R-TCATGTGCTCTCCTGTCTA
6	GLCCII	F-GCGAACCTCCTCTTTGGATAC R-GCTAGGTGTCTGAGTAGCTTTG
7	CFTR	F-GGGCTAATCTGGGAGTTGTTAC R-CCAGCTCTCTGATCTCTGTACT
8	HOXA1	F-CGTTAAATCAGGAAGCAGACCC R-GTAGCCGTA CTCTCCA ACTTTC
9	HOXA2	F-CTCAGCCACAAAGAATCCCT R-AGCTCTAGAAGCTGTGTGTTG
10	HOXA3	F-CTCCAGCTCAGGCGAAAG R-CACAGGTAGCGGTTGAAGT
11	HOXA4	F-GTCAGCGCCGTTAACCC R-GGGTCAGGTATCGATTGAAGTG
12	HOXA5	F-CTGCACATAAGTCATGACAACATAG R-GGTCAGGTAACGGTTGAAGT
13	HOXA6	F-TCCCGGACAAGACGTACAC R-CGCCACTGAGGTCCTTATCA
14	HOXA7	F-AGCTTGAAAATTCTGCTCACTTCT R-TCTGATGTCATGGCCAAATTTG
15	HOXA9	F-AAAAGCGGTGCCCTATACA R-CGGTCCCTGGTGAGGTACAT
16	HOXA10	F-GAGAGCAGCAAAGCCTCGC R-CCAGTGTCTGGTGCTTCGTG
17	HOXA11	F-TTGAGCATGCGGGACAGTT R-GTACCAGATCCGAGAGCTGGAA
18	HOXA13	F-AGCGGTGCCTTATACCAAG R-GCCGCTCAGAGAGATTCGT
19	Nup98	F-GCTGTTGGTTTCGACCCTGTT R-AACAGGGTCAACCAACAGC
20	Oct4	F-AGCAAACCCGGAGGAGT R-CCACATCGGCCCTGTGTATATC
21	Sox2	F-AGACGCTCATGAAGAAGGATAAGT R-CTGCGAGTAGGACATGCTGTAG

22	Nanog	F-GAAATCTAAGAGGTGGCAGAAAAA R-GCAGAGATTCCTCTCCACAGTTAT
23	LMNA	F-CCGCAAGACCCTTGACTCA R-TGGTATTGCGCGCTTTCAG
24	FBL	F-GCATGAGGGTGTCTTCATTTG R-ATTCCCCAGGGACCAGGTT

### 2.1.7 Immunoprecipitation (IP) and Co-IP

Cells were lysed using IP lysis buffer (50 mM HEPES - pH 8.0, 140 mM NaCl, 1% NP-40, 0.1 % Na-deoxycholate, 0.1% SDS and 1 mM EDTA) in the presence of 1X complete protease inhibitor cocktail (PIC). Lysates were pre-cleared using protein-A dynabeads (Invitrogen, 10002D), 1 hour at 4°C. Pre-cleared extracts were incubated overnight at 4°C with anti Nup93, anti Nup205, and anti Nup188 antibodies independently (2 µg/500 µg of total protein). IP complexes were captured using protein-A dynabeads (pre-blocked with 0.5 % BSA/1X PBS) and washed with lysis buffer and high salt wash buffer-1 (500 mM NaCl in lysis buffer), wash buffer-2 (20 mM Tris HCl (pH 8.0), 1 mM EDTA, 0.5% NP-40 and 50X PIC). Elution was performed using Laemmli loading buffer and analyzed by Western blotting. For Co-IP, cells were lysed in Co-IP buffer (50 mM Tris HCl, pH 8.0, 150 mM NaCl and 0.5% NP-40) supplemented with protease inhibitor cocktail. Co-IP washes were performed in the same Co-IP lysis buffer.

### 2.1.8 Chromatin Immunoprecipitation (ChIP) and ChIP-qPCR

DLD-1 cells (~1.0 X10<sup>7</sup>) were cross-linked using 1% formaldehyde for 10 min at RT. Cross-linking was quenched using 150 mM glycine, and cells were lysed in 1 ml swelling buffer (25 mM HEPES pH 8.0, 1.5 mM MgCl<sub>2</sub>, 10 mM KCl, 0.1% NP40, 1X PIC) and nuclei were recovered by centrifugation at 2000 rpm. Fixed nuclei were re-suspended in 1

ml sonication buffer (50 mM HEPES pH 8.0, 140 mM NaCl, 1 mM EDTA, 1% Triton-X-100, 0.1% Na-deoxycholate and 0.1% SDS) supplemented with protease inhibitor cocktail and sonicated using Bioruptor Tween sonicator (Diagenode) to generate fragment sizes of ~100-500 bp. Sonicated chromatin was separated by centrifugation at 13000g at 4°C for 10 min. The supernatant was pre-cleared using protein A dynabeads (Invitrogen), 1 hour at 4°C. The amount of DNA was estimated using Nano-drop 2000. Nup93 antibody validated according to ENCODE guidelines (~2 µg) was added to ~100 µg of chromatin sample and diluted to ~1 ml in sonication buffer and incubated overnight at 4°C [91]. CTCF antibody is a ChIP-grade antibody from Millipore. IP complexes were captured using protein A dynabeads (pre-blocked with 0.5 % BSA/1X PBS) and washed 3 times (at 4°C, 11 rpm on end to end rotor) each with sonication buffer, Wash buffer-1 (50 mM HEPES pH 8.0, 500 mM NaCl, 1 mM EDTA, 1% Triton X-100, 0.1% Na-deoxycholate and 0.1% SDS), wash buffer-2 (20 mM Tris HCL pH 8.0, 1 mM EDTA, 0.5% NP-40, 250 mM LiCl, 0.5% Na-deoxycholate and 1X PIC) and TE buffer. Immunoprecipitated chromatin was eluted twice in 200 µl of elution buffer (50 mM Tris pH 8.0, 1 mM EDTA, 1% SDS, 50 mM NaHCO<sub>3</sub>) at 65°C for 10 min. Input and IP fractions were treated with 20 µg RNase A for 1h at 42°C followed by 40 µg Proteinase K for 1 h at 65°C. Reverse crosslinking was performed overnight at 65°C. DNA was extracted with phenol:chloroform: isoamyl alcohol (25:24:1), ethanol precipitated using 3M sodium acetate (pH 5.2) and 2 µg of glycogen. DNA samples were washed with 70% ethanol and re-suspended in 10 µl of nuclease-free water. DNA was quantified by Real-Time qPCR and fold enrichment over input was calculated by % input method from  $2^{-\Delta\Delta C_t}$  (Haring et al., 2007; Livak and Schmittgen, 2001). All ChIP-qPCR experiments were performed in two independent biological replicates as



recommended in the ENCODE guidelines(Landt et al., 2012). CHIP-PCR primers used in this study are listed in Table-2.4.

**Table 2.4: List of ChIP-qPCR primer used in this study**

Gene name	Primer pair	Sequence
HOXA1 promoter	P1	F-CCCGGTGCAAACTGAGT R-AATGGAGGGGAAGAGCG
	P2	F-CGCTCTTCCCCCTCCATT R-ACCGTTCAATGAAAGATGAACTG
	P3	F-CTCGCCAGTTCATCTTTCATT R-CCTCCTGCAAAAGTTTGCC
	P4	F-AAATGCCACTAAAACGGTGATC R-TCTTGCAATGTCCATCTGTCA
HOXA3 Promoter	P1	F-TGCAGTGGTACGATCTCAGC R-AAAATTAGCCAGGCATGGTG
	P2	F-GGTCTCGAACTGCTGACCTC R-AGGGACCTGGAGGTATTGCT
	P3	F-TATGAGGCAGGCAGCAGTAA R-TCTCAGGTTTGGGGATAGA
	P4	F-TTTGGACAACCCATGAACAA R-TGGCTATGCCTGAGTGTGAG
HOXA5 Promoter	P1	F-AAGACCCAGTAACCCGC R-TTTGTGTAGTGTCTCCAAGGC
	P2	F-TGTATGGAATTTGACCTCGC R-CAACAACCTTATTTCCTCCG
	P3	F-CGGGGGAAATAAAGTTGTTG R-TGCACTAATAGGGGAGTTGGG
	P4	F-CCCAACTCCCCTATTAGTGCA R-GATATGTGTGCTTGATTTGTGGC
GLCCI1 promoter	P1	F-AGCTTGTGAGTGTGGGCAG R-TCTTGGGAGGAATAAATACCAGA
	P2	F-AAGCTATCTGCTTCGGAAAAGC R-AATTTGCAAGTACACCTGCATCC
	P3	F-TAAAGTTTGCCTCATGTGTCCTG R-CTCGAGTGATTGGTTCTGGAA
GAPDH		Diagenode, High Cell ChIP Kit GAPDH primer, Cat. Kch-913-050, Lot no.- D002
GRM8	Positive control	F- CCAGTACTTGGGGAGGTTGA R- GCAAACCACACCTGGCTAAT
Outside promoter regions of HOXA1	Upstream region	F-CTGAAAGAGGCGTTTTGAGC R-GGAGCTGGTCTCTTTCAACG
	Downstream region	F-ATGAATGCAGTGATGGGTCA R-AACCAAGAGGGGAGAGGAAA
Primers within	Region1	F-CCCGAGAAGAAAGGGGTAGA R-CAGATGCCTCAGAGGGTAGC

HOXA1 gene body	Region2	F-GACTCGCCTTTCGCTATATCC R-CCCTTTGCCAACAGAAACAT
	Region3	GACTCGCCTTTCGCTATATCC CCCTTTGCCAACAGAAACAT
	Region4	GCCTCAGTGGGAGGTAGTCA AGGGTCTCTTGCCCATCTCT
CTCF- ChIP	CBS 5 6	F-GCGGTCGTTTGTGCGTCTAT R-CCTCCACCCAACCTCCCCTATT
CTCF- ChIP	CBS 6 7	F-AATCCCAAAGCCAGAGTGTT R-GCTGGACGCCGTTATAGACT
CTCF- ChIP	CBS 7 9	F-AAATATAGGGCGGCTGTTCACT R-CAGTGTGGCTCCATGCAAGAG
CTCF- ChIP	CBS 10 11	F-GGGTGAGTCCCCTTTTTCTGTT R-GCGCACTTCCGATCAATGTC
CTCF- ChIP	CBS 11 13	F-GGAGGATGCTCGCAGGACAC R-GGGCGGGAAGGGGAGTAT
CFTR Promoter	P1	F-AGGAGGGCGGGTTAGTTTAC R-GTAAACTAACCCGCCCTCCT
	P2	F-TTTTCGGCTCTCTAAGGCTG R-CAGCCTTAGAGAGCCGAAAA
	P3	F-CTAAAGAGAGGCCGCGACT R-AGTCGCGGCCTCTCTTAG
	P4	F-AAAAGGAAGGGGTGGTGTG R-CACACCACCCCTTCCTTTT

### **2.1.9 Three-dimensional fluorescence in situ hybridization (3D-FISH)**

#### ***Probe preparation***

Bacterial artificial chromosome (BAC) DNA for HOXA locus (RP11-1132K14) was purchased from CHORI BACPAC Resources. BAC DNA extraction was done using Hi-Pure Plasmid DNA Extraction Kit (Invitrogen K210017). Nick translation of BAC DNA was performed using the Nick Translation kit (Roche 11 745 808 910). Nick translation reaction was carried out at 15 °C for 90 min and the reaction was stopped by adding 2µl of 0.5M EDTA (pH 8.0) at 65 °C for 10 min. Nick-translated DNA was precipitated using ethanol precipitation method at -80° C for overnight followed by centrifugation at 13000 rpm for 45min. Precipitated DNA was resuspended in hybridization mix (50% deionized Formamide + Master mix containing 10% Dextran Sulphate, 0.1 mg salmon Sperm DNA in 2X SSC solution, pH-7.4)

#### ***Hybridization***

DLD-1 cells ( $\sim 0.2 \times 10^6$ ) were seeded on coverslips in a six-well plate. After 48 h of Nup93 knockdown, the cells were washed with ice-cold 1× PBS and treated with cytoskeletal (CSK) digestion buffer (0.1 M NaCl, 0.3 M sucrose, 3 mM MgCl<sub>2</sub>, 10 mM PIPES (pH 7.4), 0.5% Triton X-100) for 5 min followed by fixation with 4% PFA in 1X PBS (pH 7.4) for 10 min at RT. The cells were permeabilized in 0.5% Triton X-100 (prepared in 1× PBS) for 10 min and incubated in 20% glycerol (prepared in 1× PBS) for 60 min followed by four freeze-thaw cycles in liquid nitrogen. The cells were washed three times with 1× PBS and treated with 0.1 N HCl for 10 min followed by three washes in 1× PBS for 5 min each. The cells were incubated in 50% formamide (FA)/2 × saline sodium citrate (SSC) (pH 7.4)

overnight at 4 °C or until used for hybridization. Cells were hybridized with 3 µl of human whole chromosome 7 paint (Applied Spectral Imaging (ASI), Israel, or MetaSystems, USA) and nick-translated BAC DNA probe for HOXA gene locus (3 µl). Post-hybridization, coverslips were washed in 50% FA/2× SSC (pH 7.4), thrice for 5 min each at 45 °C, followed by three washes for 5 min each in 0.1× SSC at 60 °C. Coverslips were then counterstained with DAPI for 2 min, washed in 2× SSC and mounted in Slowfade Gold antifade (Invitro- gen S36937).

### **2.1.10 RNA FISH**

#### ***Probe preparation***

The probe for RNA FISH for HOXA locus was prepared BAC clone by nick translation as described in section 2.1.9. The probe was resuspended in 10 µL of deionized FA and mixed with equal volume of 2× hybridization mix (10% Dextran Sulphate and 0.1 mg salmon Sperm DNA in 2X SSC solution, pH-7.4) containing 2mM vanadyl ribonucleoside complex (VRC), and incubated on ice for 30 min.

#### ***Fixation and hybridization***

Cells were washed thrice in ice-cold 1× PBS/ 2mM VRC (5 min each) and treated with CSK buffer/2mM VRC on ice for 5 min followed by fixation using 4 % PFA/ 2mMVRC (7 min RT). The cells were incubated with 70 % ethanol at –20 °C for 60 mins (or stored in 70 % ethanol at –20 °C until further use) followed by washes with ethanol series (70–90–100 % ethanol) and air-dried. Cells were then hybridized with HOXA RNA probe by incubating at 37 °C overnight, followed by washes with 50 % FA/2× SSC (with 2mM VRC) and 2× SSC (with 2mM VRC, pH 7.2-7.4) at 42 °C (three washes each of 5 min

each). The cells were mounted using DAPI–Antifade followed by imaging on a confocal microscope.

### **2.1.11 Microscopy and Image analysis**

Image acquisition was performed on a Leica SP8 confocal microscope with a 63X Plan-Apo1.4 NA oil immersion objective using scan zoom of 2.5. Acquisition of Z-stacked images (voxel size of  $0.105\ \mu\text{m} \times 0.105\ \mu\text{m} \times 0.30\ \mu\text{m}$ ) was at  $512 \times 512$  pixels per frame using 8-bit pixel depth for each channel. The line averaging was set to 4, and images were collected sequentially in a three-channel mode.

High-resolution imaging of Nup93-GFP and Mab414 (Alexa Fluor 568) was performed on Leica TCS STED 3X Nano-scope with 100X HC Plan-Apochromat 1.4 NA oil immersion objective. Depletion lasers of 592 nm and 660 nm were used for GFP and Alexa Fluor 568 respectively. Acquisition of Z-stacks (voxel size of  $0.03\ \mu\text{m} \times 0.03\ \mu\text{m} \times 1\ \mu\text{m}$ ) was performed at  $1352 \times 1352$  pixels per frame using the LASX software.

Distances of gene loci from the nuclear periphery were measured (in  $\mu\text{m}$ ) in 3D using the boundary of the DAPI signal as a marker of the nuclear periphery (Shachar et al., 2015). For quantification, confocal images were loaded into the object analysis tool of the Huygens Professional software. This tool performs surface rendering according to the threshold segmentation of different group of voxels that are separated from the background into a 3D object. 3D reconstruction was performed using surface rendering for the nucleus (blue channel), HOXA gene locus (red channel), CT7 (green channel). Identical threshold and seeding levels were used for surface rendering for all images. The nucleus was selected

as an anchor and the shortest distance of each gene locus (Object) from the nuclear periphery was measured using the ‘analyze object tool’ in Huygens software.

#### **2.1.12 Poly(A) Fluorescence *In situ* Hybridization (FISH)**

DLD1 cells ( $\sim 0.2 \times 10^6$ ) were seeded on coverslips in a 6-well plate. After 48 h of Nup93 knockdown, the cells were fixed with 4% PFA in 1X PBS (pH=7.4) for 15 minutes at RT. Cells were re-fixed and permeabilized with chilled methanol for 5 minutes, followed by incubation in 2X SSC at RT for 10 minutes. Cells were hybridized with 100  $\mu$ l of hybridization mix (40% Formamide, 10% Dextran Sulphate, 0.1 mg salmon Sperm DNA and 5 ng/ml of FAM oligo dT prepared in 2X SSC solution) at 37°C for 3 hours. Coverslips were washed twice with 2X SSC, followed by washes with 0.1X SSC. Cells were stained with DAPI and mounted in an antifade solution. Images were acquired using confocal microscopy using a 63X objective/N.A. 1.4 using 488nm and 405nm lasers, zoom set to 1.0. The mean fluorescence intensity of the FISH signal was determined for each cell and nucleus (demarcated by DAPI) and expressed as a ratio of the nuclear to cytoplasmic fluorescence intensity using the Cell Profiler software [94]. Nuclear/cytoplasmic (N/C) fluorescence intensity ratios were calculated and plotted using GraphPad Prism software. Statistical analysis was performed using the Mann-Whitney U test.

#### **2.1.13 Nuclear import assay**

Nuclear import assay was performed as described previously (Hutten et al., 2009). DLD1 cells ( $\sim 0.2 \times 10^6$ ) were seeded on coverslips in a six-well plate. After 24 h of siRNA transfection, cells were transfected with the vector encoding GR2-GFP2-M9core fusion protein. After 48 h of transfection, cells were treated with 5  $\mu$ M dexamethasone (Sigma)

for 30 min at 37 °C and fixed with 4% paraformaldehyde. Cells were permeabilized with 0.5% Triton X-100 and immunostained with Phalloidin-Alexa 594 (Invitrogen, cat. A12381) to mark the cell boundary. Finally, cells were stained with DAPI and mounted in an antifade solution. Images were acquired using Leica SP8 confocal microscopy using a 63× objective/N.A. 1.4 using 405, 488 and 594 nm and lasers, zoom set to 2.0. The mean fluorescence intensity of the GFP signal was determined for each cell (demarcated by phalloidin) and nucleus (demarcated by DAPI) and expressed as a ratio of the nuclear to cytoplasmic fluorescence intensity using ImageJ.



## **2.2 Materials and method specific for Chapter 4**

### **2.2.1 ChIP-sequencing**

Chromatin immunoprecipitation of Nup93 associated DNA was performed as mentioned in section 2.1.8. Nup93 ChIP-DNA (Two biological replicates) and Input DNA was outsourced for high throughput sequencing to Genotypic Technology, Bangalore, India. The library preparation was performed using the TruSeq ChIP Library Preparation Kit. Libraries were sequenced on the Illumina Hi-seq 2500 platform using 101 bp pair-end sequencing.

### **2.2.2 ChIP-seq analysis**

#### **A) Quality control**

Quality control for all Illumina sequence reads was performed using a FastQC tool (Version 0.72) on GALAXY ChIP-seq analysis platform (Afgan et al., 2018)

#### **B) Read alignment**

All quality-controlled reads were mapped against reference Human genome (hg19) using Bowtie2 (Version 2.2.6) on Galaxy server. Default parameters for pair-end reads were used for all FASTQ files. Bowtie2 generated ‘. bam’ files for each replicate

**Table 2.2.1: Parameters used for alignment using Bowtie2**

Input Parameter	Value
Is this single or paired library	paired
Write unaligned reads (in fastq format) to separate file(s)	False
Write aligned reads (in fastq format) to separate file(s)	False
Do you want to set paired-end options?	no
Will you select a reference genome from your history or use a built-in index?	indexed
Select reference genome	hg19canon
Set read groups information?	do_not_set
Select analysis mode	simple
Do you want to use presets?	No, just use defaults
Save the bowtie2 mapping statistics to the history	False
Job Resource Parameters	no

### **C) Heatmaps and Correlation plots between two biological replicates**

Correlation between two biological replicates of ChIP-seq was determined using multiBamSummary and plotCorelation tool on GALAXY server. Further, we used bamCompare tool to generate sequence depth normalized ‘. bigwig’ files for each replicate which can be used comparing two biological replicates by visualizing raw data on genome browser such as the UCSC genome browser. Heatmaps and average profile plots were generated using ‘computeMatrix’, ‘bamCoverage’ and ‘plot profile’ tools in the deep Tools section of GALAXY platform.

### **D) Peak calling**

MACS peak (Version 2.1.1.20160309.0) calling algorithm was used to find peaks representing likely binding sites for Nup93. Peak calling with MACS was done using the online Galaxy platform with the parameters mentioned in Table.2 Significant peaks identified by MACS were further filtered and ranked based on fold enrichment compared to input, and a false-discovery rate, p-value and tag density.

**Table 2.2.2: Parameter used for Peak calling using MACS**

Input Parameter	Value
Are your inputs Paired-end BAM files?	True
Effective genome size	2451960000
Bandwidth for picking regions to compute fragment size	300
Set lower mfold bound	10
Set upper mfold bound	20
Peak detection based on	p-value
p-value cutoff for peak detection	1e <sup>-05</sup>
Build Model	No model
Set extension size	200
Set shift size	0
When set, scale the small sample up to the bigger sample	False
Use fixed background lambda as local lambda for every peak region	False
When set, use a custom scaling ratio of ChIP/control (e.g. calculated using NCIS) for linear scaling	1.0
The small nearby region in basepairs to calculate dynamic lambda	1000
The large nearby region in basepairs to calculate dynamic lambda	10000
Composite broad regions	nobroad
Use a more sophisticated signal processing approach to find subpeak summits in each enriched peak region	False
How many duplicate tags at the exact same location are allowed?	1

#### **D) Gene annotation of ChIP-Seq peaks**

Statistically significant peaks obtained from MACS peak caller were used for peak annotation. Peak annotation was performed by intersecting peak summit file (. BED file) with genomic coordinates of genes in the Human genome (hg19) using GALAXY server. We also performed peak annotation using online tools PAVIS (Peak Annotation and Visualization) and CEAS (cis-regulatory element annotation system) (Huang et al., 2013; Shin et al., 2009). CEAS annotate each peak summit with the genomic annotations in the following four categories: (a) promoters, (b) bidirectional promoters, (c) downstream of a

gene, and (d) gene bodies (3'UTRs, 5'UTRs, coding exons, and introns). Promoter regions were defined as -1 kb, -2kb and -3kb upstream of the TSS. Downstream regions were defined as +1kb, +2kb and +3kb downstream of the TTS. Each peak was annotated with the closest gene found within a 500 kb window from the center of the summit. Average ChIP enrichment signal within/around important gene features such as a promoter, exon, intron and gene body were also plotted using CEAS.

#### **E) Gene ontology analysis**

Gene ontology analysis was performed using two online tools DAVID (<https://david.ncifcrf.gov/home.jsp>). and Gorilla (<http://cbl-gorilla.cs.technion.ac.il/>). We also performed KEGG pathway analysis of Nup93 associated genes (Kyoto Encyclopedia of Genes and Genomes, <http://www.genome.jp/kegg/>).

#### **F) Motif enrichment analysis**

First, we extracted FASTA sequences corresponding to Nup93 binding peaks using fetch genomic DNA tool in GALAXY. All FASTA sequences were submitted as an input to MEME ChIP suit in GALAXY and motifs analysis was performed with default parameters against HOCOMOCO Human (v11 FULL) database (Machanick and Bailey, 2011). Out of 20 motifs identified by MEME-ChIP, top 6 motifs were selected for further analysis. We performed TOMTOM (Tomtom compares one or more motifs against a database of known motifs) analysis on to 6 motifs to identify similar motifs from HOCOMOCO Human (v11 FULL) database.

### **G) Transcription factors and Histone mark enrichment analysis**

We performed transcription factor enrichment analysis of Nup93 associated peaks using online tool ReMap (Regulatory Map of TF Binding Sites) (Chèneby et al., 2018). Nup93 peaks summit file (. bed) was submitted to ReMap analysis. Nup93 peaks were overlapped (10 % Minimum overlap) against the ReMap catalog of transcription factor binding peaks.

ChIP-atlas database (<http://chip-atlas.org/>) was used to look at the enrichment of transcription factors and histone marks specifically in DLD-1 cells. In ChIP Atlas, two-bed files are compared using 'intersect' command in BEDTools2. P-values are calculated with the two-tailed Fisher's exact probability test We extracted 'bigwig' files for CTCF (DRX 013180), H3K4me1(DRX013183), H3K4me3 (DRX013175) H3K27ac (SRX 1528524), H3K27me3 (DRX013182) and H3K36me3 (DRX013172) from DLD-1 cells. Correlation plots and heatmaps were generated using deepTools on GALAXY server.

We also used online gene set enrichment analysis web server Enricher to determine the enrichment of histone marks on Nup93 binding regions (<http://amp.pharm.mssm.edu/Enrichr/>).

## **2.3 Materials and method specific for Chapter 5**

### **2.3.1 NT2/D1 cell culture and differentiation**

NTERA-2 cl.D1 (NT2/D1) cells were obtained from Prof. Sanjeev Galande Lab (IISER Pune) with the permission from origin lab of Prof. Peter Andrews (The University of Sheffield). Cells were cultured in Dulbecco's modified Eagle's medium (DMEM) (Gibco, 11995) supplemented with 10% fetal bovine serum (Sigma, 2959), 100 U/ml penicillin, 100 g/ml streptomycin (Gibco, 15070-063), and 2mM L-glutamine (1X Gibco® GlutaMAX™ Supplement, 35050061) at 37°C with 5% CO<sub>2</sub>. Cells were sub-cultured by scraping and maintained at high confluency to preserve their undifferentiated state. NT2/D1 cells are known to differentiate at low confluency.

For differentiation, NT2/D1 cells were grown in reduced serum (5% FBS) and treated with 10μM retinoic acid (RA). Retinoic acid stocks (10mM in DMSO) were prepared in dark and stored at -80 due to its extreme instability in the light. RA treatment was carried out in 60mm and 100mm dishes (separate dish for each day) for 8 days, cells were harvested every day (From Day0 to Day8 and at Day21) and the medium was replaced after every 2 days with fresh retinoic acid. Cells were either processed for RNA extraction or western blot analysis.

We ensured that cultures were free of Mycoplasma contamination by DAPI staining cells periodically. The authenticity of DLD1 cells was validated periodically by DAPI karyotyping.

NT2/D1 cells: Modal chromosome number = 62-63

### **2.3.2 CTCF and Nup93 ChIP in DLD-1 cells**

48h knockdown of Nup93 or CTCF was performed in multiple wells of 6 well plate as described previously in section 2.1.3. Nup93 or CTCF depleted cells were then harvested and combined from multiple wells to get the desired cell number ( $10^6$  cells). Chromatin immunoprecipitation for Nup93 and CTCF was performed as described in section 2.1.8. Lis of ChIP-PCR primers for CTCF binding sites is given in Table 2.1.4.

### **2.3.3 CTCF and Nup93 ChIP in NT2/D1 cells**

Differentiation of NT2/D1 cells was performed as described in section 2.3.1. Cells were harvested at Day0, Day4, and Day8 of differentiation. CTCF and Nup93 ChIP was performed as described in section 2.1.8.

### **2.3.4 Nup93 and CTCF knockdown followed by RA treatment**

48h knockdown of Nup93 (Oligo-1 20nM) or CTCF (Oligo-1 50nM) was performed in multiple wells of 6 well plate as described previously in section 2.1.3. After 48h of knockdown, cells were treated with 10 $\mu$ M RA for 24h. Cells were then harvested and processed for RNA extraction as described in section 2.1.6.

### **2.3.5 3D-FISH for HOXA locus in NT2/D1 cells**

NT2/D1 cells ( $0.5 \times 10^6$ ) were seeded on the coverslips in 6 well dish. RA treatment was performed as described in section 2.3.1. Cells were fixed at different intervals (Day0, Day2, Day4, and Day8) during differentiation. The 3D FISH protocol described in section 2.1.9

was followed. Image acquisition and data analysis were performed as described in section 2.1.1.

## **Chapter 3: Nup93 sub-complex mediated repression of HOXA gene cluster in differentiated cells**

**Results from this chapter are published as a part of the following paper-**

Labade, A.S., Karmodiya, K., and Sengupta, K. (2016). HOXA repression is mediated by nucleoporin Nup93 assisted by its interactors Nup188 and Nup205. *Epigenetics Chromatin* 9, 54.



### **3.1 Introduction**

The nucleus is a highly compartmentalized organelle inside the cell. Compartmentalization of the nucleus achieves regulated genome organization and function. The non-random positioning of chromosome territories or gene loci largely correlates with their transcriptional status (Ferrai et al., 2010; Sexton et al., 2007). Gene poor chromosomes are located at the nuclear periphery while gene-rich chromosomes are more centrally localized inside the nucleus. Interaction of chromatin with nuclear structures such as nuclear bodies and nuclear landmarks also facilitates non-random organization of chromosomes and gene loci (Cheung and Reddy, 2012; Sexton and Cavalli, 2015; Sexton et al., 2007). In principle, the interaction of the chromatin with a particular nuclear landmark provides a suitable platform for genome organization and gene regulation (Sexton et al., 2007). Two major nuclear landmarks are (i) nuclear envelope (NE) and (ii) Nucleolus (Nu). The nuclear envelope is composed of a double lipid bilayer, an outer nuclear membrane (ONM) and inner nuclear membrane (INM) and is perforated at multiple sites by nuclear pore complexes (NPC). In addition, the nuclear envelope also consists of a meshwork of intermediate filament proteins that underlie the NE known as the nuclear lamina. High-resolution electron microscopy images of the nuclear periphery show that the NE is underlined with electron dense heterochromatin (Cherkezyan et al., 2014). This observation is consistent with the role of the nuclear lamina in transcriptional repression of

large chromatin domains at the nuclear periphery known as lamina-associated domains (LADs) (Guelen et al., 2008; Zullo et al., 2012). In contrast, genomic regions below the nuclear pore complexes are devoid of heterochromatin. NPC is another major component of the nuclear envelope whose role in gene regulation has been a subject of intense investigation in recent years.

The Nuclear Pore Complex (NPC) is a large (100-120 MDa) macromolecular protein assembly, localized at the nuclear periphery. The traditionally known function of the NPC is to import and export proteins and RNA across the nuclear membrane (Wälde and Kehlenbach, 2010; Wentz and Rout, 2010). The NPC consists of several copies of 30 different proteins referred to as Nucleoporins (Nups). Structurally, nucleoporins are classified into (i) Scaffold nucleoporins (ii) peripheral nucleoporins. Scaffold nucleoporins such as the Nup93-Nup188 and Nup107-Nup160 subcomplexes are highly stable. Peripheral nucleoporins such as Nup153, Nup98, and Tpr are mobile nucleoporins (D'Angelo and Hetzer, 2008). In addition to their well-characterized role in nuclear transport, studies in *Saccharomyces cerevisiae*, *Drosophila melanogaster*, and mammalian cells revealed that NPC components are also involved in transcriptional regulation (Brown and Silver, 2007; Capelson et al., 2010a; Jacinto et al., 2015; Kalverda et al., 2010; Taddei et al., 2006), transcriptional memory (Light and Brickner, 2013; Light et al., 2010, 2013), differentiation, development (Buchwalter et al., 2014; D'Angelo et al., 2012; Kalverda et al., 2010; Liang et al., 2013), demarcating chromatin boundaries (Ishii et al., 2002; Kalverda and Fornerod, 2010), and chromatin organization (Breuer and Ohkura, 2015; Strambio-De-Castillia et al., 2010). These functions are likely to involve chromatin contacts with nucleoporins. Typically, Nups contact chromatin in either an off-pore or on-

pore manner. In humans, Nup98 contacts chromatin in an off-pore manner inside the nucleoplasm away from the nuclear periphery (Griffis, 2002; Liang et al., 2013). In *Drosophila*, Nup98, Sec13 and Nup50 re-localize to the nucleoplasm and contact chromatin (Hou and Corces, 2010). Nup153 and Megator (Mtor) are mobile nucleoporins that associate with ~25% of the *Drosophila* genome at Nucleoporin Associated Regions (NARs) (Vaquerizas et al., 2010)(Vaquerizas et al., 2010). In neural progenitor cells, nucleoporins contact chromatin in an on-pore manner, for instance, a group of genes that include *GRIK1*, *NRG1* and *MAP2* are specifically associated with the artificially tethered Nup98-NDC1 fusion protein at the nuclear envelope upon transcriptional activation (Liang et al., 2013). The yeast Nup170p associates with the RSC chromatin remodeling complex and silencing factor Sir4p which cooperatively mediates the association of telomeres with the nuclear envelope, resulting in sub-telomeric gene silencing (Van deaaa 1Vosse et al., 2013)(Van deaaa 1Vosse et al., 2013). These studies suggest an association of nucleoporins with chromatin. However, the molecular mechanisms of nucleoporins and their interaction with chromatin in transcription regulation remain unclear. Nucleoporins in addition to their primary role in nuclear transport also function in chromatin organization. However, for stable and on-pore nucleoporins it is unclear as to how they regulate chromatin organization.

The nucleoporin Nup93 sub-complex is composed of Nup93, Nup188, Nup205, Nup155 and Nup53 (Grandi et al., 1997; Kosinski et al., 2016; Miller et al., 2000; Sachdev et al., 2012; Vollmer and Antonin, 2014). Nup93 is a highly stable nucleoporin with a relatively low dissociation rate from the nuclear pore complex ( $K_{\text{off}}: 4.0 \pm 3.4 \times 10^{-6} \text{ s}^{-1}$ ) (Rabut et al., 2004). Interestingly, Nup93 ChIP-Chip study using tiling microarrays for

human chromosomes 5, 7 and 16 in HeLa cells for the first time showed that Nup93 contacts chromatin sub-domains on these chromosomes (Brown et al., 2008). In addition, Dam-ID of Nup93 in U2OS cells showed that Nup93 associates super-enhancers and regulates the expression of cell identity genes. These experiments revealed a novel role of a stable nucleoporin Nup93 in gene regulation by associating with the chromatin. Notably, ChIP-chip study by Brown et al shows that Nup93 associates with the promoters of HOXA1, HOXA3, and HOXA5 on human chromosome 7. However, the potential role of Nup93 in regulating HOX gene expression is unclear. This raises the intriguing possibility of Nup93 to function as an additional modulator of the HOXA chromatin sub-cluster and therefore HOXA gene expression during differentiation.

The HOXA gene locus (Chr.7p15.3) spans ~107 kb of the sub-genomic region (27,112,593bp-27,254,038bp, hg19 assembly) and encodes for 11 transcription factors that are involved in pattern formation in early development (Rousseau et al., 2014). Expression of HOXA gene is restricted to the early stages of development and differentiation. However, aberrant expression of HOXA genes in adult tissues can lead to diseases such as cancer. For example, HOXA genes are upregulated in breast carcinoma, human cutaneous melanoma and oral cancer (Bhatlekar et al., 2014; Bitu et al., 2012; Maeda et al., 2005; Makiyama et al., 2005; Mustafa et al., 2015; Novak et al., 2006). Chromosome conformation capture studies have shown that chromatin at the HOXA locus is spatially organized and its spatial organization is correlated with its expression status. For instance, in NT2D1 cells, the repressed HOXA gene cluster adopts a packaged chromatin state organized as “multiple chromatin loops” (Narendra et al., 2015; Xu et al., 2014). These loops of the HOXA gene loci are disrupted by the combined action of retinoic acid

treatment and depletion of CTCF or PRC2 that transcriptionally activate HOXA gene expression (Xu et al., 2014). Similarly, a 5C in THP-1 cells showed that repressed HOXA locus is present in the folded cluster organization (Fraser et al., 2009). Wang et al showed that silenced HOXA locus adopts a linear configuration, whereas the active locus showed a high level of interaction (Wang et al., 2011). These studies indicate that HOXA locus shows spatial dynamics in its organization, depending on the cell type and its transcriptional status. However, regulatory mechanisms that control different architectures of HOXA locus remains unclear.

Brown et al showed that Nup93 associates with HOXA1, HOXA3 and HOXA5 promoters in HeLa cells (Brown et al., 2008). We hypothesized that Nup93 is potentially involved in the spatial organization and transcriptional control of the HOXA locus. To address this, we determined the consequences of depleting Nup93 on HOXA gene expression in differentiated cells. Here we show that Nup93 associates with and represses HOXA gene expression. In addition, we observed that Nup93 mediated repression of HOXA gene locus is dependent on its interacting partners – Nup188 and Nup205. The depletion of Nup93 or its interacting partners - Nup188 and Nup205 de-represses the HOXA gene cluster. Additionally, depression of HOXA genes is facilitated by increased levels of the active histone marks (H3K9ac) and decreased levels of repressive histone marks (H3K27me3) on the HOXA1 promoter. Similarly, we observed enrichment of the transcription elongation mark (H3K36me3) within the HOXA1 gene. Taken together, Nup93 along with its interacting partners - Nup188 and Nup205 mediates repression of HOXA gene expression in terminally differentiated cells.



## **3.2 Results**

### **3.2.1 Effect of Nup93 depletion on nuclear morphology, nuclear volume, and ploidy levels**

Nup93 is a scaffold nucleoporin present at the core of the nuclear pore complex. Immunoelectron microscopy studies have revealed the octagonal symmetry of the NPC. Nup93 is present in 32 copies in each nuclear pore complex and each nucleus consists of >2000 copies of the NPC (Sachdev et al., 2012). Considering these observations, we first decided to test expression levels of Nup93 in different cell lines. Initially, we compared the expression levels of Nup93 in silico from protein expression databases such as Cancer cell line encyclopedia (CCLE) and Human Protein Atlas (HPA). We observed that Nup93 is abundantly expressed across the different cell and tissue types in both CCLE and HPA databases (Figure 3.1 A and B), suggesting that Nup93 is abundantly expressed across different cell lines.

Next, we tested expression levels of Nup93 across cell lines. We performed western blotting of Nup93 using whole cell lysates of MCF7, HT1080, HEK293, A549, SW40 and DLD-1 cells. Nup93 showed abundant expression in these cell lines. However, HEK293 and DLD-1 cells showed a relatively higher expression of Nup93 as compared to other cell lines. DLD-1 is a diploid colorectal cancer cell line maintains near-diploid chromosome numbers (45-46) across passages (Ranade et al., 2017; Sengupta et al., 2007). We, therefore, performed all experiments in DLD-1 cells.

**Figure 3.1**

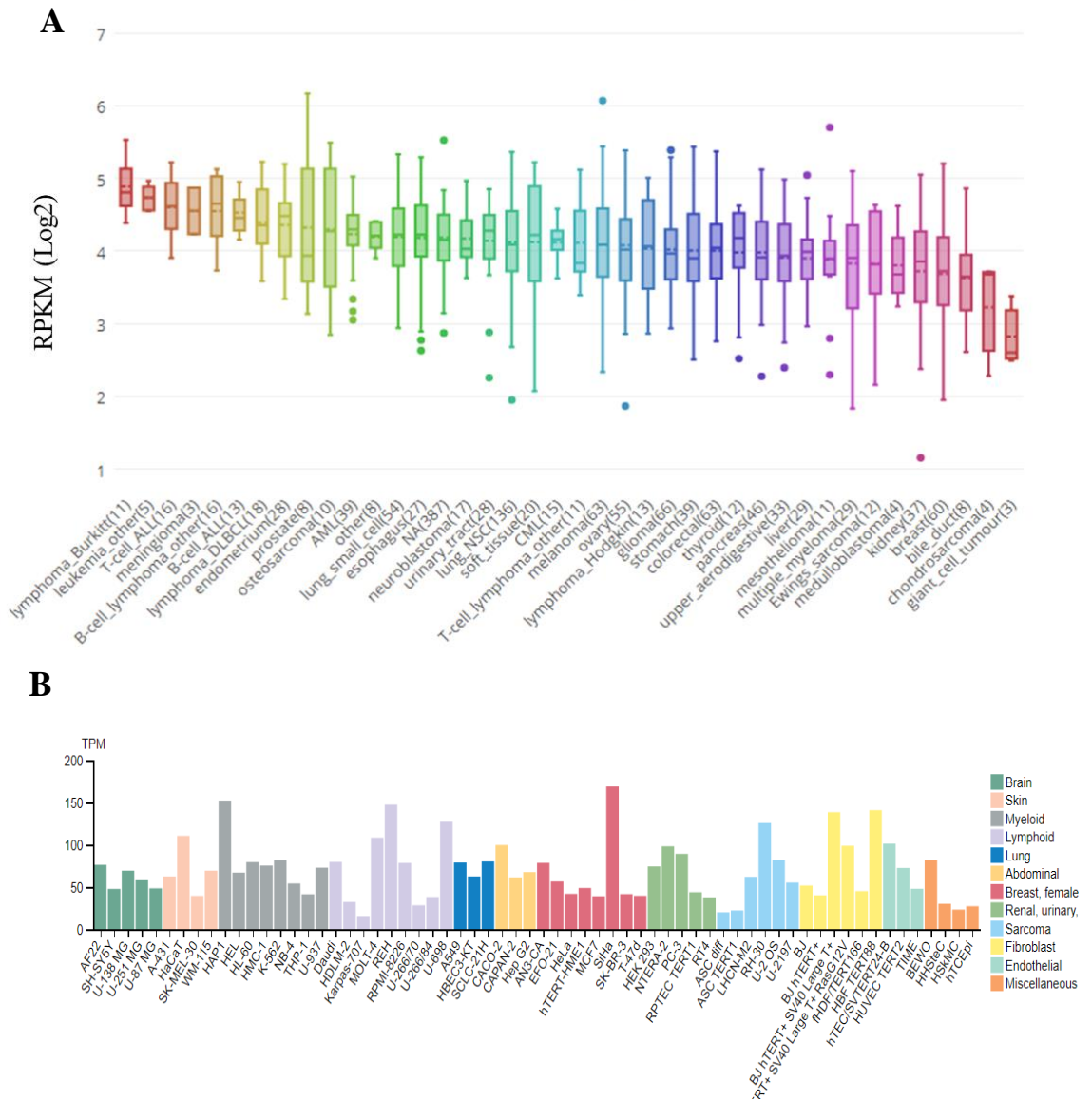


**Figure 3.1 Expression levels of Nup93 across different cell lines: A)** mRNA expression plot of Nup93 for cell lines of various origin using Cancer Cell Line Encyclopedia (CCLE) database. Y-axis represents normalized RPKM(Log2) values. **B)** Gene expression plot of Nup93 across different cell lines using the Human Protein Atlas (HPA) data.



We determined the effect of Nup93 depletion on nuclear morphology, nuclear volume and ploidy levels of DLD-1 cells. We performed siRNA mediated depletion of Nup93 followed by immunostaining of Nup93 and Lamin B2 (as a marker of nuclear envelope) in control and Nup93 depleted cells (Figure 3.2 B and C). Immunofluorescence analyses showed that the depletion of Nup93 does not affect nuclear morphology (Figure 3.2 C). However, nuclear volumes showed a significant increase upon depletion of Nup93 (Figure 3.2 D). Since Nup93-depleted cells showed an increase in nuclear volume, we examined if the ploidy of DLD-1 cells was altered (Figure 3.2 E). We performed chromosome counting on metaphase of DLD-1 cells. Interestingly, we did not observe significant changes in ploidy level upon Nup93 depletion, indicating that the increase in nuclear volume does not correlate and is independent of ploidy levels (Figure 3.2 E). This is further corroborated by an independent study which showed an increase in nuclear volumes upon immunodepletion of Nup188 - an interactor of Nup93 (Theerthagiri et al., 2010). This study also showed that the increase in nuclear volume does not correlate with an increase in DNA content but involves enhanced translocation of integral membrane proteins through the NPC (Theerthagiri et al., 2010). In summary, Nup93 depletion in DLD-1 cells increases nuclear volume but does not perturb nuclear morphology or chromosomal ploidy levels.

**Figure 3.2**

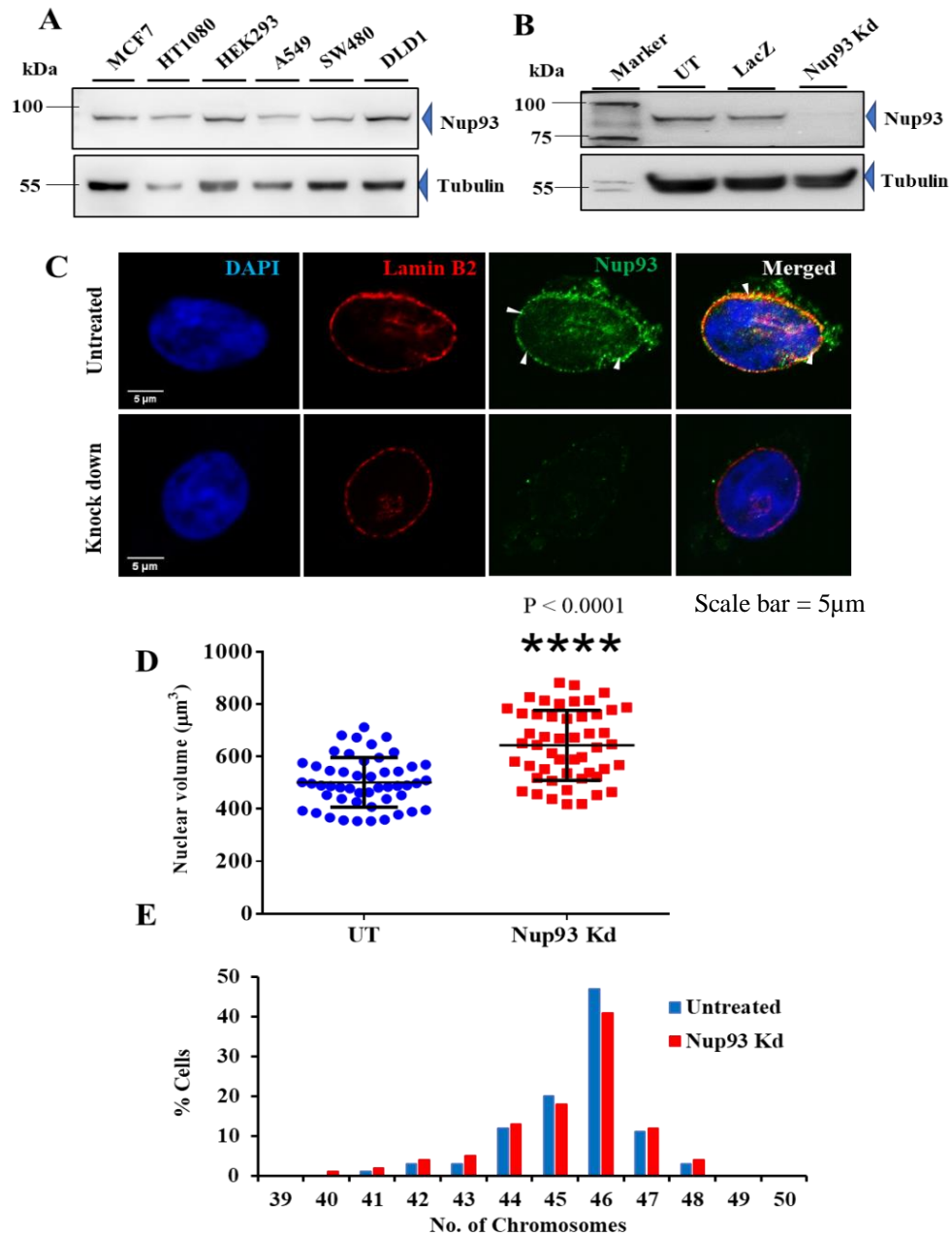


**Figure 3.2. Effect of Nup93 depletion on nuclear morphology, nuclear volume and ploidy levels. A)** Western blot showing the levels of Nup93 in different cancer cell lines, **B)** Western blot showing the levels of Nup93 untreated and Nup93 knockdown (Nup93 Kd) cells **C)** Immunofluorescence assay representing LaminB2 (Red) and Nup93(Green) staining in untreated and Nup93 knockdown cells, (63X magnification, zoom 2.5) **D)** Scatter plot showing the distribution of Nuclear volumes in untreated (UT, n=50) and Nup93 Kd (n=50) cells. Mann-Whitney U test was used to determine the statistical significance. ( $P < 0.0001$ ), **E)** Histograms showing quantification of chromosome number in Untreated and in Nup93 Kd cells. At least 100 metaphase spreads were counted for both Untreated and Nup93 knockdown cells.

### **3.2.2 Nup93 associates with the HOXA gene locus**

Chromatin immunoprecipitation of a stable nucleoporin Nup93 followed by tiling? microarray in HeLa cells showed that Nup93 associates with human chromosomes 5, 7 and 16 (Brown et al., 2008). Interestingly, Nup93 associates with promoter regions [~1000 bp upstream of the Transcription Start Site (TSS)] of HOXA1, HOXA3 and HOXA5 (Brown et al., 2008). However, the functional importance of this association was unclear from this study. Since HOXA locus organizes as “loops”, we asked if Nup93 is involved in the organization of the HOXA gene locus.

To investigate whether Nup93 associates with the promoter of the HOXA gene locus, we performed ChIP of Nup93. We first validated the Nup93 antibody for its immunoprecipitation efficiency. Immunoprecipitation assay with anti-Nup93 antibody robustly pulled down Nup93 as compared to that of input (Figure 3.3 A). We performed siRNA mediated knockdown of Nup93 followed by immunoblotting and observed >70% depletion of Nup93 upon siRNA mediated knockdown, underscoring the specificity of the Nup93 antibody (Figure 3.3 B).

**Figure 3.3**

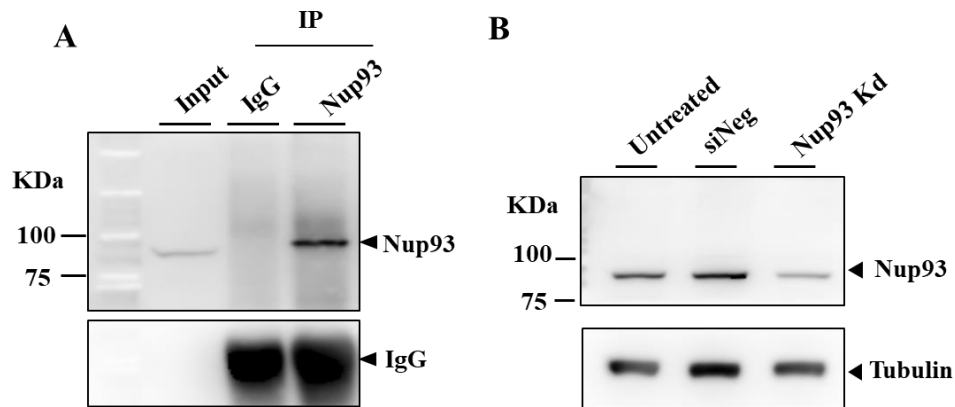


**Figure 3.3. Validation of Nup93 antibody:** **A)** Immunoprecipitation of Nup93 using anti-Nup93 antibody on whole-cell extracts of DLD1 cells (a representative full blot from three independent biological replicates, N = 3). Anti-rabbit heavy chain IgG shows equal precipitation efficiency in IgG and Nup93 lanes, **B)** A representative full Western blot showing siRNA-mediated depletion of Nup93 in DLD1 cells (lane Nup93 Kd), Control cells (Untreated), siNeg (ON-TARGET plus non-targeting siRNA control (a representative blot from three independent biological replicates, N=3).

Next, we performed ChIP of Nup93 followed by qPCR for specific sub-regions of the HOXA1 promoter. We designed overlapping primers on the promoter region of HOXA1, HOXA3, and HOXA5 (Figure 3.4 A, Primer P1 to P4). We found that Nup93 was indeed enriched on specific sub-regions and promoters of HOXA1, A3 and A5 genes (Figure 3.4 B i-iii). Primer pair P3 for HOXA1, P4 for HOXA3 and P2 for HOXA5 showed maximum enrichment of Nup93, suggesting that Nup93 is highly enriched on these promoters (Figure 3.4 B i-iii). We also performed ChIP-qPCR for the gene GLCCI1 – a gene locus ~19 Mb upstream of HOXA, which did not show an association with Nup93. ChIP-PCR corroborated this result since Nup93 was not enriched on the GLCCI1 promoter (Figure 3.4 B-iv) (Brown et al., 2008). In addition to ChIP-qPCR, we performed ChIP-PCR using selected primer sets P3, P4, P2 and P1 for HOXA1, HOXA3, HOXA5, and GLCCI1

respectively (Figure 3.4 C). Nup93 showed a significant enrichment on HOXA1, HOXA3, and HOXA5 but not on GLCCI1, which further validated the specificity of Nup93 and its association with the HOXA1, HOXA3, and HOXA5 promoter sequences respectively (Figure 3.4 C). In addition to the HOXA gene locus, we also performed ChIP-PCR for another gene CFTR (7q31.2) - a gene locus 89Mb downstream of HOXA and bound by Nup93 (Brown et al., 2008). As expected, Nup93 was significantly enriched on the promoter regions of CFTR, further validating the specificity of the ChIP experiment (Figure 3.4 C). ChIP validation was also performed in Nup93 depleted cells. ChIP-qPCR results showed that Nup93 ChIP efficiency was significantly decreased upon Nup93 knockdown indicating the specificity of our Nup93 ChIP experiment (Figure 3.3 D-i). To further validate our results, we designed ChIP-qPCR primers on outside promoter regions of the HOXA1 gene (~3000 bp upstream and downstream from TSS of HOXA1) (Figure 3.3 D-ii). We also tested an independent gene GRM8 (7q31.11) where Nup93 has a binding site within its gene body region and not on its promoter. We found that Nup93 does not associate with any of the outside promoter regions of HOXA1 (Figure 3.3 D-ii). In contrast, Nup93 showed significant enrichment on GRM8 (Figure 3.3 D-ii). In summary, these results reveal that Nup93 associates with the promoter regions of HOXA1, HOXA3 and HOXA5 in differentiated cells.

**Figure 3.4**

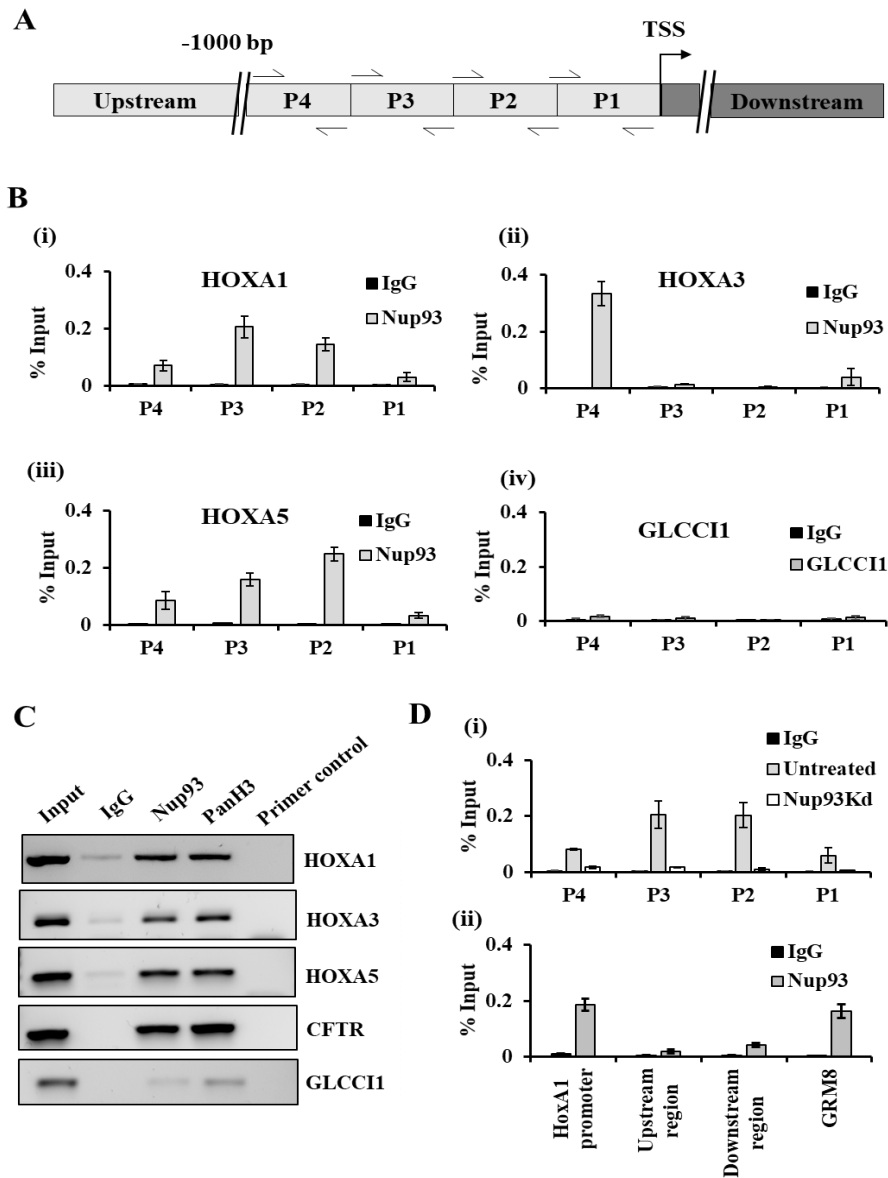


**Figure 3.4. Nup93 associates with HOXA1, HOXA3 and HOXA5 promoters:** **A)** Pictorial representation of primer pair positions (P1–P4) on the promoter of HOXA1, HOXA3 and HOXA5 genes, respectively, upstream region and downstream region indicates primer position outside the HOXA1 promoter, an arrow indicates transcription start site (TSS). **B)** ChIP experiments were performed using antibodies specific to Nup93 and IgG control. Nup93 ChIP-qPCR on (i) HOXA1 (ii) HOXA3 (iii) HOXA5 and (iv) GLCC11 promoters, respectively. Y-axis: immunoprecipitated DNA relative to 1% input, corrected for ChIP using non-specific IgG (N = 2, data from two independent biological replicates that include a total of six technical replicates), error bar- standard error of the mean (SEM). **C)** ChIP-PCR amplification of HOXA1, HOXA3 and HOXA5. CFTR is used as an independent positive control other than HOXA locus. GLCC11 promoter region was used as negative control. **D)** (i) Nup93 ChIP-qPCR was performed in untreated and Nup93 knockdown cells for HOXA1 promoter using primer pairs P1–P4. (ii) ChIP-qPCR using primer pairs outside HOXA1 promoter regions (upstream region and downstream region) and primers for a Nup93-associated gene (GRM8), used as a positive control. (N = 2, representative data from two independent biological replicates) error bar- standard error of the mean

### 3.2.3 Nup93 interacts with Nup188 and Nup205

The Nup93-subcomplex is composed of 5 nucleoporins, Nup93, Nup188, Nup205, Nup35, and Nup155. Previous studies have shown that Nup93 directly interacts with Nup188 and Nup205 (Theerthagiri et al., 2010). Therefore, we asked if the interactors of Nup93 i.e. Nup188 and Nup205, are required for the association of Nup93 with the promoter region of HOXA1. We first ascertained if Nup93 interacts with Nup188 and Nup205 in DLD-1 cells. We performed co-immunoprecipitation of Nup93 from a whole cell lysate of DLD-1 cells, which showed that Nup93 interacts with Nup188 and Nup205 (Figure 3.5 A) (Braun et al., 2016; Theerthagiri et al., 2010). However, Nup93 does not associate with Nup98 (Figure 3.5A), consistent with previous data that Nup98 is not an interactor of Nup93 (Theerthagiri et al., 2010). Reverse co-immunoprecipitation assays with Nup188 showed that Nup188 associates with Nup93 but not with Nup205 or Nup98 (Figure 3.5B). Furthermore, we performed Nup93 Co-IP upon Nup188 or Nup205 depletion (Figure 3.5C and D). Interestingly, we observed that Nup93 shows reduced interaction with Nup188 in Nup205 depleted cells (Figure 3.5D). In contrast, Nup188 depletion does not affect the interaction between Nup93 and Nup205 (Figure 3.5C). This result suggests the requirement for Nup205 in the interaction between Nup93 and Nup188. Taken together, these results suggest that Nup93 associates with Nup188 and Nup205 consistent with co-immunoprecipitation assays performed in *C. elegans* and *S. cerevisiae* (Braun et al., 2016; Grandi et al., 1997; Miller et al., 2000; Theerthagiri et al., 2010; von Appen et al., 2015). We speculate that Nup93 directly interacts with Nup188 and Nup205, however, Nup188 and Nup205 do not interact with each other (Figure 3.5E).

**Figure 3.5**

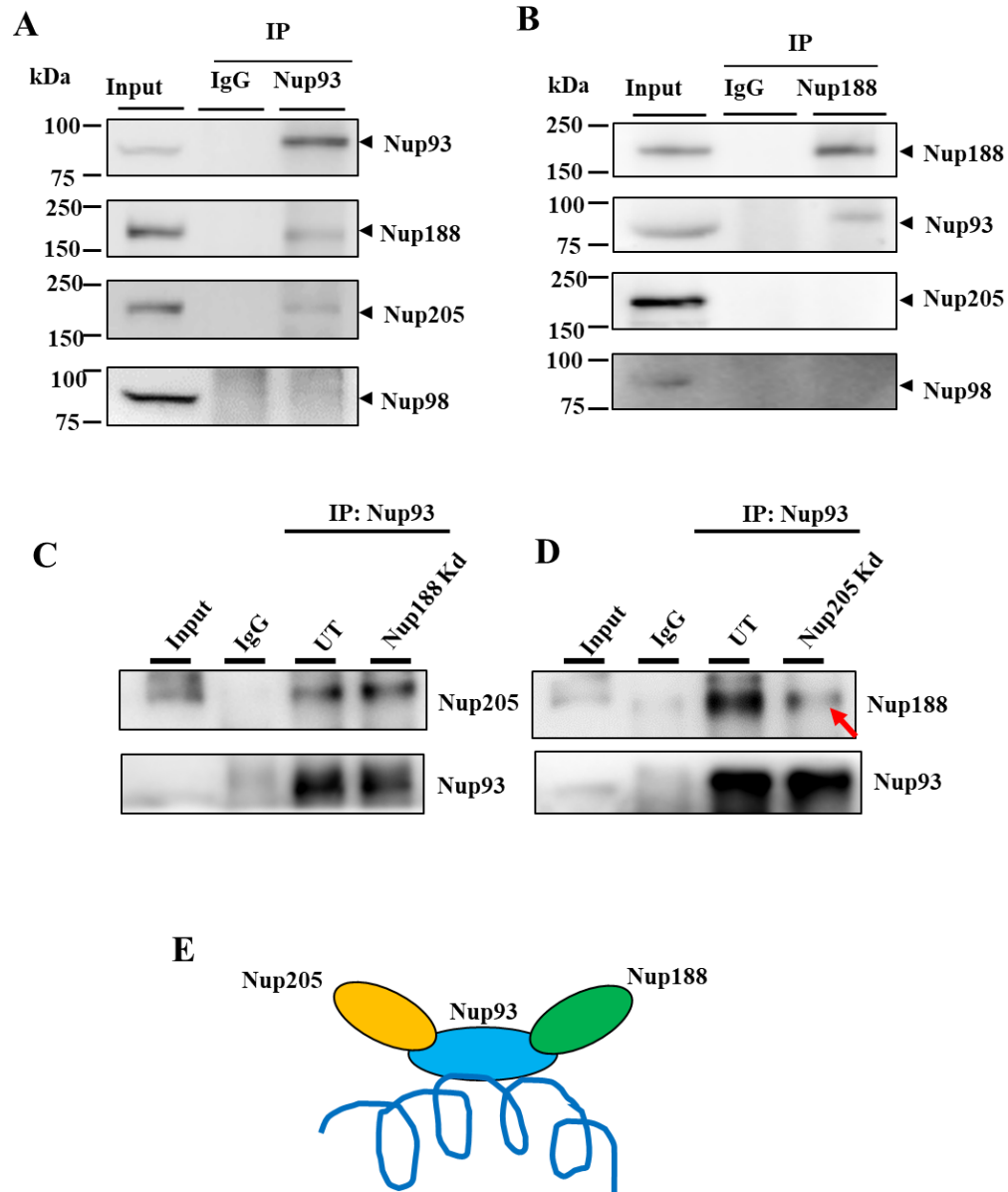


**Figure 3.5. Interaction of Nup93 with Nup188 and Nup205:** **A and B)** Immunoprecipitation was performed using antibodies specific for (A) Nup93; (B) Nup188 and IgG followed by Western blotting for Nup93, Nup188, Nup205 and negative control—Nup98 (representative data from three independent biological replicates, N = 3, single experiment for Nup98). **C and D)** Immunoprecipitation of Nup93 was performed in the background of (C) Nup188 and (D) Nup205 depletion. Reduced interaction of Nup93 with Nup188 was observed in Nup205 depleted cells (red arrow) **E)** Speculative model representing probable order of interaction between Nup93, Nup188 and Nup205.



### **3.2.4 Nup93 requires Nup188 and Nup205 to associate with the HOXA1 promoter**

Considering the interaction of Nup93 with Nup188 and Nup205, we asked if the interactors of Nup93 are required for Nup93 to associate with the HOXA1 promoter region? We performed ChIP with Nup93, in a background of Nup188 or Nup205 depletion in DLD-1 cells (Figure 3.6 A and B). ChIP-PCR and Chip-qPCR results revealed that Nup188 and Nup205 depletion decreased the occupancy of Nup93 by >70% on the HOXA1 promoter (Figure 3.6 C and D). Further, to validate this effect, we performed ChIP with core histone H3 (ChIP with an anti-PanH3 antibody that detects core histone H3) in a background of Nup188 and Nup205 depletion. Notably, we found that the occupancy of the core histone H3 (ChIP with an anti-PanH3 antibody that detects core histone H3) was unaltered on either HOXA1 or GLCCI1 promoters upon Nup188 or Nup205 depletion (Figure 3.6 E). In conclusion, this suggests that Nup93 does not associate with the HOXA1 promoter in absence of its interactors. The implications of these results are of two-fold. First, they raise the possibility that the decrease in the levels of Nup188 or Nup205 may decrease Nup93 levels, consequently lowering its occupancy on the HOXA1 promoter. Second, this suggests the requirement of a stable Nup188-Nup93-Nup205 complex for its association with the HOXA1 promoter.

**Figure 3.6**

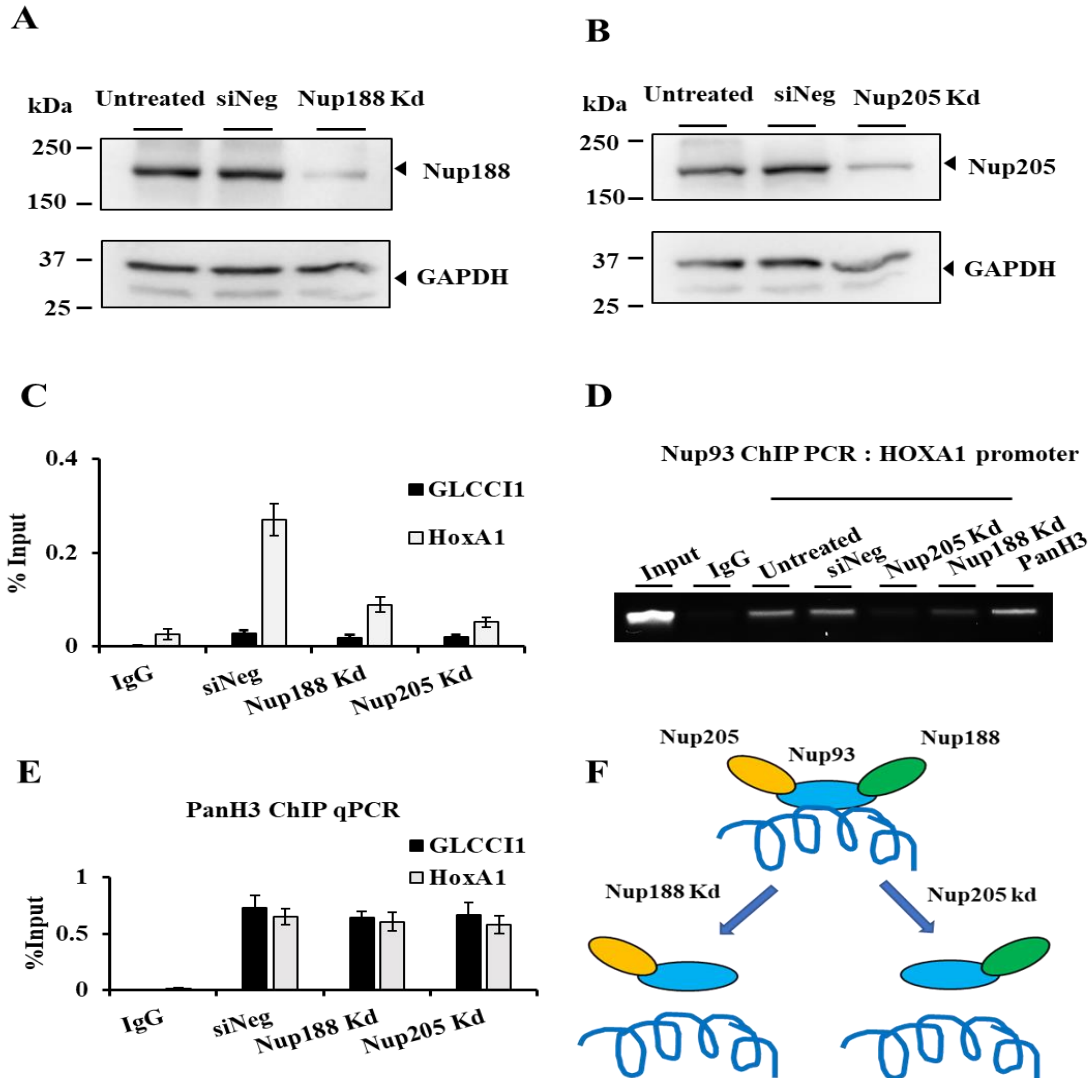
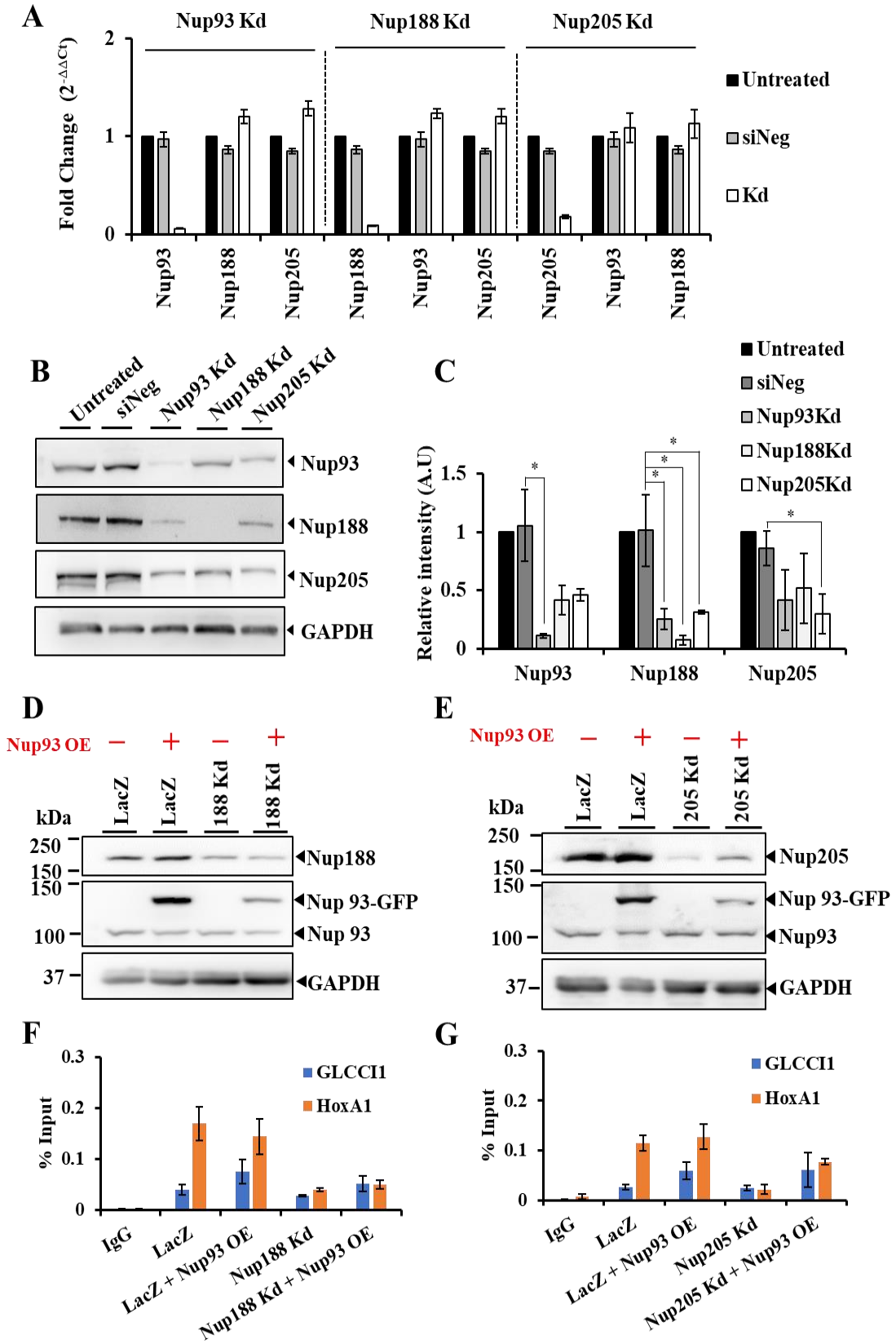


**Figure 3.6. Requirement of Nup188 and Nup205 for Nup93-HOXA1 interaction:** **A and B**) (A) Nup188 and (B) Nup205 were knocked down in DLD1 cells using siRNA. A representative Western blot showing the extent of knockdown (representative Western blot from three independent biological replicates, N = 3). **C and D**) ChIP experiment was performed using an anti-Nup93 antibody in untreated, non-targeting siRNA control (siNeg), Nup188 Kd (Knockdown) and Nup205 Kd cells. (C) ChIP-qPCR analysis was used to determine the extent of Nup93 association with the HOXA1 promoter in Nup188 and Nup205 knockdown cells. Y-axis: immunoprecipitated DNA relative to 1% input, corrected for ChIP using non-specific IgG (N = 2, data from two independent biological replicates that include a total of six technical replicates), error bar: standard error of mean (SEM). **D**) Agarose gel representing ChIP-PCR enrichment of Nup93 on HOXA1 promoter in Nup188 and Nup205 knockdown cells (Input and PanH3 are from Nup205 Kd sample) **E**) In a control experiment PanH3 ChIP-qPCR was performed on HOXA1 promoter in the background of Nup188 and Nup205 depletion, (N = 2, data from two independent biological replicates), error bar: SEM. **F**) Speculative model showing the effect of Nup188 and Nup205 knockdown on Nup93-HOXA1 interaction.

### **3.2.5 Interdependence of Nup93 sub-complex proteins**

To probe if the depletion of Nup188 and Nup205 decreases Nup93 levels, we determined the effect of Nup93, Nup188 and Nup205 knockdown on the levels of one another. We first determined if their transcript levels are interdependent (Figure 3.7 A). Interestingly, we found that independent knockdowns of Nup93, Nup188, and Nup205 did not affect the transcript levels of one another (Figure 3.7 A). However, we detected a decrease in their relative protein levels upon knockdown of one another, suggesting that depletion of one nucleoporin reduces the levels of other from Nup93 subcomplex (Figure 3.7 B and C). Next, to account for the decrease in Nup93 levels in the background of Nup188 or Nup205 depletion, we overexpressed Nup93-GFP in cells depleted of Nup188 or Nup205 (Figure 3.7 D and E). We observed significant overexpression of Nup93 in Nup188 or Nup205 depleted cells (Figure 3.7D and E). Interestingly, ChIP-qPCR analysis of HOXA1 promoter showed a reduced occupancy of Nup93 in Nup188 or Nup205 depleted cells (Figure 3.7 F and G). Taken together these results show that Nup93 requires its interactors Nup188 and Nup205 to associate with the HOXA1 promoter. Furthermore, a stable of Nup93 sub-complex (Nup188-Nup93-Nup205), is essential for its association with the HOXA1 promoter.

**Figure 3.7**



(See figure on previous page)

**Figure 3.7. Interdependence of Nup93 sub-complex proteins:** **A)** Transcript levels of Nup93, Nup188 and Nup205 in independent depletions of Nup93, Nup188 and Nup205. Error bars: S.E.M, data from a single experiment that includes 3 technical replicates. **B)** A representative Western blot showing the effect of Nup93, Nup188 and Nup205 depletion on one another (three independent biological replicates, N = 3), **C)** Western blot quantification of relative band intensities normalized to GAPDH from three independent biological replicates (For western blot shown in 'B'). **D and E)** a representative Western blot showing overexpression of Nup93 upon Nup188 (D) and Nup205 knockdown (E). GAPDH was used as a loading control. **F and G)** ChIP-qPCR was performed upon overexpression of (F) Nup93 in Nup188 and, (G) Nup205-depleted cells. Y-axis: immunoprecipitated DNA relative to 1% input, corrected for ChIP using non-specific IgG (N = 2, data from two independent biological replicates that include a total of six technical replicates), error bar: standard error of mean (SEM)

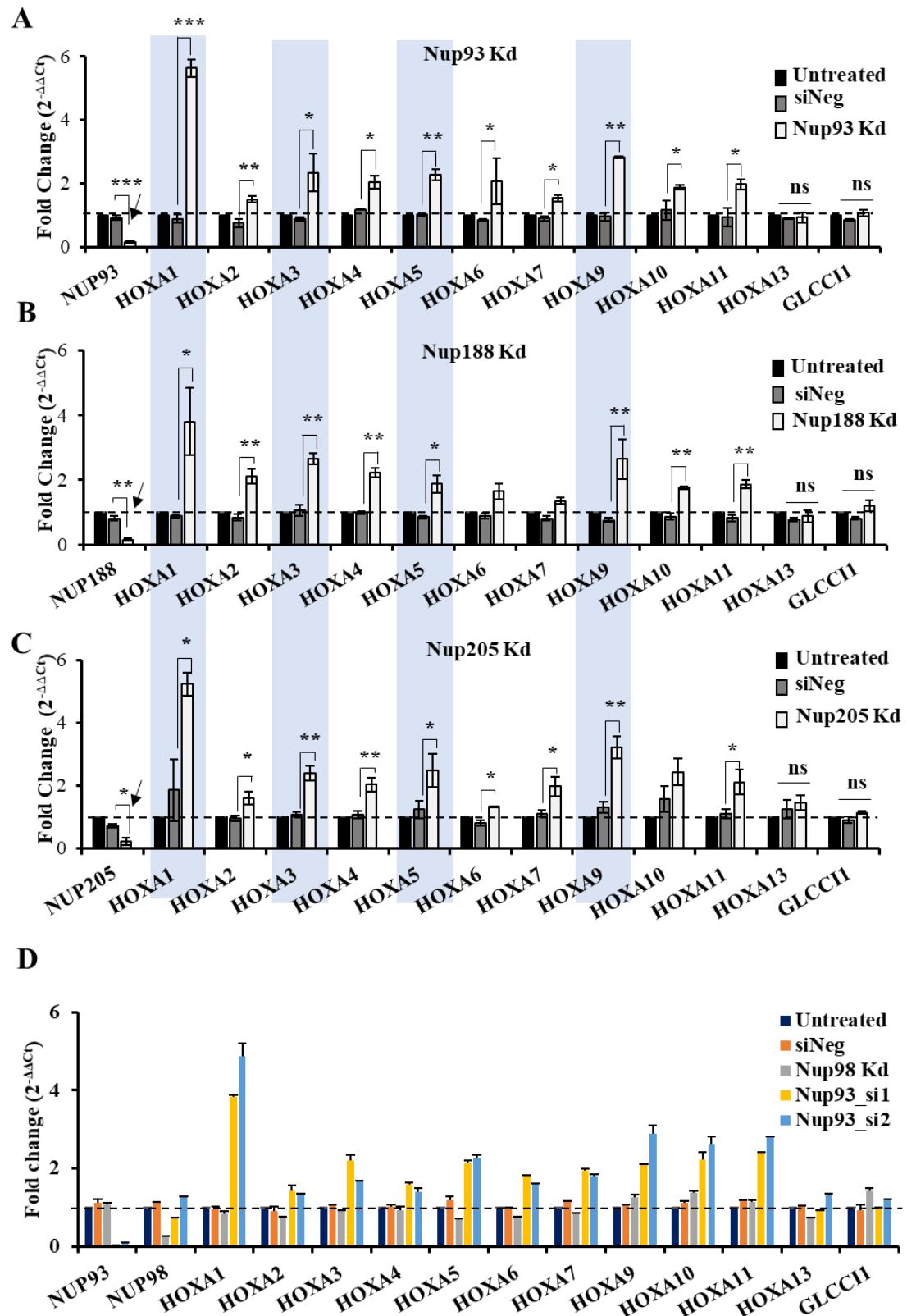
### 3.2.6 HOXA gene expression is upregulated in Nup93, Nup188 or Nup205 depleted

#### cells

As the association of Nup93 with the promoters of HOXA1, HOXA3 and HOXA5 genes suggested a regulatory role in HOXA gene expression, we investigated if depletion of Nup93 or its interactors affects HOXA gene expression. We performed independent knockdowns of Nup93, Nup188, and Nup205 in DLD-1 cells and assessed expression levels of all HOXA genes within the HOXA gene cluster (HOXA1-HOXA13). We detected a >80% reduction in the transcript levels of Nup93, Nup188, and Nup205 in their respective knockdowns (Figure 3.8 A-C). Remarkably, the transcript levels of HOXA genes (HOXA1, HOXA3, HOXA5, and HOXA9) were strikingly upregulated (fold change >2.0 fold) upon Nup93 depletion (Figure 3.8 A). HOXA1 showed an increase in transcript levels in all three nucleoporin knockdowns to ~4-6.0 fold, suggesting a significantly greater impact on HOXA1 expression levels upon Nup93, Nup188, and Nup205 knockdown (Figure 3.8 A-C). Furthermore, HOXA1, HOXA3, HOXA5, and HOXA9 were significantly upregulated in Nup188 and Nup205 depleted cells (Figure 3.8 B-C). Interestingly, the expression levels of HOXA13 and GLCCI1 were unaffected in all the

three Nup knockdowns (HOXA13, GLCCI1, Figure 3.8 A-C). We also used two independent siRNA oligonucleotides to knockdown Nup93 (Figure 3.8D), which showed a striking upregulation of HOXA1, HOXA3, HOXA5 and HOXA9 genes, but not of HOXA13 or GLCCI1 (Figure 3.8 A-C), consistent with previous results. Of note, the depletion of Nup98 did not alter gene expression levels of HOXA1, HOXA9, HOXA13 and GLCC1 (Figure 3.8 A-C), further suggesting a specific role for Nup93, Nup188, and Nup205 in regulating HOXA gene expression in differentiated cells.

**Figure 3.8**



(See figure on previous page)

**Figure 3.8. Depletion of Nup93, Nup188 and Nup205 de-represses HOXA gene cluster: A-C)** qRT-PCR analyses was used to determine mRNA levels of all HOXA genes (HOXA1 to HOXA13) upon (A) Nup93, (B) Nup188 and (C) Nup205 knockdowns in DLD1 cells. Graph represents fold change ( $2^{-\Delta\Delta Ct}$ ) in levels of mRNA normalized to untreated cells. Error bars: SEM, data from three independent biological replicates that include total of nine technical replicates, \* $p < 0.05$ ; \*\* $p < 0.01$ ; \*\*\* $p < 0.001$  (Students t-test between siNeg and knockdown). GLCCI, served as a negative control. **D)** qRT-PCR was performed for entire HOXA cluster upon Nup93, Nup188, Nup205 and Nup98 depletion using two independent siRNA oligos. Y-Axis represent fold change normalized to untreated. Data from two independent biological replicates, Error bars: S.E.M.

### **3.2.7 Overexpression of Nup93 in the background of Nup188 and Nup205 depletion does not rescue de-repression of HOXA**

We observed that overexpressed Nup93 was unable to associate with the HOXA1 promoter in Nup188 and Nup205 depleted cells (Figure 3.7 F and G). We determined the effect of Nup93 overexpression on HOXA levels in Nup188 and Nup205 depleted cells. GFP tagged Nup93 (Nup93-GFP) was localized at the nuclear periphery (Figure 3.9 A). We performed immunostaining of nuclear pores using the anti-nucleoporin antibody-Mab414 (Red) and determined its colocalization with Nup93-GFP (Green). High-resolution imaging of Mab414 and Nup93-GFP labeled cells using structured illumination microscopy (SIM), showed that Nup93-GFP localized at the nuclear periphery (Figure 3.9 A). Notably, Nup93-GFP colocalizes with Mab414 at the nuclear periphery (Figure 3.9 A). However, we did not detect nucleoplasmic localization of Nup93-GFP further reiterating the on-pore localization of Nup93 (Figure 3.9 A). We determined the effect of Nup93 overexpression on HOXA gene expression in the background of Nup188 and Nup205 depletion (Figure 3.9 B and C). Interestingly, overexpressed Nup93 did not rescue HOXA gene expression in Nup188 and Nup205 depleted cells (Figure 3.9 B and C). Taken together, these results



reiterate that Nup93 requires its interactors Nup188 and Nup205 for repression of HOXA gene expression.

**Figure 3.9**

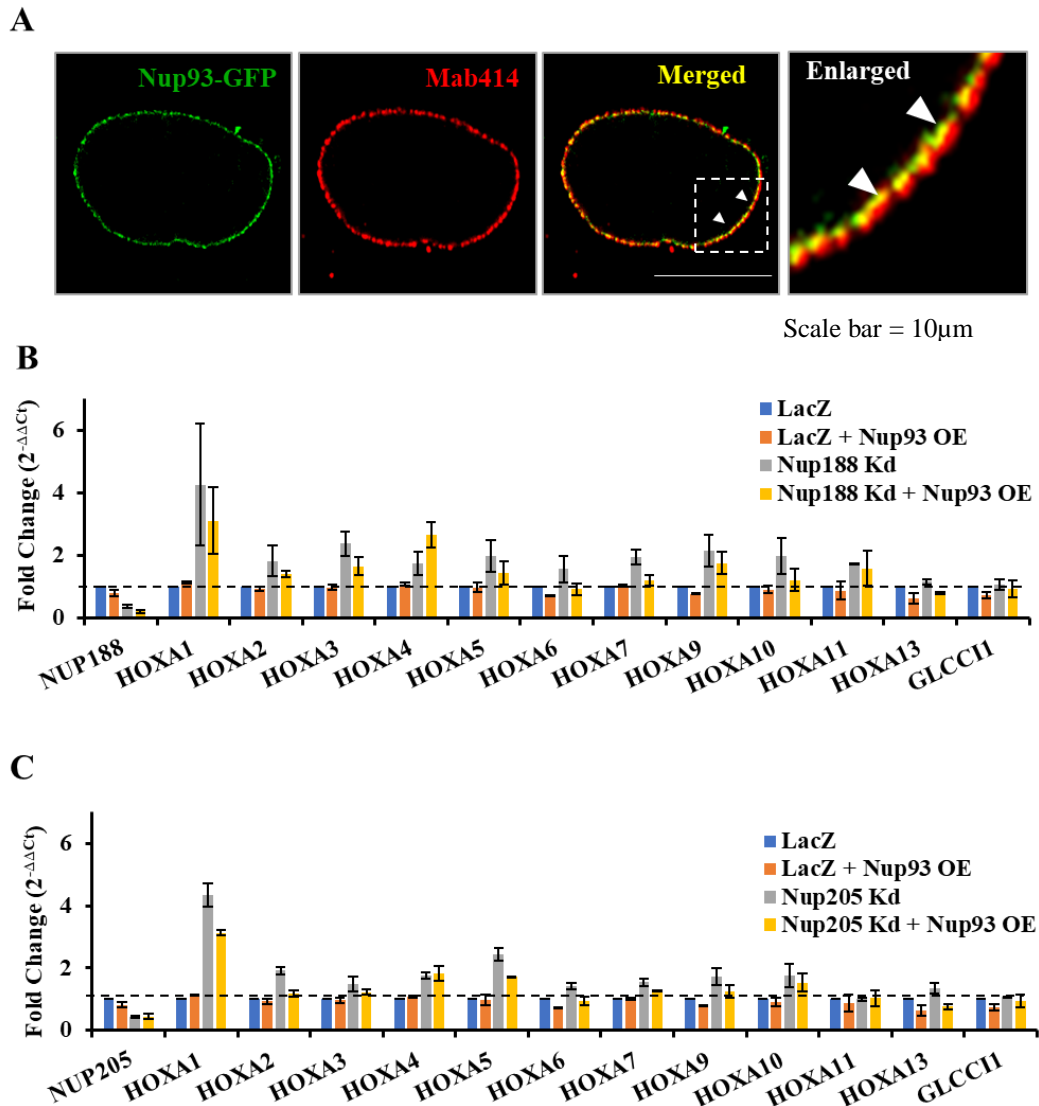


**Figure 3.9. Overexpression of Nup93 in the background of Nup188 and Nup205 depletion does not rescue de-repression of HOXA** **A)** Structured illumination microscopy images of Nup93-GFP expressing nuclei stained for Mab414, white arrows in merged enlarged panel indicates the co-localization of Nup93-GFP with Mab414. (63X magnification, zoom 2.5) **B and C)** qRT-PCR analyses was used to determine mRNA levels of all HOXA genes (HOXA1 to HOXA13) upon Nup93 overexpression in (B) Nup188- and (C) Nup205- depleted cells. Graph represents fold change ( $2^{-\Delta\Delta C_t}$ ) in levels of mRNA normalized to untreated cells. Error bars: SEM, data from two independent biological replicates that include total of six technical replicates. GLCCI1, served as a negative control.

### **3.2.8 Rescue of HOXA upregulation**

Next, we determined if cells allowed to recover after Nup93 depletion showed any change or reversibility of HOXA gene expression. It is possible that an irreversible upregulation of HOXA may imply a feedback effect to sustain HOXA upregulation. We allowed cells to recover in culture for 8 days after 48 hours of Nup93, Nup188 and Nup205 knockdown in DLD-1 cells. We detected a significant restoration in the transcript levels of Nup93, Nup188, and Nup205 after 8 days (Figure 3.10 A-C), accompanied by the downregulation of HOXA1 and HOX9. However, HOXA13 levels remained unaltered (Figure 3.10 A-C). Taken together, these results showed that HOXA upregulation is repressed upon restoration of Nup93, indicating that the association of Nup93 with HOXA gene is required for its repression. Furthermore, our results uncover a novel role for Nup93 and its interacting partners in the repression of the HOXA gene cluster in differentiated cells.

**Figure 3.10**

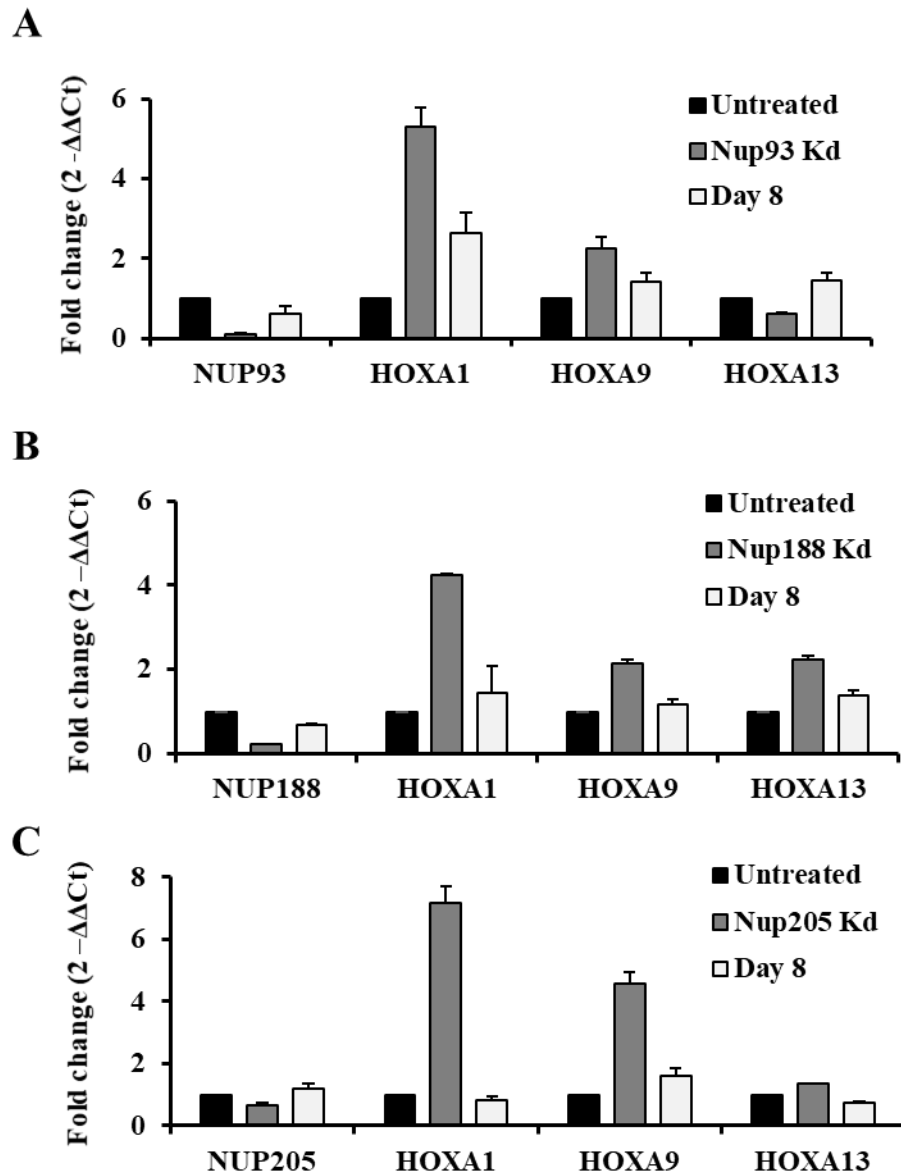
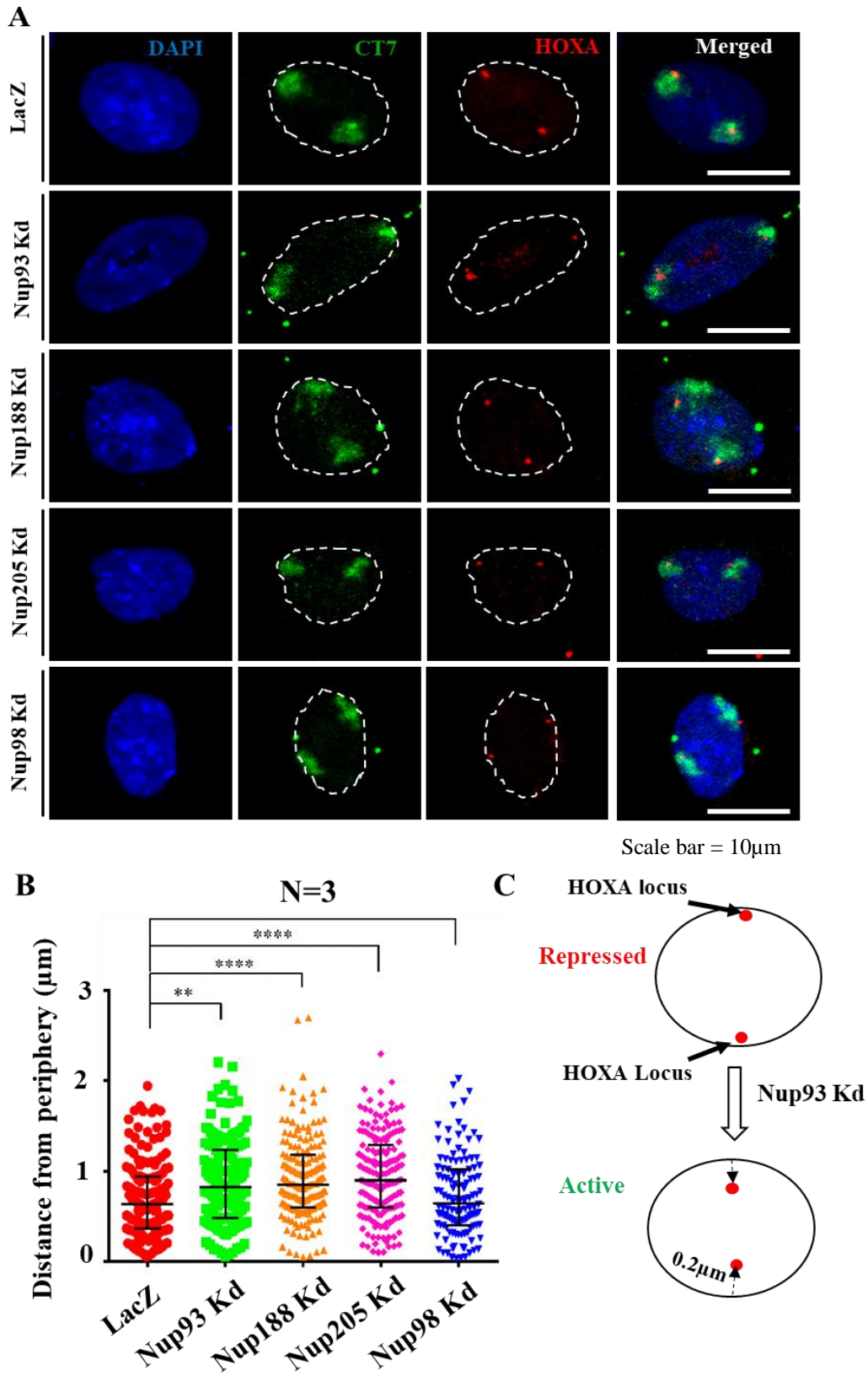


**Figure 3.10: A-C)** Effect of allowing cells to recover for 8 days after 48 hours of knockdown of (A) Nup93; (B) Nup188 and (C) Nup205, qRT-PCR analysis was used to determine mRNA levels of HOXA1, HOXA9 and HOXA13 genes after 48 h knockdown and 8 days of recovery. Error bars-S.E.M, data from one biological replicate that includes 3 technical replicates. Nup93, Nup188 and Nup205 recover to comparable levels as that of untreated cells after 8 days, along with a concomitant repression of HOXA1, HOXA9 and HOXA13 transcript levels.

### **3.2.9 HOXA gene locus is untethered from the nuclear periphery in Nup93, Nup188, Nup205 depleted cells**

As the de-repression of HOXA genes upon Nup93, Nup188, and Nup205 depletion suggests unraveling of the HOXA locus, we determined the spatial localization of HOXA upon Nup93, Nup188 or Nup205 depletion in DLD-1 cells. We performed 3-Dimensional Fluorescence In situ hybridization (3D-FISH) for the HOXA locus. 3D-FISH was performed in cells independently depleted of Nup93, Nup188, and Nup205, followed by confocal imaging of the HOXA locus (Red) and chromosome 7 territories (Green) (Figure 3.11A). We measured the shortest distance of the HOXA gene locus from the nuclear periphery considering the edge of the DAPI stained nucleus as the nuclear border (refs cite Misteli, Hetzer). We found that the HOXA gene loci are predominantly localized near the nuclear periphery in control cells (Median=0.64 $\mu$ m from the DAPI edge) (Figure 3.11B). Interestingly, Nup93, Nup188 or Nup205 depleted cells showed an ~0.2  $\mu$ m displacement of the HOXA gene loci away from the nuclear periphery (Figure 3.11B). In contrast, Nup98 depletion did not affect the positioning of the HOXA locus with respect to the nuclear periphery (Figure 3.11B). Taken together, this suggests that Nup93 and its interactors are likely to tether the HOXA gene locus, while depletion of the Nup93 sub-complex results in untethering of the HOXA gene locus from the nuclear periphery (Figure 3.11C).

**Figure 3.11**



(See figure on previous page)

**Figure 3.11. HOXA gene loci is untethered from the nuclear periphery upon Nup93, Nup188 and Nup205 depletion:** **A)** Representative images (maximum intensity projection of a confocal image stack) of 3D-FISH for HOXA (red), CT7 (green) and DAPI (blue) performed on siLacZ-, Nup93-, Nup188-, Nup205- and Nup98-depleted DLD1 cells. Scale bar ~10  $\mu\text{m}$ , white dotted line indicates nuclear boundary. (63X magnification, zoom 2.5) **B)** Dot scatter plot showing shortest distance of HOXA gene locus from nuclear periphery demarcated by DAPI in siLacZ (n = 164 loci signals)-, Nup93 (n = 154)-, Nup188 (n = 178)-, Nup205 (n = 178)- and Nup98 (n = 124)-depleted DLD1 cells, horizontal bar represents median with interquartile range. Data from two independent biological replicates, \*\*p < 0.01; \*\*\*p < 0.001 (Kolmogorov–Smirnov test). **C)** Cartoon illustration of HOXA locus movement from the nuclear periphery upon Nup93 sub-complex depletion.

### 3.2.10 HOXA transcripts are enriched upon Nup93 depletion

Since HOXA was strikingly upregulated upon Nup93 depletion, we employed RNA-FISH as an independent approach to examine HOXA transcripts in Nup93 depleted cells. We designed RNA-FISH probes that represent the HOXA locus. These intronic probes typically label active transcriptional sites (Wada et al., 2009). RNA-FISH revealed an increase in HOXA transcript levels upon Nup93 knockdown (LacZ) (Figure 3.12 A and B). Collectively, this result suggests an increase in transcript levels of HOXA genes upon Nup93 depletion.

**Figure 3.12**

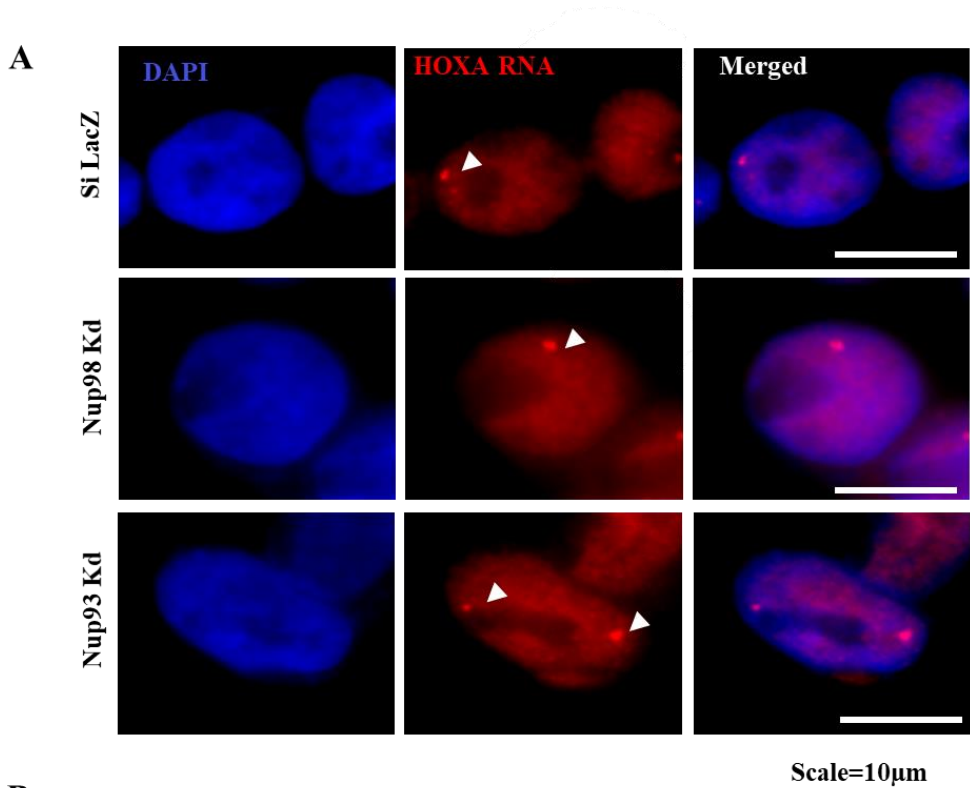


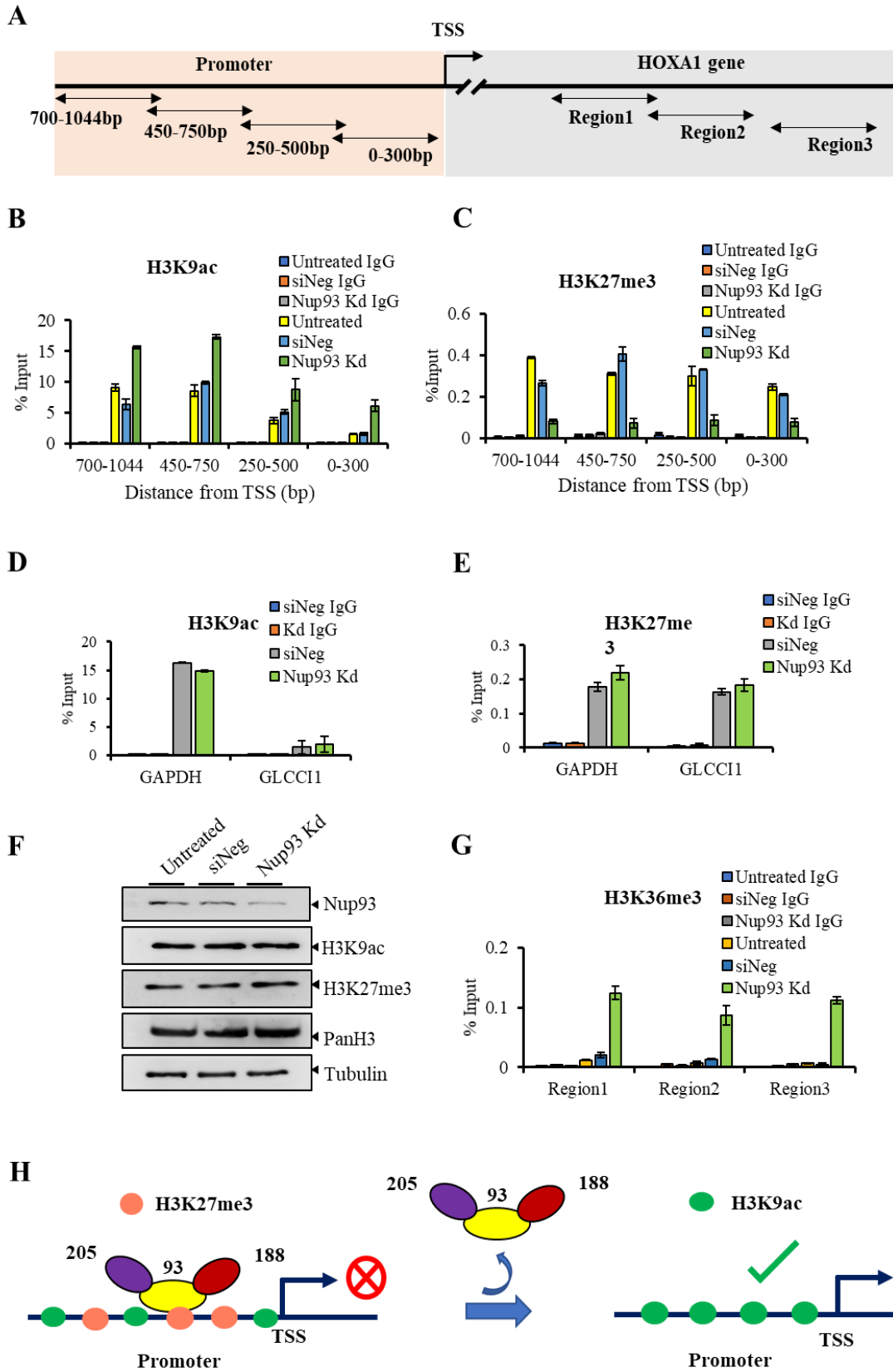
**Figure 3.12. HOXA RNA-FISH upon Nup93depletion:** **A)** Representative images of RNA-FISH for HOXA (red) and DAPI (blue) performed on siLacZ-, Nup98 and Nup93-depleted DLD1 cells. Scale bar ~10  $\mu$ m, white arrow indicates RNA-FISH signal (63X magnification, zoom 2.5) **B)** Histogram showing percentage of cells with one active locus (Blue bar) or two active loci (Orange) in SiLacZ (n = 47 nuclei)-, Nup98 (n=37) and Nup93 (n=34) depleted DLD1 cells, Data from one experiment RNA-FISH experiment. Scale bar =10 $\mu$ m

### **3.2.11 Nup93 depletion alters the relative occupancy of histone marks on the HOXA1 promoter**

A precise control of the spatiotemporal activation of the HOXA gene cluster during differentiation is often accompanied by epigenetic modifications (Atkinson et al., 2008). HOXA gene cluster is occupied by repressive (H3K9me3 and H3K27me3) and active (H3K4me3 and H3K9Ac) histone marks in its repressed and active state respectively (Vieux-Rochas et al., 2015; Xu et al., 2014). Similarly, Polycomb group of proteins (PcG e.e PRC2) silence HOXA gene cluster recruiting repressive histone mark H3K27me3 to HOXA gene cluster (Bantignies and Cavalli, 2011; Xu et al., 2014). In addition, Nup93 binding sites are enriched for repressive histone marks (H3K27me3) in HeLa cells (Brown et al., 2008). We asked if the observed de-repression of the HOXA gene cluster upon Nup93 depletion is accompanied by altered occupancy of active and inactive histone marks on the HOXA1 promoter region (Figure 3.13A). We performed ChIP with active (H3K9ac) and repressive (H3K27me3) histone marks on the HOXA1 promoter in Nup93 depleted cells (Figure 3.13A and B). We examined the levels of active and repressive histone marks on the HOXA1 promoter upon Nup93 knockdown since HOXA1 showed the highest increase in transcript levels (>4.0-6.0 fold) in cells depleted of Nup93 or its interactor Nup188 or Nup205 (Figure 3.8A-C). We performed ChIP-qPCR with overlapping primers ~1Kb upstream of the HOXA1 transcription start site (Figure 3.13A). Strikingly, depletion of Nup93 showed a significant enrichment of the active histone mark (H3K9ac) and decrease in the repressive histone mark (H3K37me3) on HOXA1 promoter region (Figure 3.13B). By contrast, there was no significant change in the levels of active and repressive histone marks on GAPDH and GLCCI1 genes upon Nup93 depletion (Figure 3.13 D and



**Figure 3.13**



(See figure on previous page)

**Figure 3.13. Nup93 depletion alters the occupancy of histone marks on HOXA1 promoter:** A) Pictorial representation of the HOXA1 promoter and regions within the HOXA1 gene (Region 1–Region 3). Left (light red) promoter of HOXA1 gene, double arrowheads: overlapping primer positions on HOXA1 promoter. Right (light gray) regions within HOXA1 gene, double arrowheads: ChIP-qPCR primer positions within HOXA1 gene (Region 1–Region 3), TSS-Transcription start site. B and C) ChIP experiments were performed using antibodies specific to (B) H3K9ac, (C) H3K27me3 and IgG in Untreated, siNeg and Nup93 knockdown cells (IgG is below detection limit <0.2% of input in ‘b–d’). D and E) GAPDH promoter and GLCC11 promoter were used as positive and negative controls, respectively. Y-axis: immunoprecipitated DNA is relative to 1% input, corrected for ChIP using non-specific IgG (All ChIP-qPCR data is from two independent biological replicates that include a total of six technical replicates), error bars: SEM. F) Representative Western blot of untreated, siNeg and Nup93 Kd cells showing that total levels of H3K9ac and H3K27me3 are unaltered. PanH3 and Tubulin were used as loading controls (data from a single experiment). G) Elongation mark (H3K36me3) shows increased occupancy on the HOXA1 gene (Region 1, Region 2 and Region 3), data from two independent biological replicates that include a total of six technical replicates, error bars: SEM. H) Speculative model representing possible role of Nup93 in modulating epigenetic marks on HOXA1 promoter region.

E). Furthermore, the total levels of H3K9ac, H3K27me3, and PanH3 were unaffected by Nup93 depletion in DLD-1 cells (Figure 3.13F). Next, we asked if the HOXA1 gene expression also correlates transcriptional elongation of HOXA upon Nup93 depletion. We determined levels of the transcriptional elongation mark - H3K36me3 (Sims and Reinberg, 2009) on the HOXA1 gene body region upon Nup93 depletion (Figure 3.13A). We detected a specific enrichment of H3K36me3 in the HOXA1 gene body region (Region1-Region3) upon Nup93 depletion (Figure 3.13G). In summary, an active transcription of the HOXA1 gene upon depletion of Nup93 is associated with an increased occupancy of active histone marks and decreased levels of repressive histone marks on its promoter (Figure 3.13H).

### **3.2.12 Nuclear import in cells depleted of Nup93, Nup188 or Nup205**

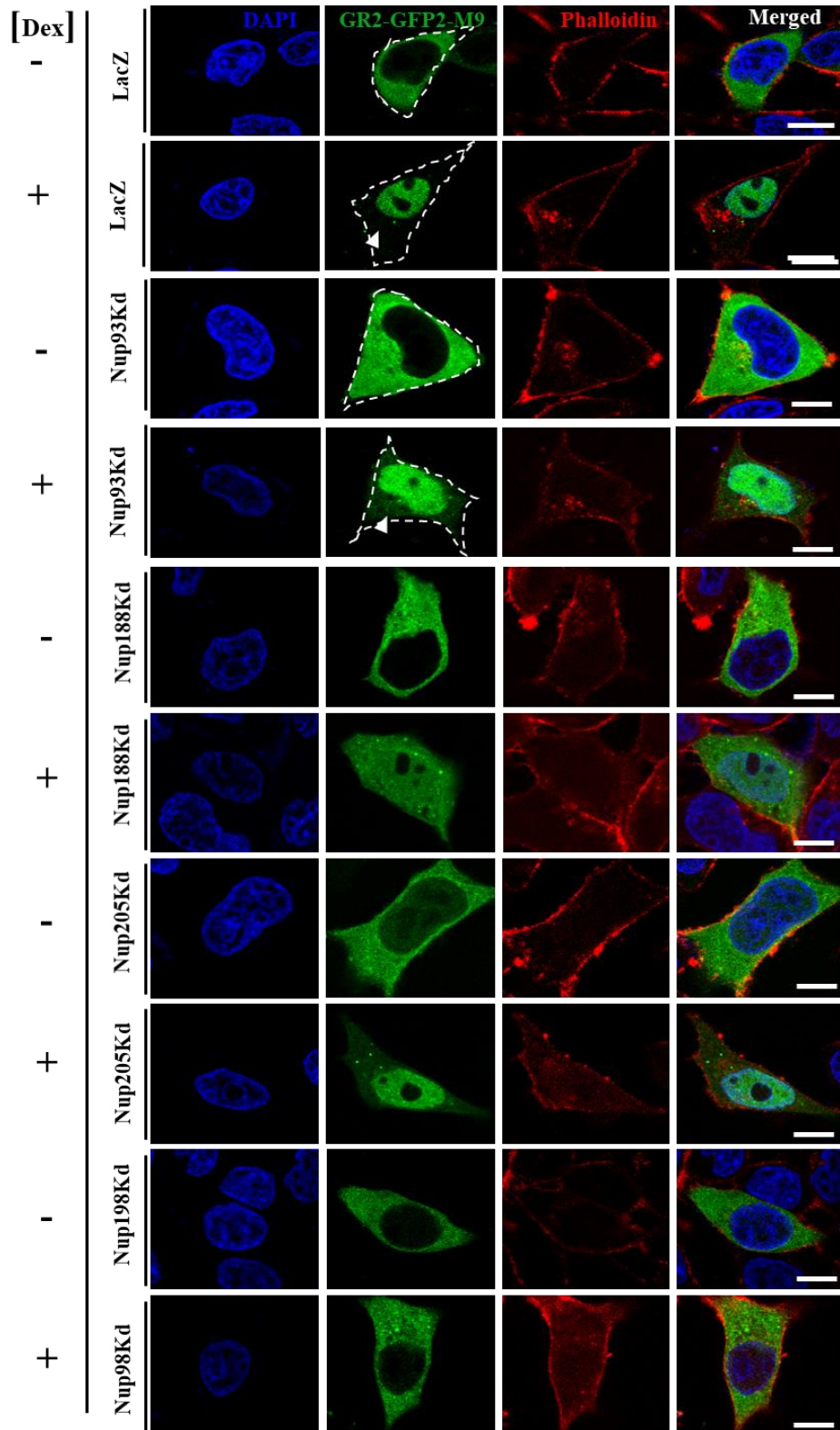
Since the Nup93-subcomplex is a major subcomplex within the nuclear pore complex, we examined the effect of depleting Nup93 and its interactors on nuclear transport. It is possible that altered nuclear transport may affect HOXA gene expression levels. In order to address the role of Nup93 and its interactors in HOXA gene expression, we determined if nuclear transport was affected in cells depleted of Nup93 or either of its interactors Nup188 or Nup205. We determined the effect of Nup93 depletion on nuclear import. We transfected DLD-1 cells with a dexamethasone-inducible reporter construct consisting of the hormone-responsive domain of glucocorticoid and GFP fused to the M9 core domain (GR2-GFP2-M9core). In the absence of dexamethasone, this reporter GFP localizes in the cytoplasm and is translocated in the nucleus in response to dexamethasone treatment. We independently transfected DLD-1 cells with the reporter GFP constructs (GR2-GFP2-M9core) in Nup93, Nup188, Nup205, and Nup98 depleted cells. Next, we quantified nuclear (N)-cytoplasmic (C) ratio (N/C ratio) of reporter GFP in control (LacZ) and Nup depleted cells before and after dexamethasone treatment. We found that the reporter GFP is exclusively localized in the cytoplasm but translocated to the nucleus within ~30 mins of 5 $\mu$ M Dexamethasone (Glucocorticoid hormone analog) treatment in control cells (LacZ) (Figure 3.14 A). Analyses of nuclear to cytoplasmic ratio showed a significant translocation of reporter GFP into the nucleus upon dexamethasone treatment in control cells (LacZ) (Figure 3.14B). Interestingly, Nup93, Nup188 or Nup205 depletion showed a reduced nuclear import of the reporter GFP as compared to control cells (Figure 3.14A and B). Notably, Nup98 depletion inhibited nuclear import of the reporter GFP construct (Figure 3.14A and B) as revealed by the N/C ratio analysis. This result, suggests that

depletion of Nup93 sub-complex reduces the import of reporter GFP. However, Nup93 depletion does not inhibit nuclear import. Furthermore, Nup188 or Nup205 depletion also showed a reduced import, albeit to a lesser extent than Nup93 depletion. In summary, this data suggests that the depletion of individual nucleoporin from the Nup93 subcomplex does not block the nuclear import.

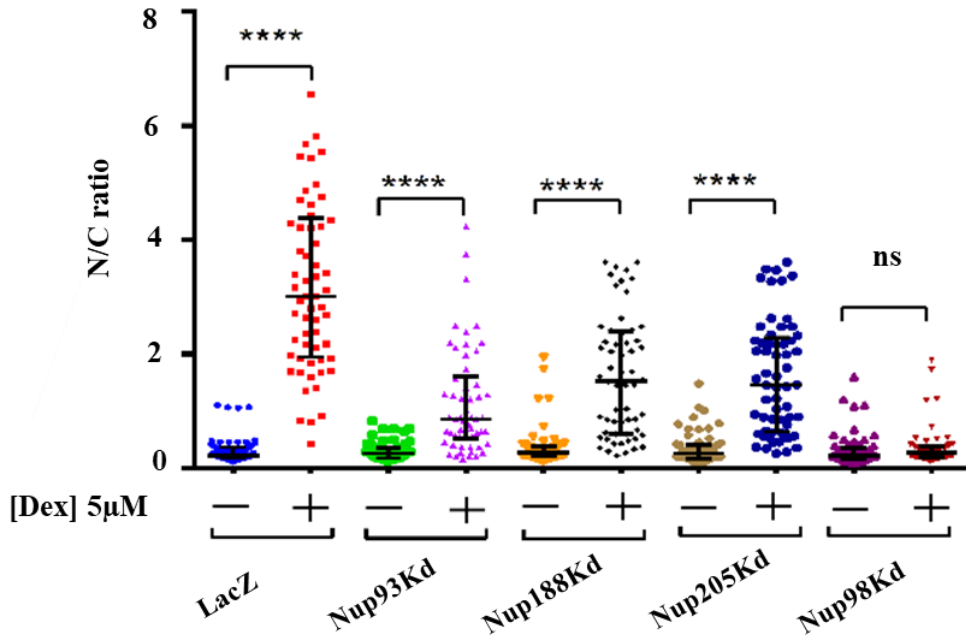
**Figure 3.14**

**A**

**Nuclear import assay**



Scale bar = 10µm

**B**

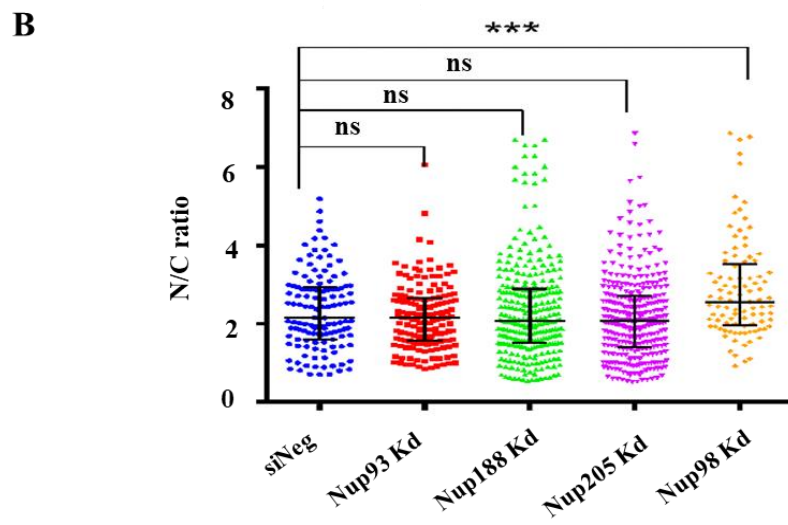
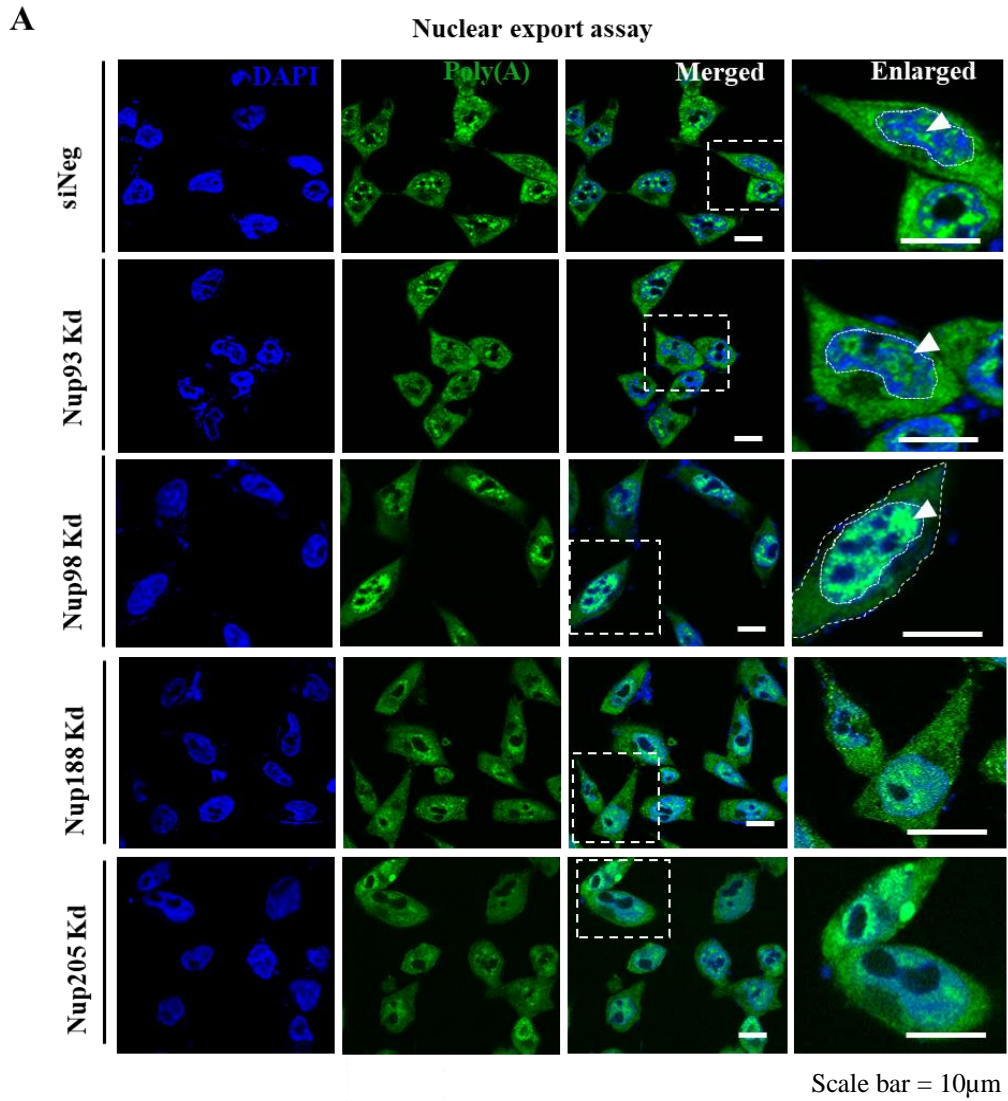
**Figure 3.14. Nup93 depletion reduces nuclear import but does not affect nuclear export:** A) A representative image of nuclear import assay performed using GR2-GFP2-M9 construct transfected in cells treated independently with LacZ-, siNup93-, siNup188-, siNup205-, and siNup98. To induce nuclear import of GR2-GFP2-M9 fusion protein, cells were treated with dexamethasone (Dex) (5 µM) for 30 min, white arrowhead indicates absence of cytoplasmic GFP in LacZ + Dex and residual cytoplasmic GFP in Nup93 Kd + Dex. Scale bar ~10 µm. (63X magnification, zoom 2.5) B) Nuclear/cytoplasmic (N/C) ratio of GR2-GFP2-M9 was determined by quantifying its relative fluorescence intensity in the nucleus and cytoplasm. Scatter plot of GFP signals expressed as nuclear-to-cytoplasmic ratios from LacZ (n = 60 cells), Nup93 Kd (n = 57), Nup188 Kd (n = 60), Nup205 Kd (n = 59) and Nup98 Kd (n = 60), data from 2 independent biological replicates (\*\*\*\*p < 0.0001).

### 3.2.13 Nuclear export in cells depleted of Nup93, Nup188 or Nup205

For the nuclear export assay, we examined the nucleocytoplasmic distribution of fluorescently labeled Poly(A) RNA in Nup93, Nup188 or Nup205 depleted cells (Figure 3.15A and B), since Poly(A) RNA is abundant in cells and is typically associated with mature transcripts (Chakraborty et al., 2006). Poly(A) RNA is detectable within the nucleus as foci and diffusely within the cytoplasm (Figure 3.15A, siNeg panel) (Figure 3.15A). We did not detect a significantly altered distribution of Poly(A) signals in the nucleus or cytoplasm in Nup93, Nup188 or Nup205 depleted cells, as compared to control cells (siNeg, Figure 3.15A and B). This is consistent with a normal nuclear transport in nuclear reassembly assays performed in Nup188-Nup93 immuno-depleted *Xenopus* egg extracts (Theerthagiri et al., 2010). While depletion of Nup98 – an established regulator of nuclear export showed a retention of Poly(A) RNA in the nucleus, evidenced by a significant increase in the nuclear to cytoplasmic ratio of Poly(A) RNA in DLD-1 cells (Figure 3.15 A and B) (Fabre et al., 1994; Powers et al., 1997; Pritchard et al., 1999).

Taken together, these assays suggest that nuclear export was not significantly affected in cells depleted of Nup93 or its interacting partners. Notably, depletion of Nup93 complex proteins does not completely block nuclear import, whereas Nup98 depletion inhibits nuclear import. We conclude that Nup93 and its interactors repress HOXA gene cluster in a manner independent of nuclear transport.

Figure 3.15





(See figure on previous page)

**Figure 3.15. Nuclear Export upon Nup93 complex depletion:** **A)** A representative image of Poly(A) RNA FISH performed using FAM-labeled oligo(dT) probe (green) in siNeg, Nup93 Kd, Nup188 Kd, Nup205 Kd and Nup98 Kd, scale bar ~10  $\mu$ m, white arrowhead indicates Poly(A) RNA foci in the nucleus. Nuclear boundary is marked by dotted line in enlarged panel. Nup98 enlarged panel shows both nuclear and cell boundary with white dotted line. (63X magnification, Zoom 1) **B)** Poly(A) RNA distribution was determined by quantifying its fluorescence intensity in the nucleus and cytoplasm. Scatter plot of Poly(A) signals expressed as nuclear (N)-to-cytoplasmic (C) ratios from siNeg (n = 127 cells), Nup93 Kd (n = 158), Nup188 Kd (n = 288), Nup205 Kd (n = 288); N/C ratio was not significant (ns) when compared to siNeg ( $p > 0.05$ ), while Nup98 Kd (n = 97) shows a relatively higher nuclear-to-cytoplasmic ratio (N/C ratio) of Poly(A) signals (\*\* $p = 0.0017$ ). Two independent biological replicates for siNeg, Nup93 Kd and Nup98 Kd. Data from a single experiment for Nup188 Kd and Nup205 Kd. Horizontal line represents median, p values obtained from Mann–Whitney U test.

### 3.2.14 Nup93 does not interact with CTCF or PRC2 complex proteins

CTCF and PRC2 complex proteins regulate chromatin looping and the expression of the HOXA gene cluster in embryonic stem cells (Li et al., 2011; Narendra et al., 2015; Peña-Hernández et al., 2015; Rousseau et al., 2014; Sakamoto et al., 2007; Vieux-Rochas et al., 2015; Xu et al., 2014). Both CTCF and PRC2 complex proteins associated with the HOXA gene cluster of differentiated and undifferentiated cells. We determined if CTCF or PRC2 complex proteins associate with Nup93 to regulate HOXA gene expression levels in differentiated cells. We performed co-immunoprecipitation assay with Nup93 and checked for the association of CTCF and PRC2 complex proteins (Figure 3.16 A and B). Interestingly, co-immunoprecipitation (Co-IP) assays did not reveal an association between Nup93 and CTCF (Figure 3.16 A), or between Nup93 and PRC2 complex proteins (EED or Suz12) in DLD-1 cells (Figure 3.16 C). Furthermore, we examined the levels of CTCF or the PRC2 complex proteins (EZH2, Suz12, and EED) in Nup93, Nup188 or Nup205 depleted cells. Levels of CTCF or PRC2 complex proteins (EZH2, Suz12, and EED) were unaltered in Nup93, Nup188 or Nup205 depleted cells (Figure 3.16 C). In summary, these

results suggest that Nup93 subcomplex represses HOXA gene cluster independent of its known regulators.

**Figure 3.16**

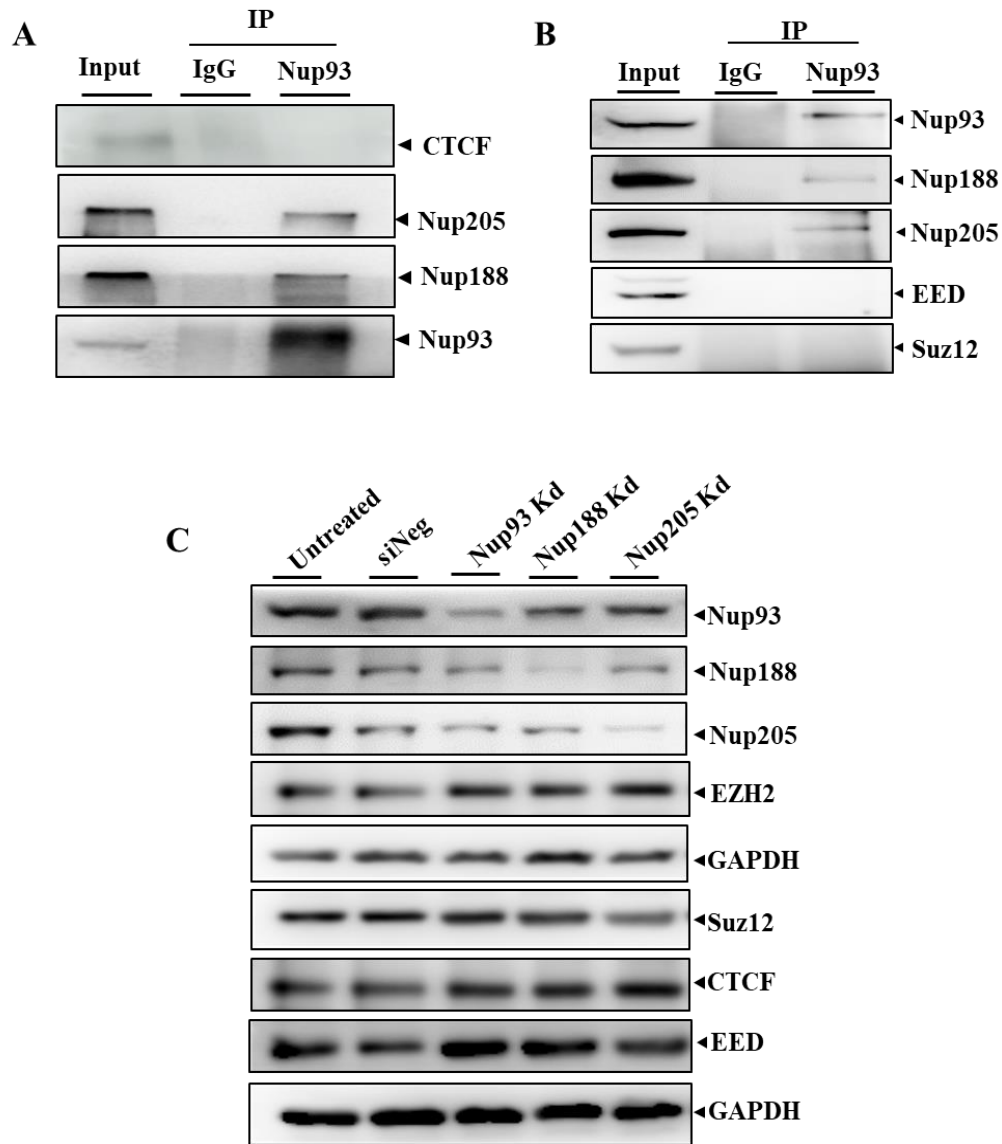


**Figure 3.16. Nup93 does not interact with CTCF or PRC2 complex proteins:** **A)** Co-immunoprecipitation was performed using anti-Nup93 antibody and negative control IgG followed by Western blotting for CTCF, Nup205, Nup188 and Nup93 (data from two independent biological replicates, N = 2), **B)** Co-IP for Nup93 and Western blot for Nup93, Nup188, Nup205 (data from three independent biological replicates, N = 3), PRC2 complex proteins EED and Suz12 (data from a single experiment). **C)** Representative Western blot showing the levels of Nup93, Nup188, Nup205, Nup98, EZH2, Suz12, CTCF, EED upon Nup93, Nup188 and Nup205 Kd (data from a single experiment).

### 3.3 Discussion

Expression of HOXA genes is restricted to early stages of development and differentiation. Aberrant expression of HOXA genes in differentiated cells is associated with disease (Bhatlekar et al., 2014; Bitu et al., 2012; Calvo et al., 2000; Maeda et al., 2005). Mechanisms that control the spatiotemporal expression of HOXA gene cluster are unclear. Moreover, the silenced HOXA gene cluster is organized in the form of a clustered loop in differentiated cells. Although, CTCF and PRC2 complex proteins occupy the silenced HOXA gene cluster, the regulatory role of these proteins in maintaining the silenced state of the HOXA gene locus remains elusive. Here we investigated the role of the stable nucleoporin Nup93 in the regulation of HOXA gene silencing in differentiated DLD-1 cells.

Previous ChIP-chip studies using tiling microarrays of human chromosomes 5, 7 and 16 revealed the association of Nup93 with sub-regions of these chromosomes (Brown et al., 2008). Nup93 was associated with the HOXA sub-cluster of human chromosome 7 (Brown et al., 2008). However, this study did not address the functional implications of Nup93-HOXA association. Here we show that Nup93 associates with the HOXA gene cluster in a manner dependent on its interactors Nup188 and Nup205. Furthermore, depletion of these nucleoporins showed a significant increase in the expression levels of HOXA genes. The upregulation of HOXA genes upon Nup93 depletion was associated with an increase in active histone marks, reduced inactive marks, and enrichment of a transcription elongation mark.

### **3.3.1 Implications of the association of nucleoporins with chromatin**

Several studies across organisms have consistently shown an association of mobile nucleoporins such as Nup98, Nup50 and Nup153 with chromatin in addition to regulating nuclear transport (Van deaaa 1Vosse et al., 2013; Buchwalter et al., 2014; Capelson et al., 2010a; Jacinto et al., 2015; Liang et al., 2013; Light et al., 2013; Vaquerizas et al., 2010). However, the mechanisms by which nucleoporins regulate both nuclear transport and chromatin organization are largely unclear. We corroborated previous findings of Brown et al (Brown et al., 2008) and show that Nup93 indeed associates with the promoters of HOXA1, HOXA3, and HOXA5 and represses HOXA gene expression in terminally differentiated cells (Figure 3.8A-C). Chromatin conformation capture assays (such as 5C) have shown that the silenced HOXA gene cluster adopts a folded loop structure in a human myeloid leukemia cell line THP-1 (Fraser et al., 2009). However, the role of nucleoporins in silencing the HOXA gene cluster is unclear. Interestingly, Nup155 - an interactor of Nup93, also interacts with class-II HDAC4 at the nuclear periphery (Kehat et al., 2011). It remains to be demonstrated if Nup93 associates with histone deacetylases to form a repressive complex during differentiation. Our studies provide evidence to the growing body of literature which reinforces the role of nucleoporins in regulating chromatin organization and gene expression.

Previous findings and co-immunoprecipitation studies reveal an association of Nup93 with its interactors Nup188 and Nup205 (Figure 3.5A and B) (Braun et al., 2016; Grandi et al., 1997; Theerthagiri et al., 2010). We, therefore, tested the potential role of the interactors of Nup93, in regulating its association with HOXA (Figure 3.6C and D).

Interestingly, the protein levels of Nup93, Nup188, and Nup205 are interdependent, suggesting that Nup188 and Nup205 are required for (i) Nup93 to form a stable complex with its interactors (ii) for Nup93 to associate with HOXA (Figure 3.7B and C). This is consistent with a reduced occupancy of Nup93 on the HOXA1 promoter in Nup188 or Nup205 depleted cells (Figure 3.6C and D). This is further supported by (i) a loss of interaction between Nup93 and Nup188 in Nup205 depleted cells (Figure 3.5D) (ii) Nup188 and Nup205 knockdowns independently reduce the levels of Nup93 (Figure 3.7B and C). The effect of the combined depletion of two or more Nups on gene expression or nuclear transport could not be ascertained as this led to massive cell death (>80%).

Regulation of gene expression is typically accompanied by an altered occupancy of active and inactive histone marks on gene promoters (Atkinson et al., 2008; Gonzalez-Sandoval and Gasser, 2016). The active state of the HOXA gene cluster is marked by active histone marks such as H3K9ac and H3K4me3, while the inactive state shows an enrichment of inactive marks such as H3K9me3 and H3K27me3 (Atkinson et al., 2008; Novak et al., 2006; Srivastava et al., 2015). Histone deacetylases and PRC2 complex proteins modify levels of active and inactive histone marks on the HOXA gene cluster in NT2/D1 embryonal carcinoma cells (Xu et al., 2014). We found that active HOXA gene expression upon Nup93 knockdown is associated with (i) an increase in the relative levels of active histone marks (H3K9ac) (ii) a decrease in inactive histone marks (H3K27me3) on the HOXA1 promoter (Fig. 4b-e) and (iii) an increase in the elongation mark (H3K36me3) within the HOXA1 gene (Figure 3.13 B-G). Considering the localization of the HOXA gene cluster on the gene-poor chromosome 7 territory, proximal to the nuclear periphery, we speculate a potential sequestration of the HOXA gene cluster to the nuclear

envelope mediated by Nup93 along with other chromatin-associated proteins (CTCF, HDACs or transcription factors). We surmise that the depletion of Nup93, Nup188 or Nup205 and their reduced stability, enhances the accessibility of the HOXA gene cluster to transcriptional activators and epigenetic modulators that facilitate the untimely expression of HOXA genes – the physiological ramifications of which remain unclear.

### **3.3.2 Role of nucleoporins in nuclear transport and chromatin organization**

Nucleoporins regulate nuclear import and export of mRNA, RNA, and proteins (Wente and Rout, 2010). In addition, various evidences implicate nucleoporins in gene regulation (Arib and Akhtar, 2011; Ibarra and Hetzer, 2015; Ikegami and Lieb, 2010; Kalverda et al., 2010; Köhler and Hurt, 2010; Liang and Hetzer, 2011; Schmid et al., 2006). Furthermore, the composition of the nuclear pore complex (NPC) is variable across cell types, which interestingly has a limited effect on nuclear transport (D'Angelo et al., 2012). In embryonic stem cells, Nup210 is absent but is specifically incorporated into the NPC during differentiation (D'Angelo et al., 2012). In contrast, Nup98 is involved in both nucleocytoplasmic transport and gene regulation (Capelson et al., 2010a; Iwamoto et al., 2010; Liang et al., 2013; Pascual-Garcia et al., 2014), since Nup98 interacts with the mRNA export factor Rae1 and regulates mRNA export (Pritchard et al., 1999). Nup98 associates with developmentally active genes such as *GRK2*, *ERBB4*, *NRG1*, and *DCC* and regulates their expression levels during differentiation (Liang et al., 2013). The Nup98-HOXA9 fusion protein associates with and activates the HOX gene cluster in an untimely manner in mouse embryonic stem cells dependent on the Crm1 protein (Oka et al., 2016). Interestingly, Nup98 depletion in DLD-1 cells does not alter HOXA gene expression

(Figure 3.8D) but altered nuclear transport (Figure 3.14 and 3.15), suggesting an independent role for Nup98 in regulating nuclear transport but not HOXA gene expression in differentiated cells. However, in cells depleted of Nup93, Nup188 or Nup205, nuclear transport was unaffected (Figure 3.14 and 3.15), consistent with previous findings of normal nuclear transport, despite the depletion of Nup188-Nup93 in nuclear re-assembly studies with *Xenopus* egg extracts (Theerthagiri et al., 2010). We have observed that co-depletion of Nup93-Nup188 or Nup93-Nup205 is lethal in DLD-1 cells. Taken together, these findings implicate nucleoporins such as Nup93, as modulators of chromatin organization in differentiated cells in addition to their nuclear transport functions.

### **3.3.3 Potential mechanisms of nucleoporin-chromatin interactions**

The mechanisms by which core nucleoporins associate with DNA are unclear. More importantly, several findings suggest that nucleoporins are involved in chromatin remodeling owing to their association with chromatin modifiers such as the SAGA complex, HDACs, RSC complex, SUMO proteases, SENP1, SENP2 and MSL complex (Van deaaa 1Vosse et al., 2013; Chow et al., 2012; Kehat et al., 2011; Mendjan et al., 2006; Pascual-Garcia et al., 2014; Rohner et al., 2013). Chromatin remodeling complexes such as the SAGA complex - a transcriptional activator, associates with the nuclear pore complex and activates *HXK1*, *INO1* and *GAL* genes when recruited to the NPC (Brickner and Walter, 2004; Casolari et al., 2004; Dieppois and Stutz, 2010; García-Oliver et al., 2012; Light et al., 2010; Rodríguez-Navarro et al., 2004; Taddei et al., 2006). Nup2, Nup60, Nic96, Nup116, Mlp1, and Mlp2 are enriched on transcriptionally active regions in *S. cerevisiae* (Casolari et al., 2004, 2005). Furthermore, ARP6 links the active housekeeping gene *RPPIA*, involved in ribosome biogenesis to the nuclear pore complex

(Yoshida et al., 2010). Nup170p represses ribosomal biogenesis genes and genes on the sub-telomeric region (Van deaaa 1Vosse et al., 2013; Yoshida et al., 2010). Nup120 and Nup133 also core nucleoporins repress *SUC2* gene expression in yeast (Sarma et al., 2011). There are relatively few instances of gene repression mediated by the Nup93 and its interactors. The repression of the HOXA gene cluster in a differentiated cell type such as DLD-1, adds to the repertoire of nucleoporin mediated gene repression events. Analyses of protein-protein interaction networks using BIOGRID (Stark et al., 2006) of human Nup93 shows that Nup93 interacts with chromatin modifiers such as HDAC11, HDAC9, HDAC5 and PCR2 complex proteins - EED and Suz12 (Figure 3.18). It is conceivable that Nup93 and its interactors associate with transcriptional repressors in repressing the HOXA gene cluster in differentiated cells, although we did not uncover a direct association between Nup93 and the chromatin repressive complex (PRC2) (Figure 3.16). ChIP-Mass spectrometric approaches may identify putative interactors of Nup93.



**Figure 3.17**

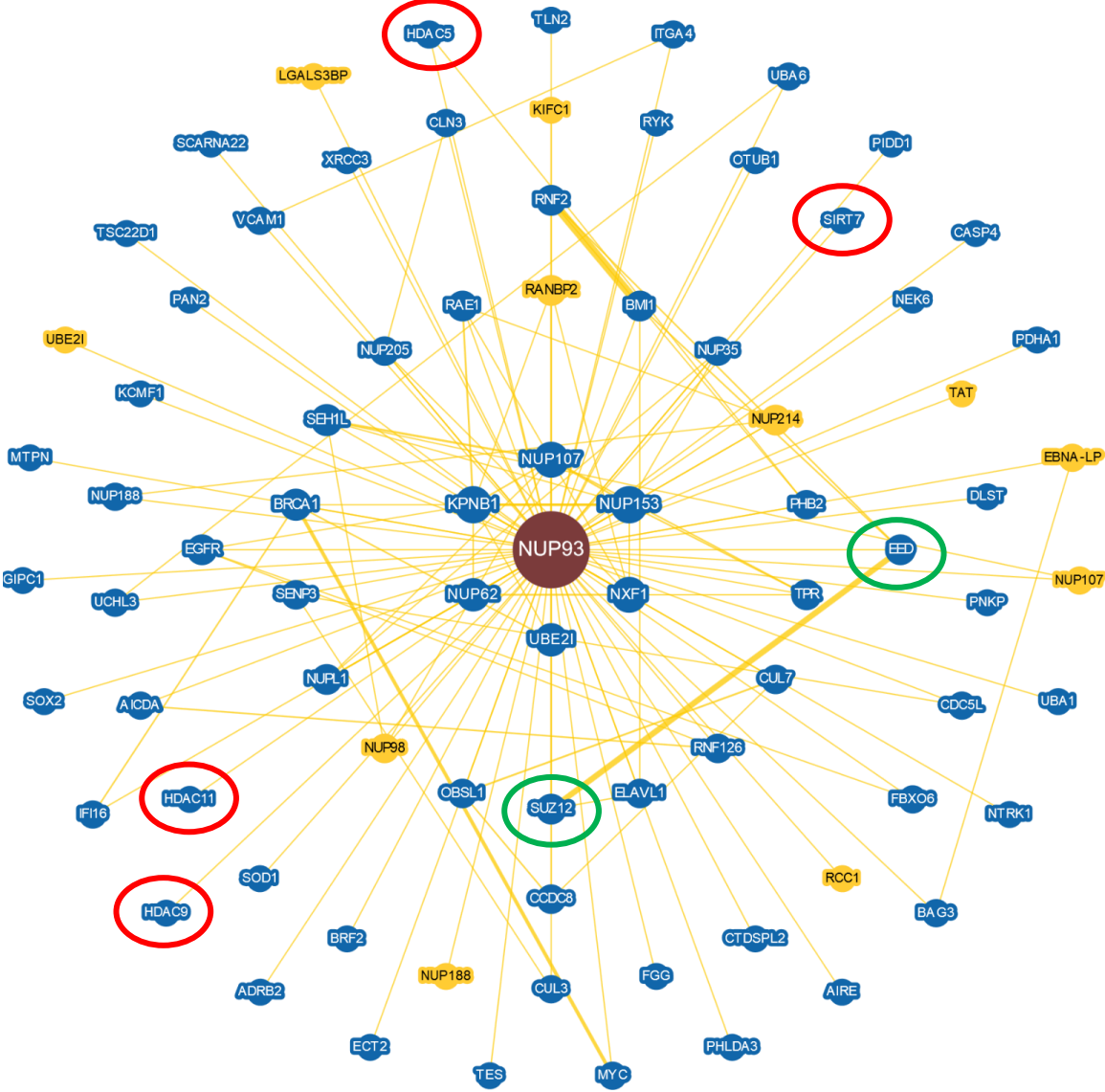


**Figure 3.17. BIOGRID interaction map of Nup93:** Schematic representation of Nup93 interactome using BIOGRID. Only a limited number of protein–protein interactions are shown. Orange lines indicates association with physical evidence. Greater node size represents increased connectivity and thicker edge sizes represent increased evidence supporting the association. Red circles indicate chromatin modifiers and green circle indicates PRC2 complex proteins.

### **3.3.4 Nucleoporins as repressors of HOXA gene expression in differentiated cells**

Regulation of HOXA gene expression is essential during early development since the aberrant expression of HOX genes leads to developmental defects (Aubin et al., 1997; Izon et al., 1998; Seifert et al., 2015). Similarly, HOXA gene silencing is also important in adult tissues since their aberrant expression is associated with various cancers (Bhatlekar et al., 2014). CTCF is an important organizer of 3D architecture and silencing HOXA gene cluster in differentiated cells (Ferraiuolo et al., 2010). Notably, CTCF is associated closer to the 5' region of the HOX gene cluster, in a manner that does not overlap with Nup93 binding sites, suggesting the complementary and potentially independent role of Nup93 and CTCF in the maintenance of HOXA gene repression. However, it is unclear if CTCF silences HOXA gene cluster in differentiated cells by recruiting regulatory proteins such as PRC2. We showed that Nup93 depletion in DLD-1 cells did not alter the levels of CTCF or PRC2 complex proteins - Ezh2, Suz12 and EED (Figure 3.16). We surmise that CTCF or PRC2 proteins may have altered chromatin occupancy in the absence of Nup93 in differentiated cells, distinct from undifferentiated cells (Xu et al., 2014). This raises the remarkable possibility of Nup93 in functioning as a partner of genome organizers in a manner that compensates for the altered occupancy of CTCF in the genome. This remains to be elucidated by ChIP-Sequencing of CTCF or PRC2 complex proteins in the absence of Nup93.

We speculate a novel role for Nup93 and its interactors in regulating chromatin compaction during later stages of differentiation, particularly of genes such as HOXA – as a mechanism that curtails its aberrant expression in differentiated cells (Figure 3.19). Our studies open- up challenging new frontiers for identifying the structural and molecular

mechanisms of nucleoporin mediated chromatin organization and function in paradigms of development, differentiation, and disease.

**Figure 3.18**

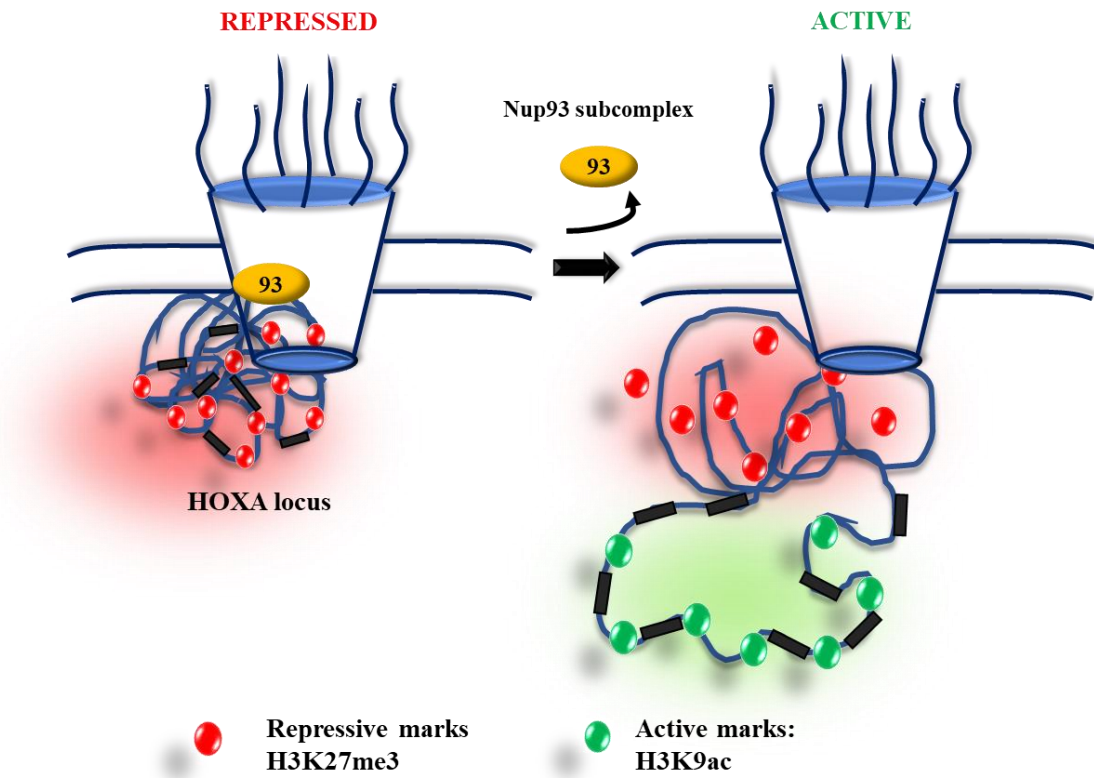


**Figure 3.19: Nup93 mediated silencing of HOXA gene cluster.** A speculative representation of HOXA gene silencing mediated by Nup93 sub-complex. In A repressed state, HOXA genes could be clustered together at the nuclear periphery and tethered by Nup93 subcomplex. Removal of Nup93 or its interactors may lead to opening of HOXA gene cluster and makes it accessible for histone modifying enzymes. Repressive histone marks are then replaced by active histone marks to de-repress the previously repressed HOXA gene cluster

## **Chapter 4: Genome-wide functions of Nup93**

## 4.1 Introduction

Nuclear pore complex is a large protein assembly embedded into the nuclear membrane. It consists of multiple copies of 30 different subunits forming a selective nuclear-cytoplasmic transport channel (D'Angelo and Hetzer, 2008). In addition to their canonical function in nuclear transport, nucleoporins play an important role in gene regulation by associating with chromatin (Capelson and Hetzer, 2009; Capelson et al., 2010a; Ibarra et al., 2016; Kalverda et al., 2010; Sood and Brickner, 2014; Vaquerizas et al., 2010). Various lines of evidence have demonstrated chromatin binding activity of Nups across different systems (Yeast, metazoan, and mammals) and have implicated Nups in the function of gene regulation (Ptak and Wozniak, 2016; Ptak et al., 2014). Based on their stability and location inside the nucleus nucleoporins are classified as 1) the scaffold Nups, which forms highly stable core ring-like structure of the NPC and (2) the peripheral Nups, which forms central channel, inner and outer ring, nuclear basket and cytoplasmic filaments (D'Angelo and Hetzer, 2008).

In mammals, nucleoporin mediated gene expression is not fully understood, and emerging evidence suggests that similar to lower organisms, nuclear pores also regulates gene expression in mammals. The first ChIP-chip (Chromatin immunoprecipitation followed by tiling microarray) study that identified the association of mammalian nucleoporin Nup93 with the genome showed that Nup93 binds to heterochromatic regions on human chromosomes 5, 7 and 16 in HeLa cells (Brown et al., 2008). Notably, this initial finding in HeLa cells suggested that mammalian nucleoporins also associate with chromatin and regulate gene expression (Brown et al., 2008)). Recently, Nup93-DamID seq analysis in U2OS cells unveiled a genome-wide interaction map of Nup93.

Interestingly, this study showed that Nup93 associates with super-enhancers and regulates expression of cell identity genes (Ibarra et al., 2016). Likewise, a transmembrane nucleoporin - Nup210 shows tissue-specific expression and assists in muscle cell differentiation as well as maturation and survival of differentiated cells (D'Angelo et al., 2012; Raices et al., 2017). Depletion of Nup50 in C2C12 cells inhibits its differentiation into myotubes (Buchwalter et al., 2014). Similarly, a mobile nucleoporin Nup98 (a phenylalanine-glycine (FG) repeat-containing nucleoporin) associates with developmental and differentiation-related genes during neuronal differentiation (Liang et al., 2013). Interestingly, Nup98 associates with genes that are in the initial stage of induction at the nuclear periphery and with the induced and active genes in the nuclear interior (Liang et al., 2013). This finding indicates that Nucleoporin might differentially regulate gene expression depending on their spatial localization inside the nucleus. In addition to gene activation, mobile nucleoporins are also implicated in gene repression. The mobile nucleoporin Nup153 represses expression of developmental genes by recruiting PRC2 complex at the promoter of these genes in mouse embryonic stem cells (Jacinto et al., 2015). Altogether, these findings highlight the role of the mammalian nuclear pore complex in gene regulation. However, whether NPC acts as a tether for modulating the regulatory activity of specific genes at the nuclear periphery is unclear. Chromatin immunoprecipitation (ChIP) followed by whole-genome sequencing of Nup93 serves as a useful paradigm to understand the gene regulatory role of Nup93 at the nuclear periphery.

Nup93 is one of the highly stable nucleoporins at the NPC (Daigle et al., 2001). Studies using Fluorescent Recovery After Photobleaching (FRAP) have identified that Nup93 has the highest residence time at the NPC with the lowest diffusion rate ( $K_{\text{off}}$ :  $4.0 \pm$

$3.4 \times 10^{-6} \text{ s}^{-1}$ ) (Rabut et al., 2004). Because of its high stability, low diffusion rate and lack of mobility, Nup93 function as a potential anchor for chromatin at the nuclear periphery. However, the organization of chromatin inside the nucleus may determine the specific association of nucleoporins with the chromatin, considering that chromosome territories are non-randomly organized in the interphase nucleus (Misteli, 2013). Interestingly, the positioning of chromosomes and genes inside the nucleus correlates with their transcriptional activity (Ranade et al., 2017; Talamas and Capelson, 2015). Gene poor chromosomes localize at the nuclear periphery while gene-rich chromosomes occupy the nuclear center. Considering the stable localization of Nup93 at the nuclear pore, we surmise that Nup93 is likely to associate predominantly with peripheral chromatin in the nucleus.

We investigated into the genome-wide binding propensity of Nup93 using ChIP-Sequencing. Here we show that Nup93 shows an association with all human chromosomes except the human X-chromosome. Further, we found that Nup93 associates with developmentally regulated genes. Moreover, ChIP-seq analysis revealed that Nup93 associates with chromatin enriched for repressive histone mark H3K27me3. Furthermore, Nup93 binding sequences significantly overlap with the binding sites of CTCF - a well-established organizer of the genome. In summary, these findings uncover a previously uncharacterized role of Nup93 in functioning as genome organizer and particularly of genes involved in the regulation of developmental processes.

## **4.2 Results**

### **4.2.1 Validating the specificity of Nup93 antibody ChIP-sequencing**

The success of any Chromatin Immunoprecipitation experiment is primarily governed by the quality of the antibody. Antibody quality is determined by its specificity and degree of enrichment in an immunoprecipitation experiment. Lack of specificity leads to cross-reactivity of the antibody with other DNA associated proteins while poor pull-down efficiency leads to the failure of ChIP experiments. For these reasons, we followed a set of working standards and guidelines of antibody characterization provided by ENCODE (Landt et al., 2012). We have performed a set of experiments to validate Nup93 antibody as suggested by ENCODE. 1) Immunoblotting showing a single band corresponding to Nup93, 2) siRNA mediated knockdown of Nup93, showing a marked (70%) decrease in protein levels upon immunoblotting, 3) Immunoprecipitation showing that the antibody specifically pulls down the cognate protein, which is sufficiently enriched over IgG, 4) Immunofluorescence assay showing the sub-nuclear localization of Nup93 at the nuclear envelope. We have performed these experiments in multiple independent biological replicates to validate the antibody against Nup93 before employing the same for ChIP-Sequencing.

#### **A) Nup93 antibody specifically recognizes Nup93 protein**

We sought to examine the specificity of Nup93 antibody using whole cell lysates prepared from DLD-1 cells. We performed immunoblotting and detected a single band corresponding to Nup93 at a molecular weight ~100 kDa at all different dilutions of



antibody. Together, this result suggests the specificity of a Nup93 antibody which is a prior requirement of ChIP-seq experiment.

### B) siRNA mediated knockdown of Nup93

We performed siRNA mediated knockdown of Nup93 using two different siRNA oligos, with a concentration gradient from 20 nM to 150 nM. Independently, scrambled siRNA and non-targeting siRNA served as negative controls. Transfection was performed for six hours, and the cell lysate was prepared after 48 hours of incubation. Both siRNA oligos showed significant knockdown of Nup93 above 20 nM (Figure.4.1 C).

**Figure 4.1**

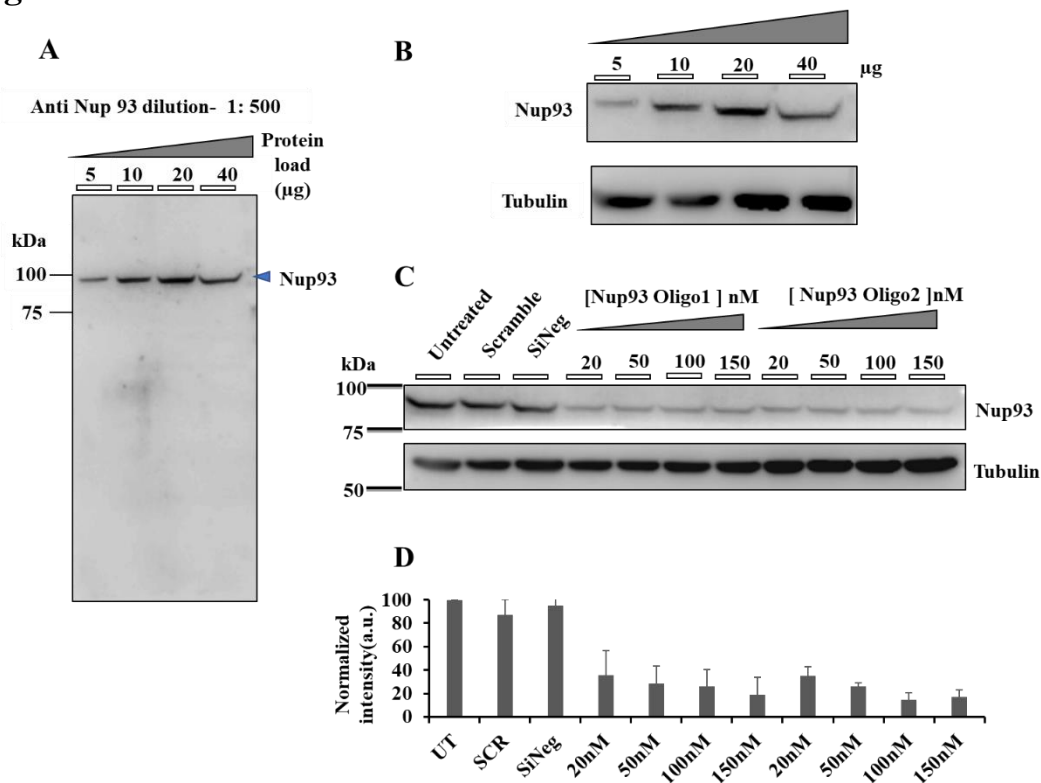


**Figure 4.1. Specificity of Nup93 antibody:** **A)** Full Immunoblot with increase in protein load showing specificity of Nup93 antibody with single band at 100kDa, **B)** Enlarged image of Nup93 with Tubulin as an internal control, **C)** Immunoblot showing the knockdown of Nup93 using two (Oligo1 and Oligo2) different siRNA oligos at different concentrations. Tubulin served as a loading control. **D)** Western blot quantification of knockdown from two independent biological replicates. Graph represents normalized band intensity compare to untreated (UT). Error bar= standard deviation (S.D.)

### C) Depletion of Nup93 does not affect cell viability

The viability of DLD-1 cells was assessed upon knockdown of Nup93 using MTT assay. We used a concentration gradient of siRNA oligos from 10 nM to 200 nM. Cells were also treated with 100 nM of scrambled (SCR) and non-targeting oligos (siNEG) and an oligo targeting the Polo-like Kinase-1 gene (PLK-1), which served as a positive control. Cell viability assays were performed at the end of 48h of siRNA transfection. At the highest concentration of oligo, cell viability was ~57% (Figure 4.2). Cell viability assay, at the end of 48h of transfection, does not show a significant decline in the viability of DLD-1 cells, suggesting that Nup93 knockdown does not appreciably affect cell viability. In contrast, knockdown of an essential gene *PLK-1* drastically reduces cell viability to ~30-35%,

**Figure 4.2**

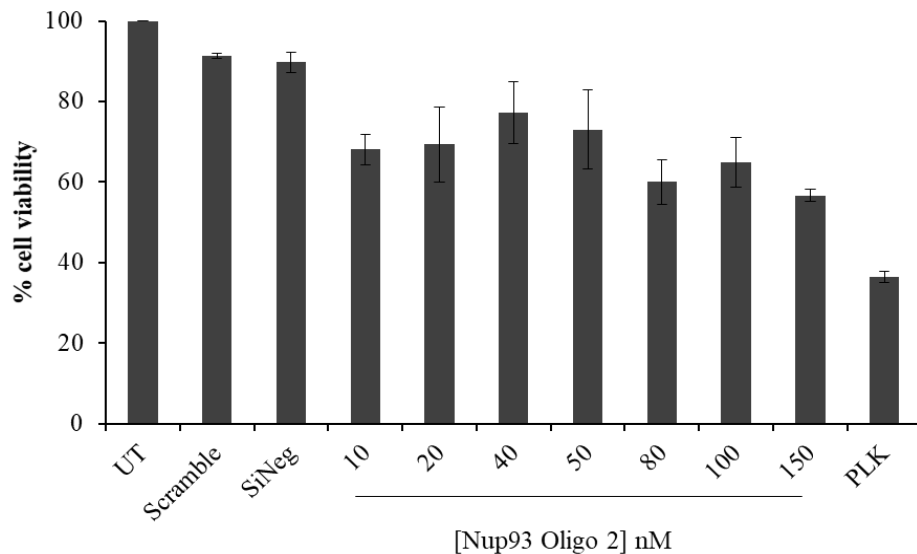


**Figure 4.2. Cell viability upon Nup93 knockdown:** Plot shows viability of DLD1 cells estimated by MTT assay upon Nup93 knockdown using different concentrations (10 -150nM) of siRNA oligo 2. N=3, Error bar -S.E.M

showing effective transfection efficiency under similar conditions in DLD-1 cells (Figure 4.2).

#### D) Nup93 is enriched in the nuclear extract

Since nuclear pore proteins are confined to the nuclear envelope, we were curious to examine the abundance of Nup93 in nuclear fraction and a cytoplasmic fraction. We separated the nuclear and cytoplasmic fractions followed by western blotting and found that Nup93 highly enriched in the nuclear fraction as compared to the cytoplasmic fraction (Figure 4.3). To establish the purity of the extracts, we used Lamin B1 and paxillin as a marker for the nuclear fraction and cytoplasmic fraction. Lamin B1 was hardly detected in cytoplasmic extract and similarly, paxillin was not detectable in nuclear extract suggesting that the cytoplasmic and nuclear fraction is pure (Figure 4.3). Glyceraldehyde

**Figure 4.3**

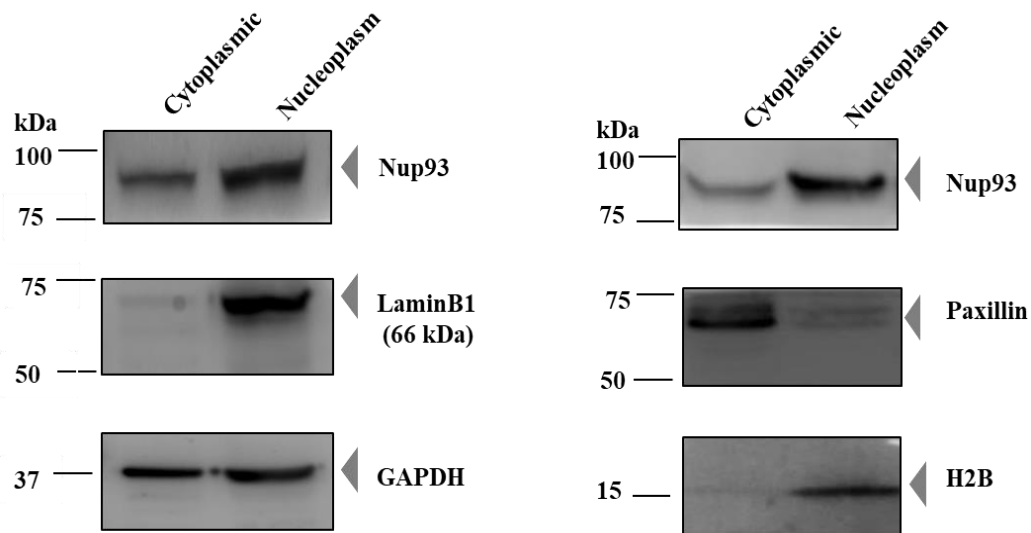


**Figure 4.3. Nuclear cytoplasmic extraction:** Western blot image of nuclear and cytoplasmic distribution of Nup93. Lamin B1 and H2B were used as a nucleoplasmic control and paxillin was used as a cytoplasmic control.

dehydrogenase phosphate is present in both the extracts at similar levels as reported (Figure 4.3) (Krynetski et al., 2001).

### E) Immunofluorescence assay (IFA)

IFA was performed on control DLD-1 cells and Nup93 knockdown cells. DLD-1 cells were fixed with 4% PFA and stained with Mab414 (Nuclear pore complex antibody) and anti Nup93 antibody. Nuclei were counterstained with DAPI. IFA assay showed that Nup93 antibody specifically stained Nup93 at the nuclear periphery (Figure 4.4). Knockdown of Nup93 showed a marked decrease in Nup93 staining further confirming the specificity of the Nup93 antibody (Figure 4.4).

**Figure 4.4**

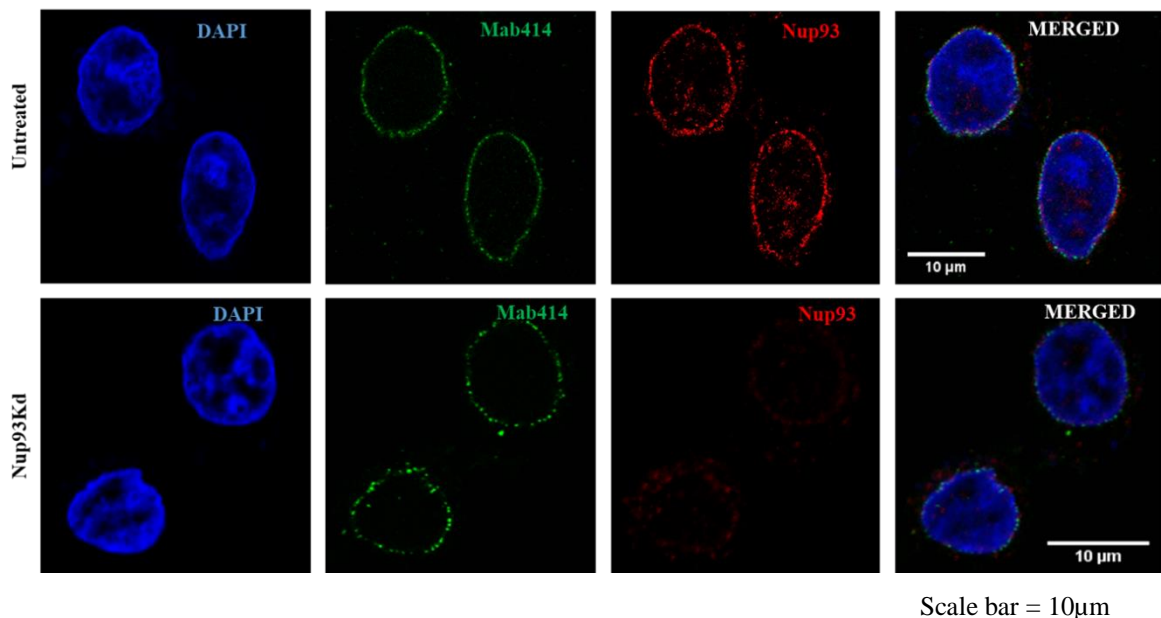


**Figure 4.4. Immunofluorescence assay:** DLD1 cells stained with DAPI (Blue), anti-nuclear pore complex antibody (Mab414, Green) and Nup93 antibody (Red). Upper panel- Untreated cells, lower panel- Nup93 knockdown cells (63X magnification , zoom 2.5)

## F) Immunoprecipitation of Nup93 with ChIP buffer

Before performing ChIP experiment, we determined the immunoprecipitation efficiency of Nup93 antibody in sonication buffer used in ChIP protocol. We performed immunoprecipitation of Nup93 from the whole-cell lysate of DLD-1 cells prepared in sonication buffer. We used the same buffer composition and conditions that were used for ChIP experiments. Several pilot experiments were performed to standardize salt

**Figure 4.5**

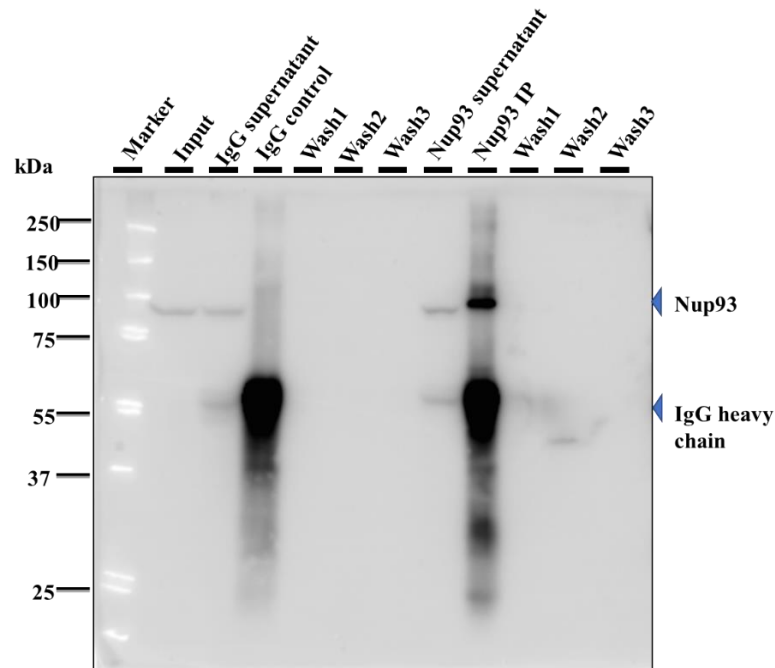


**Figure 4.5. Immunoprecipitation of Nup93:** Immunoprecipitation of Nup93 was performed in ChIP buffer. All samples including Input, IgG supernatant (leftover supernatant from control IgG sample), three washes of control IgG, Nup93 supernatant (leftover supernatant from Nup93 IP), Nup93 IP and three washes from Nup93 IP sample. Nup93 antibody specifically immunoprecipitated Nup93 (Nup93 IP lane). Significant pull-down of Nup93 was observed as compared to control IgG. Immunoprecipitation was performed using 2 $\mu$ g of antibody for 500 $\mu$ g of total protein.

concentrations, incubation time and washing conditions. Normal rabbit IgG was used as a control. Immunoprecipitation was performed using 2 $\mu$ g of antibody for 500 $\mu$ g of total protein. A single prominent band of Nup93 was observed in Nup93 pulled down a fraction as against IgG control (Figure 4.5).

#### **4.2.2 Optimizing chromatin immunoprecipitation assay to determine putative chromatin binding sites of Nup93**

To identify genome-wide occupancy of Nup93, we optimized the chromatin immunoprecipitation assay for Nup93. We crosslinked DLD-1 cells with 1% formaldehyde, cross-linking time, sonication frequency and elution conditions were optimized in pilot experiments. 10 minutes and five rounds (10 min each with the 30s on/off) of sonication produces DNA fragments between ~100 to 500 bp (Figure 4.6 A). To validate the ChIP experiment, we performed ChIP PCR for known targets of Nup93. We designed ChIP-PCR primers on the promoter regions HOXA1, HOXA3, HOXA5 and CFTR genes. The promoter region of GLCCI1 was selected as negative control. ChIP-PCR data showed that Nup93 ChIP DNA was enriched on promoter regions of its binding targets - HOXA1, HOXA3, HOXA5 and CFTR (Figure. 4.6 B). The GLCCI1 (negative control) did not show an enrichment of Nup93 on its promoter (Figure. 4.6B). PanH3 (Positive control) showed a significant enrichment on the promoters of all genes (Figure. 4.6B). We did not observe any enrichment for IgG (Figure. 4.6B). In conclusion, Nup93 ChIP-PCR showed a specific enrichment of Nup93 on its known targets, thereby validating the ChIP experiment.

**Figure 4.6**

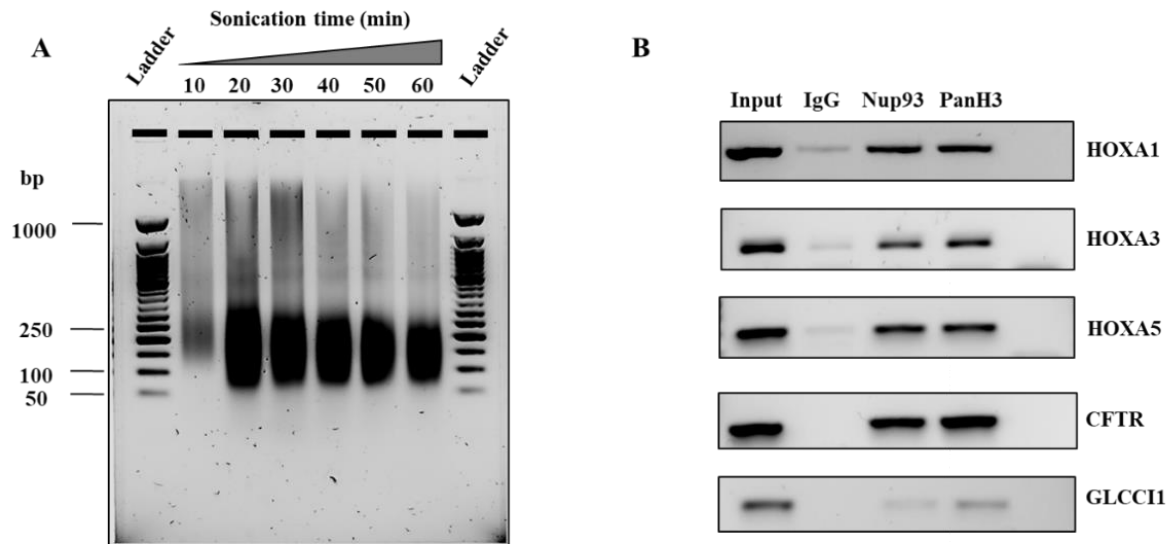


**Figure 4.6. Standardization of ChIP:** **A)** Optimization of sonication time using bioruptor. 40 minutes of sonication at high frequency gives optimum chromatin size between 100-300bp. **B)** ChIP-PCR for known targets of Nup93 (HOA1, HOXA3, HOXA5 and CFTR). GLCCI served as a negative control.

#### 4.2.3 Analysis of ChIP Seq data to investigate the genome-wide binding of Nup93

**A) Quality control:** ChIP DNA from two independent biological replicates was outsourced for sequencing to Genotypic. Pair-end sequencing was performed on Illumina2500 platform. We followed standard ChIP-seq analysis pipeline for analysis (Figure.4.7). Initially, we performed quality control checks on raw sequencing data using FastQC. The FastQc report did not show any problem related to sequencing or library

preparation (Table 4.1). All major quality control checks including per base sequencing quality, per sequence quality score, sequence length distribution were passed.

**Figure 4.7**

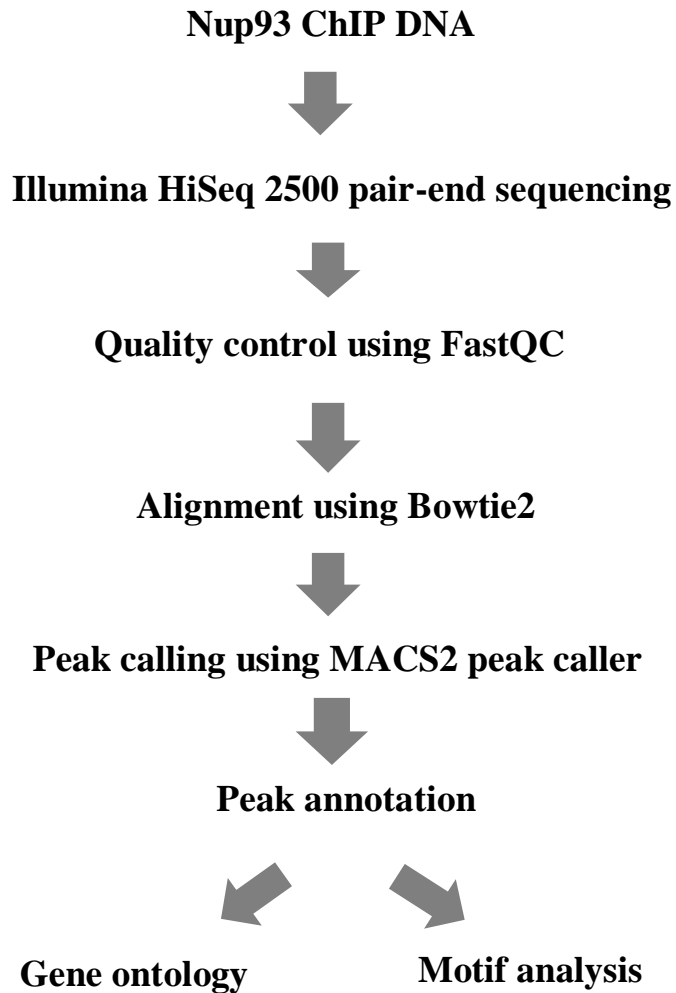


**Figure 4.7: Nup93 ChIP seq analysis pipeline**



**Table 4.2 Details of FastQC reports**

FastQC report	Input Forward	Input Reverse	Rep-1 Forward	Rep-1 Reverse	Rep-2 Forward	Rep-2 Reverse
Basic Statistics	PASS	PASS	PASS	PASS	PASS	PASS
Per base sequence quality-	PASS	PASS	PASS	PASS	PASS	PASS
Per tile sequence quality	Warning	PASS	Warning	Warning	Warning	Warning
Per sequence quality scores	PASS	PASS	PASS	PASS	PASS	PASS
Per base sequence content	Warning	Warning	Warning	Warning	Warning	Warning
Per-sequence GC content	Warning	Warning	Warning	Warning	Warning	Warning
Per base N content	PASS	PASS	PASS	PASS	PASS	PASS
Sequence Length Distribution	PASS	PASS	PASS	PASS	PASS	PASS
Sequence Duplication Levels	PASS	PASS	PASS	PASS	PASS	PASS
Overrepresented sequences	PASS	PASS	Warning	Warning	Warning	PASS
Adapter Content	PASS	PASS	PASS	PASS	PASS	PASS
Kmer Content	FAILED	FAILED	FAILED	FAILED	FAILED	FAILED

**B) Alignment:** Raw FastQ sequences were aligned to the latest human genome assembly hg19 using Bowtie2 sequence aligner. Alignment results showed that >67% reads were perfectly aligned to the human genome confirming high sequencing depth (Table 4.3, Figure. 4.8 A). BAM files generated after alignment for each replicate were compared with each other to determine the correlation between two independent biological replicates. We performed correlation analysis using an open source web-based platform GALAXY. Two

biological replicates were examined with each other using the multiBamSummary tool under NGS deepTools package on the galaxy. The two independent ChIP-seq replicates showed a significant correlation with one another (Pearson correlation coefficient- 0.97) (Figure. 4.8 B). In addition, we visualized raw BAM files on UCSC genome browser and observed a high level of correlation at each genomic position (Figure. 4.8 C). We performed further analyses with replicate 2.

**Table 4.3 Details of alignment result**

<b>Read alignment</b>	<b>Input</b>	<b>Replicate-1</b>	<b>Replicate-2</b>
Aligned concordantly 0 times	7932825	13692901	7713455
Aligned concordantly exactly 1 time	56235663	50453796	24564814
Aligned concordantly >1 times	9497806	8294016	4345938

**C) Peak calling:** Peak calling was performed using the model-based analysis of ChIP-Seq MACS (Zhang et al., 2008). Detailed list of parameters used for peak calling is given in materials and methods. We used different criteria such as tag density, fold enrichment over input and p-value and false discovery rate (FDR) to enrich for significant peaks out of false peaks. We identified 404 peaks with a significantly enriched peak (mfold >20). To further establish the quality of our ChIP-seq experiment, we examined peaks from both the replicates using the UCSC genome browser. Consistently, clear peaks could be identified in both the replicates matching to the same genomic position providing initial confidence in the data (Figure 4.8 C).

**Figure 4.8**

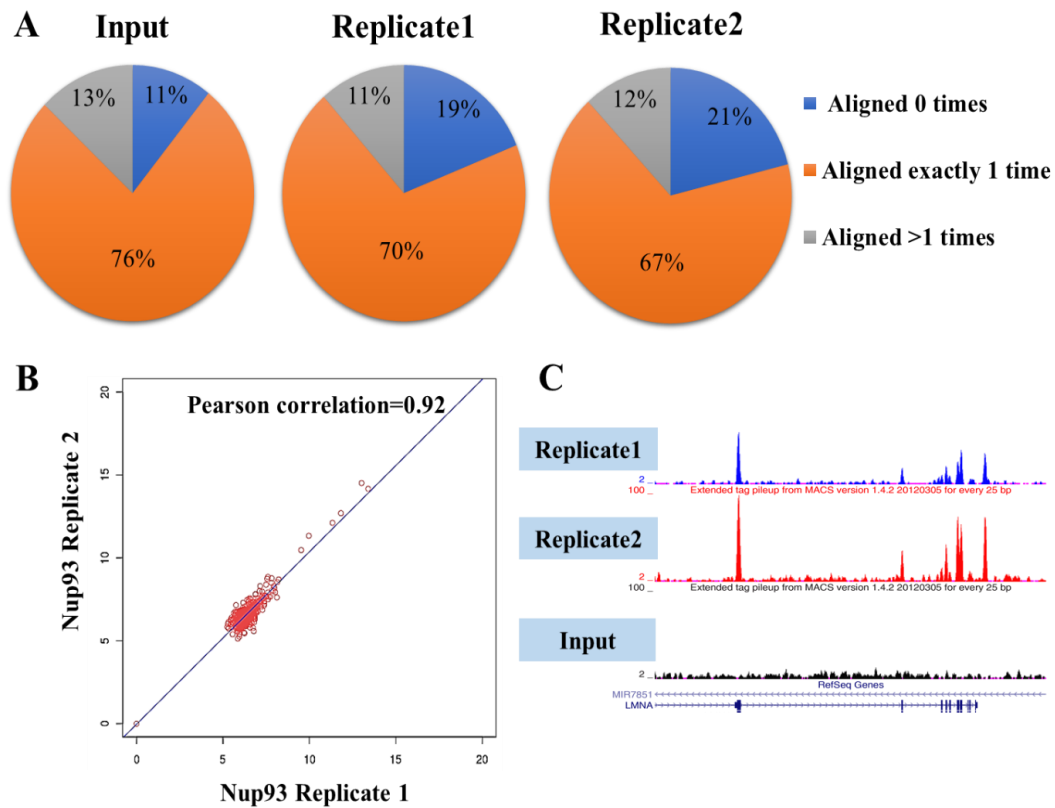


**Figure 4.8. Alignment of ChIP seq reads to Human genome:** **A)** Raw ChIP-seq reads were aligned to Human genome (hg19 assembly) using Bowtie2 aligner. Pie chart showing percentage of perfectly aligned sequences from Input, Replicate1 and Replicate 2. **B)** Two BAM files from replicate1 and replicate2 were correlated with each other to determine to correlation between two replicates. Pearson correlation coefficient between replicate is 0.92. **C)** UCSC genome browser view of both replicates at LMNA gene locus. Peaks from bothe replicates showed high level of correlation at the genomic locus

#### 4.2.4 Mapping of Nup93 peaks to the human genome

We performed annotation of Nup93 ChIP seq peaks using Cis-regulatory Element Annotation System (CEAS)(Shin et al., 2009). These results revealed that Nup93 associates with and associates with all chromosomes in the human genome (Figure. 4.9). Percent occupancy of Nup93 on each chromosome is variable. We compared percent mappable regions (Blue bars) with percent Nup93 ChIP regions (Brown bars) on each chromosome (Figure. 4.9). We found that Chromosome 2 showed the highest percentage of Nup93 ChIP regions (10.9%) with the p-value of 0.048 as compared % mappable regions on Chromosome 2 (Figure. 4.9). Chromosome 16 showed a significant occupancy of Nup93 (p-value -  $1.9e^{-6}$ ) as compared to total mappable regions on that chromosome (Figure. 4.9). Surprisingly, despite its peripheral organization, chromosome X showed the least binding of Nup93 as compared to all other chromosomes (Figure. 4.9). We asked if the occupancy of Nup93 correlates with gene density of each chromosome. This analysis showed that the occupancy of Nup93 does not correlate with the gene density (Figure. 4.10A). Gene dense chromosome 19 showed ~8.29 % occupancy of Nup93, while the gene-poor chromosome 13 showed ~6.28% occupancy of Nup93 (Figure. 4.10 A). We asked if Nup93 occupancy correlates with chromosome size. Nup93 occupancy does not correlate with chromosome size. While, chromosome 2 showed the highest occupancy of Nup93 followed by chromosomes 1, 11, 16, 17 and 19. We compared our ChIP-seq data with previously published Nup93 DamID data in U2OS cells for chromosomal occupancy

(Ibarra et al., 2016). We found that Nup93 DamID data did not show any correlation between Nup93 occupancy and gene density or chromosome size (Figure. 4.10).

**Figure 4.9**

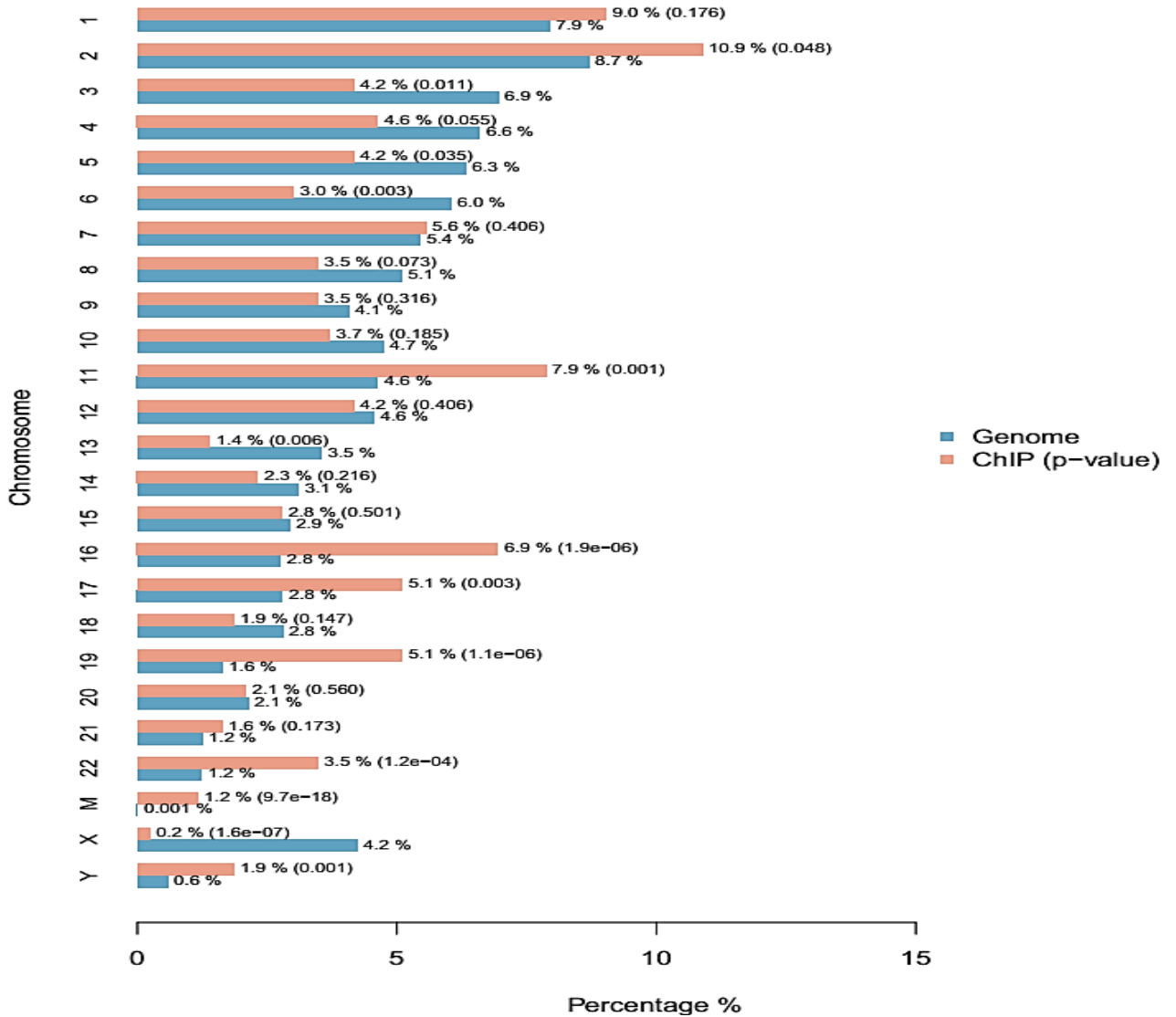
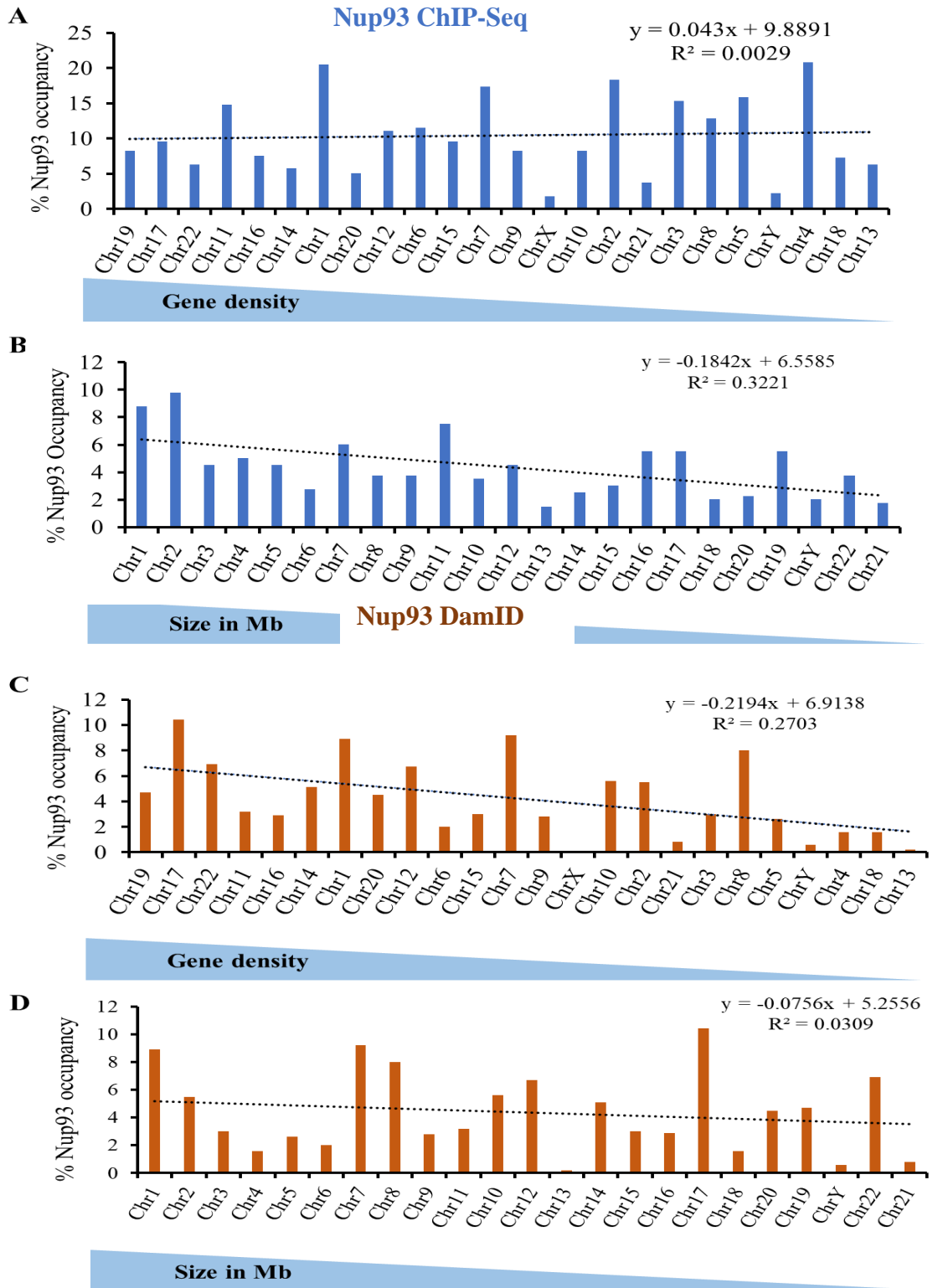


**Figure 4.9. Chromosomal distribution of ChIP regions:** The blue bars represent the percentages of the whole tiled or mappable regions in the chromosomes (genome background) and the brown bars the percentages of the Nup93 ChIP. P-values for the significance of the relative enrichment of ChIP regions with respect to the genome background are shown in bracket next to the percentages of the red bars.

**Figure 4.10**



(See figure on previous page)

**Figure 4.10. Nup93 occupancy is not correlated to gene density or chromosomal size:** **A)** Percent Nup93 occupancy (ChIP-seq data) Vs. Gene density plot for all chromosomes. **B)** Percent Nup93 occupancy (ChIP-seq data) Vs. Chromosomal size plot for all chromosomes. **C)** Percent Nup93 occupancy (DamID data) Vs. Gene density plot for all chromosomes **D)** Percent Nup93 occupancy (DamID data) Vs. Chromosomal size plot for all chromosomes

**Figure 4.11**

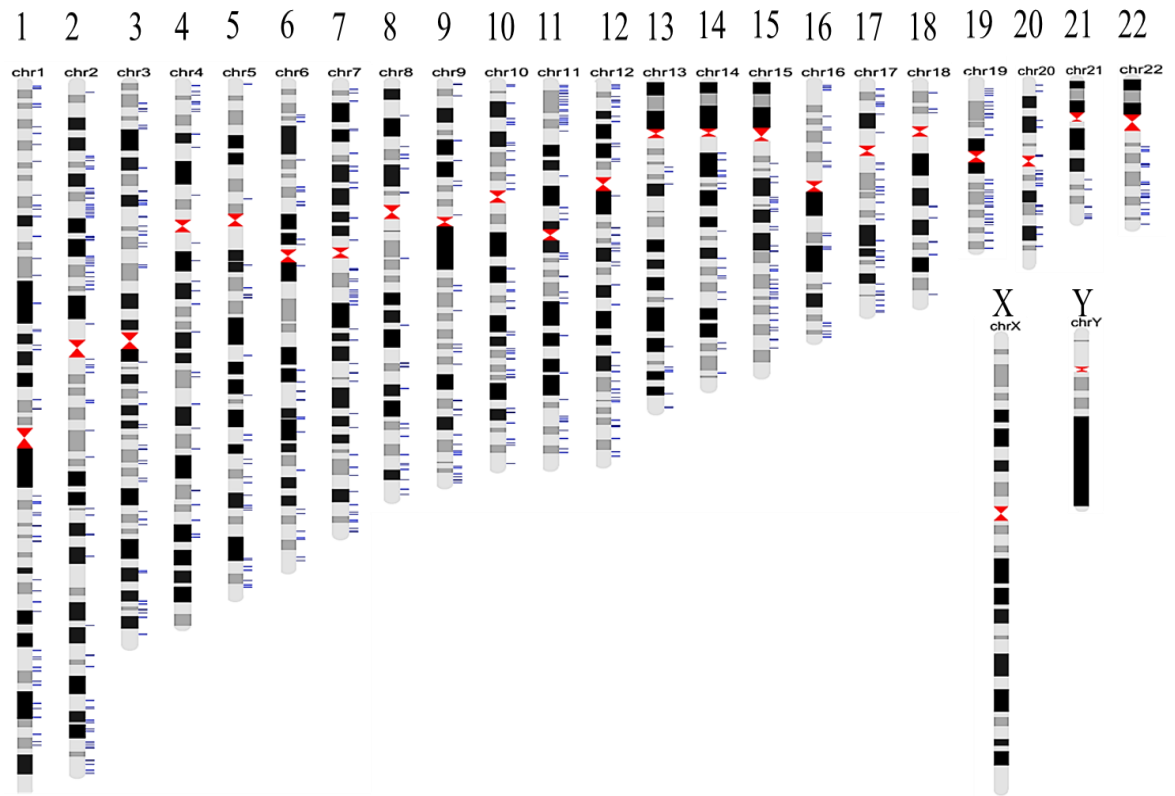


**Figure 4.11. Ideogram representing position of Nup93 peaks on all chromosomes:** Top 404 peaks of Nup93 are mapped to every human chromosome. Peak positions are shown by blue bars.

#### 4.2.5 Characterizing the location of Nup93 peaks

The locations of the high-confidence peaks were mapped to the nearest TSS of Ensembl annotated genes. Nup93 was found to enrich at intergenic regions (46%) or intronic regions (34%) of the genome (Figure. 4.12A). Interestingly, only 12% peaks of Nup93 enriched upstream or downstream ( $\pm 3$ kb from TSS, 8% Upstream + 4% Downstream) of the TSS of annotated genes, suggesting an active role of Nup93 in gene regulation (Figure. 4.12 A and B). We next examined the average profile of Nup93 on exon and intron, Nup93 is enriched at the exon or intron boundary suggesting an association of Nup93 at intron-exon junctions (Figure. 4.11C and D). Average peak size of Nup93 was  $\sim 750$ bp as revealed by peak length distribution graph (Figure 4.12 E).

We further examined the relative enrichment of Nup93 peaks in genomic features such as promoters, downstream of genes, and gene bodies (Figure 4.13). Nup93 is enriched on the promoter (Figure. 4.13) (5.8% of ChIP regions within  $\leq 1000$  bp compared to 1.1 % of the genome background) but relatively reduced enrichment in gene body region (44.9 % of Nup93 peaks as compared to 46.2% of genomic background) (Figure. 4.13). In addition, it was also observed that Nup93 associates with bidirectional promoters (Figure. 4.12). Altogether, 46% overlapped with conserved intergenic regions, suggesting that either Nup93 may act at remote distances from genes or Nup93 helps in regulation of chromatin architecture at noncoding regions. However, 12% of Nup93 binding are preferentially located close to an annotated TSS across the genome. In summary, an association of Nup93 with promoters and intron-exon junction suggests a regulatory role for Nup93 in gene regulation.



**Figure 4.12**

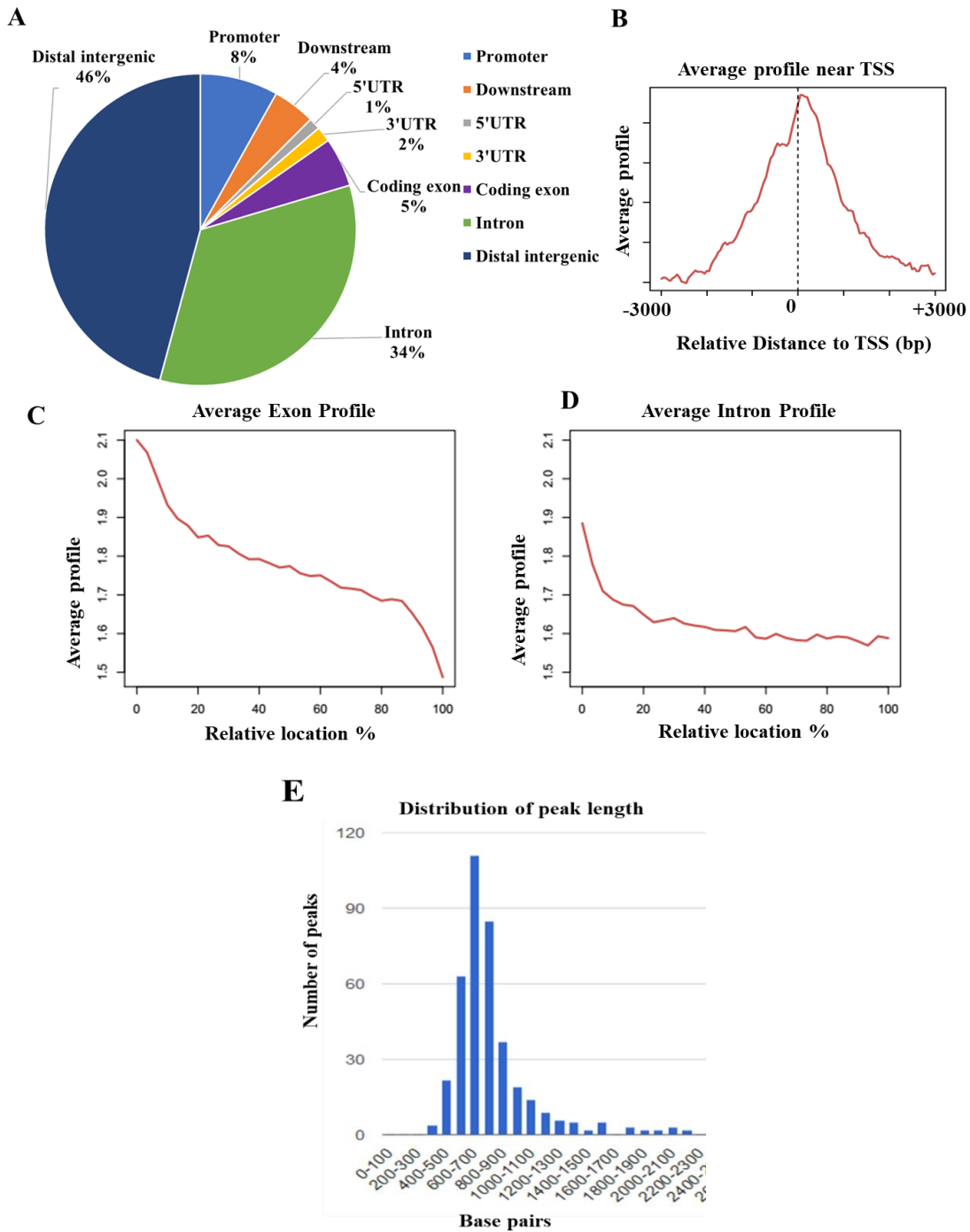


**Figure 4.12. Relative enrichments of Nup93 in important genomic features:** **A)** Pie chart showing enrichment of Nup93 peaks in different genomic regions, **B)** Average profile of Nup93 peaks around the TSS of known genes, **C)** Average profile of Nup93 peaks around the exon boundary, **D)** Average profile of Nup93 peaks around intron boundary, **E)** Peak length distribution of Nup93 peaks (Average peak length is 750bp).

**Figure 4.13**

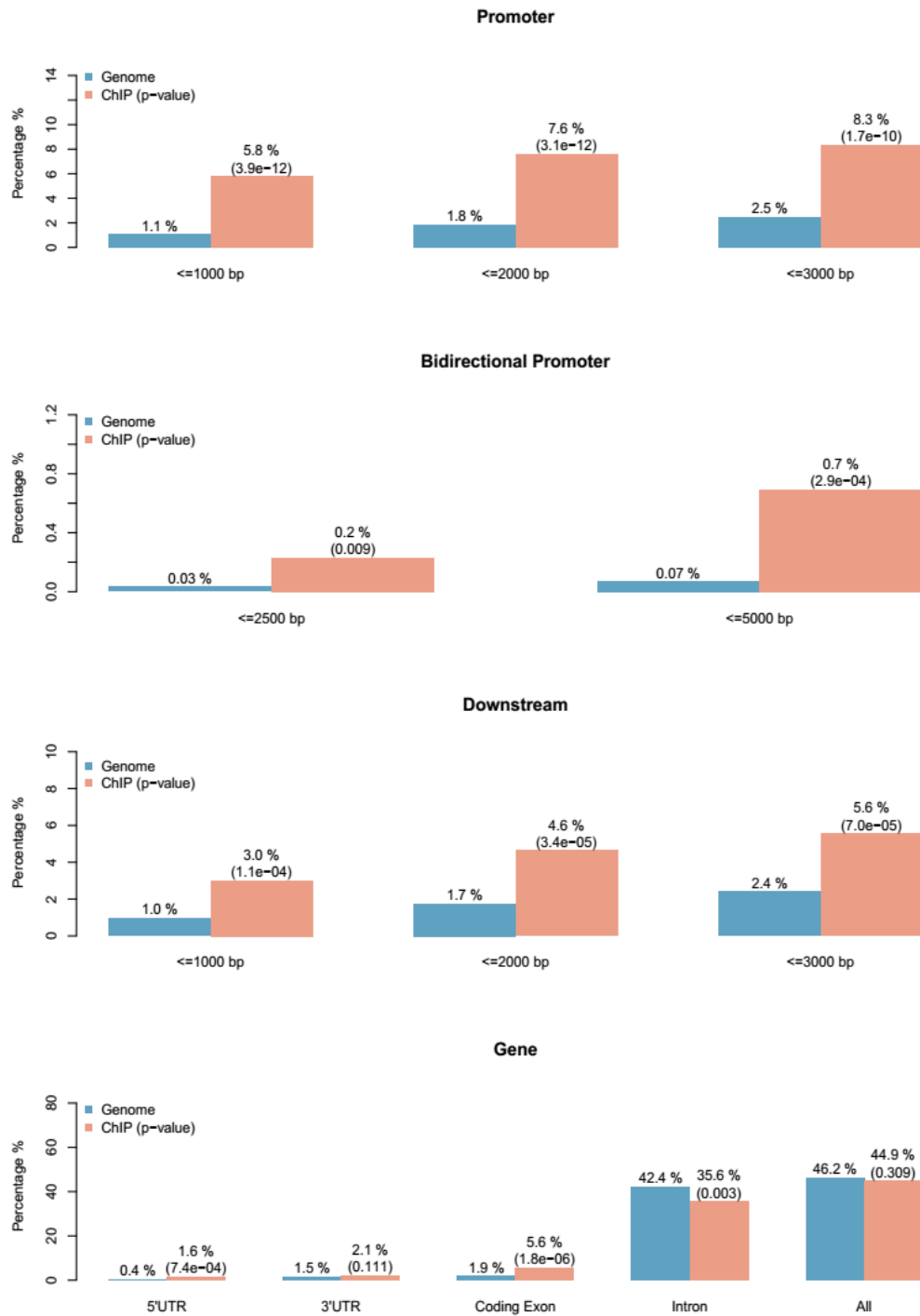


**Figure 4.13 Relative enrichments of Nup93 in important genomic features:** Nup93 is enriched (> 5% enrichment) at the promoter region (<=3000bp) compared to the genome background. Blue bars represent the total percentages of the tiled or mappable regions located in genomic regions (genome background) and the red bars the percentages of ChIP regions. In addition, Nup93 also showed significant association with bidirectional promoters and downstream regions from the promoter as compared to genome background.

#### **4.2.6 GO term analysis of Nup93 associated genes reflects its possible role during differentiation**

To investigate the functions of Nup93, we performed gene ontology analysis of Nup93 associated genes using DAVID (Huang et al., 2009a, 2009b). GO term analysis has been widely used for the association of genes identified in ChIP-seq experiments with known biological processes. Here, with the help of GO term analysis, we identified possible global functions of Nup93 in gene regulation and genome organization. Genes were categorized into the biological process, molecular function and cellular components. It was interesting to observe that the majority of Nup93 associated genes were enriched for terms involved in developmental processes such as osteoblast development, osteoblast differentiation, morphogenesis and central nervous system development (p-value < 0.005) (Figure. 4.14A). It is important to note that Nup93 is located at the nuclear periphery and its involvement in the regulation of developmental genes highlights the role of the nuclear periphery in developmental gene regulation. We found that canonical Wnt-signaling is highly significant category enriched (p-value  $3.96E^{-05}$ ) for Nup93 associated genes. Interestingly, the canonical Wnt-signaling pathway is known to involve in development and differentiation, such as cardiac differentiation and neuronal differentiation (Flaherty et al., 2012; Lange et al., 2006; Teo and Kahn, 2010). We observed that osteoblast development was the second category which was enriched (p-value  $1.09E^{-04}$ ) suggesting a role of Nup93 during early stages of development and differentiation (Figure. 4.14A). Although these functional categories are quite broad, they are consistent with the previously reported function of Nup93 in the regulation of cell identity genes (Ibarra et al., 2016).

Further, we examined KEGG pathways that were enriched for Nup93 associated genes (Figure. 4.14 B). Interestingly we found that pathways involved in developmental processes were most enriched for Nup93 associated genes (Figure. 4.14 B). It includes pathways include the Hippo signaling pathway (p-value  $5.77E^{-07}$ ), Wnt-signaling pathway (p-value 0.001) and signaling pathways regulating pluripotency of stem cells (p-value 0.0002) (Figure. 4.14B). Together, KEGG pathway analysis further suggests the possible role of Nup93 in the regulation of developmental genes.

**Figure 4.14**

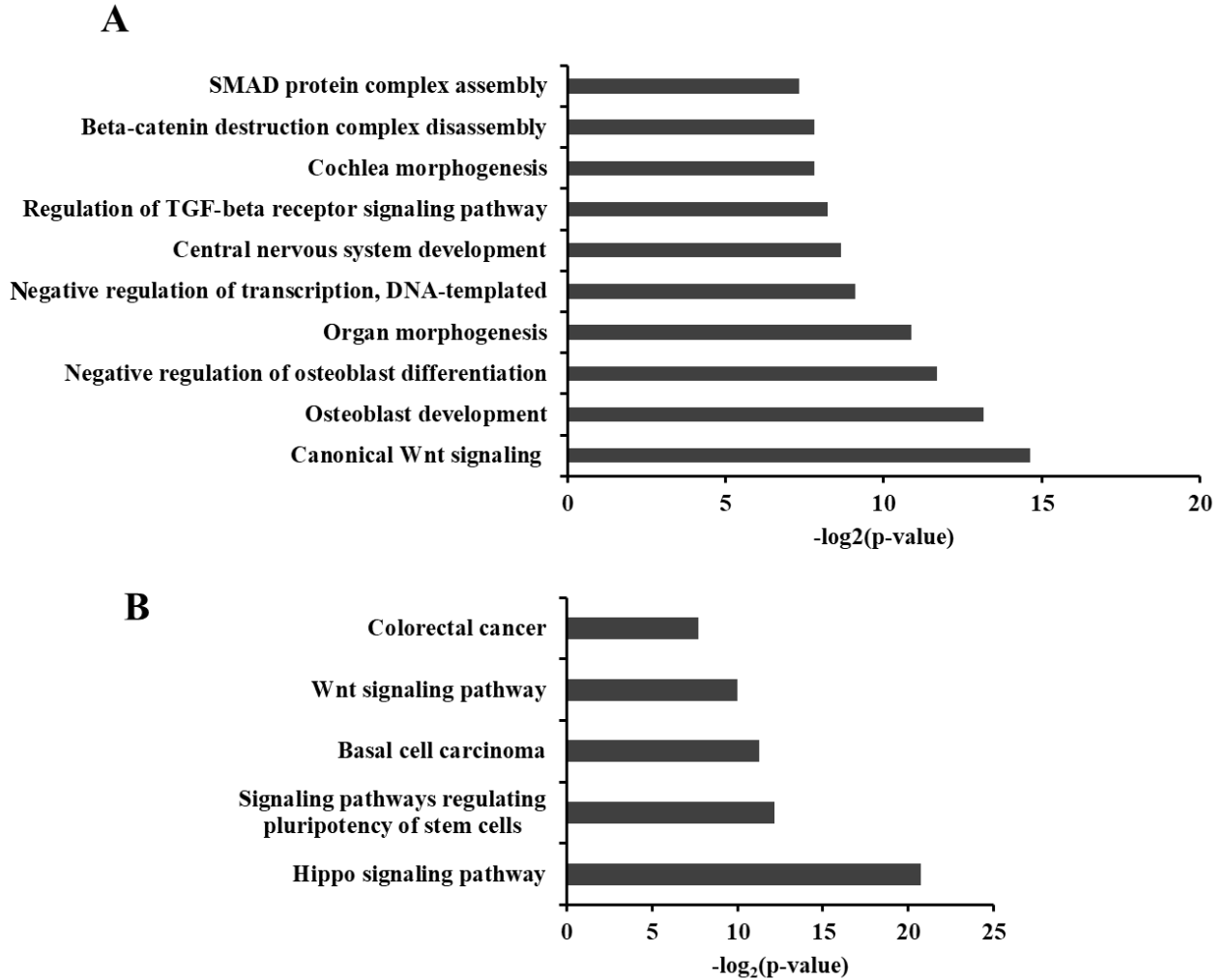


**Figure 4.14: DAVID Gene ontology analysis: A)** Biological processes discovered by Gene ontology (GO) analysis of Nup93 associated genes. Categories showing the most enriched biological processes from Nup93 ChIP-seq data set. P-value < 0.001, **B)** KEGG pathway analysis of Nup93 associated genes. All categories displayed are of p-value < 0.001 and are sorted according to fold change of the number of genes in each biological process in the experiment list over the reference list (whole genome).

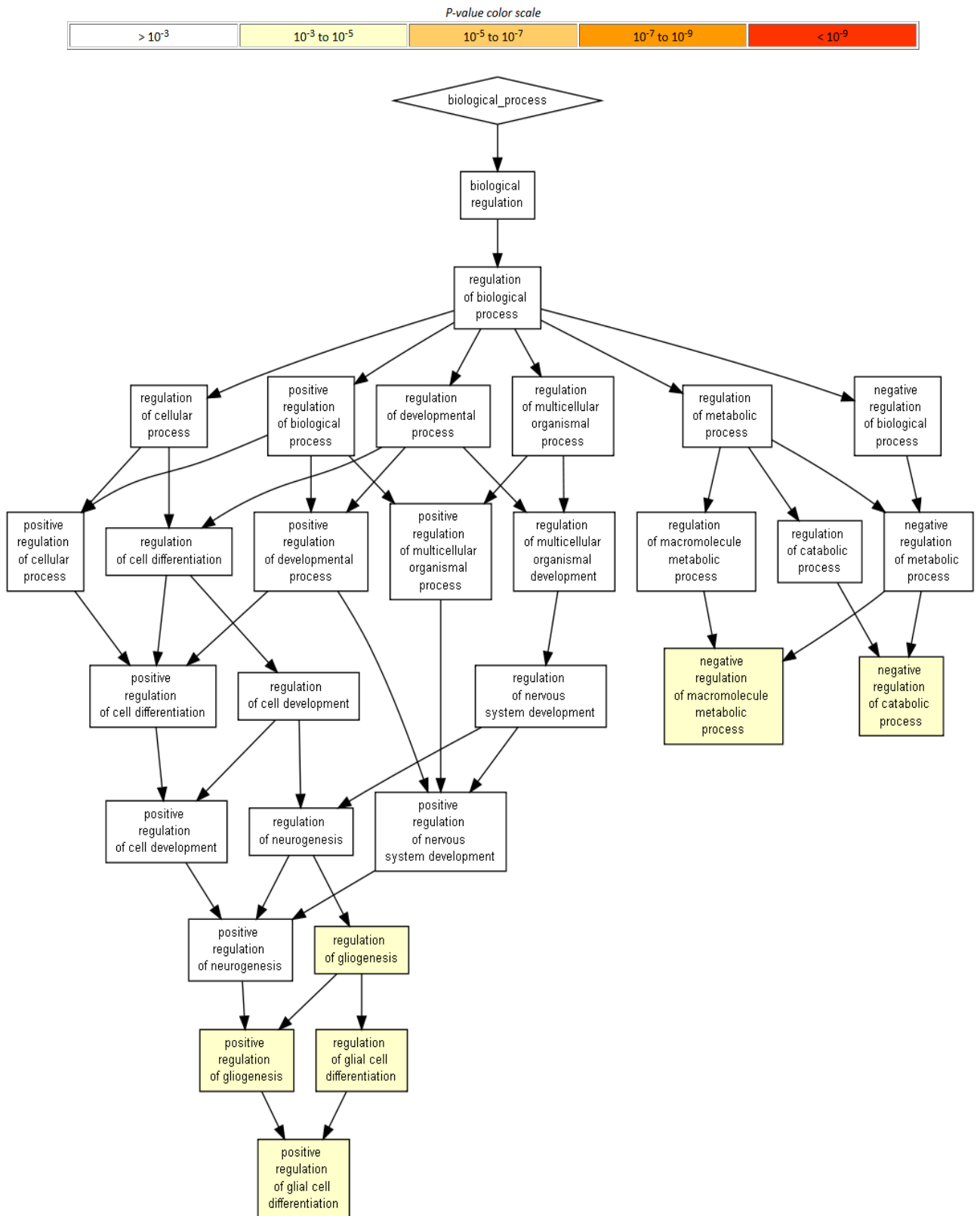
In addition to DAVID, we performed independent gene ontology analysis using online gene ontology tool Gorilla (Eden et al., 2009) (Table 4.4). We provided Nup93 associated genes (ranked according to their p-value) as an input to Gorilla. Notably, Gorilla analysis showed that GO terms related to glial cell differentiation are highly enriched for Nup93 associated genes (Table 4.4). Interestingly, Gorilla analysis specifically highlighted the role of Nup93 associated genes in neuronal differentiation which was not found in DAVID analysis (Table 4.4, Figure 4.15A). This result suggests a possible role of Nup93 in the regulation of neuronal differentiation. We then examined molecular functions enriched for Nup93 associated genes (Figure 4.15B). Surprisingly, we found that Nup93 associated genes are enriched for protein binding category. More specifically they are enriched for molecular function involved in repression of transcription factor binding (Figure 4.15B). This result suggests the speculative role of Nup93 in transcriptional repression of developmentally associated genes.

**Table 4.4: Gorilla GO terms biological processes**

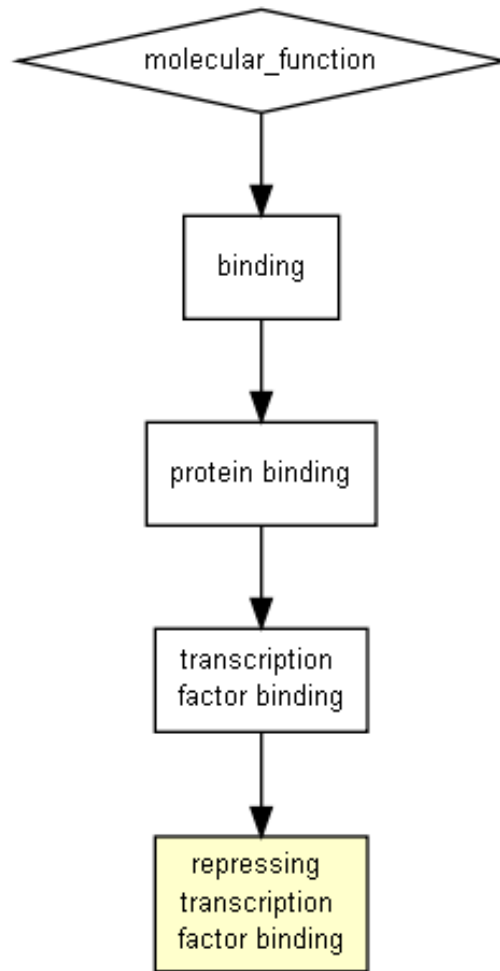
<b>GO term</b>	<b>Description</b>	<b><u>P-value</u></b>	<b><u>FDR</u></b>
<a href="#"><u>GO:0009895</u></a>	negative regulation of catabolic process	1.75E <sup>-4</sup>	6.94E <sup>-1</sup>
<a href="#"><u>GO:0045685</u></a>	regulation of glial cell differentiation	7.73E <sup>-4</sup>	1E <sup>-1</sup>
<a href="#"><u>GO:0045687</u></a>	positive regulation of glial cell differentiation	7.73E <sup>-4</sup>	1E <sup>0</sup>
<a href="#"><u>GO:0014015</u></a>	positive regulation of gliogenesis	7.73E <sup>-4</sup>	7.68E <sup>-1</sup>
<a href="#"><u>GO:0014013</u></a>	regulation of gliogenesis	7.73E <sup>-4</sup>	6.15E <sup>-1</sup>
<a href="#"><u>GO:0010605</u></a>	negative regulation of macromolecule metabolic process	8.74E <sup>-4</sup>	5.79E <sup>-1</sup>

Figure 4.15

A) Biological processes



## B) Molecular function



**Figure 4.15. Gorilla Gene ontology analysis:** A) 404 Nup93 associated genes were given as input to GOrilla. The resulting enriched GO terms are visualized using a DAG graphical representation with color coding reflecting their degree of enrichment. B) Categorization of Nup93 associated genes according to their molecular function. Repression of transcription factor binding was the most significantly enriched category.



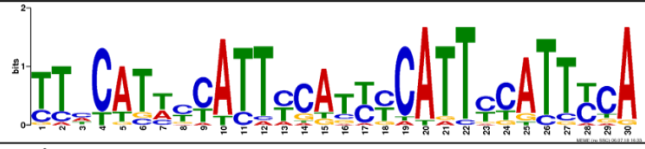
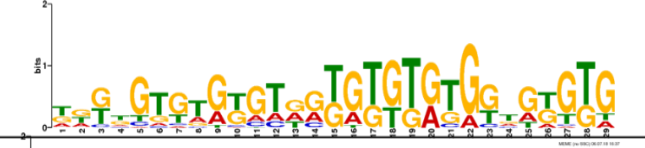
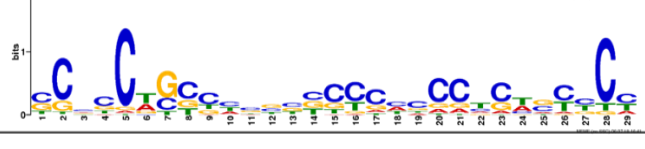



#### **4.2.7 DNA binding motifs enriched in Nup93 binding sequences**

To determine the de novo sequences recognized by Nup93 in our ChIP-Seq dataset we performed the motif search using MEME ChIP (Machanick and Bailey, 2011). First, we extracted FASTA sequences corresponding to Nup93 binding peaks using fetch genomic DNA tool in GALAXY. All FASTA sequences were submitted as an input to MEME ChIP and motifs analysis was performed with default parameters against HOCOMOCO Human (v11 FULL) database. Out of 20 motifs identified by MEME-ChIP, top 6 motifs were selected for further analysis (Figure 4.16). We performed TOMTOM (Tomtom compares one or more motifs against a database of known motifs) analysis on to 6 motifs to identify similar motifs from HOCOMOCO Human (v11 FULL) database (Figure 4.16). The first highly significant motif identified showed similarity to EGR3 motif defined by the HOCOMOCO Human database (Figure 4.16). EGR3 is a zinc finger transcription factor involved in the transcriptional regulation of circadian genes (Patwardhan et al., 1991). EGR3 is also shown to be involved in neuronal development and muscle development (Quach et al., 2013). Furthermore, a second motif was identified using this method that greatly resembled ZN394 motif as defined by the HOCOMOCO Human database (Figure 4.16). ZN394 is a zinc finger transcription factor involved in transcriptional repression of the mitogen-activated protein kinase pathway. Few more motifs identified by MEME resembles RREB1 (Ras Responsive Element Binding Protein 1), MAZ (MYC Associated Zinc Finger Protein) and FOXG1 (Figure 4.16). RREB1 is involved in Ras/Raf-mediated cell differentiation while FOXG1 is a repressor protein play a role in brain development. Altogether, motif analysis suggests that Nup93 binding motif show similarities with

different transcription factor motifs majorly involved in transcriptional regulation of developmental processes.

**Figure 4.16**

CONSENSUS	Size (bp)	E-VALUE	SIMILAR_MOTIF
	11	1.20E-54	EGR3
	21	5.60E-36	ZN394
	30	2.80E-28	ZN502
	29	3.50E-24	RREB1
	29	6.30E-22	MAZ
	15	3.70E-17	FOXG1

**Figure 4.16. Motif analysis:** DNA binding motifs identified by MEME ChIP arranged according to E-value. Last column in the table shows similar motifs identified using TOMTOM. Motif search was performed using HOCOMOCO Human database.

#### 4.2.8 Transcription factors enriched within Nup93 binding regions

To identify the transcription factors enriched within Nup93 binding regions, we used two different online tools ReMap (Chèneby et al., 2018) and ChIP Atlas. ReMap identifies enrichment of a known transcription factor within ChIP-seq binding regions. It overlaps the genomic coordinates against the ReMap database of TF peaks using a different percentage of overlap. We checked if any transcription factor shows minimum 10% overlap with Nup93 binding peaks. To our surprise, we found that CTCF showed the highest overlap with Nup93 peaks followed by c-MYC (Table 4.5). Out of 404 binding peaks of Nup93, 304 peaks showed at least 10% overlap with Nup93 peaks. Similar, 269 peaks showed minimum overlap with MYC. Top 10 transcription factors which showed the highest overlap with Nup93 peaks are shown in Table 4.5.

**Table 4.5: Transcription factors enriched on Nup93 binding regions**

No	Transcription Factor	# Observed Overlap	$-\log_{10}(\text{E-value})$
1	CTCF	304	20.921
2	MYC	269	14.243
3	AR	256	4.897
4	STAG1	251	28.708
5	BRD4	226	3.062
6	FOXA1	219	0.894
7	ZNF143	215	48.192
8	MAX	209	22.146
9	ESR1	187	17.128
10	HSF1	186	41.742

Next, we decided to determine the transcription factor enrichment on Nup93 binding regions specifically in DLD-1 cells. We performed a similar *In-silico* ChIP analysis using an independent online tool in ChIP-Atlas. We found that 64 out of 404 peaks Nup93 showed an overlap with CTCF peaks in DLD-1 cells (Table 4.6). Similarly, 54 peaks showed overlap with RAD21 (Table 4.6). In summary, these results suggest that Nup93 and CTCF have overlapping binding regions in the genome. In addition, RAD21 showed significant overlap with Nup93 peaks in DLD-1 cells. RAD 21 is a cohesion complex component protein which directly interacts with CTCF(Xiao et al., 2011). This further supports the overlap of Nup93 binding regions with CTCF.

**Table 4.6: Transcription factors enriched on Nup93 binding regions in DLD-1 cells**

	<b>Transcription Factor</b>	<b># Observed Overlap</b>	<b>-log<sub>10</sub>(p-value)</b>
1	CTCF	63/ 404	14.4
2	RAD21	55/404	12.5

#### 4.2.9 Co-occupancy of Nup93 and CTCF

Since Nup93 binds to similar regions as CTCF, we asked if Nup93 functions with CTCF in chromatin organization and gene regulation at the nuclear periphery? To answer these questions, we first compared Nup93 binding peaks with CTCF peaks. We examined the enrichment of Nup93 across all conserved CTCF binding sites. We observed significant enrichment of Nup93 peaks around the center of CTCF binding sites (Figure 4.17 A). To identify the specific enrichment of Nup93 around CTCF peaks in DLD-1 cells, we compared CTCF ChIP-seq profile with that of Nup93 ChIP-seq profile using the multiBamsummary tool in Galaxy. We plotted the correlation matrix between Nup93 and CTCF in the form of heatmap (Figure 4.17 B). Correlation analysis revealed a significant correlation (Pearson correlation coefficient 0.86, plotCorrelation tool, GALAXY) between Nup93-binding sites and CTCF binding sites genome-wide. In addition, heatmap showed an overwhelming majority of Nup93 sites co-localizing with the center of CTCF binding sites (Figure 4.17 C).

Since we did not find the CTCF motif enriched within Nup93 binding sequences, we searched ChIP-seq data set for the possible enrichment of the CTCF motif. We searched for CTCF motif within Nup93 associated sequences using MEME motif finding software [FIMO version 5.0.1 (Release date: 21-06-2018)]. FIMO helps in finding individual motif occurrences within the set of given input sequences. We provided the conserved CTCF consensus binding sequence 'CCACNAGGTGGCAG' (Kim et al., 2007) as an input motif to FIMO and searched for its occurrence in 404 Nup93 binding sequences. To confirm the presence of CTCF motif within Nup93 binding sequences, we counted the number of CTCF motifs within 404 Nup93 binding sequences. We found 141 motif occurrences in

the top 404 Nup93-associated sequences, each having a probability of less than 0.0001 ( $p < 0.0001$ ), indicating that CTCF motifs were significantly enriched within Nup93 associated chromatin. Therefore 141 Nup93 binding sequences are enriched for CTCF consensus sequence. We conclude that Nup93 binding sites overlap with CTCF binding sites in the genome.

**Figure 4.17**

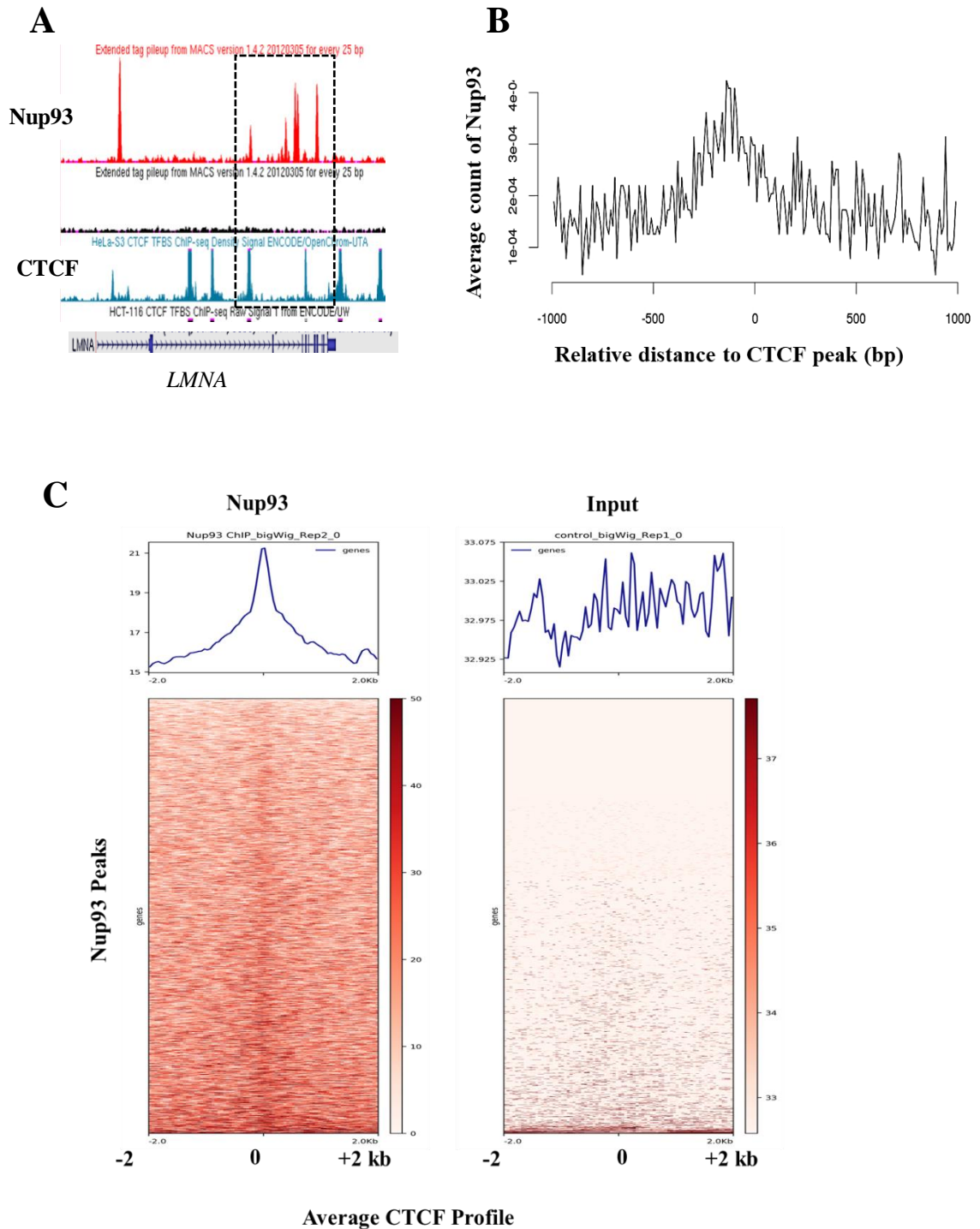


**Figure 4.17. Overlap of Nup93 and CTCF peaks:** A) Overlap of Nup93 and CTCF binding peaks on LMNA gene, Black dotted box highlights overlapping peaks B) Average profile of Nup93 relative to center of CTCF peak (All conserved CTCF binding sites) C) Enrichment heatmaps of Nup93 ChIP-seq compared with CTCF ChIP-seq (DRX013180) in DLD1 cells, sorted by CTCF occupancy around center of Nup93 binding peaks. Pearson Correlation coefficient= 0.86

#### **4.2.10 Overlapping role of Nup93 and CTCF in gene regulation**

A significant correlation between Nup93 and CTCF peaks prompted us to determine if Nup93 and CTCF colocalize at the nuclear periphery. We performed immunostaining of Mab414 (anti nucleoporin antibody) and CTCF followed by high-resolution STED imaging (STimulated Emission Depletion microscopy) microscope. Interestingly, in the normal confocal mode, we observed that CTCF colocalizes with Mab414 at the nuclear periphery (Figure 4.18A, upper panel). However, we did not observe the same colocalization between CTCF and Mab414 in high-resolution imaging using STED mode of the microscope (Figure 4.18 A, lower panel). Notably, normal confocal imaging was not able to resolve the separation between CTCF and Mab414, while STED imaging showed a clear separation between CTCF and Mab414. Together, this result suggests that CTCF does not colocalize with the NPC at the nuclear periphery, but it is present in close proximity to the NPC.

Next, we asked if Nup93 and CTCF together regulate the expression of their co-target genes. We performed siRNA mediated depletion of both Nup93 and CTCF in DLD-1 cells. LMNA and FBL overlap for Nup93 and CTCF binding sites (Figure 4.18 B and C). We tested their expression status upon depletion of both Nup93 and CTCF. qRT-PCR analysis revealed that depletion of both Nup93 and CTCF downregulates the expression of both LMNA and FBL (Figure 4.18 D). This result indicates that depletion of both Nup93 and CTCF have a similar effect on the expression of LMNA and FBL genes suggesting their common regulatory role in controlling gene expression. Interestingly, co-depletion of both Nup93 and CTCF further downregulates both LMNA and FBL genes, suggesting an additive effect of Nup93-CTCF co-depletion (Figure 4.18 D). These results suggest



overlapping roles of Nup93 and CTCF in gene regulation. However, this effect on gene expression could be gene specific. Therefore, it is important to examine the expression status of additional and common targets upon Nup93 and CTCF depletion or their co-depletion. RNA-seq analysis of their co-targets is likely to understand the co-regulatory role of Nup93 and CTCF in gene expression.

**Figure 4.18**

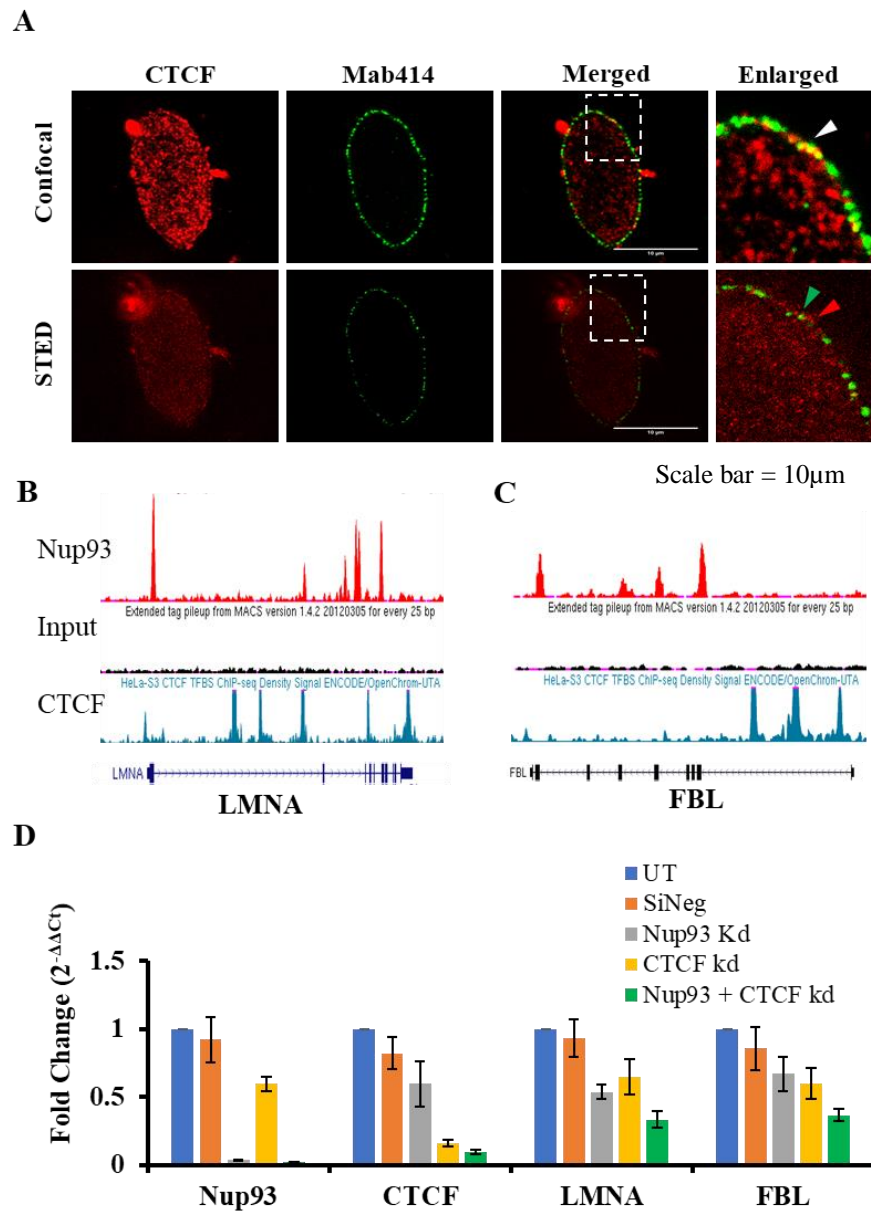


**Figure 4.18. Overlap of Nup93 and CTCF peaks:** **A**) Immunostaining of CTCF (Red) and Anti nucleoporin antibody (Mab414-Green) in DLD1 cells, upper panel- confocal mode, lower panel-STED mode. Dotted white box indicates the location of enlarged image, white arrow in upper enlarged panel indicates colocalization of Mab414 and CTCF, red and green arrows in lower enlarged panel indicates separation between Mab414 and CTCF, (100X magnification, Zoom 2.5) **B & C**) UCSC genome browser view of Nup93 and CTCF peaks on **(B)**LMNA and **(C)** FBL genes **D**) qRT-PCR analysis of LMNA and FBL upon Nup93 Kd, CTCF Kd and Nup93+CTCF Kd together. N=3, Error bar= S.E.M

#### 4.2.11 Nup93 binding sites are enriched for repressive histone marks

Since gene ontology analysis showed that Nup93 associated genes are involved in development and differentiation, we examined genomic features of Nup93 binding regions. To determine the nature of Nup93 binding sites, we examined the enrichment of different histone marks on Nup93 binding regions. We characterized epigenetic features of top Nup93 binding regions (Fold change  $\geq 2$ ) by visualizing ENCODE histone mark enrichment. We used online gene set enrichment analysis web server Enricher to determine the enrichment of histone marks on Nup93 binding regions (Chen et al., 2013; Kuleshov et al., 2016). Interestingly, we found that Nup93 binding regions are largely enriched for repressive histone marks such as H3K9me3 and H3K27me3 in across various cell lines (Table 4.6).

**Table 4.6 Histone mark enrichment on Nup93 binding regions using ENRICHER**

No	Name	P-value	Z-score	Combined score
1	H3K9me3_mononuclear cell_hg19	0.4317	-2.01	1.69
2	H3K9me3_HepG2_hg19	0.4808	-1.82	1.34
3	H3K27me3_SK-N-SH_hg19	0.5072	-1.65	1.12
4	H3K27me3_GM06990_hg19	0.5482	-1.97	1.18
5	H3K9me3_MCF-7_hg19	0.5953	-1.97	1.02
6	H3K9me3_endothelial cell of umbilical vein_hg19	0.6196	-1.77	0.85
7	H3K9me3_mammary epithelial cell_hg19	0.6804	-1.84	0.71
8	H3K27me3_Caco-2_hg19	0.7232	-1.88	0.61
9	H3K9me3_fibroblast of lung_hg19	0.7248	-1.80	0.58
10	H3K27me3_osteoblast_hg19	0.7884	-1.74	0.41

Further, we determined the enrichment of histone marks on Nup93 binding regions in DLD-1 cells. We downloaded available histone mark ChIP-seq data for DLD-1 cells from ChIP Atlas and compared it with Nup93 ChIP-seq peaks ( $FDR \geq 2$ ). We examined the distribution of previously known active histone marks (H3K4me3- DRX013182, elongation mark (H3K36me3-DRX013178) and repressive mark (H3K27me3-DRX013175) on the  $\pm 5$  kb region around the center of Nup93 binding peaks (Figure 4.19). We observed a striking correlation between Nup93-binding sites and a repressive histone mark H3K27me3-binding sites genome-wide (Figure 4.19). In contrast, we observed comparatively less enrichment of H3K4me3 (active histone mark) and H3K36me3 (elongation mark) on Nup93 binding sites. Together, these data suggest that Nup93 might mediate transcriptional silencing of a subset of genes in DLD-1 cells.

Nup93 enriches at super-enhancers (H3K27Ac peaks) in U2OS cells (Ibarra et al., 2016). Similarly, our analysis suggests a co-localization of Nup93 with architectural proteins CTCF (Figure 4.17 C). Both these observations suggest that Nup93 is enriched on enhancers for mediating long-range genome interactions. We compared the distribution of known enhancer marks on the  $\pm 5$  Kb region around the center of Nup93 binding peaks. Interestingly, the enhancer mark H3K4me1 is not enriched around the Nup93 peak (Figure 4.19). In contrast, the super enhancer mark H3K27Ac showed significant enrichment around the Nup93 binding peaks (Figure 4.19). Thus, our analysis identified a subset of Nup93 binding sites which corresponds to super-enhancers as predicted previously in U2OS cells (Ibarra et al., 2016). Since CTCF is involved in gene looping at enhancers, this result supports our conclusion on the Nup93-CTCF overlap in gene regulation. Altogether,

these results indicate the previously uncharacterized overlapping role of Nup93 and CTCF in the regulation of gene expression.

**Figure 4.19**

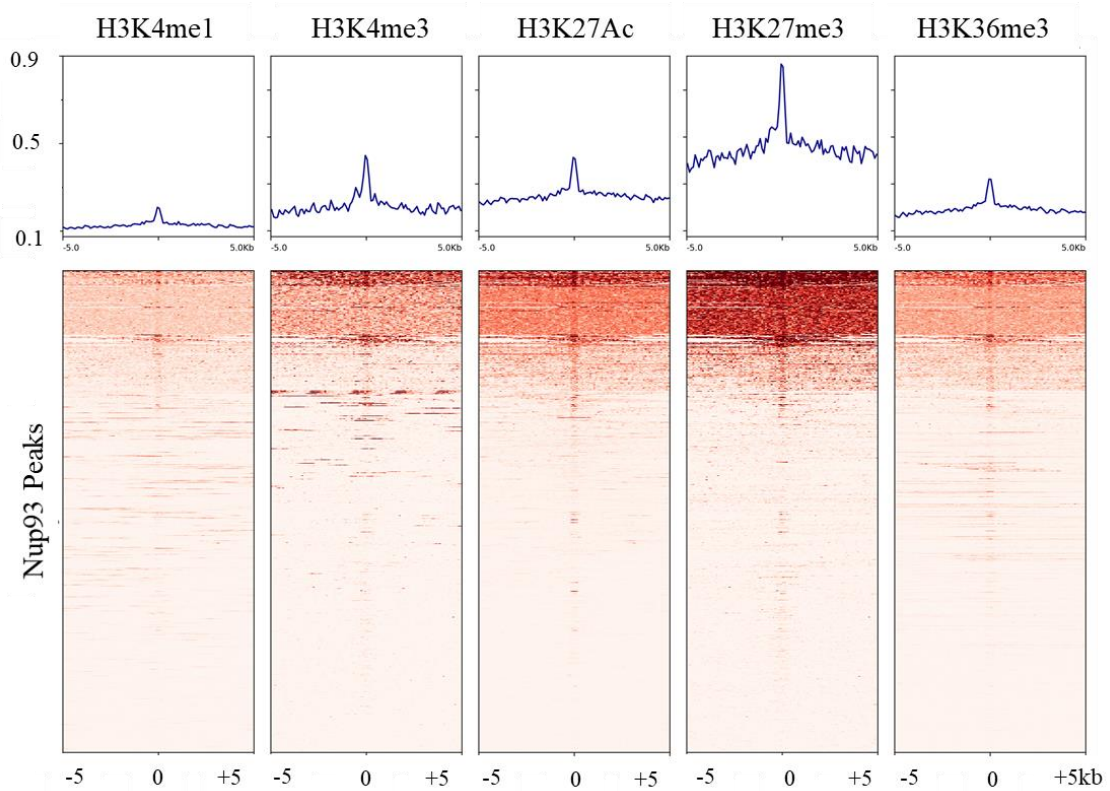


**Figure 4.19. Histone mark enrichment on Nup93 binding sites:** Enrichment heatmaps of Nup93 ChIP-seq compared with H3K4me1 (DRX013183), H3K4me3 (DRX013175), H3K27ac (SRX 1528524), H3K27me3 (DRX013182) and H3K36me3 (DRX013172) in DLD1 cells, sorted by Histone mark occupancy around center of Nup94 binding peaks.

### 4.3 Discussion

Besides their well-established role in nuclear transport, nucleoporins have been well recognized for their role in gene regulation. Nucleoporins regulate the developmental processes by direct association with developmental genes and regulatory proteins. But, the gene-specific role of many nucleoporins in transcriptional regulation is unclear. Here, we report ChIP-seq analysis for Nup93, one of the core components of the nuclear pore complex. Our study yielded a very interesting result showing a potential role of Nup93 in silencing developmental genes in DLD-1 cells. Further, we discovered that Nup93 binding sites overlap with a subset of CTCF binding sites, suggesting the overlapping role of Nup93 and CTCF in gene regulation.

We first characterized the Nup93 antibody for ChIP-seq by following ENCODE guidelines. Our aim was to generate good quality Nup93 ChIP-seq data which would be useful in understanding the biological importance of Nup93 in gene regulation and genome organization. Immunoblotting revealed a specific band of Nup93 at ~100 kDa suggesting the specificity of the Nup93 antibody (Figure 4.1). In addition, the Nup93 antibody detected a decrease in Nup93 levels upon siRNA mediated depletion, underscoring the specificity of the antibody (Figure 4.1). Nup93 is a core nuclear pore complex protein and it directly interacts with many other nucleoporins. Therefore, it was crucial to determine the immunoprecipitation efficiency of Nup93 in ChIP buffer (Figure 4.5). These initial characterizations of Nup93 antibody further reiterate the specificity of the Nup93 antibody.

To identify the target genes associated with Nup93 we applied ChIP combined with whole genome sequencing (ChIP-seq). We performed all quality checks of ChIP DNA

before Illumina sequencing. In order to minimize noise and background, we validated ChIP experiments before high-end sequencing. We performed ChIP-PCR analysis for known targets of Nup93 i.e. promoter regions of HOXA1, HOXA3, HOXA5, and CFTR. GLCCI1 served as a negative control (Figure 4.6). Our ChIP-PCR experiment showed a significant enrichment of Nup93 on its known targets as compared to negative control (Figure 4.6).

Nup93 is a stable nucleoporin with lowest dissociation rates from the nuclear pore complex ( $K_{\text{off}} = 4.0 \pm 3.4 \times 10^{-6} \text{ s}^{-1}$ ) (Rabut et al., 2004). Immunoelectron microscopy studies have mapped the spatial position of Nup93 inside the nuclear pore complex revealing that Nup93 is a core component of the nuclear pore complex (Krull et al., 2004). Given the non-random organization of chromosome territories in the interphase nucleus, with gene-poor chromosomes near the nuclear periphery and gene-rich chromosomes near the nuclear center we expected an enrichment of Nup93 to the peripheral chromosomes. In contrast, ChIP-seq analysis showed a very interesting binding profile of Nup93 across the entire genome (Figure 4.9). We found that irrespective of its peripheral localization, Nup93 associates with every human chromosome inside the nucleus except chromosome X (Figure 4.9 and 4.10). Given the dynamic nature of chromatin inside the nucleus, chromatin may associate with Nup93 at the nuclear periphery in a transient manner. In addition, since Nup93 is one of the early nucleoporins to contact chromatin during nuclear envelope reformation, we speculate that Nup93 may contact chromatin at the very early stages of nuclear envelope formation. An early association of Nup93 with chromatin might help in global chromatin organization at the nuclear periphery. However, the mechanisms behind Nup93-chromatin association are the subject of in-depth protein-chromatin association research.

It is worth mentioning that we observed no correlation between Nup93 binding and gene density of the chromosome (Figure 4.10). Similarly, we did not see a strong correlation between Nup93 binding and the size of the chromosome (Figure 4.10). But chromosome 1, chromosome 2 and chromosome 11 showed the relatively high density of Nup93 binding sites (Figure 4.10). In addition, Nup93 binding sites did not show preferential clustering in dark bands or light bands of chromosomes (Figure 4.11). Together, we observed that Nup93 associates with every chromosome irrespective of their size and gene density, though the X chromosome is an exception. We did not see Nup93 binding on X chromosome consistent with the earlier Nup93 Dam-ID study in U2OS cells (Ibarra et al., 2016).

Genome-wide analysis of Nup93-chromatin association showed that majority of Nup93 binding sites accumulate within intergenic (46%) and intronic regions (34%). It is important to note that many of these intronic and intergenic regions are essential for long-distance chromatin contacts in the genome (Figure 4.12A). This result suggests the role of Nup93 in genome organization at intergenic or intronic regions. Further, Nup93 may regulate expression of unannotated genes or noncoding RNAs within intergenic regions. The wide distribution of Nup93 binding sites within intergenic regions indicates that nucleoporins mediated gene regulation may operate via long-distance chromatin contacts within intergenic regions. Further experimentation is required for understating the distal regulatory function of Nup93 in gene regulation. This can be achieved by performing large-scale chromatin conformation capture (Hi-C) studies in the presence and absence of Nup93.



Interestingly, we further observed that Nup93 binding sites are specifically enriched on intron-exon junctions, suggesting that Nup93 might involve in regulating gene splicing (Figure 4.1C and D). However, further investigation is required to understand the involvement of Nup93 in gene splicing. This could be achieved by performing a mass-spec analysis of Nup93 to determine if any specific splicing factor interacts with Nup93. Furthermore, expression of different splice variants of the gene can be determined in the presence and absence of Nup93.

Although we found the majority of Nup93 binding sites enriched in intergenic regions and intronic regions, a subset of Nup93 binding sites (8%) showed an enrichment on promoters (Figure 4.12A). We observed that the majority of promoter-associated Nup93 binding sites are concentrated closer to the TSS of annotated genes (Figure 4.12B). This result indicates that Nup93 might be involved in the transcriptional regulation. Interestingly, gene ontology (GO) analysis of the Nup93 associated genes showed a significant enrichment for genes implicated in development and differentiation (Figure 4.14). More specifically, Gorilla analysis revealed that Nup93 associated genes are involved in glial cell differentiation suggesting a potential role of Nup93 in neuronal differentiation (Figure 4.15, Table 4.4). In addition, KEGG pathway analysis showed that Nup93 associated genes are involved in the Hippo signaling pathway and the Wnt-signaling pathway (Figure 4.14). Canonical Wnt-signalling pathway is well recognized for its role in regulating various developmental processes, further reinforcing the role of Nup93 in the regulation of development and differentiation (Flaherty et al., 2012; Lange et al., 2006; Teo and Kahn, 2010). It is important to note that many developmental genes such as HOXA genes, are expressed during early stages of differentiation and are permanently

repressed after complete differentiation. It is possible that Nup93 is acting as a tether for these permanently repressed genes at the nuclear periphery. Protein interaction studies of Nup93 with other regulators of developmental genes will provide insightful information for the mechanisms involved in the regulation of developmental genes.

Here we identified consensus motifs enriched in Nup93 binding sequences. As expected, all consensus motifs showed similarity with known transcription factor motifs such as EGR3, ZN394, ZN502, MAZ, RREB1, and FOXG1 (Figure 4.16). Interestingly, EGR3 is a zinc finger transcription factor involved in regulation of circadian genes and neuronal development. Egr3 is a nerve growth factor (NGF)-induced transcriptional regulator involved in the regulation of normal sympathetic nervous system development (Quach et al., 2013). Egr3 deficient mice showed abnormal development of the sympathetic nervous system (Eldredge et al., 2008). Similarly, MAZ (Myc associated zinc finger protein) is known to regulate neural stem cell differentiation (Wang et al., 2013). RREB1 (Ras Responsive Element Binding Protein 1) is a zinc finger transcription factor known to potentiate the transcriptional activity of NEUROD1 (Bonomo et al., 2014). FOXG1 (Forkhead box g1) is a transcriptional repressor known to regulate neuronal differentiation by localizing at mitochondria in the cytoplasm (Hanashima et al., 2004; Pancrazi et al., 2015; Regad et al., 2007). All transcription factors revealed by motif analysis suggests redundancy between their functions in developmental gene regulation. Thus, it will be interesting to examine the interaction of these transcription factors with Nup93 during differentiation. Altogether, these data support the role of Nup93 in developmental gene regulation. In addition to Nup93, other nucleoporins such as Nup153, Nup50, Nup210, Nup98 are known for their role in developmental gene regulation (Buchwalter et al., 2014;

Jacinto et al., 2015; Kalverda et al., 2010; Liang et al., 2013). Strikingly, several of these findings suggest that nucleoporins provide nuclear platform inside the nucleus for setting developmental transcriptional program and our finding is no exception.

Our results identify a specific transcriptional function of Nup93 in gene regulation which overlaps with architectural protein CTCF. Transcription factor enrichment analysis using ReMap and ChIP atlas showed that Nup93 binding sites show enrichment of CTCF (Table 4.5 and 4.6). Further, Nup93 binding sites showed a strong correlation with CTCF binding sites in DLD-1 cells (Figure 4.17). Careful examination of Nup93 binding sites using UCSC genome browser revealed that CTCF binding sites either overlaps or surrounds Nup93 binding sites (Figure 4.17A). Moreover, motif search analysis using FIMO showed that Nup93 binding sites showed enrichment of CTCF motif (FIMO analysis). In contrast, we did not observe enrichment of BORIS (a paralog of CTCF) on Nup93 binding sites, suggesting the specificity of CTCF enrichment. Supporting our result, A study in HeLa cells have shown that CTCF motif is enriched in Nup93 binding sites (Brown et al., 2008). This result suggests that Nup93 may facilitate CTCF mediated topological contacts such as those of insulators or promoter-enhancer contacts. This notion is further supported by previous findings for other nucleoporins such as Nup2 acting as insulators both in yeast and flies (Ishii et al., 2002; Kalverda and Fornerod, 2010). Furthermore, genome-wide analysis of Nup93 binding revealed that Nup93 associates with transcriptionally silenced gene loci (Table 4.6). We found that Nup93 binding regions are largely occupied by repressive histone marks such as H3K9me3 and H3K27me3 (Table 4.6). We found a strong correlation between Nup93 binding peaks and H3K27me3 binding peaks in DLD-1 cells (Figure 4.18). Interestingly, the H3K27me3 mark appears to be

common targets of the stable nucleoporin, which is supported by the previous report of Nup153 and its role in PcG mediated gene silencing (Jacinto et al., 2015). Similarly, Nup93 have been previously shown to associate with repressive histone mark (H3K27me3) in HeLa cells (Brown et al., 2008).

On the basis of these findings, we propose that a specific subset of genes associated with Nup93 at the nuclear periphery, for the purpose of permanent gene repression. Although the transcriptional repression function of Nup93 is not fully understood, it is possible that Nup93 binding may be particularly beneficial for stable tethering of genes at the nuclear periphery. NPC may provide a platform for complex regulatory interactions, such as CTCF mediated long-range interactions within the HOX gene cluster. The implications of our findings are potentially important for further understanding of developmental gene regulation. Establishment and maintenance of appropriate chromatin contacts mediated through nucleoporin-CTCF interaction may be a novel mechanism by which Nups contribute to the regulation of gene expression during cell differentiation.

**Chapter 5: Role of Nup93 and CTCF in the  
regulation of HOXA gene expression during  
differentiation**

## 5.1. Introduction

Nuclear pore complexes are channels within the nuclear envelope that selectively allow nuclear transport between the nucleoplasm and cytoplasm. It has now become evident, however, that in addition to their role in nuclear transport, NPCs are also involved in transport independent functions such as genome organization and gene regulation (Capelson and Hetzer, 2009; Ibarra and Hetzer, 2015; Raices and D'Angelo, 2018). An early hint that NPCs might involve in gene regulation originated from the 'Gene gating hypothesis' which suggested that active genes are relocated to the nuclear envelope close to the nuclear pore complex (Blobel, 1985). In support of this hypothesis, in budding yeast, several genes such as *GALI*, *HXK1*, *INO1* possess transcriptional memory and relocate to the nuclear pore complex upon activation (Light et al., 2010; Tan-Wong et al., 2009). In addition, NPCs tether DNA bearing "zip codes" at the nuclear periphery and regulate chromatin organization (Light et al., 2010).

The role of nucleoporins in gene regulation at the nuclear periphery is associated with transcriptional activation and repression. In higher eukaryotes, such as mammalian cells and *Drosophila*, the role of nucleoporins in gene regulation is largely restricted to mobile nucleoporins that regulate gene expression more towards the nuclear interior. For example, the highly mobile nucleoporins such as Nup98, Nup50, and Nup153 are involved in gene regulation away from nuclear periphery (Buchwalter et al., 2014; Griffis et al., 2004; Hase and Cordes, 2003; Liang et al., 2013). Whether nucleoporins regulate gene expression at the nuclear periphery in mammalian cells is now beginning to be understood.

However, electron microscopy shows that the region below the NPCs is a heterochromatin exclusion zone, suggesting the association of active chromatin region with the NPC at the nuclear periphery (Capelson and Hetzer, 2009). In addition, Brown et al. showed that Nup93 contacts specific sub-regions on human chromosome 5,7 and 16 in HeLa cells (Brown et al., 2008). Similarly, the recent Dam-ID study revealed that super-enhancers involved in regulation of cell identity genes are tethered to the nuclear periphery by a stable nucleoporin Nup93 (Ibarra et al., 2016). In summary, these studies implicate nucleoporins in gene regulation at the nuclear periphery.

Gene regulation function of the nucleoporin has been linked to developmental gene regulation. Recent studies suggest nucleoporins such as Nup98, Nup50, Nup153 and Nup210 in developmental gene regulation (Buchwalter et al., 2014; Griffis et al., 2004; Ibarra et al., 2016). Association of Nup98 with human genome correlate with developmental gene expression in neural progenitor cells (Liang et al., 2013). The pattern of Nup98 binding is highly cell type-specific during differentiation of neuronal progenitor cells (Liang et al., 2013). Nup50 regulates differentiation of C2C12 cells into myotubes, where knockdown of Nup50 inhibits the differentiation of C2C12 cells (Buchwalter et al., 2014). Nup93 and Nup153 associates with super-enhancers of cell identity genes, suggesting their involvement in the regulation of differentiation. Role of nucleoporins in differentiation has linked with their cell type-specific expression (D'Angelo et al., 2012; Gomez-Cavazos and Hetzer, 2015). For example, a transmembrane nucleoporins Nup210 is not expressed in embryonic stem cells but is incorporated into the NPC during differentiation. Furthermore knockdown of Nup210 inhibits the differentiation of ESCs into neuronal progenitors (D'Angelo et al., 2012). Taken together, these studies suggest

that nucleoporins modulate differentiation by controlling cell type-specific gene expression. However, mechanisms that regulate cell type-specific nucleoporin-chromatin interactions remain to be elucidated.

Here we extend our previous findings, where we found that Nup93 associates with HOXA gene clusters on chromosome 7 and represses its expression in differentiated DLD-1 cells. In addition, our ChIP-seq analysis revealed that Nup93 associates with developmentally regulated genes and Nup93 peaks significantly overlap with CTCF peaks. Our findings suggest the role of Nup93 in developmental gene regulation. CTCF (CCCTC-binding factor) is a global genome organizer (Ong and Corces, 2014). It acts as an insulator and is localized at the boundaries of active and inactive chromatin domains thereby preventing the spread of inactive chromatin into the active domain (Kim et al., 2007). In addition, CTCF regulates gene expression of specific gene loci by forming functional chromatin loops within the gene loci. For example, CTCF regulates intrachromosomal contacts between imprinting gene loci H19 and IgF2 which are located 100 kb away from each other on the human X chromosome (Singh et al., 2012; Szabó et al., 2004). Similarly, CTCF regulates interchromatin looping of the HOXA gene cluster on Human chromosome 7 (Rousseau et al., 2014; Xu et al., 2014). CTCF associates with multiple highly conserved CTCF binding sites (CBS) on the HOXA gene cluster and thereby regulates its organization and gene expression (Rousseau et al., 2014; Xu et al., 2014). There are 5 highly conserved CTCF-binding sites on 5' of the HOXA gene cluster that regulates temporal collinearity of HOXA gene expression. The Hox genes are homeobox superfamily genes that encode highly conserved developmentally regulated transcription factors. There are 39 Hox genes in humans, which are organized into four genomic clusters located on separate



chromosomes. The HOXA gene cluster is located on chromosome 7 and spans 150kb. It encodes eleven transcription factors that are colinearly expressed during early stages of differentiation. For example, the 3' end HOXA genes are expressed early during differentiation followed by expression of 5' end HOXA genes. Disruption of the temporal collinearity of HOXA gene expression during differentiation is associated with developmental defects (Aubin et al., 1997; Mallo and Alonso, 2013). In addition, ectopic expression of HOXA genes in adult tissues (e.g. Breast and lung) is linked to diseases such as cancers (Bitu et al., 2012; Novak et al., 2006). Therefore, the temporal and sequential silencing of HOXA gene expression during differentiation is the key to proper HOXA function (Mallo and Alonso, 2013; Montavon and Soshnikova, 2014). Chromatin conformation capture studies have revealed that internal chromatin looping within HOXA gene cluster is required for silencing of HOXA genes during differentiation (Narendra et al., 2015; Rousseau et al., 2014; Xu et al., 2014). CTCF and PRC2 complex protein play an important role in HOXA gene cluster silencing by recruiting inactive histone marks on HOXA gene cluster in NT2/D1 cells (Xu et al., 2014). Thus, specific and sequential chromatin looping mediated via CTCF is likely to function in transcriptional silencing of HOXA gene cluster in adult tissues. However, the role of CTCF in long-term maintenance of silent HOXA gene cluster is not elucidated.

The finding that Nup93 associates with 3' end of HOXA genes (HOXA1, HOXA3, and HOXA5) and Nup93 peaks significantly overlap with CTCF peaks may suggest an overlapping role of Nup93 and CTCF in HOXA gene regulation during differentiation. Here, we analyze the role of Nup93 and CTCF in regulating the HOXA gene expression during differentiation of NT2/D1 cells. We found that Nup93 knockdown significantly

upregulates HOXA gene expression, while CTCF depletion does not affect the expression in DLD-1 cells. However, depletion of CTCF in NT2/D1 cells significantly downregulates 3' end HOXA gene (HOXA1 and HOXA5) expression. Our preliminary result suggests that the HOXA gene cluster is potentially more responsive (since it showed enhanced expression in Nup93 depleted cells) to the RA treatment upon depletion of Nup93 in NT2/D1 cells. In contrast, CTCF depletion makes it less responsive (since it showed reduced expression in CTCF depleted cells) to RA treatment in NT2/D1 cells. 3D-FISH results revealed that HOXA gene locus shows a dynamic repositioning from the nuclear periphery during differentiation as it positions closer to the nuclear interior upon activation and relocates to the nuclear periphery that correlates with repression. We found that the untethering of HOXA locus from the nuclear periphery correlates with the reduced occupancy of Nup93 on the HOXA1 promoter during differentiation. In summary, these findings, suggest a novel mechanism of transcriptional silencing of the HOXA gene cluster during differentiation mediated via dynamic interplay between Nup93 and CTCF.

## 5.2 Results

As discussed in chapter 4, our ChIP seq analyses in DLD-1 cells revealed that Nup93 binding sites significantly overlap with CTCF binding sites. We observed that the CTCF binding motif is highly enriched within the top 404 Nup93 binding sites. Furthermore, our gene ontology analysis revealed that Nup93 associates with genes involved in development and differentiation. Consistent with these results, we previously showed that Nup93 is involved in silencing of developmentally important HOXA gene locus in DLD-1 cells. In addition to Nup93, CTCF regulates chromatin looping of the HOXA gene locus. Specific enrichment of Nup93 and CTCF on HOXA gene cluster may suggest their overlapping role in the regulation and organization of the HOXA gene cluster. Based on these observations, we hypothesized that Nup93 and CTCF might regulate the expression of key developmental genes during differentiation including HOXA gene locus. In this study, we examined the role of Nup93 and CTCF in the regulation of the HOXA gene cluster during differentiation of NT2/D1 cells.

### 5.1.1 Nup93 and CTCF binding sites do not overlap with each other on HOXA locus

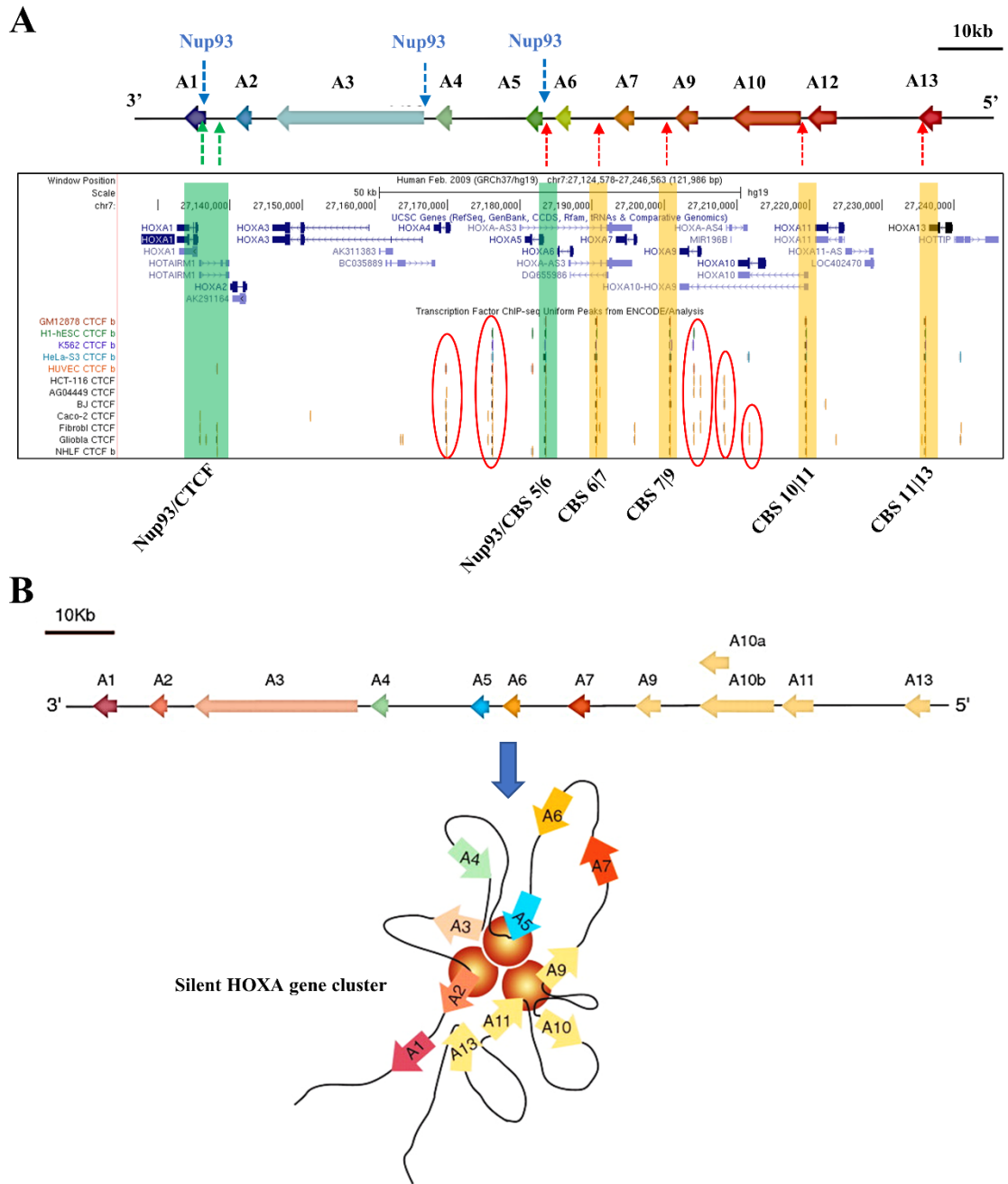
To understand the role of Nup93 and CTCF in the regulation of the HOXA gene cluster during differentiation, we determined binding sites of CTCF within the HOXA gene locus. We collated CTCF binding sites within HOXA locus across different cell lines using the UCSC genome browser. The majority of CTCF binding sites (CBS) are distributed across 5' end of the HOXA gene cluster. Amongst all, five CTCF binding sites (CBS5|6, CBS6|7, CBS7|9, CBS10|11 and CBS11|13) are highly conserved across different cell types (Figure 5.1 A). Interestingly, we observed that few non-conserved CTCF binding sites

(Highlighted in red circle) are enriched in specific cell types but absent in others (Figure 5.1 A). For example, we observed an enrichment of CTCF on HOXA1 promoter in Caco-2, fibroblast, HUVEC, and NHLF cell lines which are not detected in other cell lines (Figure 5.1A). Together, these observations suggest that CTCF may have cell type-specific enrichment on HOXA1 promoter other than its conserved binding sites.

In contrast to CTCF, we previously found that Nup93 binding sites are located within 3' end of the HOXA gene cluster with specific enrichment on the promoters of HOXA1, A3, and A5 (Figure 5.1 A, Blue arrows). Importantly, CTCF binding sites on HOXA1 and HOXA5 promoter overlap with Nup93 binding sites in Caco-2, fibroblast, HUVEC, and NHLF cell lines (Figure 5.1 A, highlighted in the green box). To further examine these overlapping Nup93-CTCF binding sites, we performed sequence analysis using *In silico* CTCFBS prediction tool (CTCFBSDB 2.0) which predicts the likelihood of CTCF binding within the DNA sequence (Ziebarth et al., 2013). We searched for CTCF enrichment within the promoter of HOXA1 gene (chr7:27135626-27136625, hg19). We found two motifs (TTCCCTCTCTCGTC and AGAAGAGCA) enriched within HOXA1 promoter having PWM (Positioned weighted matrix) score 1.56 and 10.26, indicating the likelihood of CTCF binding within HOXA1 promoter. Altogether, these data suggest that Nup93 and CTCF have overlapping binding sites on HOXA1 and HOXA5 promoter. Chromatin conformation capture studies in various cell lines including NT2/D1 and THP-1 cells have shown that silent HOXA gene locus is organized as clustered loops indicating that HOXA genes are present in a proximity with each other (Figure 5.1B) (Ferraiuolo et

al., 2010; Rousseau et al., 2014; Xu et al., 2014). However, the potentially combined role of Nup93 and CTCF in the organization of the HOXA gene cluster is not clear.

**Figure 5.1**



(See image on previous page)

**Figure 5.1. Nup93 and CTCF binding sites do not overlap with each other on HOXA locus.** **A)** Upper panel- A linear schematic of the HOXA gene cluster. Genes are indicated by arrows illustrating the direction of transcription. Nup93 and CTCF binding sites (CBS) are indicated by blue and red vertical arrows respectively. Green vertical arrows represent non-conserved CTCF binding sites on HOXA1 promoter, Lower panel- UCSC genome browser view of CTCF ChIP-seq from different cell lines on HOXA gene cluster. Conserved CTCF binding sites are highlighted in orange. Red circles represent non-conserved CTCF binding sites. Nup93 binding sites overlapping with CTCF sites are highlighted in green. **B)** Schematic representation of silent HOXA loops. Repressed HOXA genes are known to present in loop form showing higher interaction frequency between HOXA genes are revealed by 3C experiments, Reprinted with permission from (Ferraiuolo et al., 2010).

### 5.1.2 HOXA is upregulated upon Nup93 depletion independent of CTCF

Since we observed that CTCF has conserved binding sites proximal to the 5' region of the HOXA gene cluster which does not overlap with Nup93 binding sites, we first investigated the effect of Nup93-CTCF co-depletion on HOXA gene expression. We performed siRNA mediated depletion of CTCF alone and in combination with Nup93 in DLD-1 cells (Figure 3.17A). Interestingly, the depletion of CTCF alone did not affect gene expression levels of any of the genes within the HOXA cluster (Figure 3.17C). In contrast, CTCF depletion significantly upregulated the transcript levels of GLCCI1 – a gene otherwise unaffected upon Nup93 knockdown (Figure 3.17C, GLCCI1). Notably, the combined knockdown of both CTCF and Nup93 upregulated expression levels of HOXA genes, comparable to Nup93 knockdown alone (Figure 3.17C, compare green and orange bars). Additionally, GLCCI1 was upregulated to a greater extent (~3 fold) in Nup93+CTCF Kd cells, suggesting a role for CTCF even in cells subjected to a combined depletion of Nup93 and CTCF. Taken together, we conclude from these assays that Nup93 serves as an additional modulator of HOXA gene organization and prevents its untimely expression independent of CTCF in differentiated cells.

**Figure 5.2**

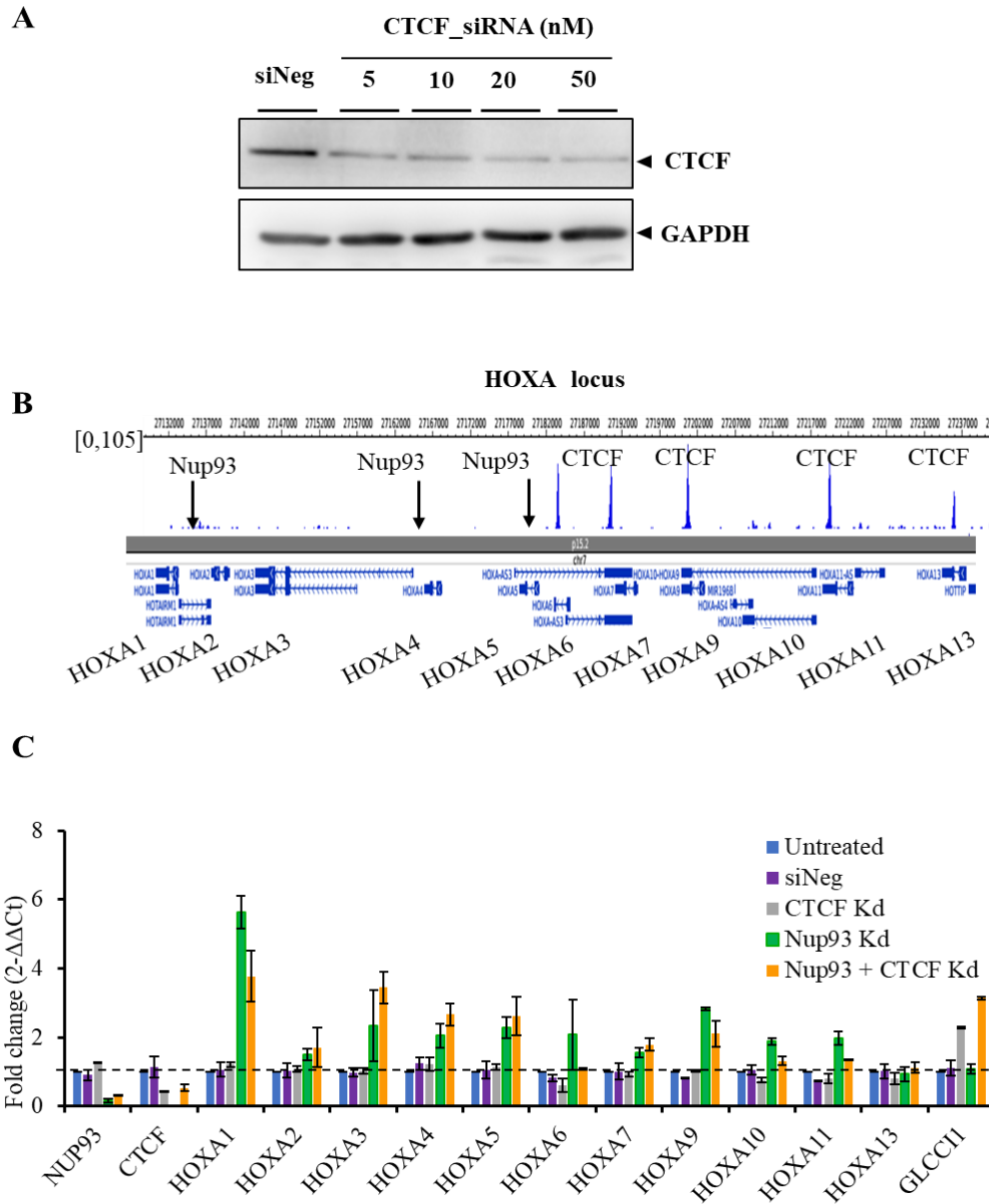


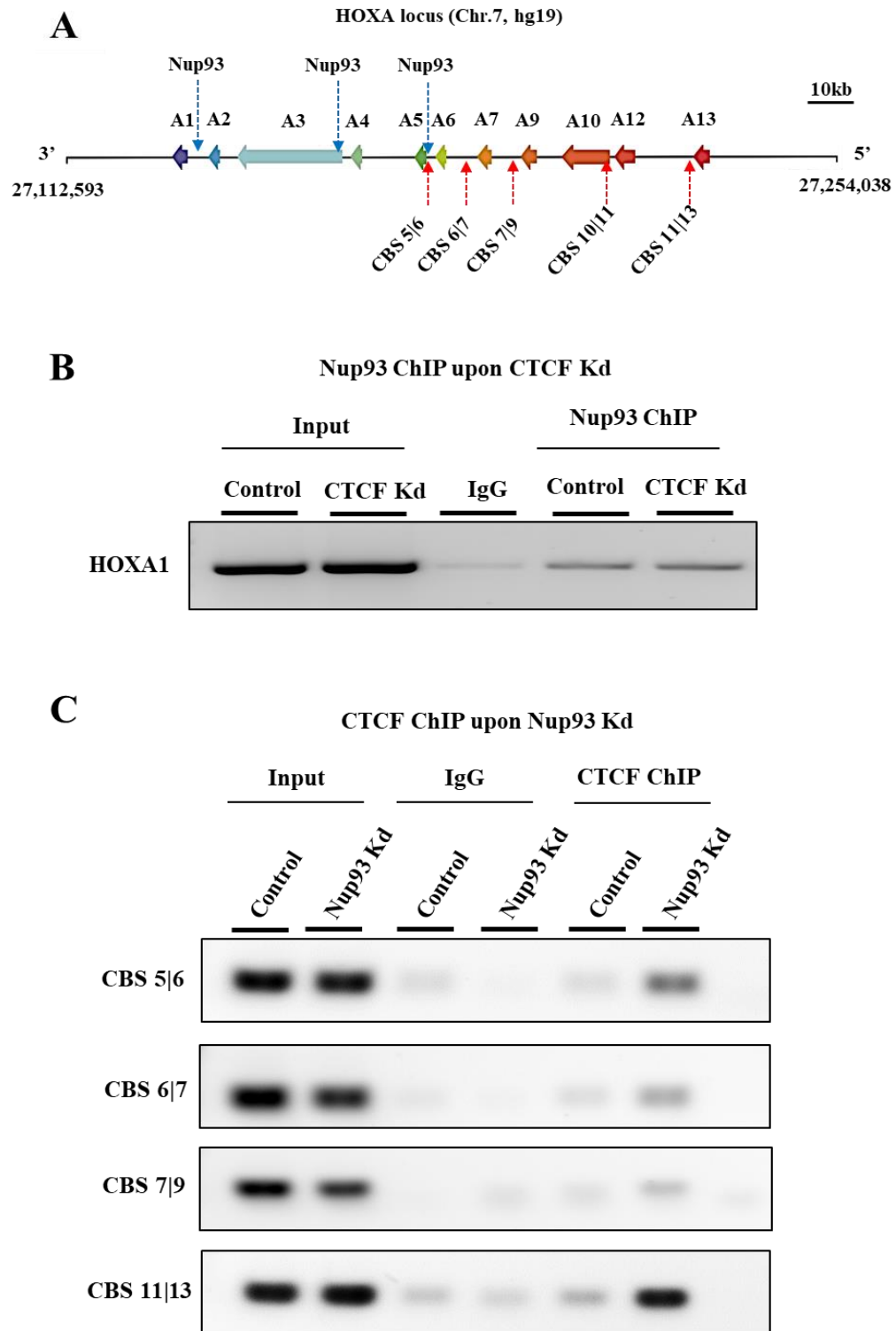
**Figure 5.2 Nup93 does not interact with CTCF or PRC2 complex proteins.** **A)** Representative Western blot showing siRNA- mediated knockdown of CTCF in DLD1 cells. **B)** Epigenome Browser view of CTCF (GSM749729) (arrow indicates potential binding sites of Nup93) on HOXA gene cluster. **C)** qRT-PCR analysis was used to determine mRNA levels of all HOXA genes (HOXA1 to HOXA13) upon CTCF and combined Nup93 + CTCF knockdowns in DLD1 cells. Graph represents fold change ( $2^{-\Delta\Delta C_t}$ ) in levels of mRNA normalized to untreated cells. Error bars SEM, data from two independent biological replicates (N = 2) that includes total of 6 technical replicates, GLCCI, served as control. Nup93 Kd data (green bars) is from Figure 3.8A, plotted here for comparison between Nup93 Kd and Nup93 + CTCF Kd (orange bars)

### **5.1.3 Nup93 depletion increases occupancy of CTCF on its conserved binding sites**

Since qRT-PCR analysis revealed that depletion of CTCF alone does not affect HOXA gene expression, we asked if CTCF depletion changes the occupancy of Nup93 on HOXA gene locus. We performed the Nup93 ChIP in the background of CTCF depletion and determined its occupancy on the HOXA1 promoter (Figure 5.3 A, a Nup93 binding site on HOXA1). Surprisingly, the ChIP-PCR analysis showed that depletion of CTCF does not affect the occupancy of Nup93 on HOXA1 promoter (Figure 5.3 B, compare Nup93 ChIP in control vs CTCF knockdown lane). This result suggests that Nup93 associates with HOXA gene locus independent of CTCF. This further underscore that CTCF depletion alone does not affect HOXA gene expression in differentiated cells. It is possible that in differentiated cells CTCF may not associate with HOXA gene cluster in presence of Nup93, since Nup93 enrichment may suppress CTCF occupancy on its binding sites. To test this possibility, we determined the CTCF enrichment on its conserved binding sites (CBS5|6, CBS6|7, CBS7|9 and CBS12|13) in the presence and absence of Nup93. We designed ChIP-PCR primers on conserved binding sites of CTCF (CBS5|6, CBS6|7, CBS7|9 and CBS12|13) and performed CTCF ChIP in control and Nup93 depleted cells (Figure 5.3 A and B). Remarkably, the ChIP-PCR analysis showed that CTCF is not enriched on its binding sites in control cells (Figure 5.3 B). In contrast, we observed a significant enrichment of CTCF on its binding sites upon Nup93 depletion. This finding suggests that Nup93 potentially functions as an independent organizer of the HOXA locus and CTCF is not required for its organization in the repressed state.



**Figure 5.3**



(See figure on previous page)

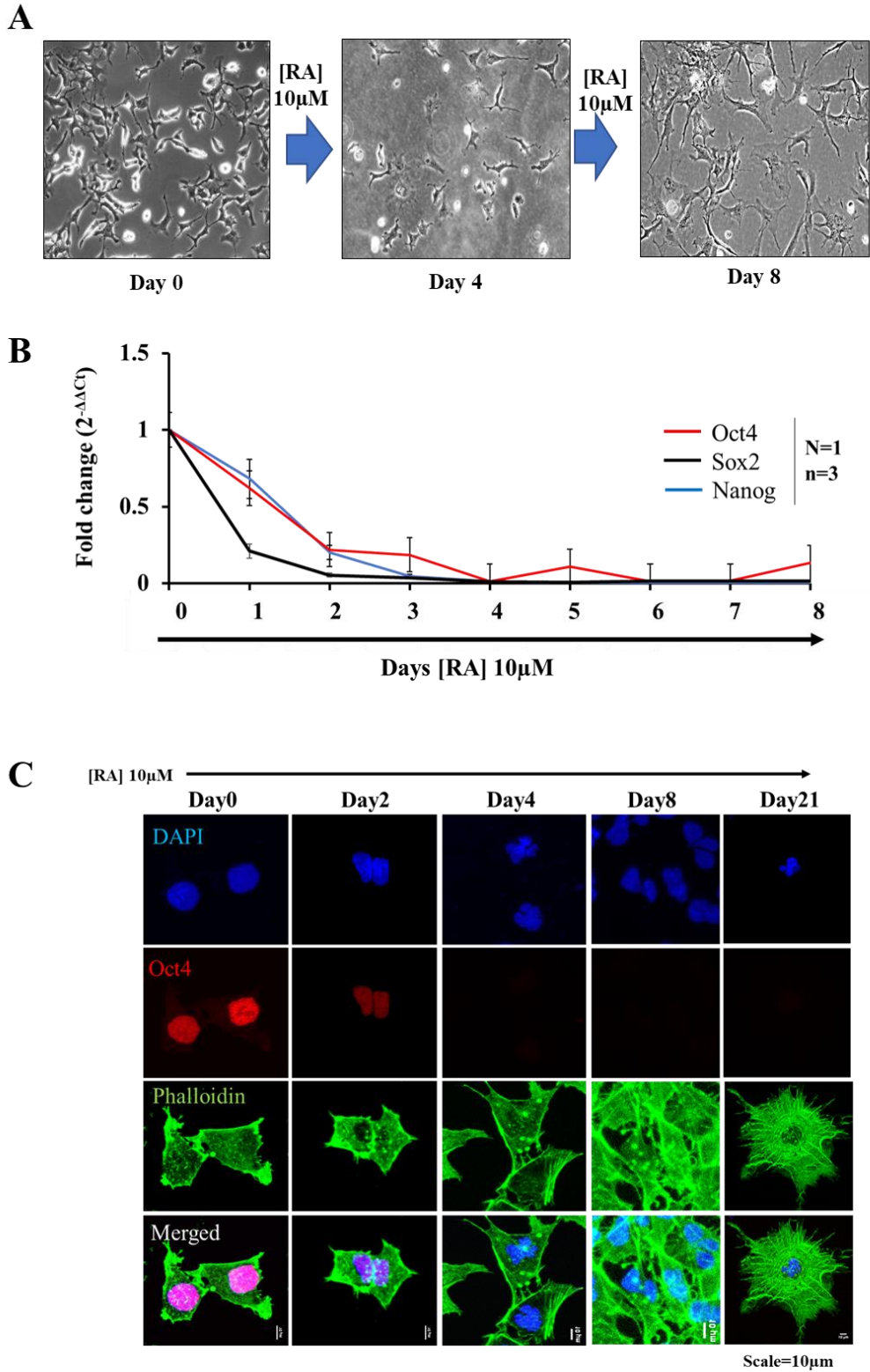
**Figure 5.3 Nup93 depletion increases occupancy of CTCF on its conserved binding sites.** **A)** A linear schematic of the HOXA gene cluster. Genes are indicated by arrows illustrating the direction of transcription. Nup93 and CTCF binding sites (CBS) are indicated by blue and red vertical arrows respectively. **B)** Nup93 ChIP-PCR performed in control and CTCF depleted cells for HOXA1 promoter. Input represents 1% of total chromatin used for ChIP Experiment **C)** CTCF ChIP-PCR performed in control and Nup93 depleted cells for CTCF binding sites (CBS) as shown in schematic of HOXA locus. Input represents 1% of total chromatin used for ChIP experiment (Data from single experiment)

#### **5.1.4 Effect of Nup93-CTCF on the dynamics of the HOXA gene cluster in RA mediated differentiation of NT2D1 cells**

To gain insights into the spatiotemporal relationship between Nup93 and CTCF in associating with HOXA locus during differentiation, we employed NT2/D1 (NTERA-2 cl. D1 human embryonal teratocarcinoma cell line) cell line as a differentiation model system. Activation of HOXA gene cluster upon induction with retinoic acid (RA) is well studied in NT2/D1 cells, accompanied by neuronal differentiation of the cells (Simeone et al., 1990; Xu et al., 2014). We first optimized RA mediated differentiation of NT2/D1 cells by performing morphological, transcriptional and immunofluorescence analysis. We performed RA [5  $\mu$ M] treatment for 8 Days and observed morphological changes in cells using bright field microscopy. We found that after 4 Days of RA treatment, NT2/D1 cells exhibited typical morphological changes such as longer projections, neuronal-like phenotype, and flattening of cells (Figure 5.4 A). Next, we examined the expression profile of well-known pluripotency marker genes Oct4, Sox2, and Nanog over an 8-Day induction of differentiation with RA (Day0 - Day8) (Figure 5.4 B). These genes are highly expressed in undifferentiated cells and their expression decreases with differentiation. We observed a gradual decrease in the expression levels of Oct4, Sox2 and Nanog upon RA treatment

from Day0 to Day8 (Figure 5.4 B). To further validate the differentiation of NT2/D1 cells, we performed immunostaining of pluripotency marker Oct4 combined with phalloidin staining on Days 2, 4 and 8 of RA treatment. Immunofluorescence analysis revealed a significant decrease in Oct4 staining upon RA treatment on Days 4, 8 and 21 indicating the differentiation of NT/2D1 cells (Figure 5.5 C). Further, we also observed typical changes in phalloidin staining upon RA treatment including polymerization actin filaments which is a typical characteristic of differentiated cells (Figure 5.4 C). Altogether, these results underscore that RA treatment successfully induces the differentiation of NT/2D1 cells.

**Figure 5.4**



(See figure on previous page)

**Figure 5.4 Standardization of NT2/D1 differentiation.** A) Bright field images of NT2/D1 cells at Day0, Day4 and Day8 of RA treatment. B) qRT-PCR analysis was used to determine mRNA levels of Oct4, Sox2 and Nanog upon RA treatment in NT2/D1 cells. Graph represents fold change ( $2^{-\Delta\Delta Ct}$ ) in levels of mRNA normalized to untreated cells. Error bars: SEM, data from one experiment that includes 3 technical replicates. Error bar = SEM. C) Immunofluorescence assay performed for Oct4 (Red) and phalloidin (Green) in NT2/D1 cells at Day0, Day2, Day4, Day8 and Day21 of differentiation. Scale bar=10 $\mu$ m, Magnification 63x.

### 5.1.5 RA mediated activation of HOXA gene cluster in NT2/D1 cells

Retinoic acid-mediated activation of HOXA gene cluster is well established in human embryonic carcinoma NT2/D1 cells (Xu et al., 2014). After optimization of RA mediated differentiation of NT/2D1 cells, we sought to examine the expression of HOXA genes in NT2/D1 cells over an 8-Day induction with 5 $\mu$ M RA. We performed qRT-PCR for selected HOXA genes representing 3'-end (HOXA1), the central region (HOXA5) and 5' end (HOXA9) of the HOXA gene cluster. qRT-PCR analysis revealed that expression levels of all HOXA genes were undetectable in untreated cells at Day0 (Figure 5.5 A-C). After RA treatment, all three HOXA genes were upregulated, however, the pattern of expression was different for each HOXA gene. We observed early activation of the HOXA1 gene upon RA induction, which peaks on Day 2, with a progressive decrease in its expression from Day2 onwards (Figure 5.5 A). HOXA5 showed a progressively slower activation as compared to HOXA1, which peaked on Days 5-6 (Figure 5.5 B). Similarly, HOXA9 was activated later Day4 onwards, which peaks at Day6 (Figure 5.5 C). Interestingly, HOXA1 showed a complete decrease in its expression levels after Day8 (Figure 5.5A). In contrast, HOXA5 and HOXA9 expression levels were not entirely decreased after Day8 (Figure 5.5 B and D). Thus, consistent with previous findings, our data suggest an early expression of

3' HOXA genes and late expression of 5' genes during the process of differentiation (Martinez-Ceballos and Gudas, 2008; Rousseau et al., 2014; Xu et al., 2014). Therefore, the temporal activation of the HOXA gene cluster serves as a reliable model for studying gene expression regulation of the HOXA cluster.

**Figure 5.5**

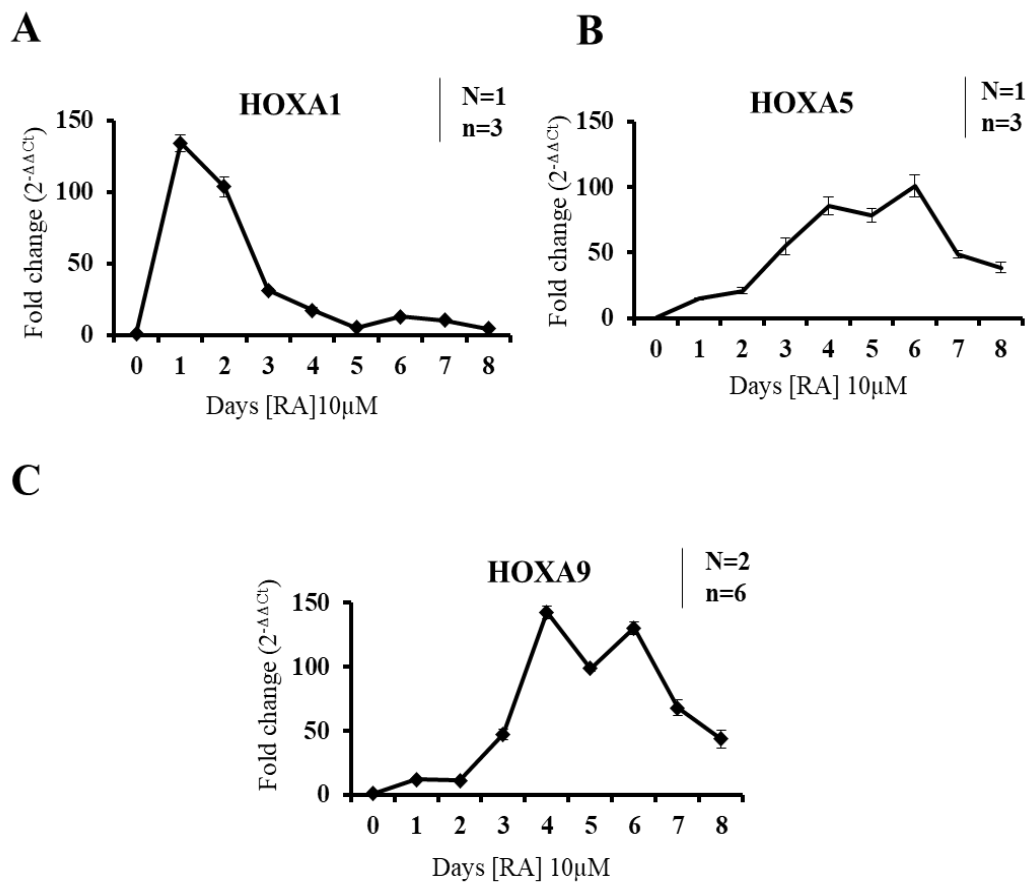


**Figure 5.5 Temporal activation of HOXA genes upon RA induction. A-D)** qRT-PCR analysis of (A) HOXA1, (B) HOXA5 and, (C) HOXA9 genes during differentiation of NT2/D1 cells from Day0 to Day8. Graph represents fold change ( $2^{-\Delta\Delta C_t}$ ) in levels of mRNA normalized to untreated cells. Error bars: SEM Data from one experiment for HOXA1 and HOXA5, and two biological replicates for HOXA9.

### **5.1.6 Expression levels of Nup93 and CTCF are unaffected upon differentiation**

We previously identified that Nup93 associates with 3' end of the HOXA gene cluster in DLD-1 cells. In contrast, CTCF has conserved binding sites on 5' end of the HOXA gene cluster. Additionally, RA mediated differentiation of NT2/D1 cells shows a temporal activation of the HOXA gene cluster (Rousseau et al., 2014; Xu et al., 2014). Based on these results, we wondered if the activation of the HOXA gene cluster during differentiation is accompanied by changes in the levels of Nup93 and CTCF. We first examined the levels of Nup93 by qRT-PCR upon RA treatment on Days 0, 2, 4 and 8 (Figure 5.6A). The extent of RA induction was tested by the observed decrease in Oct4 levels on Days 4 and 8 (Figure 5.6 A). We observed no significant change in Nup93 expression on Days 2 and 8 of RA treatment, while Day4 showed a slight increase (<1.5 fold) in Nup93 expression (Figure 5.6 A). This suggests that RA treatment does not affect the expression levels of Nup93 in NT2/D1 cells. Next, we sought to determine the protein levels of Nup93 and its interactors -Nup188 and -Nup205 along with CTCF during the process of RA mediated differentiation. Differentiation of NT2/D1 cells was first confirmed by an observed decrease in Oct4 levels (Figure 5.6 B). Interestingly, western blot analysis revealed that RA treatment did not affect the levels of Nup93 and CTCF during differentiation (Figure 5.6 B). Furthermore, Nup188 levels were unaffected upon RA treatment (Figure 5.6 B). Of note, we observed a slight decrease in the levels of Nup205 and an increase in the levels of Nup98 on Day8, however, the biological significance of this change remains elusive (Figure 5.6 B). Together, these findings suggest that RA mediated differentiation of NT2D1 cells is not associated with changes in the expression levels of Nup93 and CTCF.

**Figure 5.6**

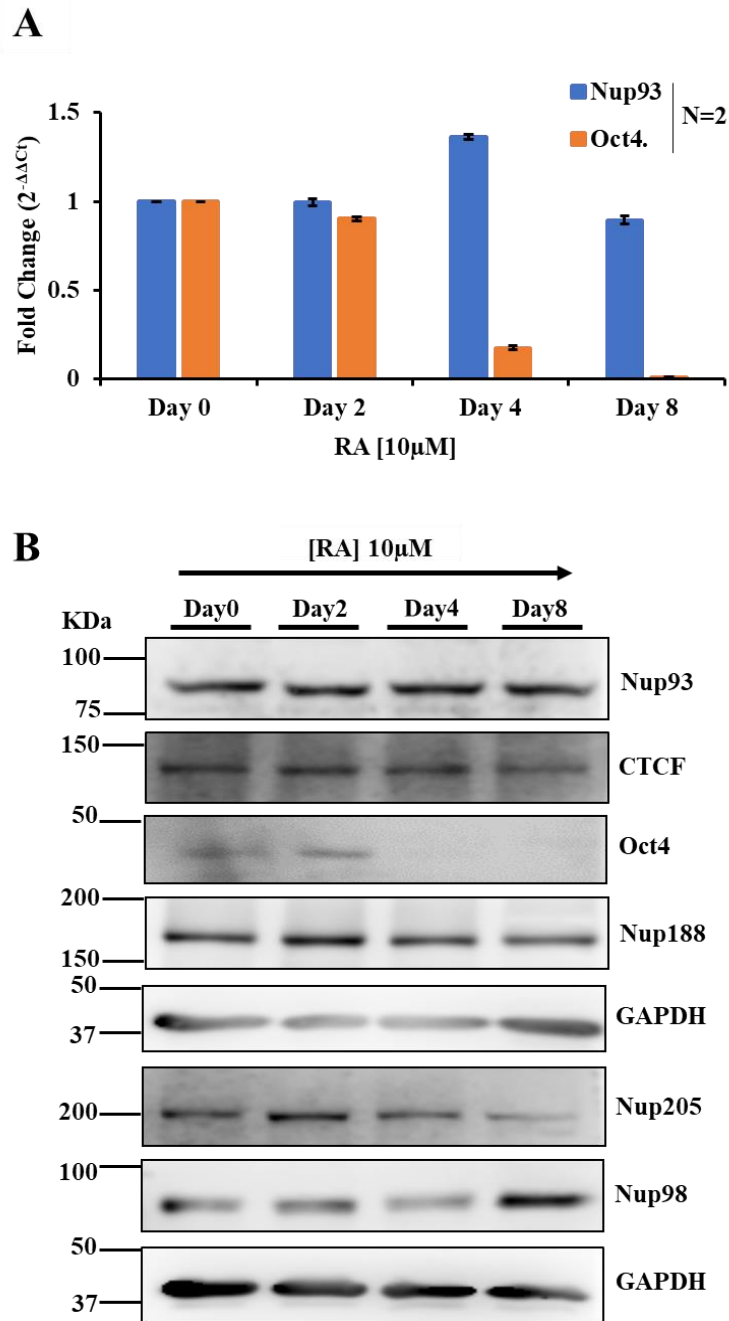


**Figure 5.6 Expression levels of Nup93 and CTCF are unaffected upon differentiation.** **A**) qRT-PCR analysis of Nup93 and Oct4 during differentiation of NT2/D1 cells at Day0, Day2, Day4 and Day8. Graph represents fold change ( $2^{-\Delta\Delta C_t}$ ) in levels of mRNA normalized to untreated cells. Error bars: SEM Data from two biological replicates that includes 6 technical replicates **B**) A representative western blot representing protein levels of Nup93, CTCF, Oct4, Nup188, Nup205 and Nup98. GAPDH was used as loading control. (N=2 biological replicates)



### 5.1.7 Antagonistic effect of Nup93 and CTCF depletion on HOXA gene expression

Given the observation that the levels of Nup93 and CTCF are unchanged during differentiation of NT2/D1 cells, we tested if their decrease affects HOXA expression in NT2/D1 cells. We analyzed the expression levels of 3' HOXA genes, HOXA1 and HOXA5 in Nup93 and CTCF depleted cells. In addition, to determine the combined effect of Nup93 and CTCF depletion on HOXA gene expression, we performed co-depletion of Nup93 and CTCF. Efficient knockdown of Nup93 and CTCF was achieved after 48h of siRNA transfection as verified by qRT-PCR (Figure 5.7 A). Consistent with our previous findings in DLD-1 cells, Nup93 knockdown resulted in a significant increase in the levels of HOXA1 and HOXA5 genes (Figure 5.7 A). Surprisingly, CTCF knockdown resulted in a significant decrease in HOXA1 and HOXA5 levels (Figure 5.7 A). This result is consistent with the previous finding in THP1 cells, where CTCF depletion led to a decrease in HOXA expression (Crutchley, 2014). Similarly, in *Drosophila*, CTCF depletion during early stages of development results in decreased expression of homeotic genes (Mohan et al., 2007). In contrast with this result, the previous finding in NT2/D1 cells has shown that CTCF depletion does not alter the expression of HOXA1 and HOXA2 but enhances the expression of HOXA5 (Xu et al., 2014). Importantly, we did not observe a decrease in HOXA expression upon CTCF depletion in DLD-1 cells (Figure 5.2 C), suggesting cell type-specific role of CTCF in HOXA regulation. Notably, we observed a marginal decrease in the levels of Nup93 upon CTCF depletion, however, CTCF levels were unchanged upon Nup93 depletion (Figure 5.7 A). Together these results suggest that depletion of CTCF and Nup93 potentially have an antagonistic effect on HOXA gene expression during differentiation

**Figure 5.7**

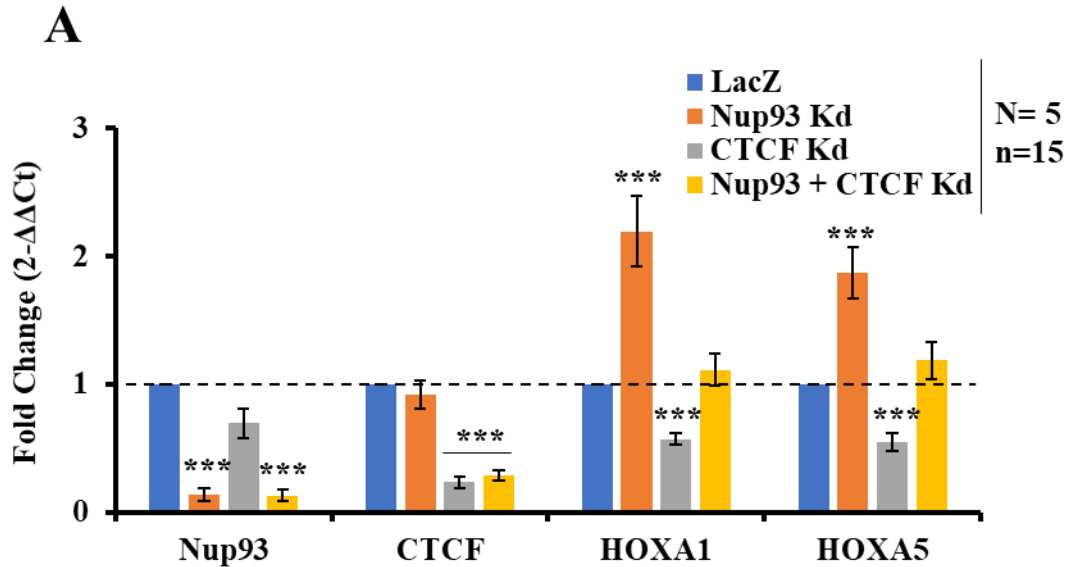


**Figure 5.7 Temporal activation of HOXA genes upon RA induction A)** qRT-PCR analysis of Nup93, CTCF, HOXA1 and, HOXA5 genes in control (LacZ), Nup93 knockdown, CTCF Kd and Nup93 + CTCF Kd cells. Graph represents fold change ( $2^{-\Delta\Delta C_t}$ ) in levels of mRNA normalized to control cells. Error bars: SEM. Data from 3 biological replicates that includes total of 9 technical replicates. \*\*\* $p < 0.001$  (Students t-test between LacZ and knockdown)

### 5.1.8 RA mediated induction of HOXA gene expression in Nup93 or CTCF depleted cells

Our results suggest that Nup93 and CTCF have an antagonistic role in modulating HOXA gene expression in NT2/D1 cells, but whether Nup93 and CTCF contribute to the RA mediated induction of HOXA gene expression is unknown. We hypothesized that RA induction enhances expression of the HOXA genes in Nup93 depleted cells and reduces expression in CTCF depleted cells. As a first approach to investigate this hypothesis, we performed 48h knockdown of Nup93 and CTCF followed by RA induction for 24h

(Schematic-Figure 5.8 A). We found that the depletion of Nup93 during RA mediated differentiation of NT2/D1 cells results in an enhanced activation of 3'HOXA genes (HOXA1 and HOXA5), whereas 5' HOXA gene (HOXA9) showed a reduced activation as compared to control cells (Figure 5.8 B). It appears that without Nup93, 3' end HOXA genes are pre-activated and are more responsive to RA treatment (Figure 5.8 D). In contrast to Nup93, CTCF depletion resulted in a reduced expression of 3' end HOXA genes (HOXA1 and HOXA5) in response to RA induction as compared to control RA treated cells (Figure 5.8 C). Both Nup93 and CTCF depletion did not show a significant effect on the activation or repression of 5' end HOXA gene (HOXA9) (Figure 5.8 B and C). It is important to note that 5' HOXA genes are activated later (after Day4) during the differentiation and 24h RA treatment is not enough for their activation. Altogether, these results indicate that 3' end HOXA genes are more responsive to RA induction upon Nup93 depletion and less responsive upon CTCF depletion. This could suggest an antagonistic role of Nup93 and CTCF in regulating HOXA gene expression. Unfortunately, we were unable to perform RA treatment for a longer period (> 24h) in Nup93 and CTCF depleted cells because of reduced cell viability.

**Figure 5.8**

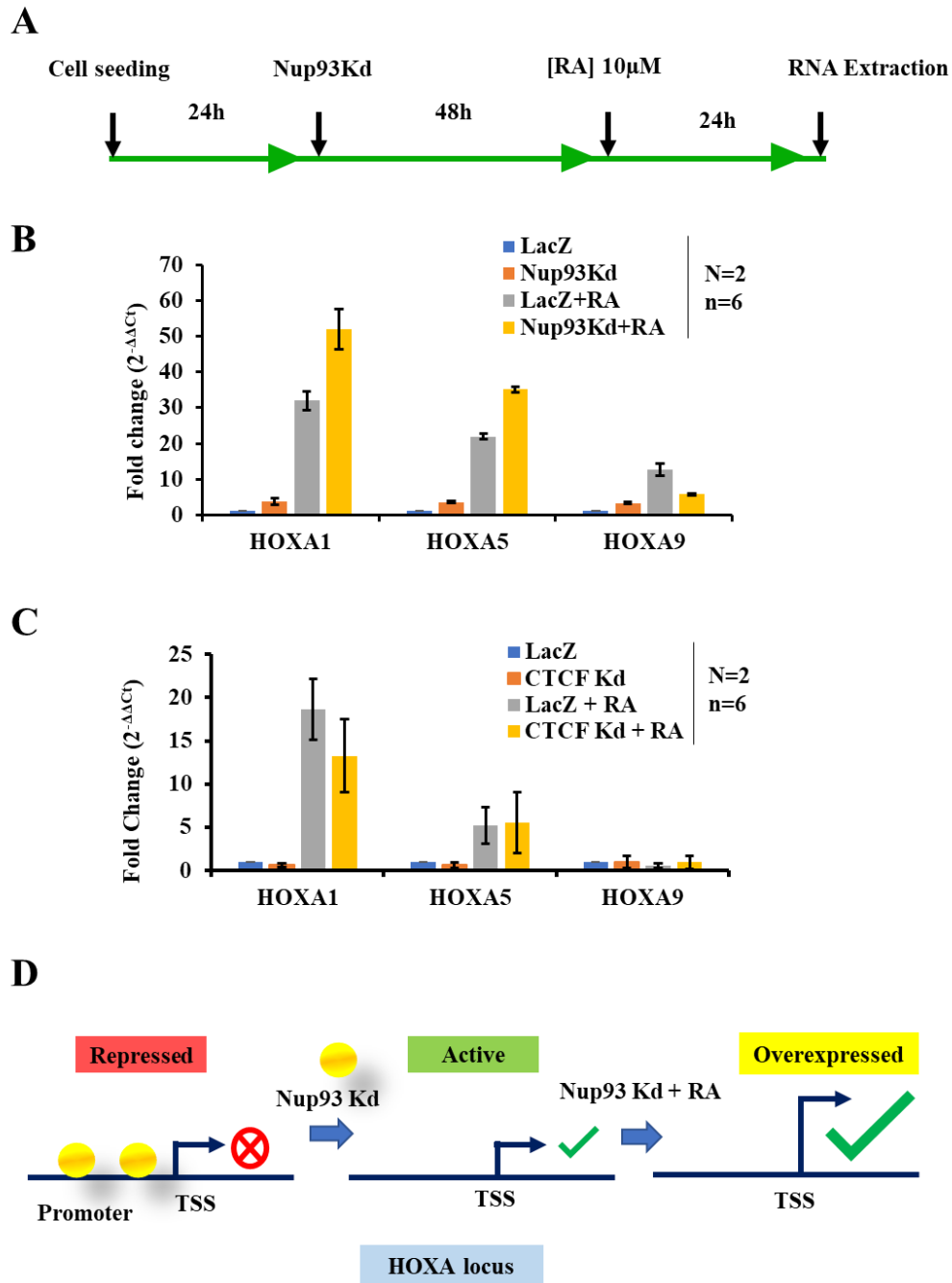


**Figure 5.8: RA mediated induction of HOXA gene expression in Nup93 or CTCF depleted cells.** A) Schematic representation of retinoic acid treatment in Nup93 or CTCF depleted cells, B) qRT-PCR analysis of HOXA1, HOXA5 and, HOXA9 genes in control (LacZ), Nup93Kd, LacZ + RA and Nup93Kd + RA treated cells. C) qRT-PCR analysis of HOXA1, HOXA5 and, HOXA9 genes in control (LacZ), CTCF Kd, LacZ + RA and CTCF Kd + RA treated cells. Graph represents fold change ( $2^{-\Delta\Delta C_t}$ ) in levels of mRNA normalized to control cells. Error bars: SEM. Data from 2 biological replicates that includes total of 6 technical replicates. D) A model representing the effect of Nup93 depletion on HOXA gene expression upon RA treatment

### **5.1.9 Dynamic association of HOXA locus with the nuclear periphery during differentiation**

Recent studies using various cellular models have shown that HOXA locus undergoes a dynamic reorganization of chromatin structure during activation (Ferraiuolo et al., 2010; Rousseau et al., 2014). In addition, we previously showed that activation of HOXA locus is accompanied by its untethering from the nuclear periphery upon Nup93 depletion. However, the spatial dynamics of HOXA locus with respect to the nuclear periphery during the process of differentiation is unclear. Therefore, we examined the 3D positioning of HOXA locus during RA mediated differentiation of NT2/D1 cells. NT2/D1 cells are embryonal carcinoma cells and are aneuploid. To reconfirm the chromosomal ploidy, we determined the modal chromosomal number of NT2/D1 cells (Figure 5.9 A). Chromosomal ploidy analysis revealed that NT2/D1 cells have a modal chromosomal number of 62-63 (Figure 5.9 A). Next, we determined the ploidy of chromosome 7 in NT2/D1 cells by 2D-FISH analysis of HOXA locus (Red) and chromosome 7 (Green) in NT2/D1 cells (Figure 5.9 B). Surprisingly, we detected 2 whole copies of chromosome 7 and 2 truncated copies of P-arm of chromosome 7 in NT2/D1 cells (Figure 5.9 B and C). Interestingly, we found that HOXA locus was present on all 4 copies of chromosome 7, indicating an aneuploidy (4 copies) of HOXA locus in NT2/D1 cells (Figure 5.9 A and B).

We then performed 3D FISH (Fluorescent In situ hybridization) of HOXA locus at 4 different time points during differentiation, (i) Day0 -Inactive state, (ii) Day2 - Induced state, (iii) Day4-Active state, and (iv) Day8-Repressed state (Figure 5.10 A). We measured the shortest distance of the HOXA gene locus from the nuclear periphery. Our distance measurement analysis revealed that HOXA gene loci were predominantly localized closer

to the nuclear periphery before RA induction at Day0 (median = 1.13  $\mu\text{m}$ ) from the edge of the nucleus (Figure 5.10 B). It is important to note that the median distance of HOXA locus from the nuclear periphery in NT2/D1 cells (1.13  $\mu\text{m}$ ) is higher as compared to DLD-1 cells (0.64  $\mu\text{m}$ ). Interestingly, we observed a significant inward movement of HOXA locus from the nuclear periphery on Day2 and Day4 of differentiation (Figure 5.10 B and C). Strikingly, we found that, on Day8 of differentiation, HOXA locus showed a significant relocation toward the nuclear periphery (Figure 5.10 B and C). This is consistent with the repression of 3' HOXA genes (HOXA1 to HOXA5) on Day8 of differentiation, further indicating the repositioning of HOXA genes at the nuclear periphery. Together, our findings suggest that the activation and repression of HOXA locus during differentiation is associated with its dynamic movement from the nuclear periphery.

**Figure 5.9**

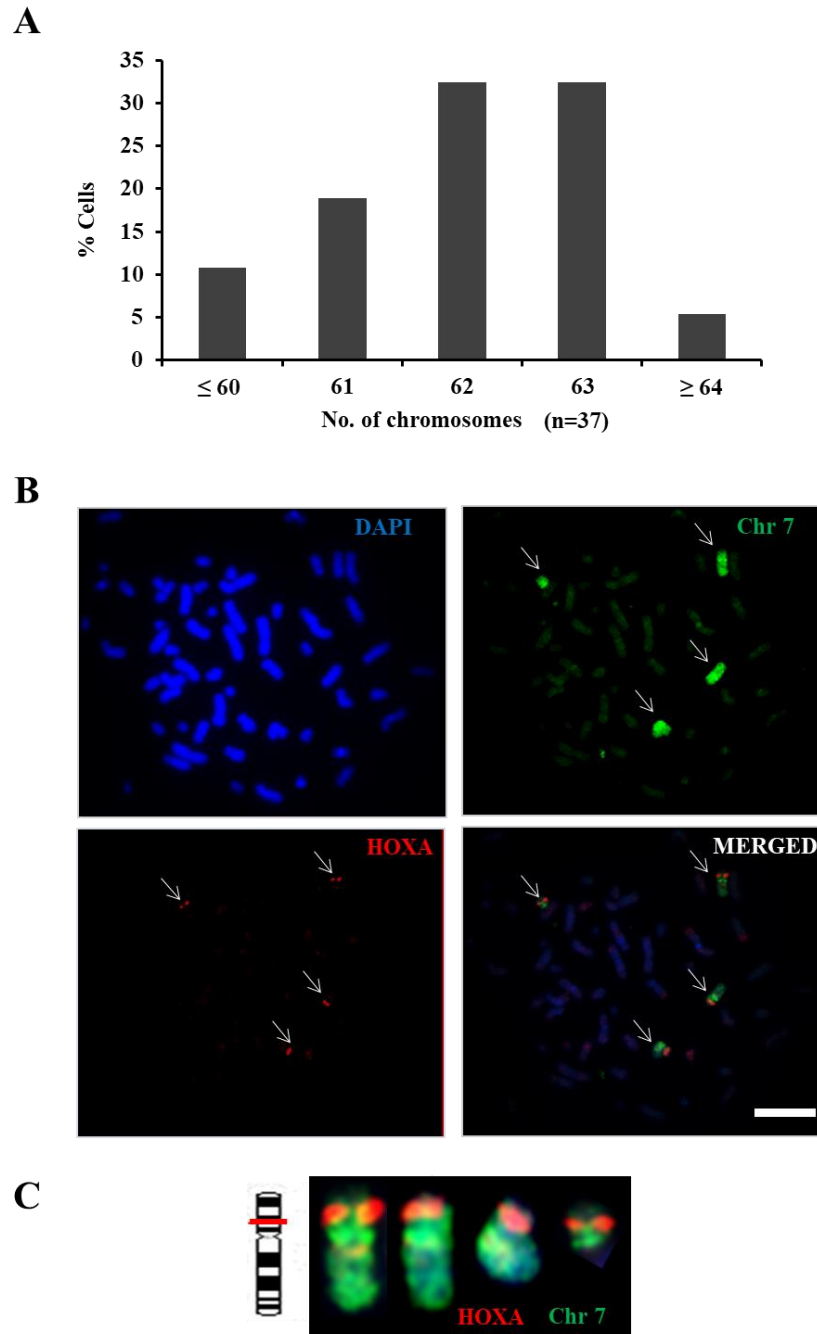
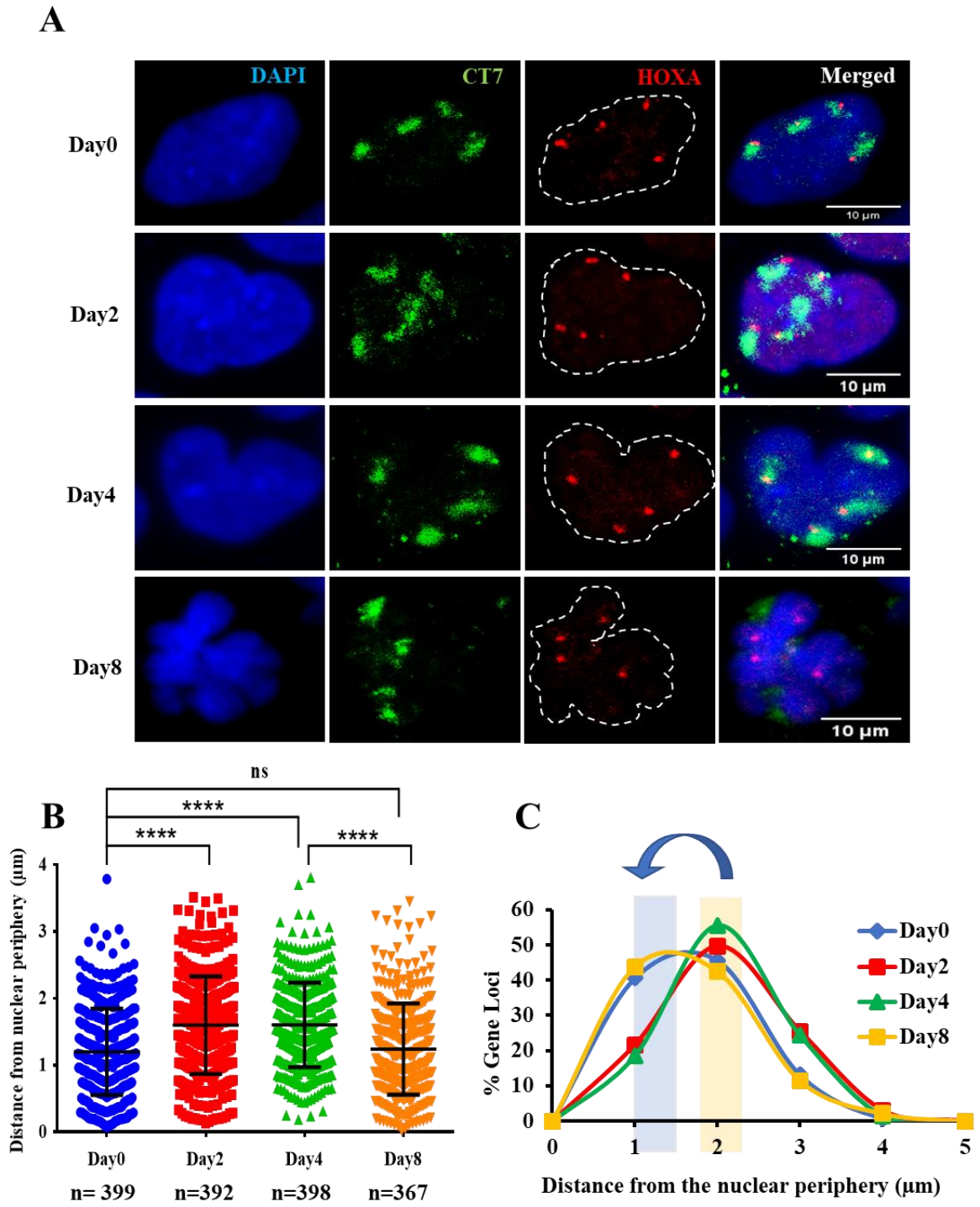


**Figure 5.9: 2D-FISH analysis of NT2/D1 cells.** **A)** Histograms showing quantification of chromosome number from NT2/D1 cells. n=38 metaphase spread, Data from one biological replicate. **B)** A representative metaphase spread from 2D-FISH analysis of Chromosome7 and HOXA gene locus in NT2/D1 cells, Magnification 63X **C)** Enlarged image of Chromosome7 and HOXA1 gene locus. Ideogram indicates the chromosomal location of HOXA (red). Two whole and two truncated copies of p-arm of chromosome7 were observed. HOXA locus is present in 4 copies.

Figure 5.10



5.1.1



(See image on previous page)

**Figure 5.10: Dynamic association of HOXA locus with the nuclear periphery during differentiation.**  
**A)** Representative images (maximum intensity projection of a confocal image stack) of 3D-FISH for HOXA (red), CT7 (green) and DAPI (blue) performed on Day0, Day2, Day4 and Day8 of differentiation of NT2/D1 cells. Scale bar ~10  $\mu\text{m}$ , white dotted line indicates nuclear boundary, magnification 63X **B)** Dot scatter plot showing shortest distance of HOXA gene locus from the nuclear periphery demarcated by DAPI. Day0 (n = 399 loci signals)-, Day2 (n = 392)-, Day4 (n = 398)- and Day8 (n = 367), horizontal bar represents median with interquartile range. Data from two independent biological replicates, \*\*\*p < 0.001 (Mann-Whitney U test). Data from two independent biological replicates **C)** Line graph showing the distribution of shortest distance of HOXA gene locus from the nuclear periphery on Day0, Day2, Day4 and Day8 of differentiation. Y-axis represents % gene loci. Curved arrow showing the repositioning of HOXA gene locus towards nuclear periphery on Day8 of differentiation

### **5.1.10 Dynamic association of Nup93 and CTCF with HOXA locus during differentiation**

Our 3D-FISH analysis indicated that HOXA locus shows dynamic repositioning from the nuclear periphery during differentiation. However, the role of Nup93 and CTCF in the positioning of HOXA locus during differentiation is unclear. As shown previously, both Nup93 and CTCF have specific binding sites on HOXA locus (Figure 5.1 A). Nup93 binding sites are predominantly enriched on 3' end HOXA genes (HOXA1, HOXA3, and HOXA5), while CTCF binding sites are enriched on 5' end HOXA genes (Figure 5.1 A). In addition, we observed that CTCF binding sites on HOXA1 and HOXA5 promoters overlap with Nup93 binding sites in Caco-2, fibroblast, HUVEC, and NHLF cell lines (Figure 5.1 A). Similarly, previous ChIP-seq study in NT2/D1 cells showed that CTCF has binding sites on HOXA1 and HOXA5 promoters (Crutchley, 2014). These observations suggest that Nup93 binding sites overlap with CTCF binding sites on HOXA1 and HOXA5 promoters in NT2/D1 cells.

We sought to determine the association of Nup93 and CTCF on HOXA1 promoter during differentiation. We performed Nup93 and CTCF ChIP at Days 0, 4, 8 of differentiation and determined the enrichment of Nup93 and CTCF on HOXA1 promoter by ChIP-PCR (Figure 5.11 A). Our ChIP-PCR analysis revealed that Nup93 is not enriched on HOXA1 promoter at Day0 (Inactive HOXA locus) and Day4 (Active HOXA locus) of differentiation (Figure 5.11 A, Nup93 ChIP, Day0 and Day4 lanes). Interestingly, we observed that Nup93 showed significant enrichment on HOXA1 promoter at Day8 (Repressed HOXA locus) of differentiation (Figure 5.11 A, Nup93 ChIP, Day8 lane). This result suggests that Nup93 is not associated with a HOXA1 promoter in its poised or active state (Day0 or Day4) but it shows specific enrichment on HOXA1 promoter in its repressed state (Day8). In contrast to Nup93, we found that CTCF showed lower occupancy on HOXA1 promoter on Day0 which is then significantly enriched on Day4 and again subsequently decreased on Day8 of differentiation (Figure 5.11 A). These data suggest the association of Nup93 and CTCF with the HOXA1 promoter is mutually exclusive. Nup93 and CTCF associates with the HOXA1 promoter in absence of one another. Finally, we speculate that CTCF is required for inducing initial looping of HOXA cluster during its active state and once the loops are formed they are tethered to the nuclear periphery by Nup93 (Figure 5.11 B). However, it is important to note here that our IgG control showed non-specific enrichment on Day0 and Day4. Further, we have not performed ChIP-qPCR analysis to quantitate the enrichment of Nup93 and CTCF on the HOXA1 promoter. Therefore, we would like to mention that the conclusion of this result is the subject of

further investigation with proper IgG control and qPCR analysis. We are in process of performing more biological replicates for this experiment.

**Figure 5.11**

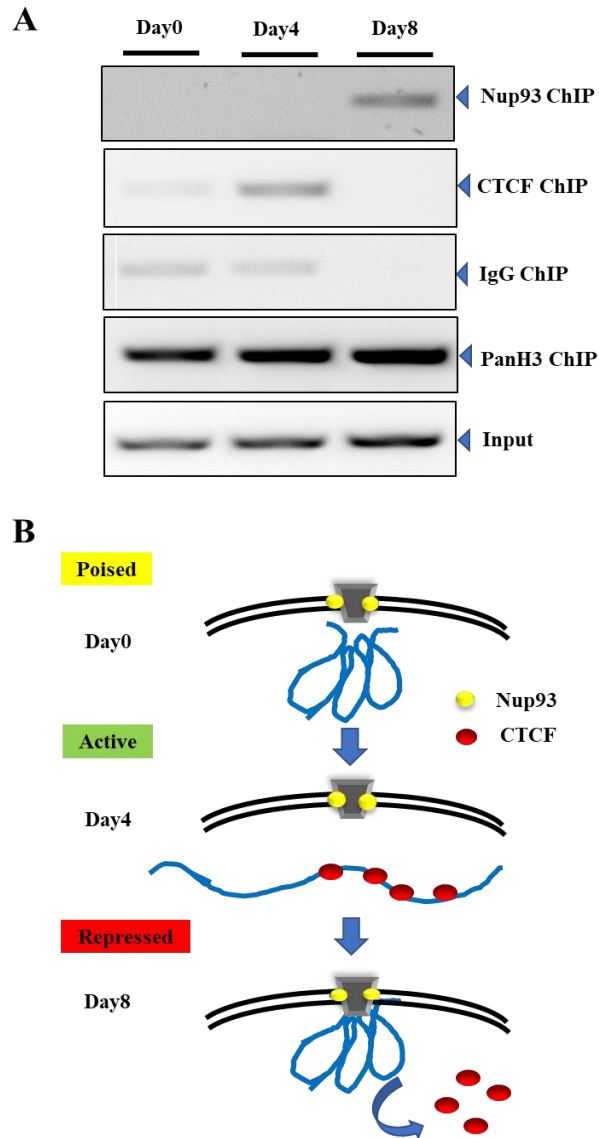


**Figure 5.11: Dynamic association of Nup93 and CTCF with HOXA locus during differentiation.** A) ChIP-analysis of Nup93 and CTCF for HOXA1 promoter on Day0, Day4 and Day8 of differentiation. Normal rabbit IgG was used as negative control. PanH3 (Anti Histone H3 antibody) was used as a positive control. Input represents 1% of total chromatin used in ChIP experiment. B) Speculative model representing the dynamic association of HOXA gene locus with the nuclear periphery during differentiation.

### 5.3 Discussion

Our study provides an early insight into the molecular interplay between the genome organizer CTCF and nucleoporin Nup93 in the dynamic organization of HOXA locus. We characterized the role of Nup93 and CTCF in the regulation of HOXA gene expression during differentiation. We demonstrated that depletion of CTCF in undifferentiated NT2/D1 cells downregulates HOXA gene expression (Figure 5.7). In contrast, depletion of CTCF in differentiated DLD-1 cells does not affect the expression of HOXA gene cluster (Figure 5.2 C). Importantly, Nup93 depletion in both DLD-1 and NT2/D1 cells upregulates HOXA gene expression (Figure 5.2-C and Figure 5.7). These results suggest that CTCF may have a cell type-specific role in controlling HOXA gene expression, while Nup93 mainly functions as a repressor of HOXA gene expression. The previous finding has shown that CTCF depletion leads to a decrease in HOXA expression in THP-1 cells (Crutchley, 2014). Similarly, in *Drosophila*, CTCF depletion during early stages of development results in decreased expression of homeotic genes (Mohan et al., 2007). However, another study in NT2/D1 cells has shown that depletion of CTCF alone does not affect the expression of HOXA genes, but Retinoic acid treatment combined with CTCF depletion enhances HOXA gene expression (Xu et al., 2014). These observations suggest that although CTCF has conserved binding sites on HOXA locus across different cell types (Figure 5.1A), it may possess a cell type-specific role in HOXA gene regulation.

We demonstrated by ChIP-PCR in DLD-1 cells that CTCF does not associate with its conserved binding sites in presence of Nup93 (Figure 5.3 C). This result can be further explained by our finding that CTCF depletion does not affect HOXA expression in DLD-1 cells (Figure 5.2 C). It is possible that silenced HOXA gene cluster is tethered to the

nuclear periphery by Nup93 independent of CTCF. Therefore, CTCF depletion alone does not affect the expression of HOXA genes in DLD-1 cells (Figure 5.2 C). We further demonstrated that depletion of Nup93 in DLD-1 cells leads to an increase in CTCF occupancy on its conserved binding sites (Figure 5.3 C). Interestingly, CTCF depletion does not alter the occupancy of Nup93 on HOXA1 promoter, further suggesting that Nup93 occupancy on HOXA1 promoter is not dependent on CTCF (Figure 5.3 B). However, our data do not exclude the possible contribution of CTCF in mediating interchromatin contacts during early stages of differentiation as demonstrated by previous chromatin conformation capture studies (Rousseau et al., 2014; Xu et al., 2014). Together, our result is consistent with a previous model whereby, HOXA gene activation is accompanied by the opening of HOXA cluster, and therefore CTCF binding sites become available for CTCF occupancy (Rousseau et al., 2014; Xu et al., 2014). It is important to note that depletion of Nup93 is not likely to entirely open of the HOXA gene cluster in DLD-1 cells for at least two reasons. First, the extent of upregulation of the HOXA gene cluster upon Nup93 depletion (3-4 fold) is less than the extent of upregulation during the process of differentiation (> 100-fold). Second, all HOXA genes are not upregulated to the comparable extent upon Nup93 depletion in DLD-1 cells. Therefore, an interplay between Nup93 and CTCF association with HOXA locus is difficult to study in terminally differentiated DLD-1 cells. For these reasons, we examined the association of Nup93 and CTCF with HOXA locus during the process of differentiation of NT2/D1 cells.

Our finding that the depletion of Nup93 in NT2/D1 cells enhances expression of HOXA genes upon RA treatment suggests that HOXA genes are more responsive to RA treatment in absence of Nup93 (Figure 5.8 B). We surmise that Nup93 depletion may result

in the opening of HOXA cluster which further increases the access of RARE (Retinoic acid response element) and thereby making HOXA more responsive to RA treatment. However, detailed investigation of interchromatin contacts between RARE elements in the presence and absence of Nup93 is required for understanding the role of Nup93 in organizing RARE elements within the HOXA gene cluster. In contrast to Nup93, we found that CTCF depletion leads to reduced expression of HOXA genes in response to RA treatment (Figure 5.8 B). The depletion of CTCF may enhance Nup93 occupancy on HOXA genes which may further repress HOXA gene expression. To test this possibility, it is important to perform Nup93 ChIP in the absence of CTCF in NT2/D1 cells.

Recent studies have revealed the dynamic organization of HOXA gene clusters during HOXA activation in various cellular models (Ferraiuolo et al., 2010; Rousseau et al., 2014; Xu et al., 2014). Here we examined the dynamic repositioning of HOXA gene locus during differentiation using 3D-FISH. In NT2/D1 cells, the HOXA gene cluster is in a relatively poised state for rapid activation upon developmental cues (Xu et al., 2014). Our 3D-FISH analysis revealed that, in control NT2/D1 cells, HOXA gene locus is positioned proximal to the nuclear periphery [median = 1.13  $\mu\text{m}$  from the edge of the nucleus] (Figure 5.10). This could suggest that the HOXA locus is not tethered to the nuclear periphery before differentiation and only positions proximal to the nuclear periphery in a 'poised state' for rapid activation upon RA treatment. However, upon RA induction, on Day2 and Day4, the active HOXA locus showed significant inward movement towards the nuclear interior (Figure 5.10). We speculate that HOXA locus moves from a repressive compartment to the active compartment during differentiation which is consistent with the previous finding that the activation of HOXA locus is accompanied by an expansion of the

repressed chromatin into the active domain (Narendra et al., 2015). Surprisingly, we observed significant repositioning of HOXA locus towards the nuclear periphery on Day8 of differentiation, this could be further explained by significant repression of 3' HOXA genes on Day8 of differentiation (Figure 5.10 and Figure 5.5). The previous study by Rousseau et al, have demonstrated the dynamic reorganization of HOXA locus during differentiation and revealed that activation of HOXA locus is associated with loss of chromatin contacts within insulators (Rousseau et al., 2014). However, the information about spatial positioning of the HOXA locus inside the nucleus during the process of differentiation was lacking. We demonstrate that HOXA locus shows dynamic movement with respect to the nuclear periphery during the process of differentiation (Figure 5.10). However, due to the limitation of the 3D-FISH experiment, our result does not distinguish between the movement of individual HOXA genes (HOXA1 to HOXA13) during the differentiation. BAC clone used for preparing FISH probes covers the entire HOXA cluster and therefore it is hard to track the sequential movement of 3' HOXA genes followed by 5' HOXA genes during its temporal activation. It will be useful to perform 3D-FISH with smaller probes specific to each HOXA gene.

CTCF has been recognized as a scaffold for attachment of chromatin loops at HOXA gene cluster (Hansen et al., 2017; Wang et al., 2015). We determined the temporal association of CTCF and Nup93 with HOXA locus during differentiation. We determined that, although HOXA genes are repressed at Day0, Nup93 is not associated with HOXA gene cluster before differentiation (Figure 5.11 A). The absence of Nup93 on HOXA locus at Day0 could be attributed to the poised status of HOXA genes in NT2/D1 cells, where the basal level of HOXA gene expression can be seen (Xu et al., 2014). We found that

Nup93 associates with HOXA1 gene at Day8 of differentiation when HOXA1 is entirely repressed (Figure 5.11 A). Therefore, the rationale for the involvement of Nup93 in the regulation of HOXA gene expression, during the early stage of differentiation, probably relates to the necessity of permanent repression of HOXA genes in adult tissues. We speculate that CTCF alone might not function as a permanent tether for repression of HOXA genes. Consistent with this assumption, we found that CTCF is enriched on active HOXA locus on Day4 and its enrichment significantly decreased on Day8 (Figure 5.11 A). This result further suggests that the association of Nup93 and CTCF with HOXA locus is mutually exclusive. CTCF might function during the early stages of repression for inducing chromatin looping and once the loops are formed they are tethered to the nuclear periphery by Nup93 (Figure 5.12). In support of this model, the previous finding has suggested that the principal role of CTCF is to initiate chromatin looping and stabilize PRC2 occupancy on HOXA locus (Xu et al., 2014). PRC2 complex proteins are known to regulate repressive histone marks on silent HOXA gene cluster (Atkinson et al., 2008; Xu et al., 2014). It is worth mentioning that, our BIOGRID analysis has revealed the interaction between Nup93 and PRC2 complex proteins EDD and Suz12 (Chapter 4, Figure 3.18). Nup93 might provide a stable platform for the organization and stabilization of PRC2 complex proteins on HOXA locus. However, the role of Nup93 in the recruitment of PRC2 complex proteins on HOXA locus remains to be elucidated.

An important question remaining relates to how the HOXA genes are contacted by a stable nucleoporin Nup93 during differentiation. One possible explanation is that the mediator proteins are required to facilitate the interaction between Nup93 and HOXA genes. Alternatively, Nup93 might associate with the HOXA gene cluster during nuclear



envelope reformation over the period of differentiation. However, the exact mechanism that triggers the silencing of HOXA locus during differentiation remains elusive. It would be interesting to determine whether CTCF mediates the interaction between Nup93 and HOXA cluster. Our study has provided insightful information about the HOXA gene cluster silencing; however, further experimentation is required to understand the spatiotemporal mechanism that regulates timely inactivation of the HOXA gene cluster during differentiation.

**Figure 5.12**

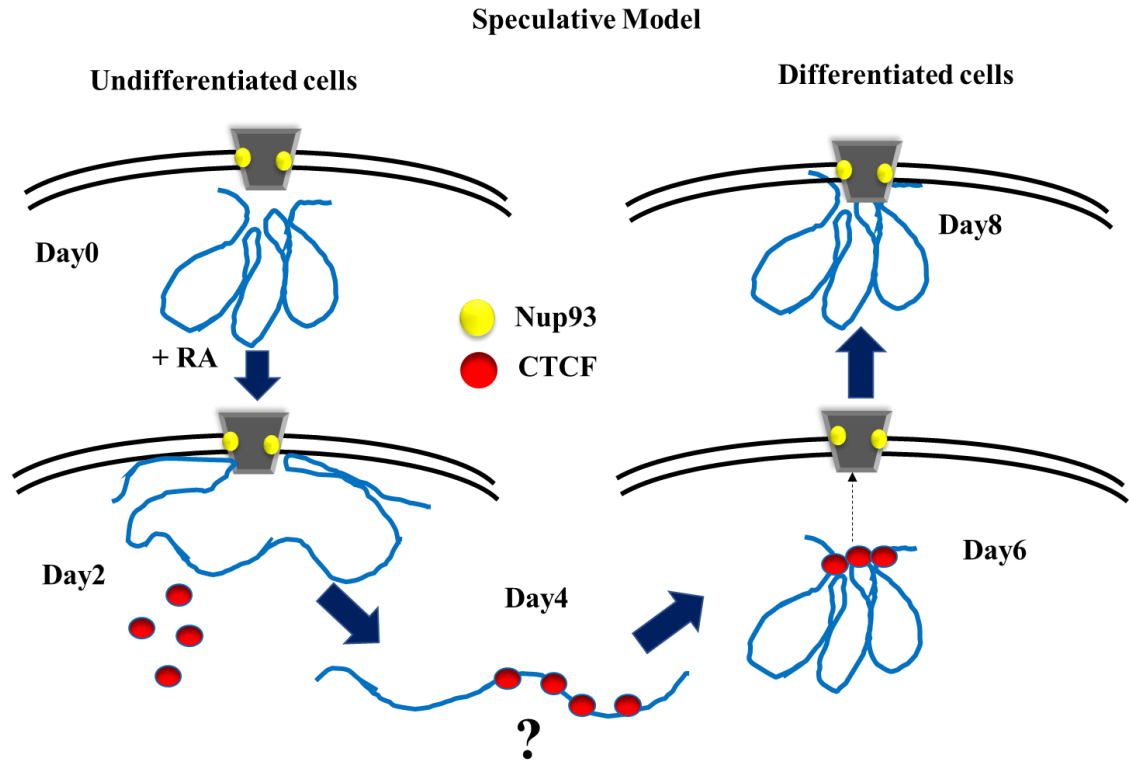


**Figure 5.12: Speculative model representing the dynamic association of HOXA gene locus with nuclear periphery during differentiation.** In undifferentiated cells HOXA gene locus is present in a poised state with some basal level of expression. Nup93 is not associated with HOXA gene locus at Day0. Upon retinoic acid treatment HOXA gene locus becomes active and chromatin looping is disturbed. In its active state CTCF occupy its binding sites and reinitiate looping of HOXA genes. HOXA gene are then tethered to the nuclear periphery by Nup93 in their repressed state.

## **Chapter 6: Conclusions and Potential Future**

### **Directions**

## 6.1 Conclusions

As discussed in Chapter 2, our study unravels a novel role for nucleoporin Nup93 and its interactors Nup188 and Nup205 in mediating the tethering and repression of the HOXA gene cluster. Our study adds to the literature which supports the additional role of nucleoporins in gene regulation. We found that depletion of Nup93, Nup188 or Nup205 significantly enhances HOXA gene expression. The elevated levels of HOXA gene expression upon the depletion of Nup93 or its interactors—Nup188 and Nup205, is associated with an increase in the occupancy of active histone marks and decreased levels of inactive histone marks with a concomitant increase in transcriptional elongation marks within the HOXA gene.

Nup93 is one of the most stable nucleoporins inside the nuclear pore complex (Rabut et al., 2004). Inverse FRAP experiments suggest that Nup93 has the longest residence time (~ 70 h) in the nuclear pore complex (Rabut et al., 2004). Each nuclear pore complex consists of 32 copies of Nup93 and each nucleus has more than 2000 copies of Nuclear pore complexes (Sachdev et al., 2012). Protein expression data from CCLE and HPA showed that Nup93 is abundantly expressed across various tissue and cell types (Chapter 3, Figure 3.1). In addition, analysis of the post-mitotic turnover rate of nucleoporins in cells and tissues indicated that scaffold nucleoporins have lower turnover rate and long half-lives at the NPC (D'Angelo et al., 2009; Savas et al., 2012; Toyama et al., 2013). Considering its high stability, low turnover rate, and abundant protein levels, it appears that nucleoporins such as Nup93 potentially provides a permanent and stable tether for chromatin at the nuclear periphery. Chromatin tethering function of Nup93 has previously been demonstrated in various systems including *Caenorhabditis elegans*,

*Drosophila*, and Human cells (Breuer and Ohkura, 2015; Brown et al., 2008; Ibarra et al., 2016; Rohner et al., 2013). In *Caenorhabditis elegans*, *hsp16.2* promoter relocates to the nuclear periphery and contacts NPP-13 (An ortholog of Nup93) upon activation (Rohner et al., 2013). Additionally, NPP-13 associates with Polymerase-III transcribed genes including snoRNA (small nucleolar RNA) and t-RNA genes (Ikegami and Lieb, 2013). An association with NPP-13 is required for processing of a subset of small nucleolar RNAs (snoRNAs) and tRNAs, while depletion of NPP-13 enhances the expression of the unprocessed long precursor of snoRNAs (T27A3.9 and Y75B12B.12) and tRNAs (F56C3.t1 and K11E4.t5) (Ikegami and Lieb, 2013). Interestingly, in *Drosophila*, Nup62 and Nup93 act as negative regulators of chromatin attachment to the NPC by suppressing chromatin interaction with Nup155. The first ChIP study with mammalian cells identified that Nup93 associates with chromatin regions on human chromosome 5, 7 and 16 (Brown et al., 2008). This study revealed that Nup93 binding sites are enriched for heterochromatic marks (H3K27me3) suggesting that Nup93 may contribute to the gene repression near the nuclear pore (Brown et al., 2008). Ibarra et al, showed that Nup93 tethers super-enhancers of cell identity genes to the nuclear periphery and depletion of Nup93 or Nup153 results in the significant upregulation of these genes (Ibarra et al., 2016). This study is consistent with the previous notion that tethering of chromatin by Nup93 at the NPC may provide a potential platform for gene expression.

In support of these previous findings, we examined if Nup93 tethers and represses HOXA locus in terminally differentiated DLD-1 cells. Our study revealed that the stable Nup93 subcomplex is required for tethering HOXA gene locus to the nuclear periphery, which correlates with the repressed status of HOXA in differentiated cells. We found that

the depletion of Nup93 or its interacting partners Nup188 or Nup205 untethers the HOXA locus from the nuclear periphery (Figure 3.11 and Figure 6.1). In addition, we found that the depletion of Nup188 or Nup205 results in a decreased occupancy of Nup93 on HOXA1 promoter, suggesting that Nup188 and Nup205 are required for the association between Nup93 and HOXA1 promoter (Figure 3.6). Furthermore, overexpression of Nup93 in a background of Nup188 or Nup205 depletion does not rescue its repressive function (Figure 3.9). Taken together, the Nup93-subcomplex functions as a tether for the HOXA gene locus at the nuclear periphery.

**Figure 6.1**

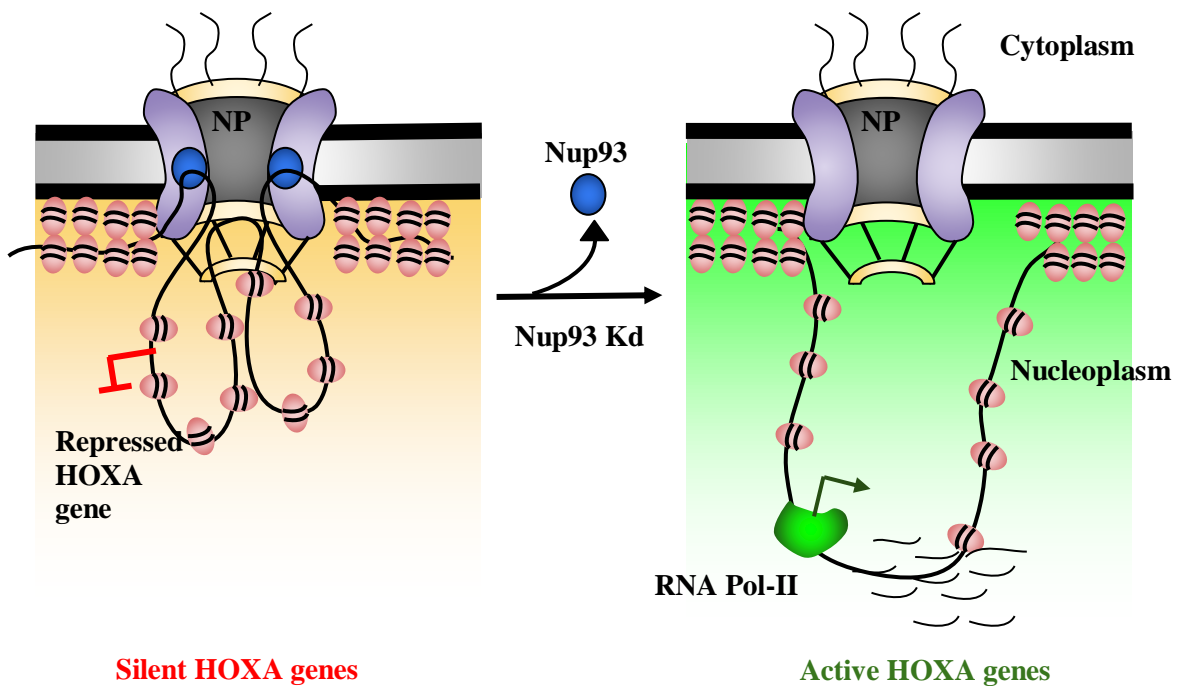


**Figure 6.1. Representative model of HOXA gene cluster silencing:** Silent HOXA gene cluster is tethered to the nuclear periphery by Nup93. Depletion of Nup93 results in activation of HOXA gene cluster accompanied by the opening of HOXA gene cluster and inward movement towards the center of the nucleus.

Notably, the association of genes with the NPC have been implicated in both gene activation and gene repression. A study by Kehat et al, in neonatal rat ventricular cardiomyocytes (NRVMs) showed that the interaction between Nup155 and HDAC4 is required for proper expression of HDAC4 target genes (e.g. *Nppb*, *Acta1*, *Cacna1*) (Kehat et al., 2011). Abolishing the interaction between Nup155 and HDAC4 by overexpressing mutant Nup155 results in a significant movement of *Nppb*, *Acta1* and *Cacna1* genes towards the nuclear periphery accompanied by their repression (Kehat et al., 2011). This finding suggests the role of Nup155 in the regulation of HDAC4 target genes at the nuclear periphery. In mouse C2C12 cells, Nup210 is important for myogenic differentiation by facilitating the expression of myogenesis genes *Asb2*, *Cand2*, *Clic5*, *GDF5*, *Igfbp4*, *Neu2*, *Ndr2*, and *Stral3* at the nuclear periphery (D'Angelo et al., 2012). Similarly, Nup210 is involved in the assembly of the Mef2C transcriptional complex for efficient transcription of structural and sarcomeric genes at the nuclear periphery (Raices et al., 2017). These findings suggest that nucleoporins regulate gene expression at the nuclear periphery. However, how nucleoporins distinguish between active and inactive chromatin or contribute to such a state of chromatin organization remains unclear. Nucleoporins could activate or represses the gene expression depending on the cell-type. More importantly, NPCs could provide a stable platform for the regulation of cell fate-specific genes for their activation or repression depending on the stage of differentiation. In support of this notion, our study showed the importance of a stable nucleoporin Nup93 in the cell type-specific regulation of HOXA gene loci - essential for normal development.

As discussed in Chapter 3, HOX family proteins are evolutionarily conserved homeobox transcription factors whose expression is temporally regulated during

development (Rousseau et al., 2014). There are 39 Hox genes in human, which are organized into four clusters located on separate chromosomes (Bhatlekar et al., 2014). HOXA gene cluster spans ~150kb on human chromosome 7. It encodes 11 transcription factors whose expression is temporally and colinearly controlled with respect to the order of their position along the chromosome during differentiation (Mallo and Alonso, 2013). Precise control of HOXA gene expression has been correlated with the sub-domain chromatin reorganization HOXA gene locus during different stages of differentiation (Rousseau et al., 2014). More importantly, the temporal regulation of transcriptional silencing of HOXA genes is essential for development and differentiation since its ectopic expression in adult tissues is linked to diseases (Calvo et al., 2000; Mustafa et al., 2015; Novak et al., 2006). Silenced HOXA cluster decorated with the inactive histone mark H3K27me3 by the combined activity of CTCF and PRC2 complex proteins (Xu et al., 2014). However, the molecular mechanism that regulates and maintain the HOXA gene cluster in a compact and silent state is unclear. Our study provided a clue into the process of repression of the HOXA gene cluster in differentiated cells. The finding that the depletion of Nup93 results in an enrichment of the active histone mark (H3K9ac) and a decrease in inactive histone mark (H3K27me3) on HOXA1 promoter suggests that Nup93 depletion is associated with epigenetic changes on HOXA gene cluster (Figure 3.13). We also observed an enrichment of elongation mark H3K36me3 on the gene body region of HOXA1 (Figure 3.13). This result supports that Nup93 may provide a stable platform which helps in the maintenance of a repressive environment (Inactive H3K27me3 marks) at the HOXA gene cluster. It is possible that nuclear pore complex may act as an anchor for transcriptional repressors such PRC2 complex proteins and histone modifiers such as



HDACs which facilitate the silencing of the HOXA gene locus at the nuclear periphery. In line with this, Kehat et al, showed that Nup155 (an interactor of Nup93) interacts with HDAC4 to negatively modulate the expression of sarcomeric genes (Kehat et al., 2011).

Here, we also found a non-canonical function for Nup93 in gene regulation, independent from its role in nuclear transport (Figure 3.14 and 3.15). Transport assays in Nup93 depleted cells did not show any change in the nucleocytoplasmic transport of polyA RNA or reporter protein (Figure 3.14). However, we cannot rule out the possibility that Nup93 depletion may inhibit the transport of specific transcriptional repressors, potentially required for silencing the HOXA gene cluster.

The mechanisms by which core nucleoporins associate with DNA are unclear. More importantly, several findings suggest that nucleoporins are involved in chromatin remodeling owing to their association with chromatin modifiers such as the SAGA complex, HDACs, RSC complex, SUMO proteases, SENP1, SENP2 and MSL complex (Van deaaa 1Vosse et al., 2013; Light et al., 2010; Mendjan et al., 2006; Rohner et al., 2013; Taddei et al., 2006) . Chromatin remodeling complexes such as the SAGA complex—a transcriptional activator, associates with the nuclear pore complex and activates HXK1, INO1, and GAL genes when recruited to the NPC (Casolari et al., 2004; Dieppois and Stutz, 2010; Mendjan et al., 2006; Rodríguez-Navarro et al., 2004). Nup2, Nup60, Nic96, Nup116, Mlp1, and Mlp2 are enriched on transcriptionally active regions in *S. cerevisiae* (Casolari et al., 2004, 2005). Furthermore, ARP6 links the active housekeeping gene RPP1A, involved in ribosome biogenesis to the nuclear pore complex (Yoshida et al., 2010). Interestingly, Nup93 tethers and regulates the expression of cell identity genes, which are predominantly localized at the nuclear periphery (Ibarra et al.,

2016). The tethering of HOXA gene cluster to the nuclear periphery and its repression by the Nup93 sub-complex adds to the repertoire of nucleoporin-mediated gene repression events. Analyses of protein-protein interaction networks using BIOGRID (Stark et al., 2006) of human Nup93 shows that Nup93 interacts with chromatin modifiers such as HDAC11, HDAC9, HDAC5 and PCR2 complex proteins—EED and Suz12. It is conceivable that Nup93 and its interactors associate with transcriptional repressors in repressing the HOXA gene cluster, although we did not detect a direct association between Nup93 and the chromatin repressive complex (PRC2). ChIP-mass spectrometric approaches may identify putative interactors of Nup93 involved in chromatin organization.

Our study also revealed an interesting link between Nup93 and CTCF in the regulation of developmental genes. Our ChIP-seq analysis revealed that Nup93 peaks significantly overlap with CTCF peaks (Figure 4.17). Furthermore, we found that Nup93 associates with genes involved in development and differentiation (Figure 4.14). This data suggests that Nup93 and CTCF may function together in the regulation of developmental genes. Interestingly, we observed that Nup93 peaks are also enriched for repressive histone marks H3K27me3 (Figure 4.19) which further underscores that Nup93 may provide a repressive environment for gene expression at the nuclear periphery. We also observed an enrichment of an enhancer mark H3K27ac on Nup93 peaks indicating the involvement of Nup93 in enhancer-promoter interactions at specific gene loci (Figure 4.19). This finding is consistent with the previous report by Ibarra et al. which supports the enhancer association of Nup93 in the regulation of cell identity genes (Ibarra et al., 2016). Specific enrichment of CTCF and H3K27ac (enhancer mark) on Nup93 binding regions suggest that NPC may act as a scaffold for long-range chromatin interactions including enhancer-

promoter interactions. We also observed an enrichment of Nup93 around the transcription start sites of genes (Figure 4.12). Investigation of promoter-enhancer interactions on co-targets of Nup93 and CTCF will help understand the potential role of Nup93 in mediating these long-range chromatin interactions. As discussed in Chapter 4, an interesting finding of our ChIP-seq data suggests that Nup93 is enriched on exon-intron boundaries of genes (Figure 4.12). However, the functional significance of this enrichment remains elusive. One possible explanation for this enrichment could be the involvement of Nup93 in co-transcriptional splicing. However, it is not known whether nucleoporins are involved in splicing of mRNA. Role of CTCF in co-transcriptional splicing has been previously elucidated (Marina et al., 2016; Ruiz-Velasco et al., 2017; Shukla et al., 2011). It will be interesting to determine the regulatory role of Nup93 and CTCF in co-transcriptional splicing of their target genes and its importance in development and differentiation.

A question that remains unanswered is how does Nup93 associate with most of the genome? (Figure 4.11) despite its exclusive peripheral localization? We surmise that Nup93 contacts chromatin at the very early stage of nuclear envelope reformation at the end of mitosis and tethers developmentally important genes at the nuclear periphery (Figure 6.2). During mitosis, chromatin is condensed in the form of chromosomes and contacts between chromatin and associated proteins is lost (Egli et al., 2008). At the end of mitosis, chromatin re-establishes contacts with transcription factors and various nuclear landmarks in a manner that restores the previous expression status of all genes. Interestingly, at the end of mitosis, nucleoporins are among the first proteins to contact chromatin (Benavente et al., 1989; Walther et al., 2003). It is possible that Nup93 may establish contacts with significant regions of the genome, which are maintained throughout

interphase (Figure 6.2). It will be interesting to understand how Nup93 recognize and associate with specific genes at end of each mitosis. In *yeast*, genes such as *GAL1*, *INO1*, *HXX1*, *HSP104*, *SUC2* relocate to the nuclear periphery and associate with the nuclear pore complex (NPC) upon activation (Brickner and Walter, 2004; Cabal et al., 2006; Casolari et al., 2004; Taddei et al., 2006; Tan-Wong et al., 2009). Interestingly, gene recruitment to the NPC is mediated via ‘memory gene loop’ formation between the promoter and ‘3 ends of *HXX1* and *GAL1::FMP27* genes which facilitate the faster access of RNA polymerase-II for rapid induction (Tan-Wong et al., 2009). Similarly, in Human and *Drosophila*, Nup98 is required for maintaining the transcriptional memory of INF- $\gamma$ -inducible *HLA-DRA* coding genes (Light et al., 2013).

In summary, the nuclear pore complex recognizes specific DNA sequences which helps them to establish specific DNA contacts during cell division cycles. Therefore, we speculate that Nup93 might associate with specific DNA sequences during early stages of nuclear envelope reformation which allow Nup93 to associate with the genome despite its peripheral nuclear localization. However, it is important to note that Nup93 association is specifically excluded from the human chromosome X as revealed by our ChIP seq analysis and an independent Nup93 Dam-ID study (Ibarra et al., 2016). Functional importance of the absence of Nup93 binding on X-chromosome remains elusive.

**Figure 6.2**

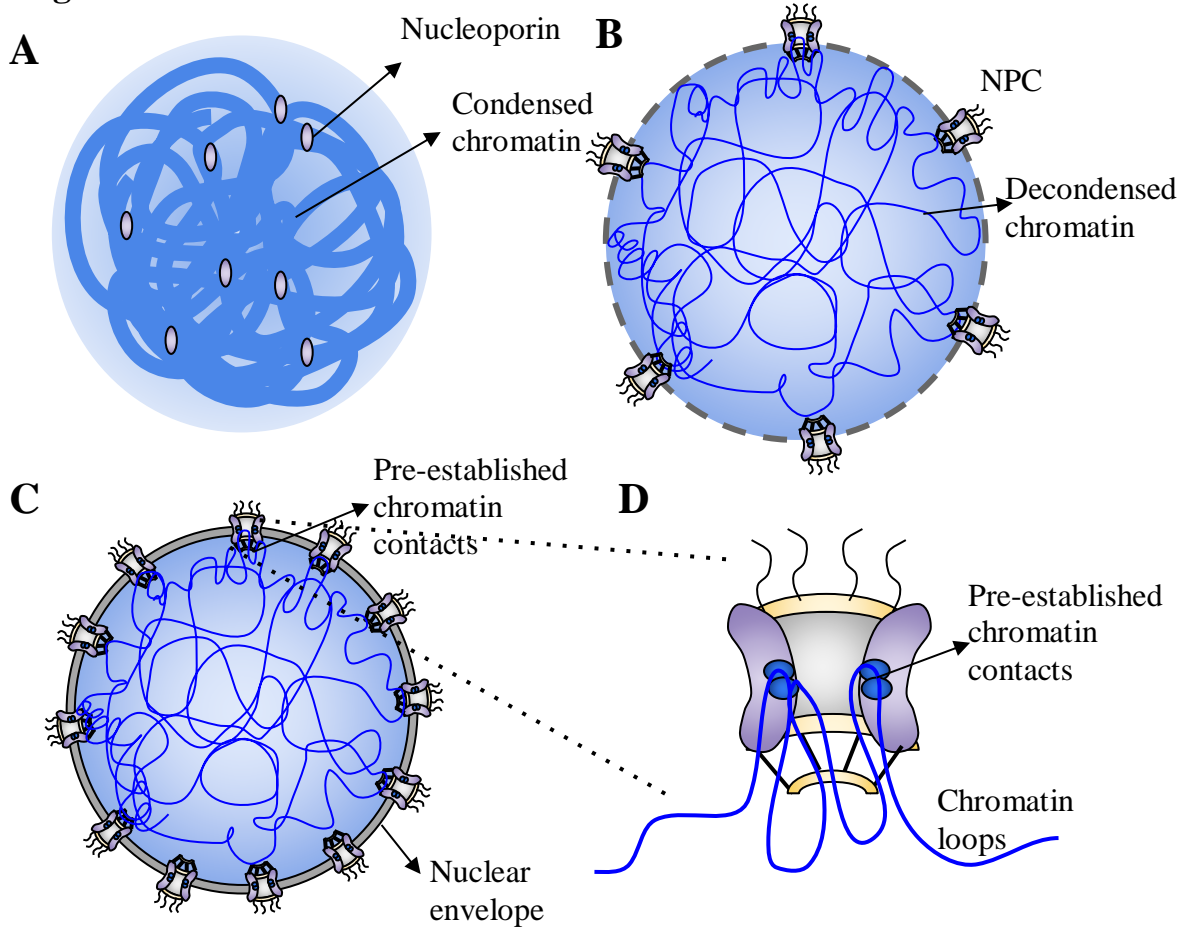


**Figure 6.2. A schematic model representing the establishment of chromatin contacts with the NPC:** **A)** At the end of late telophase nucleoporins contracts chromatin and forms seeding points for nuclear membrane formation. **B)** Maturation of nuclear membrane and assembly of nuclear pore complex. **C)** Pre-established contacts between NPC and chromatin are maintained throughout the interphase. Nucleus representing pre-established contacts between NPC and chromatin at the nuclear periphery. **D)** An enlarged view of chromatin contacts with NPC

As discussed in chapter 5, we have examined the role of Nup93 and in regulating HOXA gene dynamics during differentiation of NT2/D1 cells. Our findings reveal a previously uncharacterized mechanism of HOXA gene cluster silencing during NT2/D1 differentiation which involves the interplay between Nup93 and CTCF in regulating

HOXA gene expression. 3D-FISH analysis revealed that HOXA gene locus shows dynamic movement from the nuclear periphery, which correlates with its expression. The HOXA locus moves towards the nuclear interior upon induction by RA treatment and relocates to the nuclear periphery on day8 of differentiation (Figure 5.10). We also found that in embryonal carcinoma NT/2D1 cells, HOXA gene locus is positioned proximal to the nuclear periphery (~ 1.4  $\mu\text{m}$  from DAPI edge) (Figure 5.10). This proximal positioning may be attributed to a poised status of HOXA gene locus in NT2/D1 cells. In line with these observations, we found that the HOXA1 promoter is not occupied by Nup93 at day0 and day4, while CTCF seems to occupy the HOXA1 promoter in absence of Nup93 (Figure 5.11). The occupancy of Nup93 is significantly enriched on day8 with the loss of CTCF occupancy. These observations indicate that Nup93 and CTCF may antagonistically associate with HOXA1 promoter during differentiation. Consistent with this observation, qRT-PCR data suggests that Nup93 and CTCF depletion have an antagonistic effect on the expression of 3'-end HOXA genes where Nup93 depletion upregulates HOXA gene expression while CTCF depletion downregulates HOXA gene expression (Figure 5.7). Similarly, HOXA genes are more responsive to RA induction in Nup93 depleted cells and less responsive upon CTCF depleted cells. Based on these findings, we propose that CTCF is required for initial loop organization of HOXA genes, while Nup93 is involved in tethering of HOXA locus for the purpose of long-term maintenance of silent HOXA gene cluster.

**Figure 6.3**

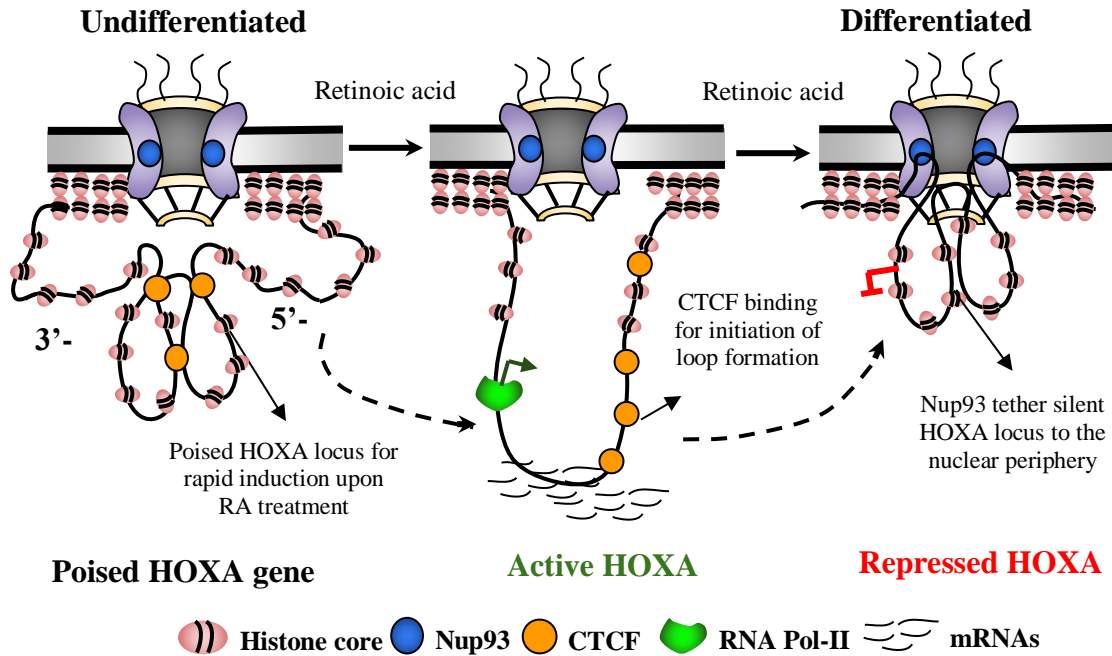


**Figure 6.3. A representative model of HOXA gene cluster silencing during differentiation:** In undifferentiated NT2/D1 cells, poised HOXA gene cluster is positioned proximal to the nuclear periphery and not tethered to the NPC by Nup93. Poised HOXA cluster is held together by CTCF for rapid activation. Retinoic acid-mediated induction of HOXA expression results in the opening of HOXA cluster accompanied by inward movement of HOXA genes towards the nuclear interior. At this stage, CTCF still bound to the HOXA locus which helps in the initiation of chromatin looping. At the end of the differentiation process, HOXA loops are tethered to the nuclear periphery by Nup93 for their permanent repression.

Implications of our findings are specifically important in the field of differential gene regulation during cell fate determination. The tethering of developmentally silenced genes to the nuclear periphery is likely to be a general mechanism by which nucleoporins regulate the repression of specific genes expressed in early stages of differentiation. NPC may act as a hub for the clustering of different transcription factors and chromatin modifiers required for developmental gene silencing. In line with this notion, our study

suggests temporal gene silencing of developmentally important HOXA genes. Furthermore, we propose that the nuclear pore complex may provide a stable platform for 3D-organization of chromatin by facilitating long-range chromatin interactions.

## **6. 2 Potential Future Directions**

Nucleoporins have been implicated in various transport independent functions such as Transcriptional regulation, transcriptional memory (Light and Brickner, 2013; Light et al., 2013) , demarcating chromatin boundaries (Ishii et al., 2002; Kalverda and Fornerod, 2010) , differentiation, development (D'Angelo et al., 2012; Kalverda et al., 2010; Liang et al., 2013; Palancade et al., 2007), DNA damage repair (Khadaroo et al., 2009; Palancade et al., 2007) and chromatin organization (Breuer and Ohkura, 2015). These functions are likely to involve chromatin contacts with nucleoporins. However, it is not known whether nucleoporins directly contact chromatin, or these contacts are mediated via other chromatin-associated proteins. Considering the dynamic interaction of chromatin with histone marks, chromatin modifying enzymes, transcription factors, DNA methylating enzymes, DNA and RNA polymerases and splicing factors. It is highly likely that nucleoporin-chromatin interactions are mediated via intermediate proteins that interact with both nucleoporins and chromatin. Whether nucleoporins interact with specific transcription regulator depending on the cell or tissue type is not yet clear. Furthermore, stable nucleoporins may have different interacting partners than mobile nucleoporins which remains to be investigated. Therefore, investigating the detailed proteome of nuclear pore-associated proteins is important for understanding the role of nucleoporins in tissue-



specific gene regulation. Independent ChIP-mass spec analysis of each nucleoporin across the cell and tissue types will help us to determine cell-specific interacting partners different nucleoporins. The long-standing question in the field of nucleoporin and gene regulation is how does a stable nucleoporin such as Nup93 which is located inside the core of the nuclear pore complex contacts chromatin? Considering the spatial restrictions on chromatin movement inside the nuclear pore complex, it is hard to determine if stable nucleoporins directly contact chromatin. Several mechanisms have been proposed in this aspect. As discussed previously, one possible hypothesis is that nucleoporins may associate with the specific gene loci at very early stages of nuclear envelope reformation since they are one of the early proteins that contact chromatin at the end of mitosis. However, detailed investigation of this early recruitment and its possible implication in gene regulation remains unclear. One possible approach is to perform chromatin immunoprecipitation of nucleoporin associated sequences at an early stage of nuclear envelope reformation. This would help us to determine if nucleoporin-chromatin contacts are pre-established before cell enters into the interphase.

Live visualization of gene-nucleoporins interaction could help us to understand the mechanism of gene recruitment at the nuclear pore complex. One possible approach is high-resolution imaging of nucleoporin chromatin interactions using the CRISPR-Cas9 system, which could give us more insights into the mechanism of dynamic chromatin movement inside the NPC to contact a stable nucleoporin such as Nup93. Another approach is to tag an endogenous gene locus by inserting a reporter sequence such as MS2 repeats using CRISPR-cas9 and then track the movement of gene locus using fluorescently tagged MS2 protein. If we could visualize a gene locus in real time, we can track its

recruitment to the nuclear pore complex in the presence and absence of specific nucleoporin. Further, we can ask what other factors affect the recruitment of specific gene locus to the NPC. This approach would be specifically helpful to track the movement of developmentally important genes such as HOXA gene locus during the process of differentiation. In addition, it would be particularly interesting to visualize nucleoporin mediated long-range chromatin contacts in real time. With regards to HOXA locus, real-time visualization of 3' HOXA gene as against 5' HOXA genes during their collinear activation would give us the better understanding of chromatin dynamics and its impact on gene activation.

Role of nucleoporins in the co-regulation of developmentally important genes has not been elucidated. Nuclear pore complex may provide a stable platform for co-regulation of developmentally important genes. The 3-dimensional organization of genome allows long-range chromatin interactions that are required for gene regulation and coexpression of genes (Arzate-Mejía et al., 2018; Gorkin et al., 2014; Ruiz-Velasco et al., 2017; Soler-Oliva et al., 2017). High throughput chromosome chromatin conformation capture technique such as Hi-C would be useful to determine the nucleoporin mediated contacts that are involved in co-regulation of developmentally important genes at the nuclear periphery.

Our ChIP-seq analysis revealed that Nup93 is specifically enriched on the exon-intron junction, suggesting its possible involvement in co-transcriptional splicing. It remains to be examined if Nup93 is involved in co-transcriptional splicing of developmentally important genes. CTCF has been shown to involve in co-transcriptional splicing (Ruiz-Velasco et al., 2017; Shukla et al., 2011) and we found that Nup93 is

enriched on CTCF binding regions, this further supports the possible role of Nup93 in co-transcriptional splicing. One would test this possibility by performing qRT-PCR for different splice variants of Nup93 associated genes in control and Nup93 depleted cells. Furthermore, RNA-seq analysis would help understand the global role of Nup93 in co-transcriptional splicing.

Genome-wide role of nucleoporins in chromosome positioning has not been elucidated previously. Since nucleoporins are one the early proteins that associates with chromatin before the reformation of the interphase nucleus, there exist the possibility that nucleoporins could regulate non-random positioning of chromosome territories inside the interphase nucleus. 3D-FISH imaging of chromosome territories upon depletion of different nucleoporins would help us understand the role of nucleoporins in chromosome positioning.

## References

- Van deaana 1Vosse, D.W., Wan, Y., Lapetina, D.L., Chen, W.-M., Chiang, J.-H., Aitchison, J.D., and Wozniak, R.W. (2013). A role for the nucleoporin Nup170p in chromatin structure and gene silencing. *Cell* 152, 969–983.
- Afgan, E., Baker, D., Batut, B., van den Beek, M., Bouvier, D., Cech, M., Chilton, J., Clements, D., Coraor, N., Grüning, B.A., et al. (2018). The Galaxy platform for accessible, reproducible and collaborative biomedical analyses: 2018 update. *Nucleic Acids Res.* 46, W537–W544.
- Alber, F., Dokudovskaya, S., Veenhoff, L.M., Zhang, W., Kipper, J., Devos, D., Suprpto, A., Karni-Schmidt, O., Williams, R., Chait, B.T., et al. (2007). The molecular architecture of the nuclear pore complex. *Nature* 450, 695–701.
- Albiez, H., Cremer, M., Tiberi, C., Vecchio, L., Schermelleh, L., Dittrich, S., Küpper, K., Joffe, B., Thormeyer, T., von Hase, J., et al. (2006). Chromatin domains and the interchromatin compartment form structurally defined and functionally interacting nuclear networks. *Chromosome Res.* 14, 707–733.
- Andrulis, E.D., Neiman, A.M., Zappulla, D.C., and Sternglanz, R. (1998). Perinuclear localization of chromatin facilitates transcriptional silencing. *Nature* 394, 592–595.
- Antonin, W., Ellenberg, J., and Dultz, E. (2008). Nuclear pore complex assembly through the cell cycle: regulation and membrane organization. *FEBS Lett.* 582, 2004–2016.
- Arib, G., and Akhtar, A. (2011). Multiple facets of nuclear periphery in gene expression control. *Curr. Opin. Cell Biol.* 23, 346–353.
- Arzate-Mejía, R.G., Recillas-Targa, F., and Corces, V.G. (2018). Developing in 3D: the role of CTCF in cell differentiation. *Development* 145.
- Atkinson, S.P., Koch, C.M., Clelland, G.K., Willcox, S., Fowler, J.C., Stewart, R., Lako, M., Dunham, I., and Armstrong, L. (2008). Epigenetic marking prepares the human HOXA cluster for activation during differentiation of pluripotent cells. *Stem Cells* 26, 1174–1185.
- Aubin, J., Lemieux, M., Tremblay, M., Bérard, J., and Jeannotte, L. (1997). Early postnatal lethality in Hoxa-5 mutant mice is attributable to respiratory tract defects. *Dev. Biol.* 192, 432–445.
- Bantignies, F., and Cavalli, G. (2011). Polycomb group proteins: repression in 3D. *Trends Genet.* 27, 454–464.
- Batrakou, D.G., Kerr, A.R.W., and Schirmer, E.C. (2009). Comparative proteomic analyses of the nuclear envelope and pore complex suggests a wide range of heretofore unexpected functions. *J. Proteomics* 72, 56–70.
- Benavente, R., Dabauvalle, M.C., Scheer, U., and Chaly, N. (1989). Functional role of newly formed pore complexes in postmitotic nuclear reorganization. *Chromosoma* 98, 233–241.
- Bermejo, R., Kumar, A., and Foiani, M. (2012). Preserving the genome by regulating chromatin association with the nuclear envelope. *Trends Cell Biol.* 22, 465–473.
- Bhatlekar, S., Fields, J.Z., and Boman, B.M. (2014). HOX genes and their role in the development of human cancers. *J. Mol. Med.* 92, 811–823.

- Bitu, C.C., Destro, M.F. de S.S., Carrera, M., da Silva, S.D., Graner, E., Kowalski, L.P., Soares, F.A., and Coletta, R.D. (2012). HOXA1 is overexpressed in oral squamous cell carcinomas and its expression is correlated with poor prognosis. *BMC Cancer* 12, 146.
- Blobel, G. (1985). Gene gating: a hypothesis. *Proc. Natl. Acad. Sci. USA* 82, 8527–8529.
- Bonomo, J.A., Guan, M., Ng, M.C.Y., Palmer, N.D., Hicks, P.J., Keaton, J.M., Lea, J.P., Langefeld, C.D., Freedman, B.I., and Bowden, D.W. (2014). The ras responsive transcription factor RREB1 is a novel candidate gene for type 2 diabetes associated end-stage kidney disease. *Hum. Mol. Genet.* 23, 6441–6447.
- Braun, D.A., Sadowski, C.E., Kohl, S., Lovric, S., Astrinidis, S.A., Pabst, W.L., Gee, H.Y., Ashraf, S., Lawson, J.A., Shril, S., et al. (2016). Mutations in nuclear pore genes NUP93, NUP205 and XPO5 cause steroid-resistant nephrotic syndrome. *Nat. Genet.* 48, 457–465.
- Breuer, M., and Ohkura, H. (2015). A negative loop within the nuclear pore complex controls global chromatin organization. *Genes Dev.* 29, 1789–1794.
- Brickner, J.H., and Walter, P. (2004). Gene recruitment of the activated INO1 locus to the nuclear membrane. *PLoS Biol.* 2, e342.
- Brickner, D.G., Ahmed, S., Meldi, L., Thompson, A., Light, W., Young, M., Hickman, T.L., Chu, F., Fabre, E., and Brickner, J.H. (2012). Transcription factor binding to a DNA zip code controls interchromosomal clustering at the nuclear periphery. *Dev. Cell* 22, 1234–1246.
- Broers, J.L.V., Ramaekers, F.C.S., Bonne, G., Yaou, R.B., and Hutchison, C.J. (2006). Nuclear lamins: laminopathies and their role in premature ageing. *Physiol. Rev.* 86, 967–1008.
- Brown, C.R., and Silver, P.A. (2007). Transcriptional regulation at the nuclear pore complex. *Curr. Opin. Genet. Dev.* 17, 100–106.
- Brown, C.R., Kennedy, C.J., Delmar, V.A., Forbes, D.J., and Silver, P.A. (2008). Global histone acetylation induces functional genomic reorganization at mammalian nuclear pore complexes. *Genes Dev.* 22, 627–639.
- Buchwalter, A.L., Liang, Y., and Hetzer, M.W. (2014). Nup50 is required for cell differentiation and exhibits transcription-dependent dynamics. *Mol. Biol. Cell* 25, 2472–2484.
- Bukata, L., Parker, S.L., and D'Angelo, M.A. (2013). Nuclear pore complexes in the maintenance of genome integrity. *Curr. Opin. Cell Biol.* 25, 378–386.
- Cabal, G.G., Genovesio, A., Rodriguez-Navarro, S., Zimmer, C., Gadal, O., Lesne, A., Buc, H., Feuerbach-Fournier, F., Olivo-Marin, J.-C., Hurt, E.C., et al. (2006). SAGA interacting factors confine sub-diffusion of transcribed genes to the nuclear envelope. *Nature* 441, 770–773.
- Calvo, R., West, J., Franklin, W., Erickson, P., Bemis, L., Li, E., Helfrich, B., Bunn, P., Roche, J., Brambilla, E., et al. (2000). Altered HOX and WNT7A expression in human lung cancer. *Proc. Natl. Acad. Sci. USA* 97, 12776–12781.
- Capelson, M., and Hetzer, M.W. (2009). The role of nuclear pores in gene regulation, development and disease. *EMBO Rep.* 10, 697–705.
- Capelson, M., Liang, Y., Schulte, R., Mair, W., Wagner, U., and Hetzer, M.W. (2010a). Chromatin-bound nuclear pore components regulate gene expression in higher eukaryotes. *Cell* 140, 372–383.
- Capelson, M., Doucet, C., and Hetzer, M.W. (2010b). Nuclear pore complexes: guardians of the nuclear genome. *Cold Spring Harb. Symp. Quant. Biol.* 75, 585–597.

- Capitanio, J.S., Montpetit, B., and Wozniak, R.W. (2017). Human Nup98 regulates the localization and activity of DExH/D-box helicase DHX9. *Elife* 6.
- Casolari, J.M., Brown, C.R., Komili, S., West, J., Hieronymus, H., and Silver, P.A. (2004). Genome-wide localization of the nuclear transport machinery couples transcriptional status and nuclear organization. *Cell* 117, 427–439.
- Casolari, J.M., Brown, C.R., Drubin, D.A., Rando, O.J., and Silver, P.A. (2005). Developmentally induced changes in transcriptional program alter spatial organization across chromosomes. *Genes Dev.* 19, 1188–1198.
- Chen, C.-K., Blanco, M., Jackson, C., Aznauryan, E., Ollikainen, N., Surka, C., Chow, A., Cerase, A., McDonel, P., and Guttman, M. (2016). Xist recruits the X chromosome to the nuclear lamina to enable chromosome-wide silencing. *Science* 354, 468–472.
- Chen, E.Y., Tan, C.M., Kou, Y., Duan, Q., Wang, Z., Meirelles, G.V., Clark, N.R., and Ma'ayan, A. (2013). Enrichr: interactive and collaborative HTML5 gene list enrichment analysis tool. *BMC Bioinformatics* 14, 128.
- Chèneby, J., Gheorghe, M., Artufel, M., Mathelier, A., and Ballester, B. (2018). ReMap 2018: an updated atlas of regulatory regions from an integrative analysis of DNA-binding ChIP-seq experiments. *Nucleic Acids Res.* 46, D267–D275.
- Cherkezyan, L., Stypula-Cyrus, Y., Subramanian, H., White, C., Dela Cruz, M., Wali, R.K., Goldberg, M.J., Bianchi, L.K., Roy, H.K., and Backman, V. (2014). Nanoscale changes in chromatin organization represent the initial steps of tumorigenesis: a transmission electron microscopy study. *BMC Cancer* 14, 189.
- Cheung, A.Y., and Reddy, A.S.N. (2012). Nuclear architecture and dynamics: territories, nuclear bodies, and nucleocytoplasmic trafficking. *Plant Physiol.* 158, 23–25.
- Ching, R.W., Dellaire, G., Eskiw, C.H., and Bazett-Jones, D.P. (2005). PML bodies: a meeting place for genomic loci? *J. Cell Sci.* 118, 847–854.
- Chow, K.-H., Elgort, S., Dasso, M., and Ullman, K.S. (2012). Two distinct sites in Nup153 mediate interaction with the SUMO proteases SENP1 and SENP2. *Nucleus* 3, 349–358.
- Collas, P., Lund, E.G., and Oldenburg, A.R. (2014). Closing the (nuclear) envelope on the genome: how nuclear lamins interact with promoters and modulate gene expression. *Bioessays* 36, 75–83.
- Crabbe, L., Cesare, A.J., Kasuboski, J.M., Fitzpatrick, J.A.J., and Karlseder, J. (2012). Human telomeres are tethered to the nuclear envelope during postmitotic nuclear assembly. *Cell Rep.* 2, 1521–1529.
- Croft, J.A., Bridger, J.M., Boyle, S., Perry, P., Teague, P., and Bickmore, W.A. (1999). Differences in the localization and morphology of chromosomes in the human nucleus. *J. Cell Biol.* 145, 1119–1131.
- Crutchley, J. (2014). Bridging chromatin architecture to gene expression: Investigating the roles of CTCF and cohesin in the regulation of the HOXA cluster.
- Czapiewski, R., Robson, M.I., and Schirmer, E.C. (2016). Anchoring a leviathan: how the nuclear membrane tethers the genome. *Front. Genet.* 7, 82.
- D'Angelo, M.A. (2018). Nuclear pore complexes as hubs for gene regulation. *Nucleus* 9, 142–148.

- D'Angelo, M.A., and Hetzer, M.W. (2008). Structure, dynamics and function of nuclear pore complexes. *Trends Cell Biol.* *18*, 456–466.
- D'Angelo, M.A., Raices, M., Panowski, S.H., and Hetzer, M.W. (2009). Age-dependent deterioration of nuclear pore complexes causes a loss of nuclear integrity in postmitotic cells. *Cell* *136*, 284–295.
- D'Angelo, M.A., Gomez-Cavazos, J.S., Mei, A., Lackner, D.H., and Hetzer, M.W. (2012). A change in nuclear pore complex composition regulates cell differentiation. *Dev. Cell* *22*, 446–458.
- Daigle, N., Beaudouin, J., Hartnell, L., Imreh, G., Hallberg, E., Lippincott-Schwartz, J., and Ellenberg, J. (2001). Nuclear pore complexes form immobile networks and have a very low turnover in live mammalian cells. *J. Cell Biol.* *154*, 71–84.
- Dechat, T., Pflieger, K., Sengupta, K., Shimi, T., Shumaker, D.K., Solimando, L., and Goldman, R.D. (2008). Nuclear lamins: major factors in the structural organization and function of the nucleus and chromatin. *Genes Dev.* *22*, 832–853.
- DeGrasse, J.A., DuBois, K.N., Devos, D., Siegel, T.N., Sali, A., Field, M.C., Rout, M.P., and Chait, B.T. (2009). Evidence for a shared nuclear pore complex architecture that is conserved from the last common eukaryotic ancestor. *Mol. Cell Proteomics* *8*, 2119–2130.
- Dieppo, G., and Stutz, F. (2010). Connecting the transcription site to the nuclear pore: a multi-tether process that regulates gene expression. *J. Cell Sci.* *123*, 1989–1999.
- Doucet, C.M., and Hetzer, M.W. (2010). Nuclear pore biogenesis into an intact nuclear envelope. *Chromosoma* *119*, 469–477.
- Dultz, E., Zanin, E., Wurzenberger, C., Braun, M., Rabut, G., Sironi, L., and Ellenberg, J. (2008). Systematic kinetic analysis of mitotic dis- and reassembly of the nuclear pore in living cells. *J. Cell Biol.* *180*, 857–865.
- Egli, D., Birkhoff, G., and Eggan, K. (2008). Mediators of reprogramming: transcription factors and transitions through mitosis. *Nat. Rev. Mol. Cell Biol.* *9*, 505–516.
- Eibauer, M., Pellanda, M., Turgay, Y., Dubrovsky, A., Wild, A., and Medalia, O. (2015). Structure and gating of the nuclear pore complex. *Nat. Commun.* *6*, 7532.
- Eisenhardt, N., Redolfi, J., and Antonin, W. (2014). Interaction of Nup53 with Ndc1 and Nup155 is required for nuclear pore complex assembly. *J. Cell Sci.* *127*, 908–921.
- Fanucchi, S., Shibayama, Y., Burd, S., Weinberg, M.S., and Mhlanga, M.M. (2013). Chromosomal contact permits transcription between coregulated genes. *Cell* *155*, 606–620.
- Fedorova, E., and Zink, D. (2008). Nuclear architecture and gene regulation. *Biochim. Biophys. Acta* *1783*, 2174–2184.
- Ferrai, C., de Castro, I.J., Lavitas, L., Chotalia, M., and Pombo, A. (2010). Gene positioning. *Cold Spring Harb. Perspect. Biol.* *2*, a000588.
- Ferraiuolo, M.A., Rousseau, M., Miyamoto, C., Shenker, S., Wang, X.Q.D., Nadler, M., Blanchette, M., and Dostie, J. (2010). The three-dimensional architecture of Hox cluster silencing. *Nucleic Acids Res.* *38*, 7472–7484.
- Fischer, T., Strässer, K., Rácz, A., Rodriguez-Navarro, S., Oppizzi, M., Ihrig, P., Lechner, J., and Hurt, E. (2002). The mRNA export machinery requires the novel Sac3p-Thp1p complex to dock at the nucleoplasmic entrance of the nuclear pores. *EMBO J.* *21*, 5843–5852.

- Fišerová, J., Efenberková, M., Sieger, T., Maninová, M., Uhlířová, J., and Hozák, P. (2017). Chromatin organization at the nuclear periphery as revealed by image analysis of structured illumination microscopy data. *J. Cell Sci.* *130*, 2066–2077.
- Flaherty, M.P., Kamerzell, T.J., and Dawn, B. (2012). Wnt signaling and cardiac differentiation. *Prog Mol Biol Transl Sci* *111*, 153–174.
- Foisner, R. (2001). Inner nuclear membrane proteins and the nuclear lamina. *J. Cell Sci.* *114*, 3791–3792.
- Franks, T.M., Benner, C., Narvaiza, I., Marchetto, M.C.N., Young, J.M., Malik, H.S., Gage, F.H., and Hetzer, M.W. (2016). Evolution of a transcriptional regulator from a transmembrane nucleoporin. *Genes Dev.* *30*, 1155–1171.
- Fraser, J., Rousseau, M., Shenker, S., Ferraiuolo, M.A., Hayashizaki, Y., Blanchette, M., and Dostie, J. (2009). Chromatin conformation signatures of cellular differentiation. *Genome Biol.* *10*, R37.
- Fritz, A.J., Barutcu, A.R., Martin-Buley, L., van Wijnen, A.J., Zaidi, S.K., Imbalzano, A.N., Lian, J.B., Stein, J.L., and Stein, G.S. (2016). Chromosomes at work: organization of chromosome territories in the interphase nucleus. *J. Cell Biochem.* *117*, 9–19.
- Funakoshi, T., Clever, M., Watanabe, A., and Imamoto, N. (2011). Localization of Pom121 to the inner nuclear membrane is required for an early step of interphase nuclear pore complex assembly. *Mol. Biol. Cell* *22*, 1058–1069.
- Galy, V., Olivo-Marin, J.C., Scherthan, H., Doye, V., Rascalou, N., and Nehrbass, U. (2000). Nuclear pore complexes in the organization of silent telomeric chromatin. *Nature* *403*, 108–112.
- Galy, V., Mattaj, I.W., and Askjaer, P. (2003). *Caenorhabditis elegans* nucleoporins Nup93 and Nup205 determine the limit of nuclear pore complex size exclusion in vivo. *Mol. Biol. Cell* *14*, 5104–5115.
- García-Oliver, E., García-Molinero, V., and Rodríguez-Navarro, S. (2012). mRNA export and gene expression: the SAGA-TREX-2 connection. *Biochim. Biophys. Acta* *1819*, 555–565.
- Gerasimova, T.I., Byrd, K., and Corces, V.G. (2000). A chromatin insulator determines the nuclear localization of DNA. *Mol. Cell* *6*, 1025–1035.
- Gibcus, J.H., and Dekker, J. (2013). The hierarchy of the 3D genome. *Mol. Cell* *49*, 773–782.
- Gomez-Cavazos, J.S., and Hetzer, M.W. (2015). The nucleoporin gp210/Nup210 controls muscle differentiation by regulating nuclear envelope/ER homeostasis. *J. Cell Biol.* *208*, 671–681.
- Gonzalez-Sandoval, A., and Gasser, S.M. (2016). On tads and lads: spatial control over gene expression. *Trends Genet.* *32*, 485–495.
- Gorkin, D.U., Leung, D., and Ren, B. (2014). The 3D genome in transcriptional regulation and pluripotency. *Cell Stem Cell* *14*, 762–775.
- Grandi, P., Dang, T., Pané, N., Shevchenko, A., Mann, M., Forbes, D., and Hurt, E. (1997). Nup93, a vertebrate homologue of yeast Nic96p, forms a complex with a novel 205-kDa protein and is required for correct nuclear pore assembly. *Mol. Biol. Cell* *8*, 2017–2038.
- Griffis, E. (2002). Nup98 Is a Mobile Nucleoporin with Transcription-dependent Dynamics. *Mol. Biol. Cell* *13*, 1282–1297.



- Griffis, E.R., Craige, B., Dimaano, C., Ullman, K.S., and Powers, M.A. (2004). Distinct functional domains within nucleoporins Nup153 and Nup98 mediate transcription-dependent mobility. *Mol. Biol. Cell* *15*, 1991–2002.
- Guelen, L., Pagie, L., Brasset, E., Meuleman, W., Faza, M.B., Talhout, W., Eussen, B.H., de Klein, A., Wessels, L., de Laat, W., et al. (2008). Domain organization of human chromosomes revealed by mapping of nuclear lamina interactions. *Nature* *453*, 948–951.
- Hanashima, C., Li, S.C., Shen, L., Lai, E., and Fishell, G. (2004). Foxg1 suppresses early cortical cell fate. *Science* *303*, 56–59.
- Hansen, A.S., Pustova, I., Cattoglio, C., Tjian, R., and Darzacq, X. (2017). CTCF and cohesin regulate chromatin loop stability with distinct dynamics. *Elife* *6*.
- Haring, M., Offermann, S., Danker, T., Horst, I., Peterhansel, C., and Stam, M. (2007). Chromatin immunoprecipitation: optimization, quantitative analysis and data normalization. *Plant Methods* *3*, 11.
- Hase, M.E., and Cordes, V.C. (2003). Direct interaction with nup153 mediates binding of Tpr to the periphery of the nuclear pore complex. *Mol. Biol. Cell* *14*, 1923–1940.
- Hawryluk-Gara, L.A. (2005). Vertebrate Nup53 Interacts with the Nuclear Lamina and Is Required for the Assembly of a Nup93-containing Complex. *Mol. Biol. Cell* *16*, 2382–2394.
- Hellemans, J., Preobrazhenska, O., Willaert, A., Debeer, P., Verdonk, P.C.M., Costa, T., Janssens, K., Menten, B., Van Roy, N., Vermeulen, S.J.T., et al. (2004). Loss-of-function mutations in LEMD3 result in osteopoikilosis, Buschke-Ollendorff syndrome and melorheostosis. *Nat. Genet.* *36*, 1213–1218.
- Hou, C., and Corces, V.G. (2010). Nups take leave of the nuclear envelope to regulate transcription. *Cell* *140*, 306–308.
- Huang, W., Loganantharaj, R., Schroeder, B., Fargo, D., and Li, L. (2013). PAVIS: a tool for Peak Annotation and Visualization. *Bioinformatics* *29*, 3097–3099.
- Hübner, M.R., and Spector, D.L. (2010). Chromatin dynamics. *Annu. Rev. Biophys.* *39*, 471–489.
- Hutten, S., Wälde, S., Spillner, C., Hauber, J., and Kehlenbach, R.H. (2009). The nuclear pore component Nup358 promotes transportin-dependent nuclear import. *J. Cell Sci.* *122*, 1100–1110.
- Ibarra, A., and Hetzer, M.W. (2015). Nuclear pore proteins and the control of genome functions. *Genes Dev.* *29*, 337–349.
- Ibarra, A., Benner, C., Tyagi, S., Cool, J., and Hetzer, M.W. (2016). Nucleoporin-mediated regulation of cell identity genes. *Genes Dev.* *30*, 2253–2258.
- Ikegami, K., and Lieb, J.D. (2010). Nucleoporins and transcription: new connections, new questions. *PLoS Genet.* *6*, e1000861.
- Ikegami, K., and Lieb, J.D. (2013). Integral nuclear pore proteins bind to Pol III-transcribed genes and are required for Pol III transcript processing in *C. elegans*. *Mol. Cell* *51*, 840–849.
- Ishii, K., Arib, G., Lin, C., Van Houwe, G., and Laemmli, U.K. (2002). Chromatin boundaries in budding yeast: the nuclear pore connection. *Cell* *109*, 551–562.
- Iwamoto, M., Asakawa, H., Hiraoka, Y., and Haraguchi, T. (2010). Nucleoporin Nup98: a gatekeeper in the eukaryotic kingdoms. *Genes Cells* *15*, 661–669.

- Izon, D.J., Rozenfeld, S., Fong, S.T., Kömüves, L., Largman, C., and Lawrence, H.J. (1998). Loss of function of the homeobox gene *Hoxa-9* perturbs early T-cell development and induces apoptosis in primitive thymocytes. *Blood* 92, 383–393.
- Jacinto, F.V., Benner, C., and Hetzer, M.W. (2015). The nucleoporin Nup153 regulates embryonic stem cell pluripotency through gene silencing. *Genes Dev.* 29, 1224–1238.
- Jamali, T., Jamali, Y., Mehrbod, M., and Mofrad, M.R.K. (2011). Nuclear pore complex: biochemistry and biophysics of nucleocytoplasmic transport in health and disease. *Int. Rev. Cell Mol. Biol.* 287, 233–286.
- Kalverda, B., and Fornerod, M. (2010). Characterization of genome-nucleoporin interactions in *Drosophila* links chromatin insulators to the nuclear pore complex. *Cell Cycle* 9, 4812–4817.
- Kalverda, B., Pickersgill, H., Shloma, V.V., and Fornerod, M. (2010). Nucleoporins directly stimulate expression of developmental and cell-cycle genes inside the nucleoplasm. *Cell* 140, 360–371.
- Kehat, I., Accornero, F., Aronow, B.J., and Molkenin, J.D. (2011). Modulation of chromatin position and gene expression by HDAC4 interaction with nucleoporins. *J. Cell Biol.* 193, 21–29.
- Kelley, K., Knockenhauer, K.E., Kabachinski, G., and Schwartz, T.U. (2015). Atomic structure of the Y complex of the nuclear pore. *Nat. Struct. Mol. Biol.* 22, 425–431.
- Khadaroo, B., Teixeira, M.T., Luciano, P., Eckert-Boulet, N., Germann, S.M., Simon, M.N., Gallina, I., Abdallah, P., Gilson, E., Géli, V., et al. (2009). The DNA damage response at eroded telomeres and tethering to the nuclear pore complex. *Nat. Cell Biol.* 11, 980–987.
- Kim, D.I., Birendra, K.C., Zhu, W., Motamedchaboki, K., Doye, V., and Roux, K.J. (2014). Probing nuclear pore complex architecture with proximity-dependent biotinylation. *Proc. Natl. Acad. Sci. USA* 111, E2453–61.
- Kim, S.H., McQueen, P.G., Lichtman, M.K., Shevach, E.M., Parada, L.A., and Misteli, T. (2004). Spatial genome organization during T-cell differentiation. *Cytogenet Genome Res* 105, 292–301.
- Kim, T.H., Abdullaev, Z.K., Smith, A.D., Ching, K.A., Loukinov, D.I., Green, R.D., Zhang, M.Q., Lobanenkov, V.V., and Ren, B. (2007). Analysis of the vertebrate insulator protein CTCF-binding sites in the human genome. *Cell* 128, 1231–1245.
- Knockenhauer, K.E., and Schwartz, T.U. (2016). The nuclear pore complex as a flexible and dynamic gate. *Cell* 164, 1162–1171.
- Köhler, A., and Hurt, E. (2010). Gene regulation by nucleoporins and links to cancer. *Mol. Cell* 38, 6–15.
- Korfali, N., Wilkie, G.S., Swanson, S.K., Srsen, V., de Las Heras, J., Batrakou, D.G., Malik, P., Zuleger, N., Kerr, A.R.W., Florens, L., et al. (2012). The nuclear envelope proteome differs notably between tissues. *Nucleus* 3, 552–564.
- Kosinski, J., Mosalaganti, S., von Appen, A., Teimer, R., DiGuilio, A.L., Wan, W., Bui, K.H., Hagen, W.J.H., Briggs, J.A.G., Glavy, J.S., et al. (2016). Molecular architecture of the inner ring scaffold of the human nuclear pore complex. *Science* 352, 363–365.
- Krull, S., Thyberg, J., Björkroth, B., Rackwitz, H.-R., and Cordes, V.C. (2004). Nucleoporins as components of the nuclear pore complex core structure and Tpr as the architectural element of the nuclear basket. *Mol. Biol. Cell* 15, 4261–4277.

- Krynetski, E.Y., Krynetskaia, N.F., Gallo, A.E., Murti, K.G., and Evans, W.E. (2001). A novel protein complex distinct from mismatch repair binds thioguanylated DNA. *Mol. Pharmacol.* *59*, 367–374.
- Kuleshov, M.V., Jones, M.R., Rouillard, A.D., Fernandez, N.F., Duan, Q., Wang, Z., Koplev, S., Jenkins, S.L., Jagodnik, K.M., Lachmann, A., et al. (2016). Enrichr: a comprehensive gene set enrichment analysis web server 2016 update. *Nucleic Acids Res.* *44*, W90–7.
- Landt, S.G., Marinov, G.K., Kundaje, A., Kheradpour, P., Pauli, F., Batzoglou, S., Bernstein, B.E., Bickel, P., Brown, J.B., Cayting, P., et al. (2012). ChIP-seq guidelines and practices of the ENCODE and modENCODE consortia. *Genome Res.* *22*, 1813–1831.
- Lange, C., Mix, E., Rateitschak, K., and Rolfs, A. (2006). Wnt signal pathways and neural stem cell differentiation. *Neurodegener Dis* *3*, 76–86.
- Leary, D.J., and Huang, S. (2001). Regulation of ribosome biogenesis within the nucleolus. *FEBS Lett.* *509*, 145–150.
- Lemaître, C., Fischer, B., Kalousi, A., Hoffbeck, A.S., Guirouilh-Barbat, J., Shahar, O.D., Genet, D., Goldberg, M., Bertrand, P., Lopez, B., et al. (2012). The nucleoporin 153, a novel factor in double-strand break repair and DNA damage response. *Oncogene* *31*, 4803–4809.
- Li, X., Isono, K.-I., Yamada, D., Endo, T.A., Endoh, M., Shinga, J., Mizutani-Koseki, Y., Otte, A.P., Casanova, M., Kitamura, H., et al. (2011). Mammalian polycomb-like Pcl2/Mtf2 is a novel regulatory component of PRC2 that can differentially modulate polycomb activity both at the Hox gene cluster and at Cdkn2a genes. *Mol. Cell. Biol.* *31*, 351–364.
- Li, Y., Hu, M., and Shen, Y. (2018). Gene regulation in the 3D genome. *Hum. Mol. Genet.* *27*, R228–R233.
- Liang, Y., and Hetzer, M.W. (2011). Functional interactions between nucleoporins and chromatin. *Curr. Opin. Cell Biol.* *23*, 65–70.
- Liang, Y., Franks, T.M., Marchetto, M.C., Gage, F.H., and Hetzer, M.W. (2013). Dynamic association of NUP98 with the human genome. *PLoS Genet.* *9*, e1003308.
- Light, W.H., and Brickner, J.H. (2013). Nuclear pore proteins regulate chromatin structure and transcriptional memory by a conserved mechanism. *Nucleus* *4*, 357–360.
- Light, W.H., Brickner, D.G., Brand, V.R., and Brickner, J.H. (2010). Interaction of a DNA zip code with the nuclear pore complex promotes H2A.Z incorporation and INO1 transcriptional memory. *Mol. Cell* *40*, 112–125.
- Light, W.H., Freaney, J., Sood, V., Thompson, A., D’Urso, A., Horvath, C.M., and Brickner, J.H. (2013). A conserved role for human Nup98 in altering chromatin structure and promoting epigenetic transcriptional memory. *PLoS Biol.* *11*, e1001524.
- Livak, K.J., and Schmittgen, T.D. (2001). Analysis of relative gene expression data using real-time quantitative PCR and the 2(-Delta Delta C(T)) Method. *Methods* *25*, 402–408.
- Machanic, P., and Bailey, T.L. (2011). MEME-ChIP: motif analysis of large DNA datasets. *Bioinformatics* *27*, 1696–1697.
- Maeda, K., Hamada, J.-I., Takahashi, Y., Tada, M., Yamamoto, Y., Sugihara, T., and Moriuchi, T. (2005). Altered expressions of HOX genes in human cutaneous malignant melanoma. *Int. J. Cancer* *114*, 436–441.

- Makiyama, K., Hamada, J.-I., Takada, M., Murakawa, K., Takahashi, Y., Tada, M., Tamoto, E., Shindo, G., Matsunaga, A., Teramoto, K.-I., et al. (2005). Aberrant expression of HOX genes in human invasive breast carcinoma. *Oncol. Rep.* *13*, 673–679.
- Mallo, M., and Alonso, C.R. (2013). The regulation of Hox gene expression during animal development. *Development* *140*, 3951–3963.
- Mansfeld, J., Güttinger, S., Hawryluk-Gara, L.A., Panté, N., Mall, M., Galy, V., Haselmann, U., Mühlhäusser, P., Wozniak, R.W., Mattaj, I.W., et al. (2006). The conserved transmembrane nucleoporin NDC1 is required for nuclear pore complex assembly in vertebrate cells. *Mol. Cell* *22*, 93–103.
- Mao, Y.S., Zhang, B., and Spector, D.L. (2011). Biogenesis and function of nuclear bodies. *Trends Genet.* *27*, 295–306.
- Marina, R.J., Sturgill, D., Bailly, M.A., Thenoz, M., Varma, G., Prigge, M.F., Nanan, K.K., Shukla, S., Haque, N., and Oberdoerffer, S. (2016). TET-catalyzed oxidation of intragenic 5-methylcytosine regulates CTCF-dependent alternative splicing. *EMBO J.* *35*, 335–355.
- Mattout-Drubezki, A., and Gruenbaum, Y. (2003). Dynamic interactions of nuclear lamina proteins with chromatin and transcriptional machinery. *Cell Mol. Life Sci.* *60*, 2053–2063.
- Meinke, P., Nguyen, T.D., and Wehnert, M.S. (2011). The LINC complex and human disease. *Biochem. Soc. Trans.* *39*, 1693–1697.
- Mekhail, K., and Moazed, D. (2010). The nuclear envelope in genome organization, expression and stability. *Nat. Rev. Mol. Cell Biol.* *11*, 317–328.
- Mendjan, S., Taipale, M., Kind, J., Holz, H., Gebhardt, P., Schelder, M., Vermeulen, M., Buscaino, A., Duncan, K., Mueller, J., et al. (2006). Nuclear pore components are involved in the transcriptional regulation of dosage compensation in *Drosophila*. *Mol. Cell* *21*, 811–823.
- Miller, B.R., Powers, M., Park, M., Fischer, W., and Forbes, D.J. (2000). Identification of a new vertebrate nucleoporin, Nup188, with the use of a novel organelle trap assay. *Mol. Biol. Cell* *11*, 3381–3396.
- Misteli, T. (2013). The cell biology of genomes: bringing the double helix to life. *Cell* *152*, 1209–1212.
- Mitchell, J.M., Mansfeld, J., Capitanio, J., Kutay, U., and Wozniak, R.W. (2010). Pom121 links two essential subcomplexes of the nuclear pore complex core to the membrane. *J. Cell Biol.* *191*, 505–521.
- Mohan, M., Bartkuhn, M., Herold, M., Philippen, A., Heintl, N., Bardenhagen, I., Leers, J., White, R.A.H., Renkawitz-Pohl, R., Saumweber, H., et al. (2007). The *Drosophila* insulator proteins CTCF and CP190 link enhancer blocking to body patterning. *EMBO J.* *26*, 4203–4214.
- Montavon, T., and Soshnikova, N. (2014). Hox gene regulation and timing in embryogenesis. *Semin. Cell Dev. Biol.* *34*, 76–84.
- Mustafa, M., Lee, J.-Y., and Kim, M.H. (2015). CTCF negatively regulates HOXA10 expression in breast cancer cells. *Biochem. Biophys. Res. Commun.* *467*, 828–834.
- Nagai, S., Dubrana, K., Tsai-Pflugfelder, M., Davidson, M.B., Roberts, T.M., Brown, G.W., Varela, E., Hediger, F., Gasser, S.M., and Krogan, N.J. (2008). Functional targeting of DNA damage to a nuclear pore-associated SUMO-dependent ubiquitin ligase. *Science* *322*, 597–602.

- Narendra, V., Rocha, P.P., An, D., Raviram, R., Skok, J.A., Mazzoni, E.O., and Reinberg, D. (2015). CTCF establishes discrete functional chromatin domains at the Hox clusters during differentiation. *Science* 347, 1017–1021.
- Neumann, N., Lundin, D., and Poole, A.M. (2010). Comparative genomic evidence for a complete nuclear pore complex in the last eukaryotic common ancestor. *PLoS One* 5, e13241.
- Nikolakaki, E., Simos, G., Georgatos, S.D., and Giannakouros, T. (1996). A nuclear envelope-associated kinase phosphorylates arginine-serine motifs and modulates interactions between the lamin B receptor and other nuclear proteins. *J. Biol. Chem.* 271, 8365–8372.
- Novak, P., Jensen, T., Oshiro, M.M., Wozniak, R.J., Nouzova, M., Watts, G.S., Klimecki, W.T., Kim, C., and Futscher, B.W. (2006). Epigenetic inactivation of the HOXA gene cluster in breast cancer. *Cancer Res.* 66, 10664–10670.
- Oka, M., Mura, S., Yamada, K., Sangel, P., Hirata, S., Maehara, K., Kawakami, K., Tachibana, T., Ohkawa, Y., Kimura, H., et al. (2016). Chromatin-prebound Crml recruits Nup98-HoxA9 fusion to induce aberrant expression of Hox cluster genes. *Elife* 5, e09540.
- Ong, C.-T., and Corces, V.G. (2014). CTCF: an architectural protein bridging genome topology and function. *Nat. Rev. Genet.* 15, 234–246.
- Onischenko, E., Stanton, L.H., Madrid, A.S., Kieselbach, T., and Weis, K. (2009). Role of the Ndc1 interaction network in yeast nuclear pore complex assembly and maintenance. *J. Cell Biol.* 185, 475–491.
- Otsuka, S., Szyzborska, A., and Ellenberg, J. (2014). Imaging the assembly, structure, and function of the nuclear pore inside cells. *Methods Cell Biol.* 122, 219–238.
- Otsuka, S., Bui, K.H., Schorb, M., Hossain, M.J., Politi, A.Z., Koch, B., Eltsov, M., Beck, M., and Ellenberg, J. (2016). Nuclear pore assembly proceeds by an inside-out extrusion of the nuclear envelope. *Elife* 5.
- Palancade, B., Liu, X., Garcia-Rubio, M., Aguilera, A., Zhao, X., and Doye, V. (2007). Nucleoporins prevent DNA damage accumulation by modulating Ulp1-dependent sumoylation processes. *Mol. Biol. Cell* 18, 2912–2923.
- Pancrazi, L., Di Benedetto, G., Colombaioni, L., Della Sala, G., Testa, G., Olimpico, F., Reyes, A., Zeviani, M., Pozzan, T., and Costa, M. (2015). Foxg1 localizes to mitochondria and coordinates cell differentiation and bioenergetics. *Proc. Natl. Acad. Sci. USA* 112, 13910–13915.
- Parada, L.A., McQueen, P.G., and Misteli, T. (2004). Tissue-specific spatial organization of genomes. *Genome Biol.* 5, R44.
- Pascual-Garcia, P., and Capelson, M. (2014). Nuclear pores as versatile platforms for gene regulation. *Curr. Opin. Genet. Dev.* 25, 110–117.
- Pascual-Garcia, P., Jeong, J., and Capelson, M. (2014). Nucleoporin Nup98 associates with Trx/MLL and NSL histone-modifying complexes and regulates Hox gene expression. *Cell Rep.* 9, 433–442.
- Pascual-Garcia, P., Debo, B., Aleman, J.R., Talamas, J.A., Lan, Y., Nguyen, N.H., Won, K.J., and Capelson, M. (2017). Metazoan Nuclear Pores Provide a Scaffold for Poised Genes and Mediate Induced Enhancer-Promoter Contacts. *Mol. Cell* 66, 63–76.e6.

- Patwardhan, S., Gashler, A., Siegel, M.G., Chang, L.C., Joseph, L.J., Shows, T.B., Le Beau, M.M., and Sukhatme, V.P. (1991). EGR3, a novel member of the Egr family of genes encoding immediate-early transcription factors. *Oncogene* 6, 917–928.
- Peña-Hernández, R., Marques, M., Hilmi, K., Zhao, T., Saad, A., Alaoui-Jamali, M.A., del Rincon, S.V., Ashworth, T., Roy, A.L., Emerson, B.M., et al. (2015). Genome-wide targeting of the epigenetic regulatory protein CTCF to gene promoters by the transcription factor TFII-I. *Proc. Natl. Acad. Sci. USA* 112, E677–86.
- Poleshko, A., and Katz, R.A. (2014). Specifying peripheral heterochromatin during nuclear lamina reassembly. *Nucleus* 5, 32–39.
- Pritchard, C.E., Fornerod, M., Kasper, L.H., and van Deursen, J.M. (1999). RAE1 is a shuttling mRNA export factor that binds to a GLEBS-like NUP98 motif at the nuclear pore complex through multiple domains. *J. Cell Biol.* 145, 237–254.
- Ptak, C., and Wozniak, R.W. (2016). Nucleoporins and chromatin metabolism. *Curr. Opin. Cell Biol.* 40, 153–160.
- Ptak, C., Aitchison, J.D., and Wozniak, R.W. (2014). The multifunctional nuclear pore complex: a platform for controlling gene expression. *Curr. Opin. Cell Biol.* 28, 46–53.
- Quach, D.H., Oliveira-Fernandes, M., Gruner, K.A., and Tourtellotte, W.G. (2013). A sympathetic neuron autonomous role for Egr3-mediated gene regulation in dendrite morphogenesis and target tissue innervation. *J. Neurosci.* 33, 4570–4583.
- Quinodoz, S.A., Ollikainen, N., Tabak, B., Palla, A., Schmidt, J.M., Detmar, E., Lai, M.M., Shishkin, A.A., Bhat, P., Takei, Y., et al. (2018). Higher-Order Inter-chromosomal Hubs Shape 3D Genome Organization in the Nucleus. *Cell* 174, 744–757.e24.
- Rabut, G., Doye, V., and Ellenberg, J. (2004). Mapping the dynamic organization of the nuclear pore complex inside single living cells. *Nat. Cell Biol.* 6, 1114–1121.
- Raices, M., and D’Angelo, M.A. (2018). Nuclear pore complexes in the organization and regulation of the mammalian genome. In *Nuclear Pore Complexes in Genome Organization, Function and Maintenance*, M. D’Angelo, ed. (Cham: Springer International Publishing), pp. 159–182.
- Raices, M., Bukata, L., Sakuma, S., Borlido, J., Hernandez, L.S., Hart, D.O., and D’Angelo, M.A. (2017). Nuclear pores regulate muscle development and maintenance by assembling a localized mef2c complex. *Dev. Cell* 41, 540–554.e7.
- Ranade, D., Koul, S., Thompson, J., Prasad, K.B., and Sengupta, K. (2017). Chromosomal aneuploidies induced upon Lamin B2 depletion are mislocalized in the interphase nucleus. *Chromosoma* 126, 223–244.
- Randise-Hinchliff, C., Coukos, R., Sood, V., and Sumner, M.C. Strategies to regulate transcription factor-mediated gene positioning and interchromosomal clustering at the nuclear periphery. [Jcb.rupress.org](http://Jcb.rupress.org).
- Rasala, B.A., Ramos, C., Harel, A., and Forbes, D.J. (2008). Capture of AT-rich chromatin by ELYS recruits POM121 and NDC1 to initiate nuclear pore assembly. *Mol. Biol. Cell* 19, 3982–3996.
- Reddy, K.L., Zullo, J.M., Bertolino, E., and Singh, H. (2008). Transcriptional repression mediated by repositioning of genes to the nuclear lamina. *Nature* 452, 243–247.

- Regad, T., Roth, M., Bredenkamp, N., Illing, N., and Papalopulu, N. (2007). The neural progenitor-specifying activity of FoxG1 is antagonistically regulated by CKI and FGF. *Nat. Cell Biol.* 9, 531–540.
- Rio, D.C., Ares, M., Hannon, G.J., and Nilsen, T.W. (2010). Purification of RNA using TRIzol (TRI reagent). *Cold Spring Harb. Protoc.* 2010, pdb.prot5439.
- Rodríguez-Navarro, S., Fischer, T., Luo, M.-J., Antúnez, O., Brettschneider, S., Lechner, J., Pérez-Ortín, J.E., Reed, R., and Hurt, E. (2004). Sus1, a functional component of the SAGA histone acetylase complex and the nuclear pore-associated mRNA export machinery. *Cell* 116, 75–86.
- Rohner, S., Kalck, V., Wang, X., Ikegami, K., Lieb, J.D., Gasser, S.M., and Meister, P. (2013). Promoter- and RNA polymerase II-dependent hsp-16 gene association with nuclear pores in *Caenorhabditis elegans*. *J. Cell Biol.* 200, 589–604.
- Rousseau, M., Crutchley, J.L., Miura, H., Suderman, M., Blanchette, M., and Dostie, J. (2014). Hox in motion: tracking HoxA cluster conformation during differentiation. *Nucleic Acids Res.* 42, 1524–1540.
- Ruiz-Velasco, M., Kumar, M., Lai, M.C., Bhat, P., Solis-Pinson, A.B., Reyes, A., Kleinsorg, S., Noh, K.-M., Gibson, T.J., and Zaugg, J.B. (2017). CTCF-Mediated Chromatin Loops between Promoter and Gene Body Regulate Alternative Splicing across Individuals. *Cell Syst.* 5, 628–637.e6.
- Sachdev, R., Sieverding, C., Flötenmeyer, M., and Antonin, W. (2012). The C-terminal domain of Nup93 is essential for assembly of the structural backbone of nuclear pore complexes. *Mol. Biol. Cell* 23, 740–749.
- Sakamoto, Y., Watanabe, S., Ichimura, T., Kawasuji, M., Koseki, H., Baba, H., and Nakao, M. (2007). Overlapping roles of the methylated DNA-binding protein MBD1 and polycomb group proteins in transcriptional repression of HOXA genes and heterochromatin foci formation. *J. Biol. Chem.* 282, 16391–16400.
- Sakiyama, Y., Panatala, R., and Lim, R.Y.H. (2017). Structural dynamics of the nuclear pore complex. *Semin. Cell Dev. Biol.* 68, 27–33.
- Sampathkumar, P., Kim, S.J., Upla, P., Rice, W.J., Phillips, J., Timney, B.L., Pieper, U., Bonanno, J.B., Fernandez-Martinez, J., Hakhverdyan, Z., et al. (2013). Structure, dynamics, evolution, and function of a major scaffold component in the nuclear pore complex. *Structure* 21, 560–571.
- Sarma, N.J., Buford, T.D., Haley, T., Barbara-Haley, K., Santangelo, G.M., and Willis, K.A. (2011). The nuclear pore complex mediates binding of the Mig1 repressor to target promoters. *PLoS One* 6, e27117.
- Savas, J.N., Toyama, B.H., Xu, T., Yates, J.R., and Hetzer, M.W. (2012). Extremely long-lived nuclear pore proteins in the rat brain. *Science* 335, 942.
- Scherthan, H., Jerratsch, M., Li, B., Smith, S., Hultén, M., Lock, T., and de Lange, T. (2000). Mammalian meiotic telomeres: protein composition and redistribution in relation to nuclear pores. *Mol. Biol. Cell* 11, 4189–4203.
- Schmid, M., Arib, G., Laemmli, C., Nishikawa, J., Durussel, T., and Laemmli, U.K. (2006). Nup-PI: the nucleopore-promoter interaction of genes in yeast. *Mol. Cell* 21, 379–391.

- Schneider, M., Hellerschmied, D., Schubert, T., Amlacher, S., Vinayachandran, V., Reja, R., Pugh, B.F., Clausen, T., and Köhler, A. (2015). The Nuclear Pore-Associated TREX-2 Complex Employs Mediator to Regulate Gene Expression. *Cell* *162*, 1016–1028.
- Schooley, A., Vollmer, B., and Antonin, W. (2012). Building a nuclear envelope at the end of mitosis: coordinating membrane reorganization, nuclear pore complex assembly, and chromatin de-condensation. *Chromosoma* *121*, 539–554.
- Seifert, A., Werheid, D.F., Knapp, S.M., and Tobiasch, E. (2015). Role of Hox genes in stem cell differentiation. *World J. Stem Cells* *7*, 583–595.
- Sengupta, K., Upender, M.B., Barenboim-Stapleton, L., Nguyen, Q.T., Wincovitch, S.M., Garfield, S.H., Difilippantonio, M.J., and Ried, T. (2007). Artificially introduced aneuploid chromosomes assume a conserved position in colon cancer cells. *PLoS One* *2*, e199.
- Sexton, T., and Cavalli, G. (2015). The role of chromosome domains in shaping the functional genome. *Cell* *160*, 1049–1059.
- Sexton, T., Schober, H., Fraser, P., and Gasser, S.M. (2007). Gene regulation through nuclear organization. *Nat. Struct. Mol. Biol.* *14*, 1049–1055.
- Shachar, S., Voss, T.C., Pegoraro, G., Sciascia, N., and Misteli, T. (2015). Identification of Gene Positioning Factors Using High-Throughput Imaging Mapping. *Cell* *162*, 911–923.
- Sharma, A., Solmaz, S.R., Blobel, G., and Melčák, I. (2015). Ordered regions of channel nucleoporins nup62, nup54, and nup58 form dynamic complexes in solution. *J. Biol. Chem.* *290*, 18370–18378.
- Shimi, T., Pflieger, K., Kojima, S., Pack, C.-G., Solovei, I., Goldman, A.E., Adam, S.A., Shumaker, D.K., Kinjo, M., Cremer, T., et al. (2008). The A- and B-type nuclear lamin networks: microdomains involved in chromatin organization and transcription. *Genes Dev.* *22*, 3409–3421.
- Shin, H., Liu, T., Manrai, A.K., and Liu, X.S. (2009). CEAS: cis-regulatory element annotation system. *Bioinformatics* *25*, 2605–2606.
- Shukla, S., Kavak, E., Gregory, M., Imashimizu, M., Shutinoski, B., Kashlev, M., Oberdoerffer, P., Sandberg, R., and Oberdoerffer, S. (2011). CTCF-promoted RNA polymerase II pausing links DNA methylation to splicing. *Nature* *479*, 74–79.
- Simeone, A., Acampora, D., Arcioni, L., Andrews, P.W., Boncinelli, E., and Mavilio, F. (1990). Sequential activation of HOX2 homeobox genes by retinoic acid in human embryonal carcinoma cells. *Nature* *346*, 763–766.
- Singh, P., Lee, D.-H., and Szabó, P.E. (2012). More than insulator: multiple roles of CTCF at the H19-Igf2 imprinted domain. *Front. Genet.* *3*, 214.
- Siniosoglou, S., Wimmer, C., Rieger, M., Doye, V., Tekotte, H., Weise, C., Emig, S., Segref, A., and Hurt, E.C. (1996). A novel complex of nucleoporins, which includes Sec13p and a Sec13p homolog, is essential for normal nuclear pores. *Cell* *84*, 265–275.
- Soler-Oliva, M.E., Guerrero-Martínez, J.A., Bachetti, V., and Reyes, J.C. (2017). Analysis of the relationship between coexpression domains and chromatin 3D organization. *PLoS Comput. Biol.* *13*, e1005708.



- Solovei, I., Wang, A.S., Thanisch, K., Schmidt, C.S., Krebs, S., Zwerger, M., Cohen, T.V., Devys, D., Foisner, R., Peichl, L., et al. (2013). LBR and lamin A/C sequentially tether peripheral heterochromatin and inversely regulate differentiation. *Cell* 152, 584–598.
- Sood, V., and Brickner, J.H. (2014). Nuclear pore interactions with the genome. *Curr. Opin. Genet. Dev.* 25, 43–49.
- Spector, D.L., and Lamond, A.I. (2011). Nuclear speckles. *Cold Spring Harb. Perspect. Biol.* 3.
- Stancheva, I., and Schirmer, E.C. (2014). Nuclear envelope: connecting structural genome organization to regulation of gene expression. *Adv. Exp. Med. Biol.* 773, 209–244.
- Stark, C., Breitkreutz, B.-J., Reguly, T., Boucher, L., Breitkreutz, A., and Tyers, M. (2006). BioGRID: a general repository for interaction datasets. *Nucleic Acids Res.* 34, D535–9.
- Stavru, F., Hülsmann, B.B., Spang, A., Hartmann, E., Cordes, V.C., and Görlich, D. (2006a). NDC1: a crucial membrane-integral nucleoporin of metazoan nuclear pore complexes. *J. Cell Biol.* 173, 509–519.
- Stavru, F., Nautrup-Pedersen, G., Cordes, V.C., and Görlich, D. (2006b). Nuclear pore complex assembly and maintenance in POM121- and gp210-deficient cells. *J. Cell Biol.* 173, 477–483.
- Steglich, B., Sazer, S., and Ekwall, K. (2013). Transcriptional regulation at the yeast nuclear envelope. *Nucleus* 4, 379–389.
- Strambio-De-Castillia, C., Niepel, M., and Rout, M.P. (2010). The nuclear pore complex: bridging nuclear transport and gene regulation. *Nat. Rev. Mol. Cell Biol.* 11, 490–501.
- Szabó, P.E., Tang, S.-H.E., Silva, F.J., Tsark, W.M.K., and Mann, J.R. (2004). Role of CTCF binding sites in the Igf2/H19 imprinting control region. *Mol. Cell Biol.* 24, 4791–4800.
- Taddei, A. (2007). Active genes at the nuclear pore complex. *Curr. Opin. Cell Biol.* 19, 305–310.
- Taddei, A., Van Houwe, G., Hediger, F., Kalck, V., Cubizolles, F., Schober, H., and Gasser, S.M. (2006). Nuclear pore association confers optimal expression levels for an inducible yeast gene. *Nature* 441, 774–778.
- Talamas, J.A., and Capelson, M. (2015). Nuclear envelope and genome interactions in cell fate. *Front. Genet.* 6, 95.
- Talamas, J.A., and Hetzer, M.W. (2011). POM121 and Sun1 play a role in early steps of interphase NPC assembly. *J. Cell Biol.* 194, 27–37.
- Tan-Wong, S.M., Wijayatilake, H.D., and Proudfoot, N.J. (2009). Gene loops function to maintain transcriptional memory through interaction with the nuclear pore complex. *Genes Dev.* 23, 2610–2624.
- Teo, J.-L., and Kahn, M. (2010). The Wnt signaling pathway in cellular proliferation and differentiation: A tale of two coactivators. *Adv. Drug Deliv. Rev.* 62, 1149–1155.
- Texari, L., Dieppois, G., Vinciguerra, P., Contreras, M.P., Groner, A., Letourneau, A., and Stutz, F. (2013). The nuclear pore regulates GAL1 gene transcription by controlling the localization of the SUMO protease Ulp1. *Mol. Cell* 51, 807–818.
- Thanisch, K., Song, C., Engelkamp, D., Koch, J., Wang, A., Hallberg, E., Foisner, R., Leonhardt, H., Stewart, C.L., Joffe, B., et al. (2017). Nuclear envelope localization of LEMD2 is

developmentally dynamic and lamin A/C dependent yet insufficient for heterochromatin tethering. *Differentiation*. *94*, 58–70.

Theerthagiri, G., Eisenhardt, N., Schwarz, H., and Antonin, W. (2010). The nucleoporin Nup188 controls passage of membrane proteins across the nuclear pore complex. *J. Cell Biol.* *189*, 1129–1142.

Toyama, B.H., Savas, J.N., Park, S.K., Harris, M.S., Ingolia, N.T., Yates, J.R., and Hetzer, M.W. (2013). Identification of long-lived proteins reveals exceptional stability of essential cellular structures. *Cell* *154*, 971–982.

Turner, E.M., and Schlieker, C. (2016). Pelger-Huët anomaly and Greenberg skeletal dysplasia: LBR-associated diseases of cholesterol metabolism. *Rare Dis.* *4*, e1241363.

Ulrich, A., Partridge, J.R., and Schwartz, T.U. (2014). The stoichiometry of the nucleoporin 62 subcomplex of the nuclear pore in solution. *Mol. Biol. Cell* *25*, 1484–1492.

van Koningsbruggen, S., Gierlinski, M., Schofield, P., Martin, D., Barton, G.J., Ariyurek, Y., den Dunnen, J.T., and Lamond, A.I. (2010). High-resolution whole-genome sequencing reveals that specific chromatin domains from most human chromosomes associate with nucleoli. *Mol. Biol. Cell* *21*, 3735–3748.

Vaquerizas, J.M., Suyama, R., Kind, J., Miura, K., Luscombe, N.M., and Akhtar, A. (2010). Nuclear pore proteins nup153 and megator define transcriptionally active regions in the *Drosophila* genome. *PLoS Genet.* *6*, e1000846.

Vieux-Rochas, M., Fabre, P.J., Leleu, M., Duboule, D., and Noordermeer, D. (2015). Clustering of mammalian Hox genes with other H3K27me3 targets within an active nuclear domain. *Proc. Natl. Acad. Sci. USA* *112*, 4672–4677.

Vollmer, B., and Antonin, W. (2014). The diverse roles of the Nup93/Nic96 complex proteins - structural scaffolds of the nuclear pore complex with additional cellular functions. *Biol. Chem.* *395*, 515–528.

von Appen, A., Kosinski, J., Sparks, L., Ori, A., DiGuilio, A.L., Vollmer, B., Mackmull, M.-T., Banterle, N., Parca, L., Kastiris, P., et al. (2015). In situ structural analysis of the human nuclear pore complex. *Nature* *526*, 140–143.

Wada, Y., Ohta, Y., Xu, M., Tsutsumi, S., Minami, T., Inoue, K., Komura, D., Kitakami, J., Oshida, N., Papantonis, A., et al. (2009). A wave of nascent transcription on activated human genes. *Proc. Natl. Acad. Sci. USA* *106*, 18357–18361.

Wälde, S., and Kehlenbach, R.H. (2010). The Part and the Whole: functions of nucleoporins in nucleocytoplasmic transport. *Trends Cell Biol.* *20*, 461–469.

Walker, C.L., Cargile, C.B., Floy, K.M., Delannoy, M., and Migeon, B.R. (1991). The Barr body is a looped X chromosome formed by telomere association. *Proc. Natl. Acad. Sci. USA* *88*, 6191–6195.

Walther, T.C., Alves, A., Pickersgill, H., Loiodice, I., Hetzer, M., Galy, V., Hülsmann, B.B., Köcher, T., Wilm, M., Allen, T., et al. (2003). The conserved Nup107-160 complex is critical for nuclear pore complex assembly. *Cell* *113*, 195–206.

Wang, K.C., Yang, Y.W., Liu, B., Sanyal, A., Corces-Zimmerman, R., Chen, Y., Lajoie, B.R., Protacio, A., Flynn, R.A., Gupta, R.A., et al. (2011). A long noncoding RNA maintains active chromatin to coordinate homeotic gene expression. *Nature* *472*, 120–124.

- Wang, X., Xu, M., Zhao, G., Liu, G., Hao, D., Lv, X., and Liu, D. (2015). Exploring CTCF and cohesin related chromatin architecture at HOXA gene cluster in primary human fibroblasts. *Sci China Life Sci* 58, 860–866.
- Wente, S.R., and Rout, M.P. (2010). The nuclear pore complex and nuclear transport. *Cold Spring Harb. Perspect. Biol.* 2, a000562.
- Williams, R.R.E., Azuara, V., Perry, P., Sauer, S., Dvorkina, M., Jørgensen, H., Roix, J., McQueen, P., Misteli, T., Merckenschlager, M., et al. (2006). Neural induction promotes large-scale chromatin reorganisation of the *Mash1* locus. *J. Cell Sci.* 119, 132–140.
- Worman, H.J., and Schirmer, E.C. (2015). Nuclear membrane diversity: underlying tissue-specific pathologies in disease? *Curr. Opin. Cell Biol.* 34, 101–112.
- Wu, X., Kasper, L.H., Mantcheva, R.T., Mantchev, G.T., Springett, M.J., and van Deursen, J.M. (2001). Disruption of the FG nucleoporin NUP98 causes selective changes in nuclear pore complex stoichiometry and function. *Proc. Natl. Acad. Sci. USA* 98, 3191–3196.
- Xiao, T., Wallace, J., and Felsenfeld, G. (2011). Specific sites in the C terminus of CTCF interact with the SA2 subunit of the cohesin complex and are required for cohesin-dependent insulation activity. *Mol. Cell. Biol.* 31, 2174–2183.
- Xu, M., Zhao, G.-N., Lv, X., Liu, G., Wang, L.Y., Hao, D.-L., Wang, J., Liu, D.-P., and Liang, C.-C. (2014). CTCF controls HOXA cluster silencing and mediates PRC2-repressive higher-order chromatin structure in NT2/D1 cells. *Mol. Cell. Biol.* 34, 3867–3879.
- Yoshida, T., Shimada, K., Oma, Y., Kalck, V., Akimura, K., Taddei, A., Iwahashi, H., Kugou, K., Ohta, K., Gasser, S.M., et al. (2010). Actin-related protein Arp6 influences H2A.Z-dependent and -independent gene expression and links ribosomal protein genes to nuclear pores. *PLoS Genet.* 6, e1000910.
- Zhang, Q., Bethmann, C., Worth, N.F., Davies, J.D., Wasner, C., Feuer, A., Ragnauth, C.D., Yi, Q., Mellad, J.A., Warren, D.T., et al. (2007). Nesprin-1 and -2 are involved in the pathogenesis of Emery Dreifuss muscular dystrophy and are critical for nuclear envelope integrity. *Hum. Mol. Genet.* 16, 2816–2833.
- Zhang, Y., Liu, T., Meyer, C.A., Eeckhoute, J., Johnson, D.S., Bernstein, B.E., Nusbaum, C., Myers, R.M., Brown, M., Li, W., et al. (2008). Model-based analysis of ChIP-Seq (MACS). *Genome Biol.* 9, R137.
- Zink, D., Amaral, M.D., Englmann, A., Lang, S., Clarke, L.A., Rudolph, C., Alt, F., Luther, K., Braz, C., Sadoni, N., et al. (2004). Transcription-dependent spatial arrangements of CFTR and adjacent genes in human cell nuclei. *J. Cell Biol.* 166, 815–825.
- Zuleger, N., Boyle, S., Kelly, D.A., de las Heras, J.I., Lazou, V., Korfali, N., Batrakou, D.G., Randles, K.N., Morris, G.E., Harrison, D.J., et al. (2013). Specific nuclear envelope transmembrane proteins can promote the location of chromosomes to and from the nuclear periphery. *Genome Biol.* 14, R14.
- Zullo, J.M., Demarco, I.A., Piqué-Regi, R., Gaffney, D.J., Epstein, C.B., Spooner, C.J., Luperchio, T.R., Bernstein, B.E., Pritchard, J.K., Reddy, K.L., et al. (2012). DNA sequence-dependent compartmentalization and silencing of chromatin at the nuclear lamina. *Cell* 149, 1474–1487.